Synthesis and Characterization
of
Novel Poly(imino ketone)s
Via Palladium-Catalyzed Aryl Amination

Dissertation zur Erlangung des Grades

"Doktor der Naturwissenschaften"

am Fachbereich Chemie und Pharmazie

der Johannes Gutenberg-Universität in Mainz

By

Ayman S. Al-Hussaini

geb. in Ägypten

Mainz 2005

Tag der mündlichen Prüfung: Friday, 22 April 2005.

Die vorliegende Arbeit wurde in der Zeit von Juli 2001 bis December 2004 am Max-Planck-Institut für Polymerforschung in Mainz unter Anleitung von Herrn Professor Dr. K. Müllen durchgeführt.

Herrn Professor Dr. K. Müllen danke ich für seine wissenschaftliche und persönliche Unterstützung sowie für zahlreiche motivierende Diskussionen.

**To
my parents and my brothers**

CHAPTER I

INTRODUCTION

CHAPTER II

CHAPTER III

CHAPTER IV

CHAPTER V

CHAPTER VI

List of acronyms:

PIKs	Poly(imino ketone)s	PEEKKs	poly(ether ether ketone ketone)s
PIAlcos	Novel poly(imino alcohol)s	PEKs	Poly(arylene ether ketone)s
PIAzos	Poly(imino azobenzene)s	PAAs	Polyaramides
PIAcs	Poly(imino acridine)s	PANI	Polyaniline
PIFOs	Poly(imino fluorenone)s	2,7-PFO	2,7-Poly-(9-fluorenone)
PICs	Poly(imino carbazole)s		

List of ligands and catalysts:

TPP	Triphenyl phosphite
$Pd_2(dba)_3$	Tris(dibenzylideneacetone)dipalladium(0)
BINAP	2,2`-bis(diphenylphosphino)-1,1`-binaphthyl
$C_{20}H_{27}P$	Di-t-butylphosphinobiphenyl
$P(t-Bu)_3$	Tri.-tert.butyl phosphine
$C_{27}H_{37}N_2^+Cl^-$	1,3-Bis(2,6-diisopropylphenyl)imidazolium chloride)
$(DPPF)PdCl_2$	1,1`-Bis{(diphenylphosphino)ferrocene)}dichloropalladium (II)
DPEphos	Bis[2-(diphenylphosphino)phenyl]ether

List of symbols:

M_n	Number average molecular weight
M_w	Weight average molecular weight
M_w / M_n	Polydispersity index
$[\eta]$	Intrinsic viscosity
T_g	glass transition temperature
T_m	Melting temperature
G'	The real component of the complex shear modulus
G''	The imaginary component of the complex shear modulus
ω	Frequency
C	Concentration

T	Temperature
λ	The X-ray wavelength
d	The spacing between the atomic planes
Θ	The angle between the X-ray beam and the atomic plane
ε^*	The complex dielectric permitivity
ε'	The real component of the dielectric constant
ε''	The imaginary component of the dielectric constant
$\tan\delta$	The dielectric loss tangent

List of abbreviations:

FT-IR	Fourier transform infrared spectroscopy
NMR	Nuclear magnetic resonance spectroscopy
GPC	Gel permeation chromatography
PL	Photoluminescence spectra
EL	Electroluminescence spectra
TGA	Thermogravimetric analysis
DSC	Differential scanning calorimetry
WAXD	Wide-angle X-ray diffraction
DMA	Dynamic mechanical analysis
CV	Cyclic voltammetry
TOF	Time of flight of charge carrier
HTL	Hole transporting layer
RT	Room temperature
TLC	Thin-layer chromatography

DMSO	Dimethylsulfoxide
DMF	N,N-Dimethylformamide
DMAc	Dimethylacetamide
DPS	Diphenylsulfone
NMP	N-Methylpyrrolidinone
THF	Tetrahydrofuran
ICT	Intramolecular charge-transfer
Mp	Melting point
Mol	Mole
Min	Minute
HTL	Hole transporting layer
LEDs	Light-emitting diodes
PLEDs	Polymer light-emitting diodes

CHAPTER I

INTRODUCTION

1.1 Poly(arylene ether ketone)s (PEKs)

This section begins with a discussion of the synthesis and properties of poly(arylene ether ketone)s (PEKs). This part includes a review of PEKs, with emphasis on the investigation of the curing mechanism. The nucleophilic aromatic substitution mechanism used in this research and the properties of the thermoplastic materials will be briefly described.

1.1.1   Synthesis and properties of poly(arylene ether ketone)s and related materials.

Poly(arylene ether ketone)s (PEKs) are semicrystalline high-performance polymers with outstanding physical properties.[1-3] Much research effort has been expended in structural variation to control and improve their properties.[4-7] Poly(arylene ether ketone)s can be prepared *via* polycondensation using electrophilic or nucleophilic aromatic substitution.[8-11] The electrophilic aromatic substitution route involves the reaction between electron-rich aromatic hydrocarbons and aromatic acid chlorides in which ketone linkages are formed. This polycondensation is carried out either in an organic solvent with aluminum chloride as a catalyst,[12,13] i.e. Friedel-Crafts acylation, or in hydrogen fluoride / boron trifluoride as a catalyst and solvent.[14,15] The nucleophilic aromatic substitution (S_NAr) route involves the reaction between activated aromatic halides (activated aromatic ketone monomers in which the carbonyl group serves as the activating moiety) and alkali metal phenoxides in which ether linkages are formed. This method is used for the production not only of PEKs, most popular representative of poly(ether ether ketone)s (PEEKs), but also of commercial polysulfones and poly(ether sulfone)s. The electrophilic route using the Friedel-Craft acylation reaction has some limitations because of mechanistic problems, therefore the nucleophilic route has been the most commonly used method to prepare various kinds of poly(arylene ether ketone)s.

While high molecular weight poly(aryl ether sulfone)s[16] and poly(ether imide)s[17] have been made by the nitro displacement reaction, the report[18] that claimed synthesis of high molecular weight crystalline PEKs has some questionable points.[8,19]

1

Most of the syntheses of poly(arylene ether ketone)s have employed fluoride as a leaving group[20] and nitro leaving groups were rarely used because of the generation of reactive nitrite ions that become reactive and tend to cause side reactions at elevated temperature.[21,22a-e] However, high molecular weight polyetherimides have been made by nitro displacement reaction.[23] In the synthesis of PEKs, the problem of the nitro leaving group in the S_NAr reaction could be avoided, if the nitro groups of a ketone monomer were easily displaced at mild conditions.[24] Trifluoromethyl group that is known as an effective activating group for the nitro displacement reaction without side reactions was selected as a second activating group.[25] Trifluoromethyl groups in the monomer exert not only an activating effect on a leaving group but also a bulky substituent effect on a polymer main chain, which may prevent crystallization, resulting in amorphous polymers. In this case, a high temperature to overcome premature crystallization during synthesis of PEKs is not necessary and nucleophilic nitro displacement can be carried out under mild conditions. The first example of the synthesis of high molecular weight amorphous poly(arylene ether ketone)s through the nucleophilic nitro displacement reaction with an AA-type monomer that is doubly activated by carbonyl and trifluoromethyl groups has been reported.[25]

According to the reported results[26, 27] the electron withdrawing carbonyl group of the amide moiety can activate the leaving groups at the para-position for nucleophilic aromatic substitution, and amide linkages survive the typical polymerization reaction of poly(aryl ether)s (Figure 1.1-1). The amide groups in the monomer may exert not only an activating effect on a leaving group but also a bulky substituent effect on a polymer main chain which may prevent crystallization of a polymer chain, resulting in an amorphous polymer with enhanced solubility in organic solvents and high glass transition temperature.[28,29] New amorphous poly(arylene ether ketone)s with amide substituents were prepared via nucleophilic nitro displacement reaction.[30]
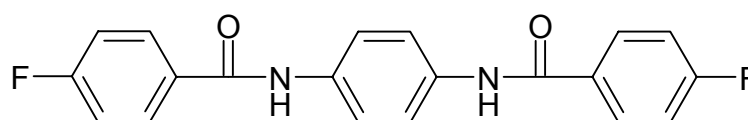
Figure 1.1-1:

1.1.2 Nucleophilic aromatic substitution with emphasis on important variables

The most important commercial routes are nucleophilic aromatic substitution[8,9] and, electrophilic aromatic substitution.[12-15] Nucleophilic aromatic substitution is also the synthetic route to the materials produced in this research, therefore the background for this mechanism will be discussed herein.

There are four important mechanisms for aromatic nucleophilic substitution.[31,32] The most important of which, the S_NAr, is applicable to poly(arylene ether ketone)s. The general S_NAr-mechanism is shown in Figure 1.1-2. Step one involves the attack of the nucleophile on the activated site to form a resonance stabilized arenium ion intermediate; this is usually the rate determining step. Step two involves the departure of the leaving group and is usually fast and results in reformation of aromaticity in the ring.
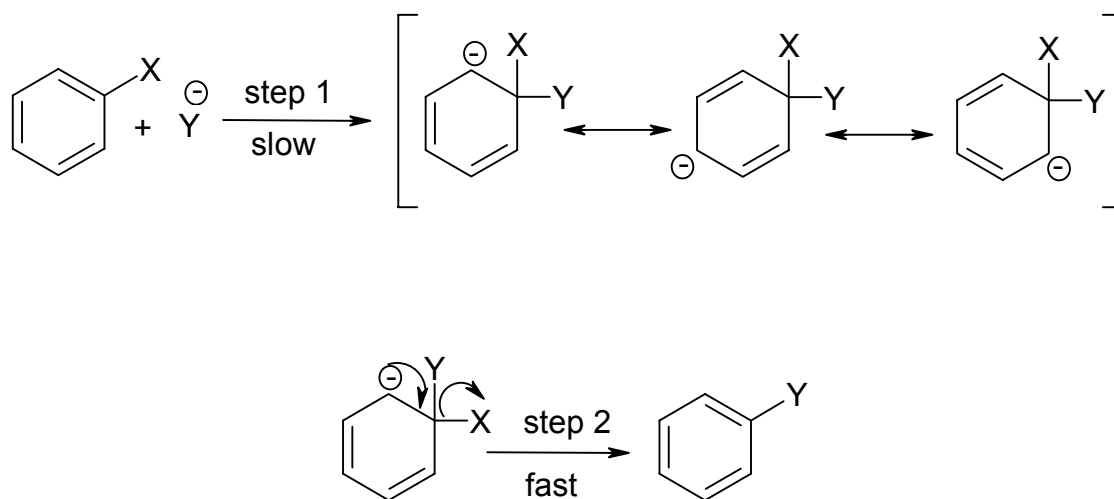
Figure 1.1-2: S_NAr Mechanism.[32]

1.1.2.1 Synthesis of poly(arylene ether ketone)s *via* nucleophilic aromatic substitution

Polyarylene ether ketone are prepared *via* nucleophilic aromatic substitution as illustrated in Scheme 1.1-1. An aromatic bisphenol is reacted with a base utilizing a metal cation, which is typically sodium carbonate or potassium carbonate. The metal carbonate can undergo a number of reactions to produce phenolate and water, which are summarized in Figure 1.1-3.[33] This reaction forms the phenolate anion, or the diphenolate with a strong base. The phenolate acts as the nucleophile to displace the halide ion after nucleophilic aromatic substitution has occured at the activated dihalide to form the diaryl ether bond.
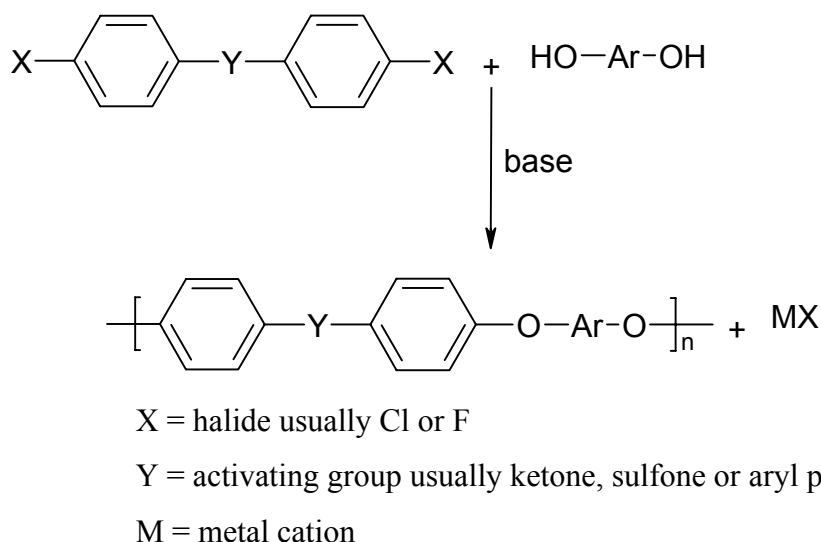
Scheme 1.1-1: Generic nucleophilic aromatic substitution polymerization.
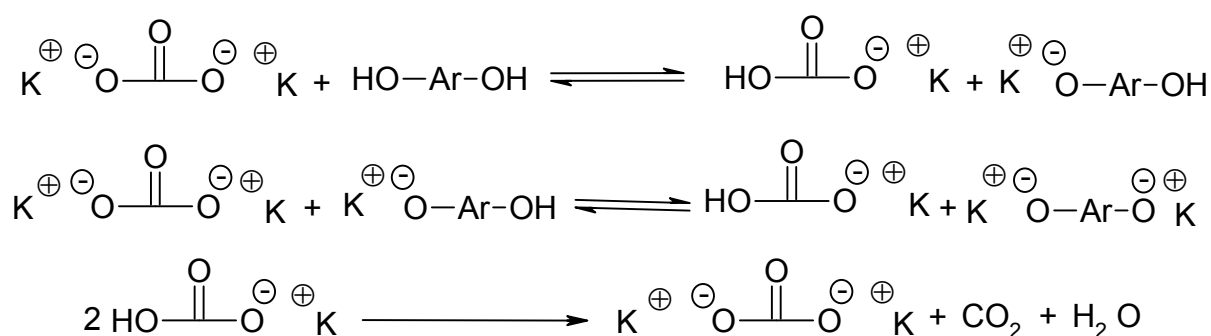
Figure 1.1-3: Reactions of potassium carbonate in the formation of phenolates and water.

1.1.2.2 The activating group

The presence of an electron withdrawing group in the ortho and/or para positions stabilizes the intermediate formed in step one; however, substitution at the ortho position can sterically hinder the attack of the nucleophile. An electron withdrawing group such as a nitro group stabilizes the intermediate by forming a Meisenheimer salt, (**1**), named after its discoverer.[34] The structure of intermediates such as (**1**) have been confirmed by NMR[35] spectroscopy and X-ray crystallography.[36] The S_NAr-mechanism is supported by the fact that these intermediates have been isolated and that the presence of the electron withdrawing group in the para-position accelerates the rate of the reaction by stabilizing the intermediate formed in the rate determining step. The reactivity order corresponds to the electron withdrawing power and has been observed to be:[31,37] $NO > NO_2 > SO_2Me > CF_3 > CN > CHO > COR > COOH >$

Br > Cl > I > H > F > CMe$_3$ > Me > OMe > NMe$_2$ > OH > NH$_2$. Nitro, ketone and ketone groups are common activating groups utilized in the synthesis of polyarylene ethers.
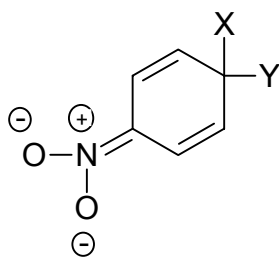
1

1.1.2.3 The leaving group

The leaving group (X-) is an important variable in the nucleophilic aromatic substitution polymerization of polyarylene ether ketones. Bunnett[38] reported that the rate of the reaction was dependent on the leaving group in the order of F >> Cl > Br > I for the halogen series. This is despite the fact that the bond strengths for carbon-halogen bonds decrease in the same order. One concludes that the leaving group is not lost in the rate determining step and that the breaking of that bond is not rate determining. The reason why it has an effect on the rate of the reaction at all is because the leaving group has an electronic effect on the activated carbon which is attacked in the rate determining step. The greater electronegativity of the fluorine atom inductively withdraws electron density from the activated carbon, further activating it for the attack of a nucleophile and stabilizies the intermediate. Steric effects can also play a role in increasing the rate. Thus, a smaller atom on the activated carbon allows for a better access to that carbon for the incoming nucleophile.[38]

1.1.2.4 The nucleophile

The nucleophilicity of the nucleophile plays an important role in the polymerization of polyarylene ether ketones by nucleophilic aromatic substitution. An approximate order of nucleophile strength is: ArS- > RO- > R$_2$NH- > ArO- > OH- > ArNH$_2$ > NH$_3$ > I- > Br- > Cl- > H$_2$O > ROH.[38] This is important in the polymerization reaction as it is vital that side reactions be avoided to obtain high molecular weight products. This order suggests that the phenoxide anion is the strongest nucleophile in the reaction with nucleophilicity above hydroxide ion, the halogens and water.

1.1.2.5 The solvent

The choice of solvent is particularly important in the nucleophilic aromatic substitution polymerization reaction. There are three major requirements of the solvent. Firstly, the solvent should not undergo any reaction with the reactants leading to side products. Next, the solvation power of the solvent must be such that all of the reactants and products have sufficient solubility. This can be a significant problem with polymers where the reacting chain end must remain in solution even when the polymer chain has grown very large. Lastly, the solvent should assist in the dissociation of the nucleophilic anion from the metal cation associated with it. Nucleophilic substitution reactions are commonly conducted in polar aprotic solvents as opposed to protic solvents. The reason for this is that the nucleophilicity of the nucleophile is highly dependent on solvent interactions.[39] Protic solvents will highly solvate the nucleophile, thereby reducing its ability to react with the activated carbon. In the absence of protic solvents the relative nucleophilicity of anions changes, presumably due to the removal of solvation effects.[40,41] Some common polar aprotic solvents are shown in Figure 1.1-4. These solvents not only reduce the solvation of the nucleophiles but also can enhance the nucleophilicity of the nucleophile by strongly solvating the cations associated with the nucleophiles.[42]

N,N-Dimethylformamide
(DMF)

Dimethylacetamide
(DMAc)

Dimethylsulfoxide
(DMSO)

N-Methylpyrrolidinone
(NMP)

Sulfolane

Diphenylsulfone
(DPS)
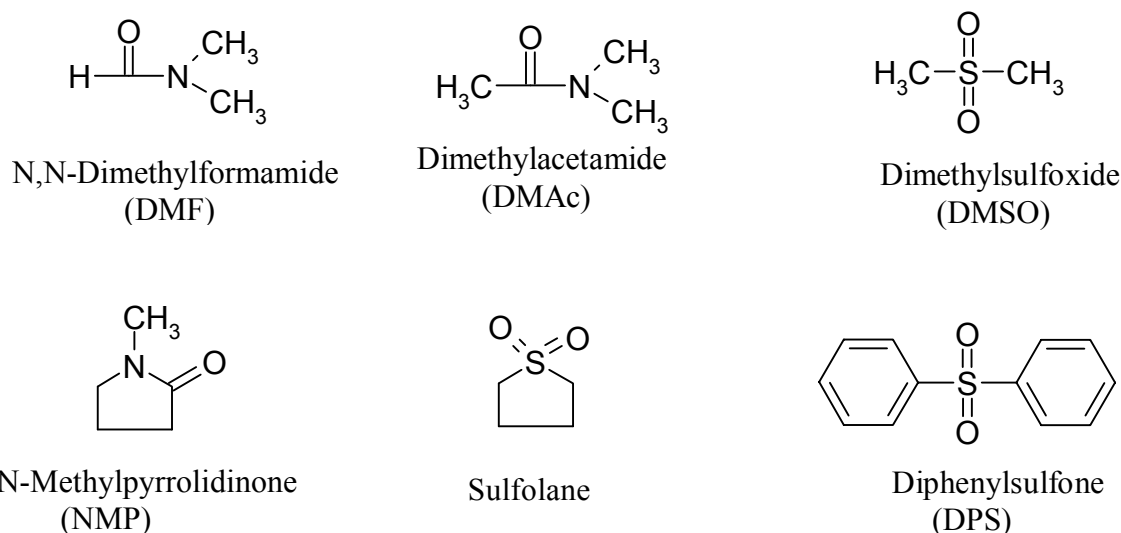
Figure 1.1-4: Examples of polar aprotic solvents.

CHAPTER I

INTRODUCTION

1.2 Polyaniline (PANI)
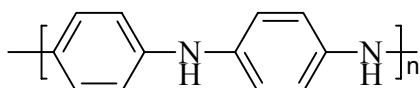
1.2.1 Synthesis, properties and structure of polyaniline

Polyaniline (PANI) has attracted considerable attention since MacDiarmid et al.[43] reinvestigated this material as a conducting polymer due to its simple synthesis, good environmental stability, and adequate level of electrical conductivity. Polyaniline is unique among conducting polymers in that its electrical properties can be reversibly controlled, both by charge-transfer doping and by protonation. The wide range of associated electrochemical and optical properties, coupled with good stability, make polyaniline potentially attractive for application as an electronic material. Recent work has shown that polyaniline prepared at room temperature is of fairly low molecular weight[44] and contains defect sites.[45] It is hoped that better-quality polyaniline, with fewer defect sites and higher molecular weight may lead to improvements in its mechanical and electrical properties.

Polyaniline can be synthesized by both electrochemical and chemical oxidative polymerization.[46] Considerable effort has been made to develop relationships between synthesis conditions and properties of polyaniline obtained by electrochemical polymerization.[47] By contrast, relatively little attention has been paid to the chemical polymerization of aniline due to its very complex and undefined structure.[48-50] Controlled polymerization of aniline at different reaction conditions using amonium peroxodisulfate as an oxidant was reported.[51] The course of this reaction was followed by determination of the yield of copolymerization, molecular weight and of its polydispersity in dependence on the reaction parameters. The influence of the reaction parameters on electrical conductivity and energy gap was determined.

7

The polyanilines can be considered as being derived from a polymer,[52] the base form of which has the generalized composition:
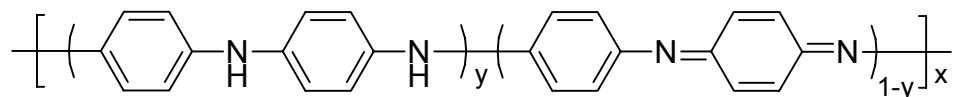
and which consists of alternating reduced,
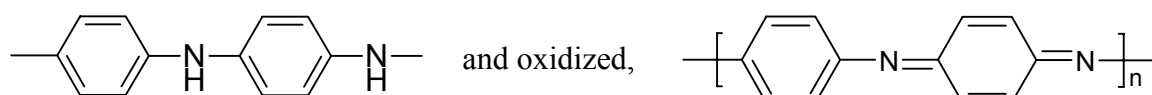
and oxidized,

repeating units.[53-55] The average oxidation state (1-y) can be varied continuously from zero to give the completely reduced polymer,
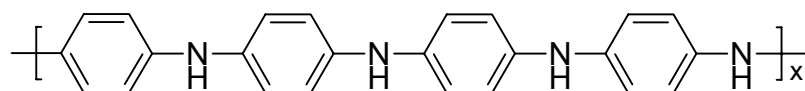
to 0.5 to give the "half-oxidized" polymer,
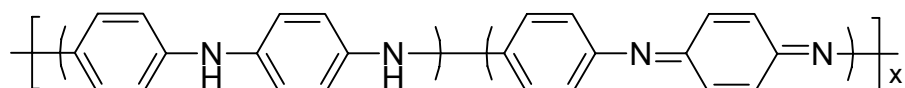
to one to give the completely oxidized polymer,
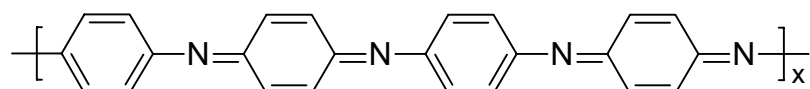
The terms "leucoemeraldine", "emeraldine", and "pernigraniline" refer to the different oxidation states of the polymer where (1-y)=0, 0.5, and 1, respectively, either in the base form, e.g. emeraldine base, or in the protonated salt form, e.g. emeraldine hydrochloride.[53-55] In principle, the imine nitrogen atoms can be protonated in whole or in part to give the corresponding salts, the degree of protonation of the polymeric base depending on its oxidation state and on the pH of the aqueous acid. Complete protonation of the imine nitrogen atoms in emeraldine base by aqueous HCl, for example, results in the formation of a delocalized polysemiquinone radical cation[53-56] and is accompanied by an increase in conductivity of $\sim 10^{10}$ S/cm.

The partly protonated emeraldine hydrochloride salt can be synthesized easily either by the chemical or electrochemical oxidative polymerization of aniline.[53-55] It can be deprotonated by aqueous ammonium hydroxide to give emeraldine base powder (a semiconductor).

Since the discovery in 1985 that doped polyaniline is capable of conducting electricity in the metallic regime,[43] research has focused on using this material in applications such as electrodes in lightweight batteries[57,58] and as flexible, hole-transport layers in electroluminescent devices.[59,60] Particularly appealing aspects of this material are the simple and inexpensive synthesis by chemical [61] or electrochemical [62-64] oxidation of aniline and the moisture and air stability of its conductive form.[43]

Although dominated by para-regiochemistry, it is likely that ortho-and meta-defects as well as biphenyl defects formed by C-C coupling occur uncontrollably during the synthesis of this material.[65] Furthermore, the derivatives of this material that can be formed by the aniline oxidation are limited. Derivatives with substituents on the aromatic rings have been prepared, [66-69] but these substituents create further structural ambiguity during the electrophilic polymerization because their directing properties may counteract the para-directing property of the amino group. Poly(m-aniline)[70-74] and oligomeric aniline derivatives with alternating meta-and para-regiochemistry have been presented recently as possible candidates for organic ferromagnetic applications. Derivatives of poly(m-aniline) have been synthesized by the copper-mediated Ullmann coupling.[70,74] However, these polymerizations are accompanied by the formation of insoluble fractions, which may have resulted from crosslinking.[71] The palladium-catalyzed amination of aryl halides and triflates,[75] an increasingly important method for the synthesis of arylamines in many applications,[76] holds great promise for the construction of the PANI framework. Polymerizations based on this reaction would be regiospecific and could afford access to modified polymers with otherwise inaccessible substituent patterns. Palladium catalysis has been used to prepare a number of arylamine polymers[77] and of the conductive p-PANI.[78]

1.2.2   The concept of doping.

Conjugated organic polymers are either electrical insulators or semiconductors. Those that can have their conductivity increased by several orders of magnitude from the semiconductor regime are generally referred to as `electronic polymers' and have become of very great scientific and technological importance since 1990 because of their use in light emitting diodes.[79,80] Trans-(CH)x and the emeraldine base form of polyaniline are used in Figure 1.2-1 to illustrate the increases in electrical conductivity of many orders of magnitude which can be obtained by doping.

Conductivity increases with increased doping
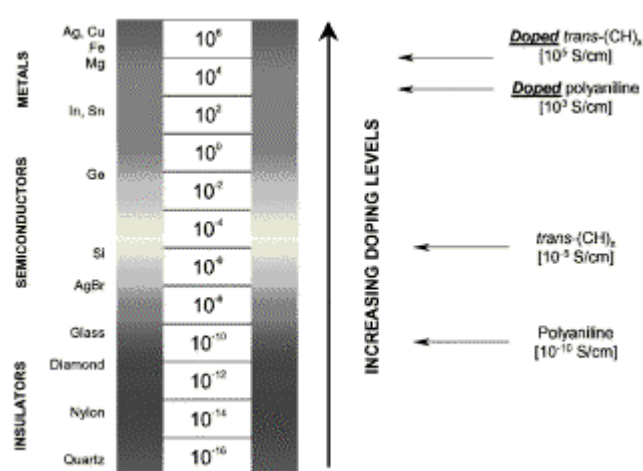
Figure 1.2-1: Conductivity of electronic polymers.

Prior to the discovery of the novel protonic acid doping of polyaniline, during which the number of electrons associated with the polymer chain remain unchanged,[81] the doping of all conducting polymers had previously been accomplished by redox doping. This involves the partial addition (reduction) or removal (oxidation) of electrons to or from the-system of the polymer backbone.[82-84]

The concept of doping is the unique theme which distinguishes conducting polymers from all other types of polymers.[85,86] During the doping process, an organic polymer, either an insulator or semiconductor having a small conductivity, typically in the range from 10^{-10} to 10^{-5} S/cm, is converted to a polymer which is in the `metallic' conducting regime (~ 1–10^4 S/cm). The controlled addition of known, usually small ($\leq 10\ \%$) non-stoichiometric quantities of chemical species results in dramatic changes in the electronic, electrical, magnetic, optical, and structural properties of the polymer. Doping is reversible to produce the original polymer with little or no degradation of the polymer backbone. Both doping and undoping processes, involving dopant counterions which stabilize the doped state, may be carried out chemically

or electrochemically.[84] Transitory doping by methods which introduce no dopant ions are also known.[87]

1.2.3 Electronic polyaniline fibers

By using a previously observed method for producing polyaniline fibers[88] highly-conducting sulfuric acid-doped polyaniline fibers have been prepared[89] (diameters: average, 139 nm; maximum, 275 nm; minimum, 96 nm) by placing a ~20 wt. % solution of polyaniline in 98 % sulfuric acid in a glass pipette with the tip ~3 cm above the surface of a copper cathode immersed in pure water at 5000 V potential difference. The fibers collect in or on the surface of the water. The conductivity of a single fiber was ~0.1 S/cm, as expected since partial fiber de-doping occurred in the water cathode. The diameter and length of the fibers appear (Figure 1.2-2) to be sensitive to the nature of the polyaniline used. No great difficulty is foreseen in producing fibers <100 nm diameter.
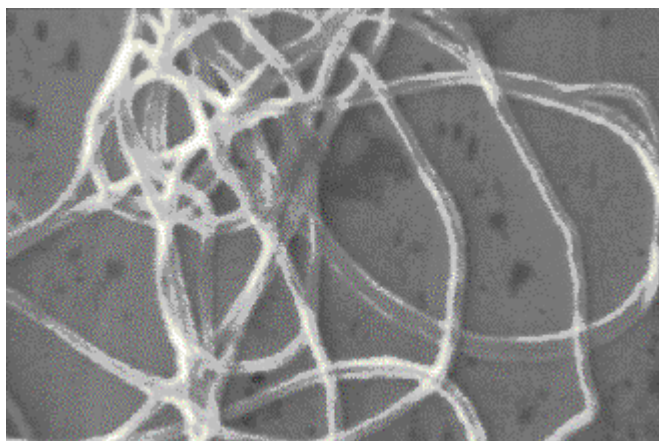
Figure 1.2-2: The 100 % polyaniline fiber with an average diameter of 139 nm.

CHAPTER I

INTRODUCTION

Poly(arylene amide)s (PAAs)

1.3.1 Structure and properties of poly(arylene amide)s (PAAs)

Aromatic polyamides consisting of aromatic rings and amide linkages are an important class of high-performance polymers.[90,91] These polymers have excellent thermal and mechanical properties mainly due to the high stiffness of the chains and strong hydrogen bonding.[92] However, the above structural characteristics make aromatic polyamides difficult to process as they exhibit poor solubility in organic solvents and high softening or melting temperatures.[93, 94] Since the beginning of their development aromatic polyamides, called „aramides", have reached many end uses. Amongst glass-, carbon- and polyethylene fibers aramid fibers are most established in high-performance composites. Their specific properties make them attractive reinforcements for polymeric composites used in aircraft and space industry, in sporting goods and numerous other applications.

In 1961 DuPont marketed the Nomex aramid fiber. It is made from poly(m-phenyleneisophthalamide) (Figure 1.3-1) and has excellent thermal and flame-resistant properties. Nomex fibers are used for example in honeycomb composite structures for aircraft flooring and in fire resistant clothing.
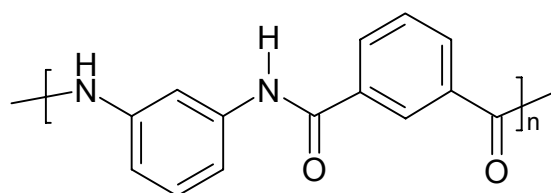
Figure 1.3-1: poly(m-phenyleneisophthalamide).

Fibers based on poly(p-phenyleneterephthalamid) (Figure 1.3-2) were commercialized in 1972 by DuPont with the trade name Kevlar.
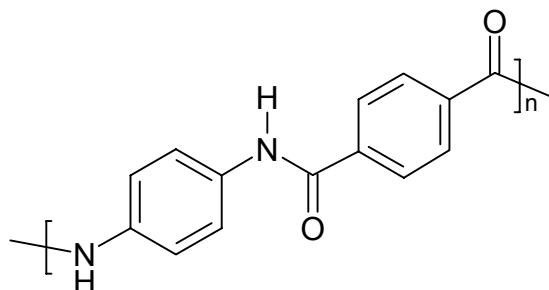
Figure 1.3-2: poly(p-phenyleneterephthalamide).

The polymer chains are orientated in a highly crystalline state and are fixed by hydrogen bonds as shown in Figure 1.3-3. In addition to their thermal stability they exhibit high tensile strength and modulus in combination with low density. Kevlar fibers have found many end uses in advanced composites, bulletproof clothing, in tires, ropes and cables. The performance of a composite material does not only depend on the applied fiber or matrix resin but also of the fiber-matrix adhesion. Aramid fibers have a very smooth and chemically inert surface and therefore the fiber-matrix adhesion in most cases is very poor.
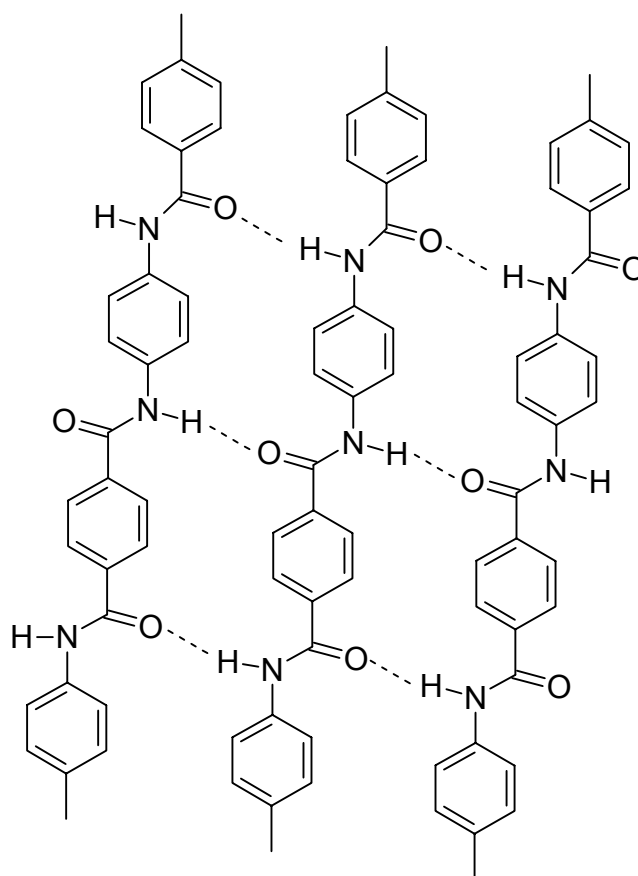
Figure 1.3-3: Hydrogen bonds in a highly crystalline state.

1.3.2 Synthesis of poly(arylene amide)s (PAAs)

Polyamides have been synthesized using low-temperature polycondensation and direct solution polycondensation.[90,95] Two principal types of low-temperature polycondensation processes[96-99] are described separately: two-phase (interfacial) polycondensation and direct low-temperature polycondensation.

The two-phase process is involved with the reaction of diacid chlorides and diamines in water-immiscible solvents of low polarity and high yields polyamides of low molecular weight due to rapid precipitation. For example, low-temperature interfacial polycondensation between terephthaloyl chloride and 1,4-phenylene diamine gave a fully aromatic

oligoamide.[100] Wholly or partially water-miscible solvents were found suitable for the synthesis of aromatic polyamides.[98-102] The disadvantages were that the polymers obtained all had a broad molecular weight distribution, making them unsuitable for fibers or films.[90] Low-temperature solution polycondensation is a convenient method for the synthesis of polyamides.[98] It involves low-temperature reaction of diacid chlorides and diamines in amide type solvents. The concentrated polymer solution thus obtained could be used for wet spinning of fibers or casting films. The solvating power of many organic solvents was increased greatly by the addition of lithium chlorides, resulting in an increase of the aggregate size. Low-temperature solution polycondensation of diamines with 4,4`-azobenzoyl diacid chloride in N,N-dimethylacetamide (DMAc) gave azopolymides with higher yield and viscosity than those prepared by interfacial polycondensation.[103]

In direct polycondensation of aromatic dicarboxylic acids and aromatic diamines, aryl phosphites are used in the presence of pyridine.[90,104] Since 1975 the phosphorylation polycondensation reaction was reported,[31] this reaction has been applied extensively to polyamide synthesis because of its convenience. This technique employs triphenyl phosphite (TPP) and pyridine as condensing agents to synthesize polyamides directly from aromatic diamines and aromatic or aliphatic dicarboxylic acids, and the reaction proceeds through N-phosphonium salts of pyridine (Scheme 1.3-1).[105] This synthetic approach proved to be more efficient and convenient compared to the acid chloride route.[106,107] The phosphorylation reaction has been extended successfully to the synthesis of high molecular poly(amide imide)s from imide-containing dicarboxylic acids and aromatic diamines.[108-113]

$$P(OC_6H_5)_3 + R`COOH \xrightarrow{\text{Pyridine}}$$

$$R``NH_2 \longrightarrow R`CONHR`` + C_6H_5OH + HO\text{-}P(OC_6H_5)_2$$
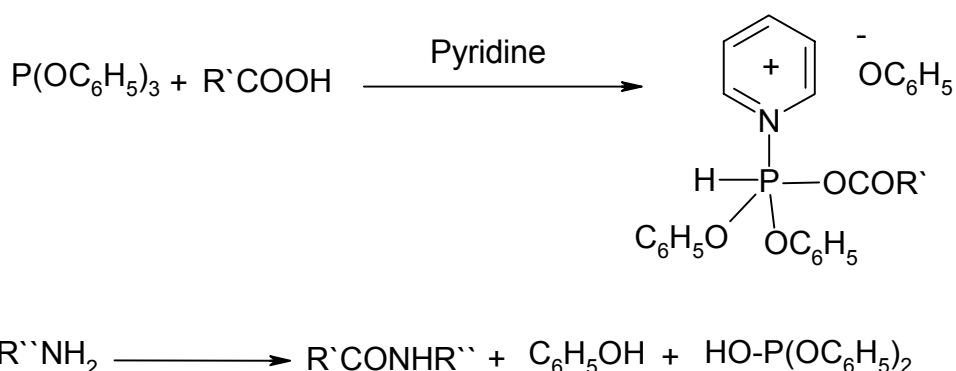
Scheme 1.3-1: Generalized polyamide synthesis using triphenyl phosphite (TPP) and pyridine as condensing agents.

Direct polycondensation of aromatic dicarboxylic acids and diamines in the presence of phosphorus oxychloride proceeded *via* bifunctional cyclic phosphoric-carboxylic anhydride gave an amide (Scheme 1.3-2).[96]
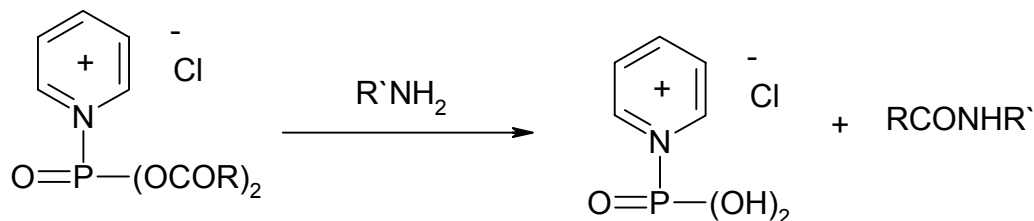
Scheme 1.3-2: Generalized polyamide synthesis using an N-phosphonium salts of pyridine.

1.3.3 Structural modification of poly(arylene amide)s (PAAs)

However, polyamides have the common problem of being difficult to process owing to their infusibility and poor solubility in organic solvents. The reasons are strong interchain forces, inherent macromolecular rigidity or semicrystallinity. Therefore, much effort has been made to develop structurally modified polymers having increased solubility, in order to improve their processability while maintaining the good thermal stability. The solubility of the polymers is often increased when flexible bonds, large pendent groups or polar substituents are incorporated into the polymer chain. The introduction of pendent bulky groups along the polymer backbone results in a less ordered polymer matrix increasing the solubility characteristics without affecting thermal and mechanical properties to any great extent.[114-117]

Modified aromatic polyamides bearing pendent N-benzylidene,[118] phthalimide,[114] benzoxazole, or benzothiazole,[119] amide[120] (Scheme 1.3-3) and ester[121] groups which exhibited an enhanced solubility in common organic solvents and higher thermal stability than the corresponding unsubstituted polyamides were reported.
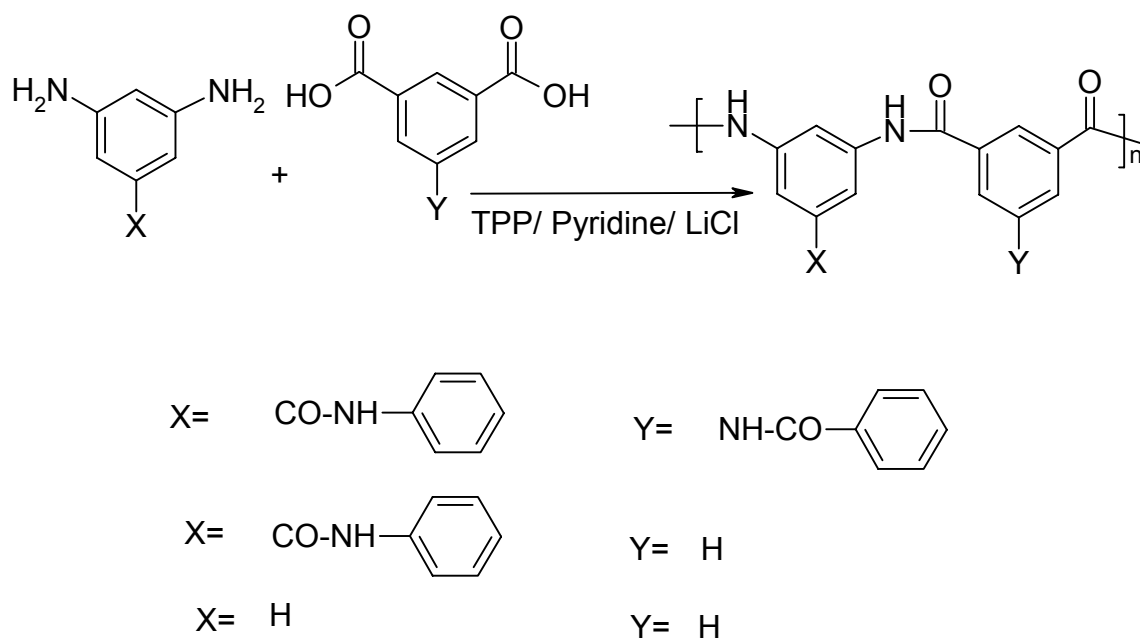
Scheme 1.3-3: Modified aromatic polyamides bearing pendent aromatic amide.

The reported studies suggest that the incorporation of bulky pendent group 5-(4-acetoxy-benzamide) into the backbone of polyamides results in polymers with enhanced solubility and processability as well as satisfactory thermal stability.[122-124]

Recently, by introducing acetoxybenzamide groups pendent to the aromatic polyamide chain together with oxadiazole or cyano-substituted benzene rings in the main chain, polymers with substantially increased solubility where obtained which could be processed into thin flexible films by casting their solutions. These polyamides show good thermal stability, reasonable high glass transition temperature and strong mechanical properties (Scheme 1.3-4).[125]
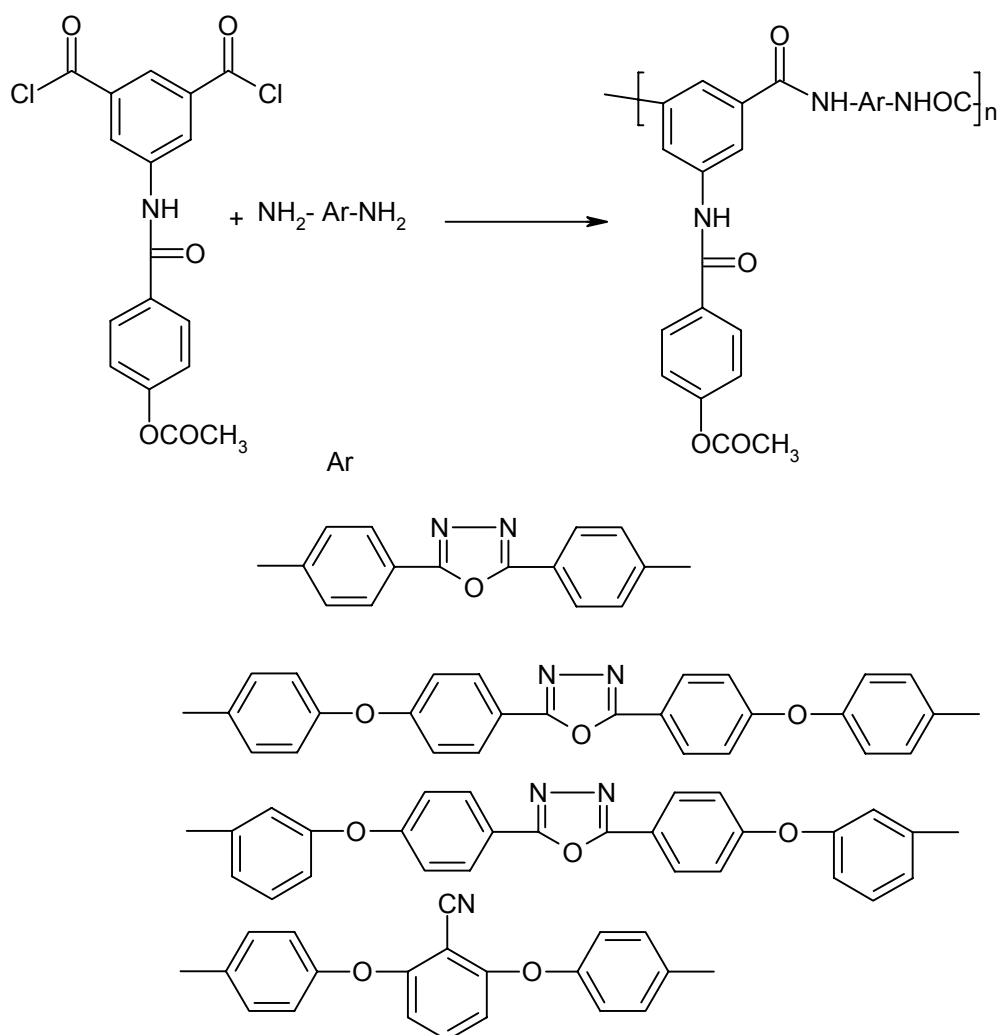
Scheme 1.3-4: Synthesis of aromatic polyamides containing oxadiazole or cyano-substituted benzene rings in the main chain with acetoxybenzamide groups.

The introduction of flexible ether linkages into the rigid polymer backbones is known to be an effective means to enhance the solubility and processability of these rigid polymers while minimizing the deterioration of their physical properties. The generation of an ether linkage as a polymer forming reaction has been intensively utilized in the synthesis of poly(arylene ether)s that are generally prepared by the step-growth condensation of activated aryl halides or nitro compounds containing phenoxide groups.[126] Most of the poly(arylene ether) syntheses employ halide, particularly fluoride, as a leaving group. The nitro group is not frequently used because of the generation of reactive nitrite ions that cause side reactions at elevated temperature.[127] However, nitro displacement reactions have been successfully utilized for the synthesis of poly(ether imide),[127d,128a] poly(ether nitrile),[128a] poly(ether

oxadiazole),[128b] poly(arylene ether ketone)s,[128c,d] and poly(biphenylene oxide)s.[128e,f] The synthesis of poly(arylene ether amide)s and similar copolymers has been reported previously, but in these cases conventional halide displacement at high reaction temperature has been observed.[129] Recently, synthesis of poly(arylene ether amide)s containing trifluoromethyl groups utilizing the nucleophilic nitro displacement reaction of AB-type monomers under mild conditions were reported.[130] In step-growth polymerizations, AB-type monomers have an inherent stoichiometric balance of the functional groups, and structure regularity of the corresponding polymers is higher than that of polymers obtained from A-A- and B-B-type monomers. The trifluoromethyl group was selected as a second functional group because it is known as an effective activating group for nitro displacement without side reactions.[128c,131] Trifluoromethyl groups in monomers exert not only an activation effect on a leaving group but also a bulky substituent effect on the polymer main chains, resulting in improved solubility (Scheme 1.3-5).[130]
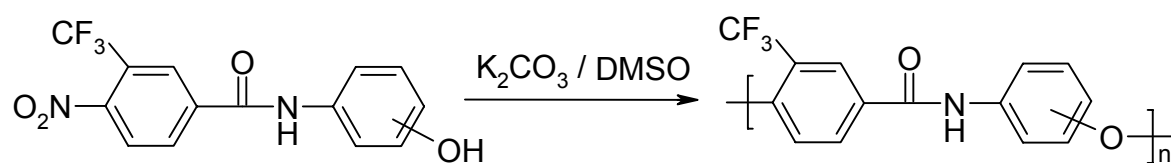
Scheme 1.3-5: The nucleophilic nitro displacement reaction to synthesis of poly(arylene ether amide)s containing trifluoromethyl groups under mild conditions.

CHAPTER I

INTRODUCTION

1.4 Palladium-catalyzed arylene amination

1.4.1 Introduction

The synthesis of compounds containing the N-aryl moiety has attracted a great deal of interest recently due to the importance of such compounds in fields as diverse as natural products,[132] photography,[133] and materials.[134] Although a number of traditional methods exist for aryl C-N- bond construction,[135-147] they typically suffer from problems such as limited generality, harsh conditions, the need to employ stoichiometric quantities of valuable reagents, numerous synthetic steps, or regiochemical ambiguities. From the standpoint of directness and atom-economy, a transition metal-catalyzed approach to C–N-bond construction is appealing because it entails simply the cross-coupling of an amine with an aryl halide. In the past few years, Buchwald's group at MIT[148-164] and Hartwig's group at Yale[165-171] have progressively and independently contributed to the development of a general, reliable, and practical methodology for the formation of aromatic carbon-nitrogen bonds. It is the purpose of this introduction to review the types of products that are now accessible using palladium-catalyzed the C–N-bond forming method. We will describe the optimal conditions now used in the preparation of tertiary amines, secondary amines, primary amines (anilines), as well as the special cases of intramolecular cyclizations. These procedures are built upon many ground-breaking studies of others which, for reasons of space, cannot be covered thoroughly in this introduction.

The reader is therefore referred to the original literature for the mechanistic insights that were gleaned from these earlier reports, and to account articles from both the Buchwald[172] and Hartwig[173] groups that chronicle the progression of exciting developments that ultimately brought C–N bond forming technology to its present state.

1.4.2 Background and outline

The first procedure for the Pd-catalyzed N-arylation reaction was provided by Migita and co-workers in 1983.[174] In this report, they showed that aryl bromides reacted with N,N-diethylaminotributyltin to afford the corresponding N,N-diethylanilines, as well as tri-n-butyltin bromide as the stoichiometric by-product (Scheme 1.4-1). A severe limitation of this protocol was that it was not readily extendable to other amine types since amino stannanes are typically not commercially available, and are both thermally and moisture sensitive.

$$n\text{-Bu}_3\text{SnNEt}_2 + \text{PhBr} \xrightarrow[\text{toluene, 100 °C, 3 h}]{\text{PdCl}_2(o\text{-tolyl}_3\text{P})_2 \ (1 \text{ mol \% Pd})} \text{PhNEt}_2 + n\text{-Bu}_3\text{SnBr}$$

81 %
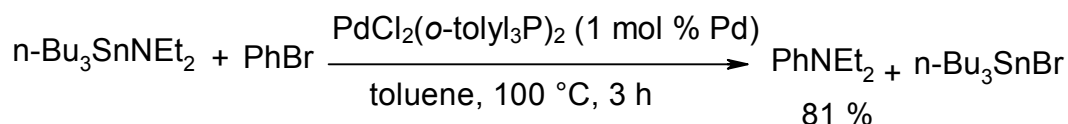
Scheme 1.4-1.

This problem was solved by Buchwald and Guram in 1994,[148] who exploited the ability of N,N-diethylaminostannane to undergo transamination reactions.[175] Aminotin compounds which they were able to prepare in-situ were found to undergo cross-coupling reactions with a variety of aryl bromides (Scheme 1.4-2).
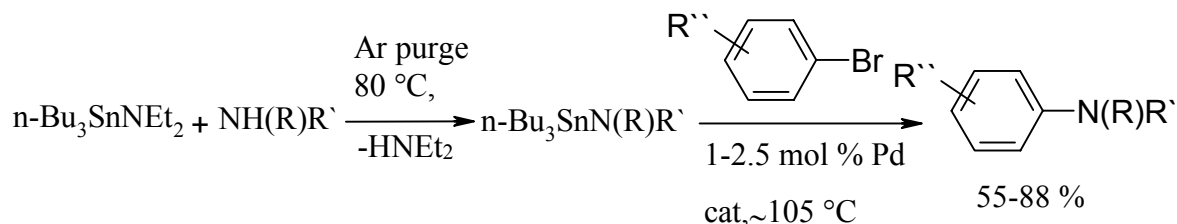
Scheme 1.4-2.

Despite the increased generality of this protocol relative to the Migita procedure, it was still undesirable that stoichiometric amounts of tin were required.

Amination of aryl bromides under tin-free conditions was achieved nearly simultaneously by both the Buchwald[149] and Hartwig[166] groups. Using P(o-tolyl)$_3$ as ligand, a palladium catalyst, and an appropriate base, most commonly NaOt-Bu, they were able to cross-couple a variety of different amines and aryl bromides (Scheme 1.4-3). Although this method has expanded greatly over the past few years, now encompassing a variety of other nitrogen-containing species and other aryl `halides' (bromides, iodides, chlorides, and sulfonates), the basic features of this catalytic cycle are operative in all of these transformations.

Pd(dba)$_2$ / 2 P(o-tolyl)$_3$

or PdCl$_2$(o-tolyl$_3$P)$_2$

R``⟨benzene⟩—Br + NH(R)R` → R``⟨benzene⟩—N(R)R`

NaOt-Bu, toluene
65 or 100 °C

67-89 %
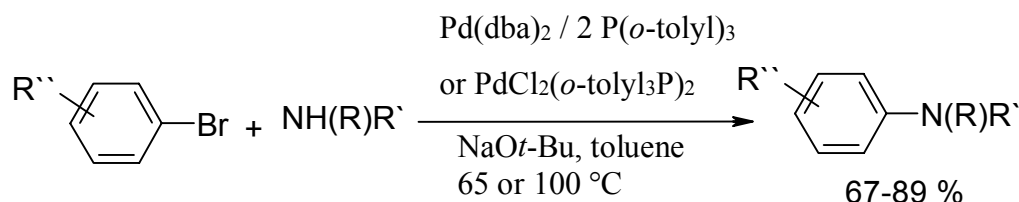
Scheme 1.4-3.

1.4.3 N-Arylation of secondary amines

1.4.3.1 Cross-coupling of amines with aryl bromides

Although in some cases monodentate ligands such as P(o-tol)$_3$ were suitable ligands for the cross-coupling of N-methyl(aryl) or N-methyl(alkyl) amines with aryl bromides,[149] chelating bidentate phosphine ligands were more often preferable,[151] typically providing less of the reduced arene side-product. For instance, N-methylaniline was N-arylated with 2-bromoanisole in the absence of solvent in 75 % yield using tris(dibenzylideneacetone)dipalladium(0) (Pd$_2$(dba)$_3$) and 2,2`-bis(diphenylphosphino)-1,1`-binaphthyl (BINAP)[176,177] as ligand, while the same reaction with P(o-tolyl)$_3$ in toluene did not afford the desired product (Scheme 1.4-4).

Pd$_2$(dba)$_3$ (0.5 mol % Pd)

BINAP or P(o-tolyl)$_3$

(0.75 mol %)

NaOt-Bu
80 °C, 29 h

⟨2-OMe-phenyl⟩—Br + MeNH—⟨phenyl⟩ → ⟨2-OMe-phenyl⟩—N(Me)—⟨phenyl⟩

BINAP   75 %

P(o-tolyl)$_3$ 0 %

(in toluene)
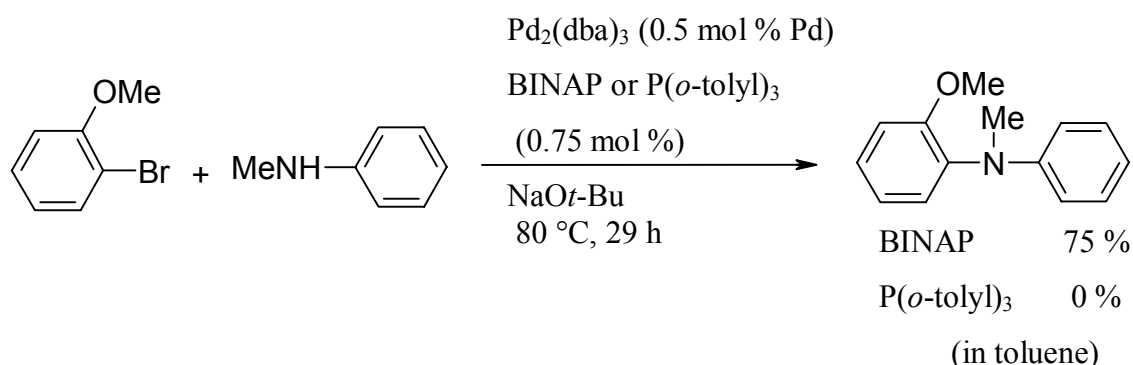
Scheme 1.4-4.

Similarly, N-arylation of N-methylaniline with 2-bromo-p-xylene using BINAP as ligand afforded the corresponding tertiary amine in 79 % yield, whereas the same reaction with P(o-tolyl)$_3$ as ligand proceeded in only 5 % yield (Scheme 1.4-5).

Pd$_2$(dba)$_3$ (2 mol % Pd)

BINAP or P(o-tolyl)$_3$ (3 mol %)

NaOt-Bu

toluene, 80 °C, 4 h

⟨dimethylphenyl⟩—Br + MeNH—⟨phenyl⟩ → ⟨dimethylphenyl⟩—N(Me)—⟨phenyl⟩

BINAP   79 %

P(o-tolyl)$_3$ 5 %
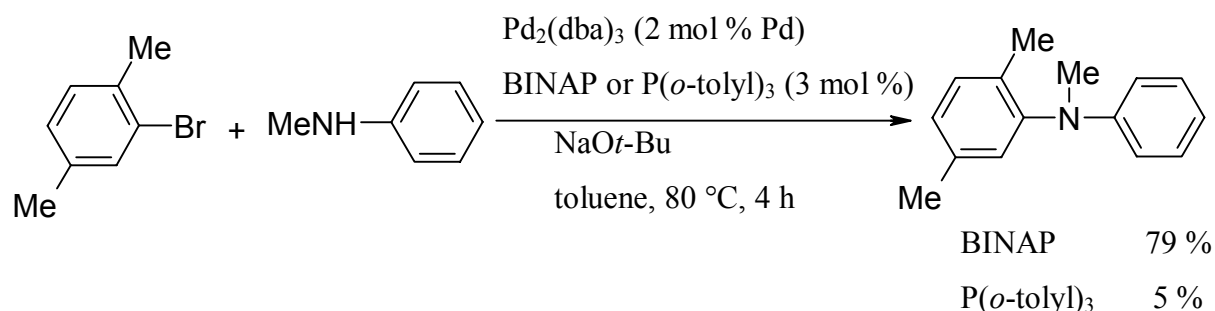
Scheme 1.4-5.

Concurrent with Buchwald's group investigations into the uses of BINAP as ligand, Hartwig and co-workers found that 1,1`-bis{(diphenylphosphino)ferrocene)}dichloropalladium (II) ((DPPF)PdCl$_2$) also constitutes an effective catalyst system for the amination of a secondary amine[167] although its utility in this context was demonstrated only in a cross-coupling reaction with a p-substituted electron-deficient aryl bromide (Scheme 1.4-6).
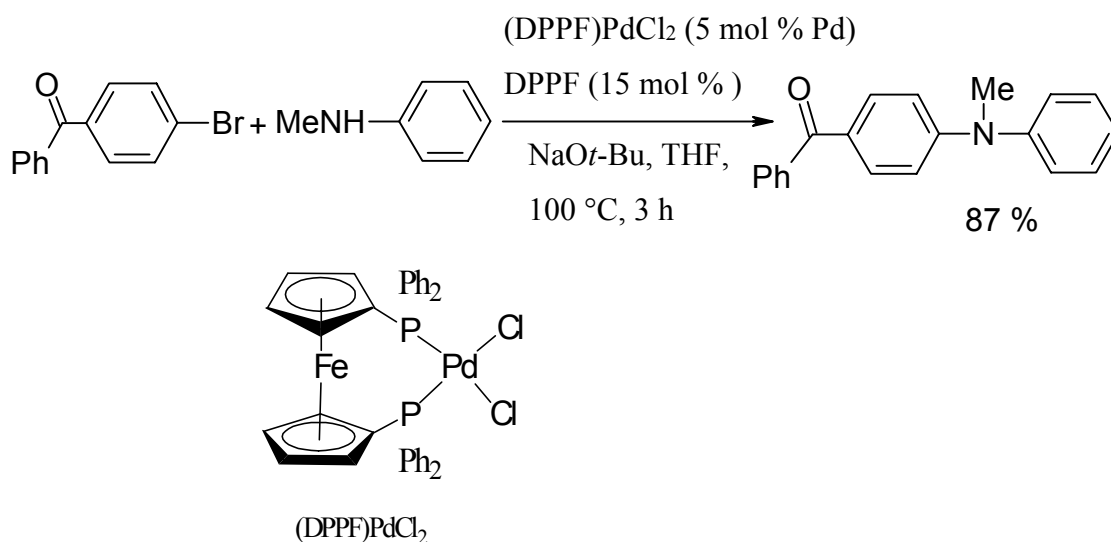
Scheme 1.4-6.

It is nevertheless worth noting that although BINAP was found to be superior to P(o-tolyl)$_3$ in these instances, in some cases cross-coupling reactions with BINAP as ligand still formed significant quantities of reduced arene side products. This was particularly problematic when acyclic (alkyl) aryl secondary amines (with groups larger than methyl) and/or electron-rich aryl bromides are employed, as well as in the cross-coupling reactions of acyclic dialkylamines.

The benefits associated with the use of chelating ligands should not detract from the role of monodentate phosphine ligands in synthetic applications of C–N-bond-forming methodol. In particular, bulky electron-rich monophosphine ligands have not only found considerable application in synthetic organic chemistry, but they are also in some instances the most efficient and active ligands. Yamamoto, Nishiyama, and Koie have disclosed an efficient method for the preparation of triarylamines from the Pd-catalyzed N-arylation of diarylamines.[178] Using P(t-Bu)$_3$ as ligand for the Pd-catalyst, they report that N-(3-methylphenyl)diphenylamine is prepared in 99 % yield from bromobenzene and N-(3-methylphenyl)aniline, whereas the use of BINAP as ligand resulted in an 18 % yield, and employing P(o-tolyl)$_3$ furnished only a 5 % yield of product (Scheme 1.4-7).

Pd(OAc)$_2$ (0.025 mol % Pd)

Ligand (0.1 mol %)

NaOt-Bu, O-xylene,

120 °C, 3 h

GC yield:

P(t-Bu)$_3$ 99 %

BINAP   18 %

P(o-tolyl)$_3$ 5 %
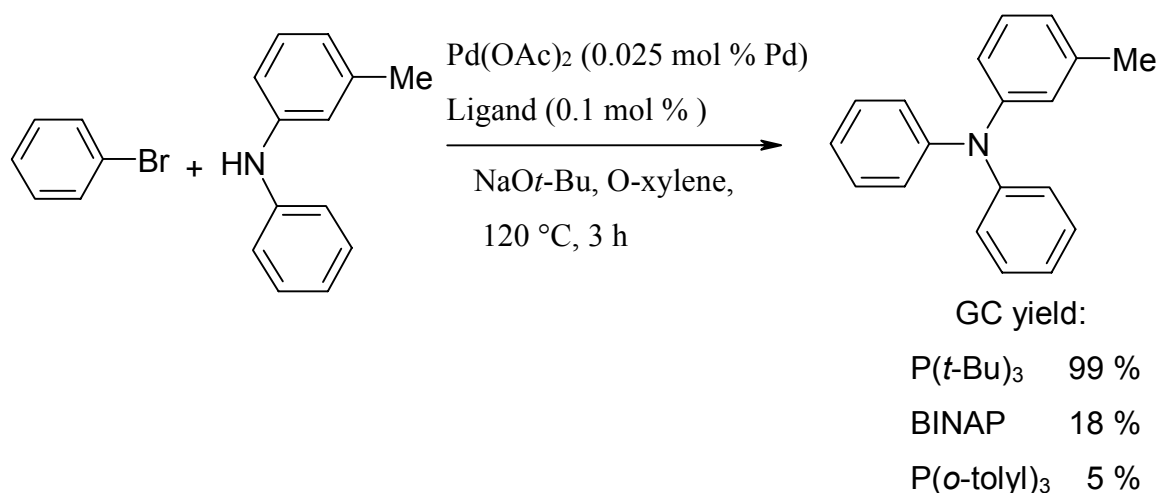
Scheme 1.4-7.

1.4.3.2 Cross-coupling of amines with aryl chlorides

Using a protocol resembling that developed for the amination of aryl bromides, it was found that aryl chlorides were less reactive than aryl bromides in Pd-catalyzed aminations, thus neither P(o-tolyl)$_3$ nor BINAP were effective ligands for the amination of aryl chlorides.

Using P(t-Bu)$_3$ as ligand, Yamamoto, Nishiyama, and Koie have prepared triarylamines via a Pd-catalyzed coupling of a diarylamine with chlorobenzene using NaOt-Bu as base, without any other additives (Scheme 1.4-8).[178]

Pd(OAc)$_2$ (0.025 mol % Pd)

P(t-Bu)$_3$, (0.10 mol %)

NaOt-Bu, o-xylene,

130 °C, 3 h

GC yield

99 %
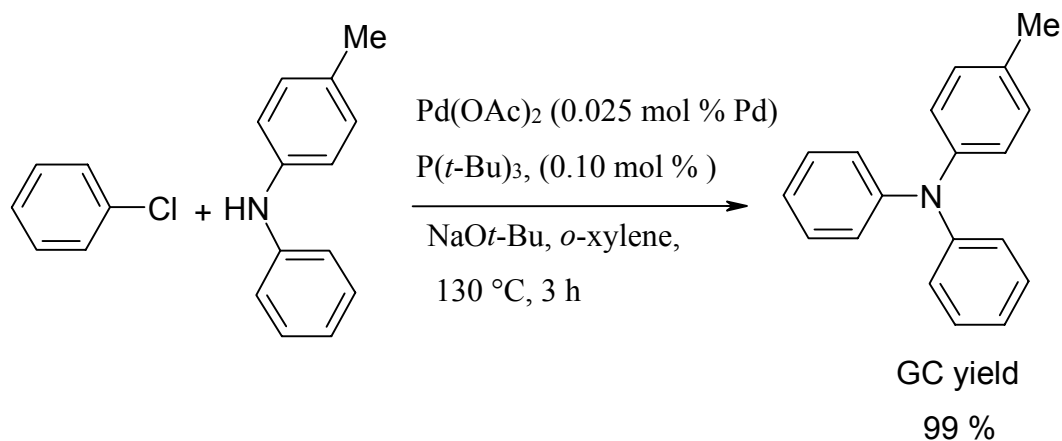
Scheme 1.4-8.

It should be noted that compared to the analogous reaction using bromobenzene, this reaction did require higher temperatures, higher concentration of halide, and more halide (130 °C, 8.0 M, two equivalents vs. 100 °C, 0.7 M, one equivalent). With the electron-rich ligand tricyclohexylphosphine, Reddy and Tanaka noted that the cross-couplings of N-methylaniline with 4-chlorobenzonitrile proceeded in good yield at 120 °C without additives (e.g. LiBr), using NaOt-Bu as base (Scheme 1.4-9).[179]
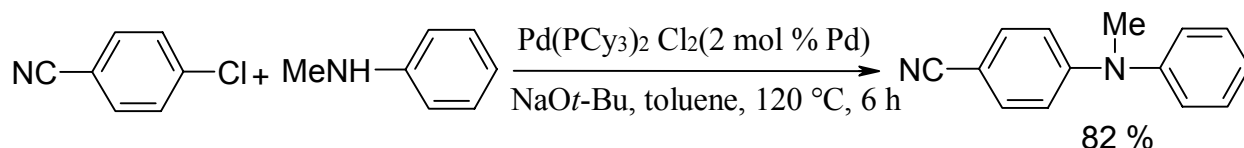
Scheme 1.4-9.

1.4.3.3. Cross-couplings of amines with aryl triflates

Using conditions similar to those developed for the amination of aryl bromides, Buchwald's group and Hartwig's group found that good yields could be obtained utilizing electronically neutral or electron-rich aryl triflates.[157,168] Electron-deficient aryl triflates in general gave low product yields, due to NaOt-Bu-induced cleavage of the aryl triflate, with subsequent liberation of the corresponding sodium phenoxide (Scheme 1.4-10).
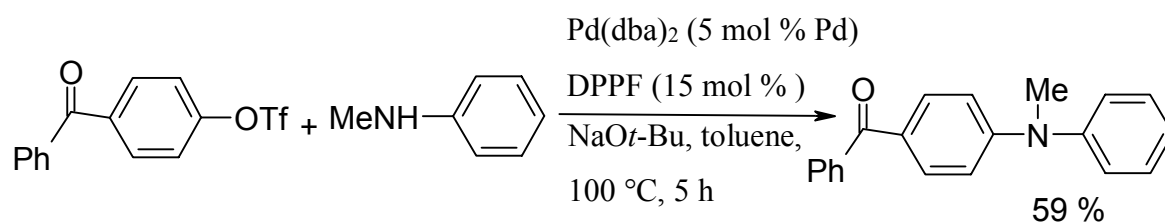
Scheme 1.4-10.

Use of BINAP/Cs$_2$CO$_3$ with electron-rich aryl triflates afforded cross-coupled products in high yields (Scheme 1.4-11).
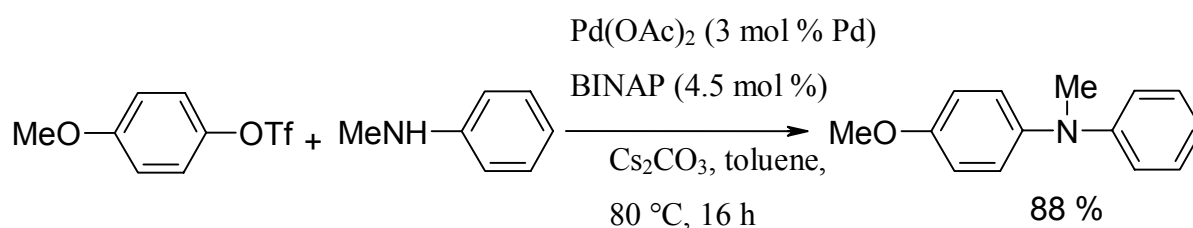
Scheme 1.4-11.

1.4.4. N-Arylation of primary amines

1.4.4.1 Cross-coupling of primary anilines with aryl bromides and iodides

An interest in the synthesis of oligoanilines were an inspiration for Buchwald's group to develop Pd-catalyzed couplings of primary anilines with aryl bromides. Using standard conditions [Pd$_2$(dba)$_3$ and BINAP], they found that anilines were effectively coupled with a variety of aryl bromides.[151] Reactions of electron-poor aromatic halides and electron-rich amines give the highest yields in the amination protocol (Scheme 1.4-12).[180]
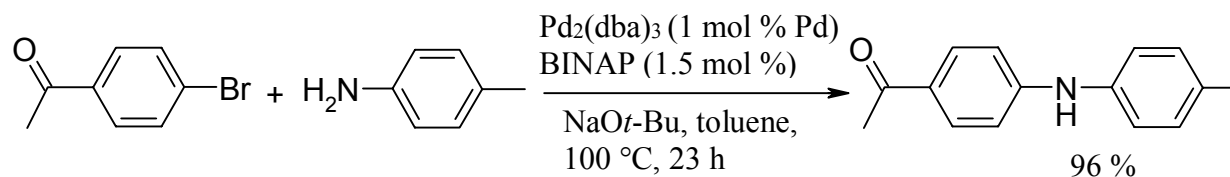
Scheme 1.4-112.

Similarly, Hartwig and co-workers have demonstrated the utility of (DPPF)PdCl$_2$-catalyzed reactions of aryl bromides and iodides with anilines (Scheme 1.4-13).[167]
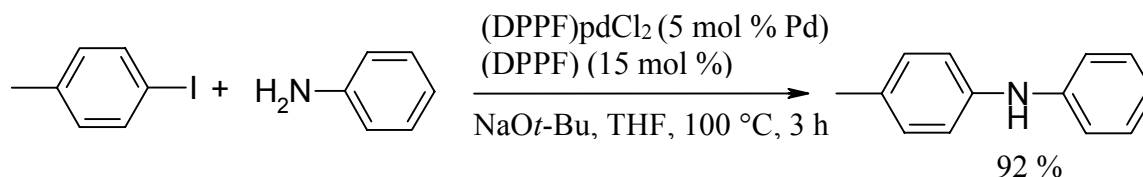
Scheme 1.4-13.

During a search for inexpensive ligands we investigated the use of bis[2-(diphenylphosphino)phenyl]ether (DPEphos). This ligand, reported by van Leeuwen et al.[181] is easily prepared from diphenyl ether by double lithiation, followed by trapping with chlorodiphenylphosphine. In a comparative study, DPEphos, BINAP, and DPPF were combined with Pd(OAc)$_2$, and the resulting systems were tested for their effectiveness in catalyzing the N-arylation of primary anilines. DPEphos was found to be as good BINAP in the cases studied, and as good as or superior to DPPF (Scheme 1.4-14).[164]
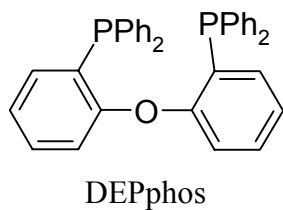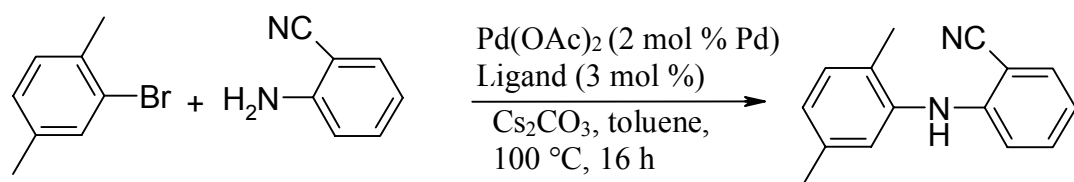
Scheme 1.4-14.

Ligand	yield
DEPphos	87 %
BINAP	82 %
DPPF	20 %

1.4.4.1.1 Catalytic cycle of Pd-amination of aryl bromides with primary amines

The catalytic cycle for this process is similar to that postulated for many palladium-catalyzed C-C-bond-forming processes (Scheme 1.4-15).[182] Mixing BINAP with Pd$_2$(dba)$_3$ initially leads to the formation of the isolable complex (BINAP)Pd(dba) (**2**).[183] This complex probably undergoes dissociation of a dba-ligand prior to oxidative addition of the aryl bromide to form the isolable oxidative addition complex **3**. However, Amatore has shown that direct oxidative addition to (L-L)Pd(dba) is possible.[183] Coordination of the amine to **3**,[184] followed by deprotonation, would form amido complex **5**, which then undergoes reductive elimination to form the desired product and to regenerate the Pd(0) catalyst. It is also possible that the reaction proceeds *via* tert-butoxide complex **6** when NaO*t*-Bu is used as a base.[185]
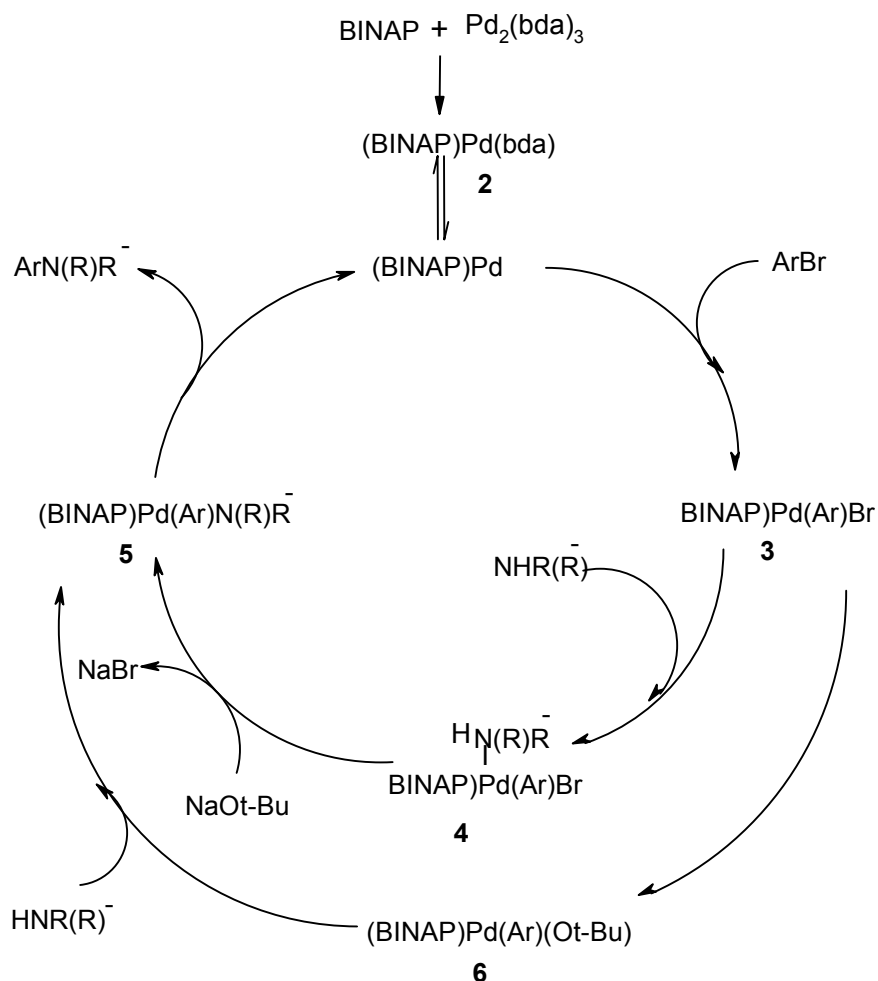
Scheme 1.4-15: Proposed Pd / BINAP-catalytic cycle of amination of aryl bromides with primary amines.

1.4.4.2 Cross-coupling of anilines with aryl chlorides

Aryl chlorides displayed the lower reactivity than ary bromides in Pd-catalyzed aminations. Since aryl iodides are often more expensive and less readily available than their aryl bromide counterparts and aryl chlorides are less reactive than aryl bromides in Pd-catalyzed aminations. This liability must be weighed against the greater availability and lower cost of aryl chlorides, therefore, aryl bromides are still the most widely used aryl halides in Pd-catalyzed aminations.

1.4.4.3 Cross-coupling of anilines with aryl sulfonates

Buchwald's group has shown that using standard conditions, [Pd(OAc)$_2$, BINAP, Cs$_2$CO$_3$ as base] primary anilines can be coupled with electron-poor triflates in high yields, even with substrates containing an enolizable ketone (Scheme 1.4-16).[160]
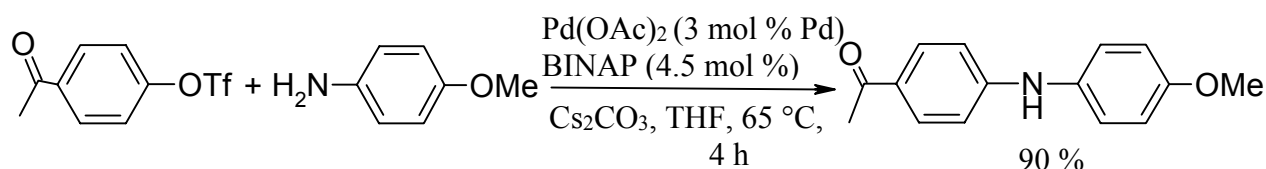
Scheme 1.4-16.

With NaOt-Bu as base, Hartwig and co-workers have demonstrated the utility of DPPF as ligand in cross-couplings of anilines with unactivated aryl triflates (Scheme 1.4-17).[168]
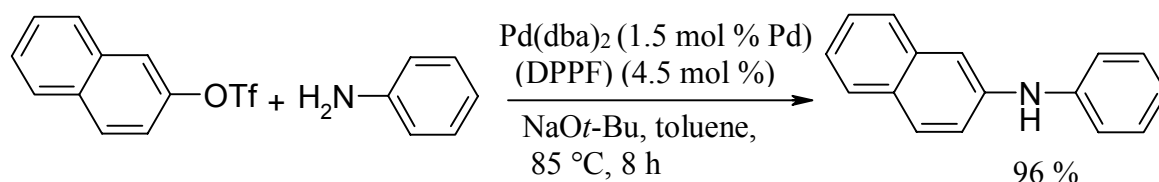
Scheme 1.4-17.

Hartwig and Hamann have since shown that even the less reactive tosylate functionality can participate in aniline coupling reactions. Using the ferrocenyl-derived ligand 4, they succeeded in the cross-coupling of aniline with the tosylate of 4-cyanophenol in 79 % yield (Scheme 1.4-18).[186]
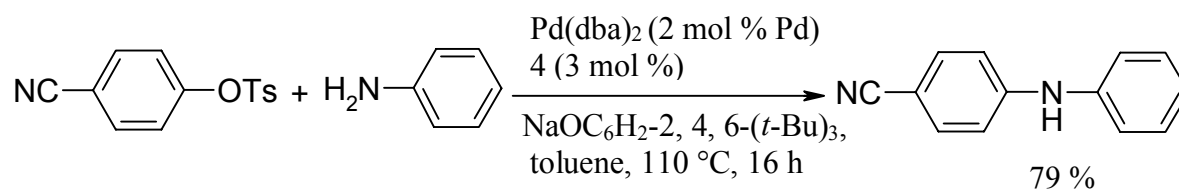
Scheme 1.4-18.

28

1.4.5 N-Arylation of ammonia surrogates

Benzophenone imine has been used extensively in Buchwald's group as a surrogate for ammonia in Pd-catalyzed aminations of aryl halides and aryl triflates. In addition to the practical feature that it is commercially available, it has also been found to impart high crystallinity to its derivatives, is stable to base and mild acid, yet can be cleaved under a variety of controlled conditions. They have found benzophenone imine to undergo the widest range of N-arylation reactions, wherein the use of Pd/BINAP conditions are suitable in reactions with aryl bromides, iodides, and triflates, as is shown below.[161] Upon completion of reaction, the benzophenone moiety of the coupled products can be cleaved by catalytic hydrogenation with ammonium formate using Pd/C,[187] or alternatively by treatment with wet HCl and wet THF[188] to liberate the corresponding primary aniline derivative (Scheme 1.4-19).
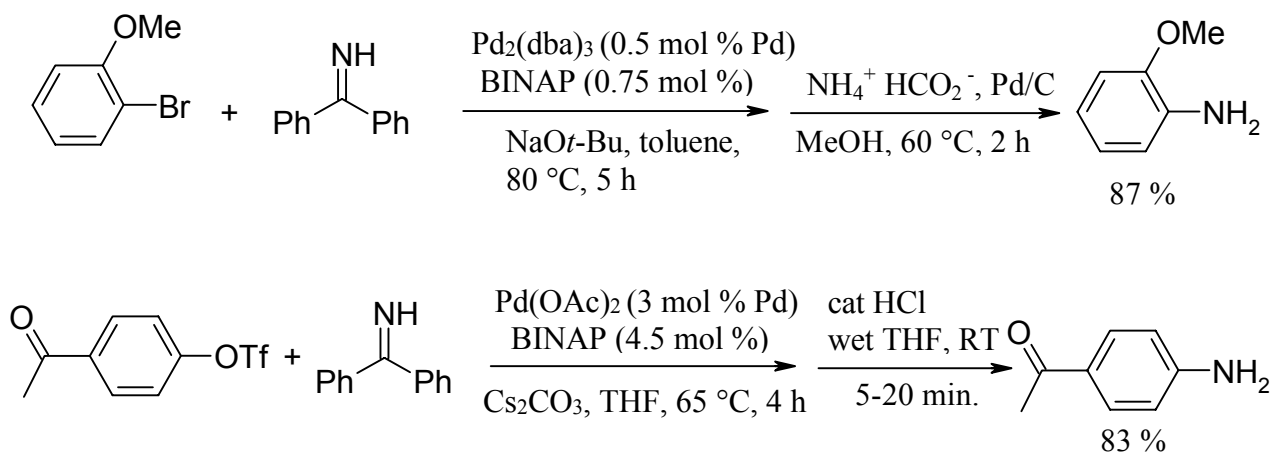
Scheme 1.4-19.

1.4. 6. N-Arylation of other nitrogen-containing substrates

Pyrroles, indoles, and carbazoles constitute a special class of nitrogenous bases. Under standard Pd-catalyzed N-arylation conditions, these compounds can be prepared in high yield using both electron-rich and electron-poor aryl bromides. However, the former requires long reaction times at high temperatures, and no examples of o-substituted aryl bromide substrates were reported (Scheme 1.4-20).[171]
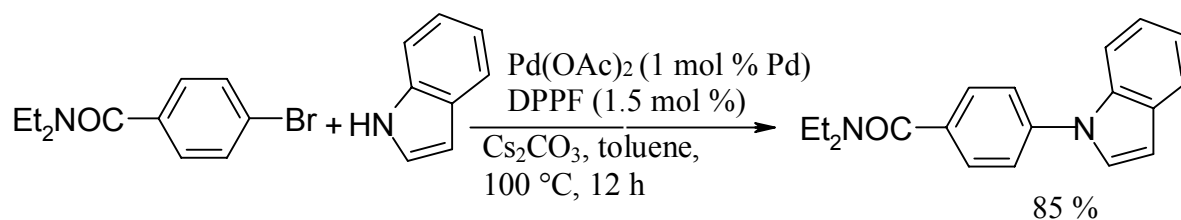
Scheme 1.4-20.

1.4.7. Intramolecular N-arylation reactions

Boger and co-workers were the first to disclose a palladium-mediated intramolecular closure of an amine onto an aryl bromide, although this reaction required stoichiometric quantities of palladium.[189-191] Buchwald's group was able to adapt that concept to intramolecular ring closures (Scheme 1.4-21).[154]

Pd$_2$(dba)$_3$ (1 mol % Pd)
NaO*t*-Bu/K$_2$CO$_3$, toluene,
65 °C, 2 h, 96 %

or

Pd(ph$_3$P)$_4$ (5 mol % Pd)
Et$_3$N, RT, 15 h, 87 %
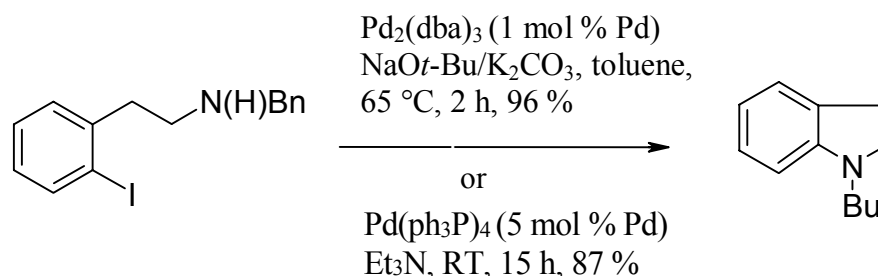
Scheme 1.4-21.

As in the case of intermolecular cyclizations, the Pd-catalyzed N-arylation reaction could be conducted in the absence of a main group metal. In this study, the aryl iodides were found to be better substrates than aryl bromides in the intramolecular cyclizations.[154] This is due to the fact that in the intramolecular cyclizations the deprotonation of nitrogen occures after the coordination to the metal in contrast to the intermolecular cyclizations.[154] It was noted that the ring closure could also be carried out at room temperature, using Et$_3$N as solvent (and also functioning as base).[154]

Though Buchwald's group attempts at conducting the intermolecular version were not successful, they have developed conditions for intramolecular amide cyclizations, as well as cyclizations of benzamides (to generate lactams) (Scheme 1.4-22).[150]

Pd$_2$(dba)$_3$ (10 mol % Pd)
P(*o*- tolyl)$_3$ (20 %)

K$_2$CO$_3$, toluene,
100 °C, 91 h,

82 %
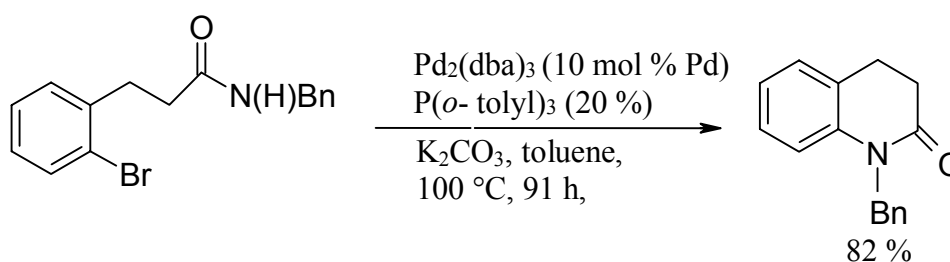
Scheme 1.4-22.

In summary, the Pd-catalyzed N-arylation reaction is a broadly useful method for the construction of a wide variety of substrates. Central to the development was the ongoing development of new ligand systems and the careful optimization of reaction conditions and reagents, supplemented by a sound mechanistic understanding of both organic and organometallic chemistry. It is anticipated that future studies will not only improve the scope and understanding of this process, but like the predecessors before[192-194] will lead to new applications of Pd-catalyzed cross-coupling reactions.

2-Motivation and objectives

2.1 Motivation

In view of the considerations formulated in the introduction, the catalytic amination reaction of arylene halides with primary amines using palladium complexes has become an important synthetic procedure for a variety of arylene amines including pharmaceuticals, electronic materials, and ligands for metal catalysts. The Pd-catalyzed aryl amination has also been applied to polycondensation reactions to give various polyamines and its related poly(iminoarylene)s with no or scarcely crosslinked structures.[195a-c]

Herein the idea is to use Pd-catalyzed aryl amination to synthesize new types of polymers. This approach has aimed at developing new conditions for Hartwig-Buchwald reactions[196a-o] and to apply them to obtain new polymer structures. It was expected that the polycondensation of different aromatic dihalides with primary aromatic diamines using the catalytic system generated from tris(dibenzylideneacetone)dipalladium (0) $Pd_2(dba)_3$ and 2,2´-bis(diphenylphosphino)-1,1´-binaphthyl (BINAP) (Figure 3.1-6) would produce soluble novel polymers. The use of inexpensive monomers with bromine or chlorine leaving groups instead of expensive fluorine containing monomers is, as has already been shown for PEEKKs (poly(ether ether ketone ketone)s), very attractive for obtaining aromatic polymers.[7] It was anticipated from the presence of both imino and carbonyl functions that the obtained PIKs would form intermolecular hydrogen bonds like KEVLAR and thus lead to good thermal and mechanical properties, essential requirements for a new class of high-performance polymers.[197] This approach was focused on synthesizing aromatic poly(imino ketone)s (PIKs) as possible new high-performance polymers. PIKs can be considered as being a hybrid structure of poly(arylene ether ketone)s (PEKs), polyaramides (PAAs) and polyaniline (PANI) (Figure 2.1-1).

Hydrogen bonding interactions are crucial in establishing a molecular network in solution and in the solid state. The presence of hydrogen bonding in a polymeric material significantly influences its characterization and structural properties. One of the more striking consequences of the formation of the hydrogen bonding appears in the vibrational spectrum. Therefore it was also the aim to record the hydrogen bonding interactions of the newly synthesized polymers by FT-IR and ^{1}H-NMR spectroscopy.

PEEKK

PANI

PAA

PIK
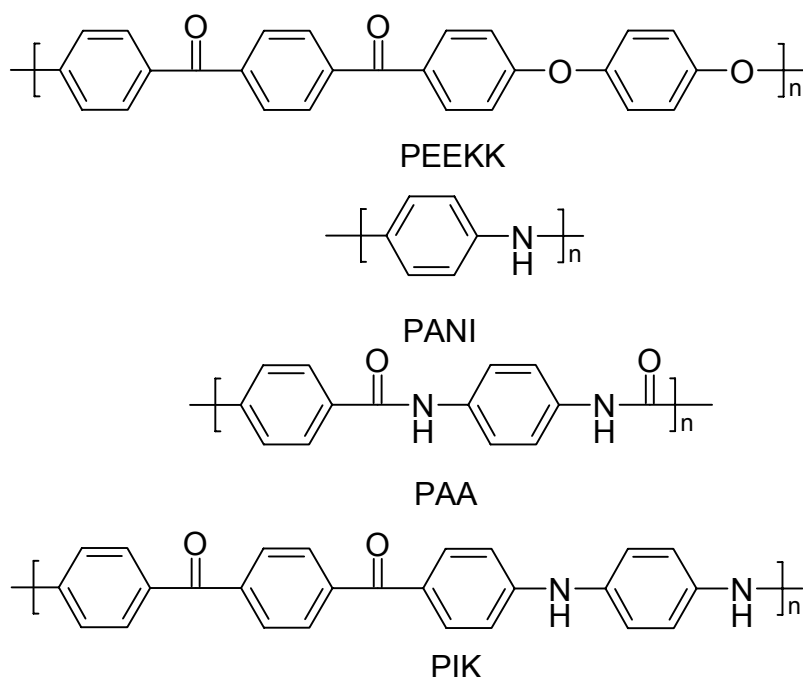
Figure 2.1-1: PIK as hybrid material of PEK, PANI and PAA.

There has been a tremendous growth of interest in the field of polymer containing chromophores since polymeric materials offer the attractive combinations of optical, structural and processing properties over simple organic materials. Therefore, our synthetic concept was extended to synthesize novel polymers containing chromophores such as acridine, azobenzenes, fluorenone and carbazole. There have been few reports on the preparation[288] and photoactivities[288c] of polymers containing the proflavine structure. For this reason, this thesis is aimed at synthesizing poly(imino acridine)s as new polymers containing acridine units in the main chain by palladium-catalyzed aryl amination of aryl dibromides with 3,6-diaminoacridine free base.

The azobenzene group is a well-known photosensitive chromophore, which undergoes photoinduced cis-trans isomerization. Owing to their photoactivities, polymers containing azobenzene units have attracted interest because of their potential uses in various photonic applications.[304] On the other hand, polymer syntheses using organotransition-metal complexes as catalysts are the subject of recent interest.[305] The azobenzene group in a polymer backbone increases the chain stiffness and imparts color to the polymer. Therefore the synthesis of new poly(imino azobenzene)s *via* diamine and dibromo compounds reaction has been performed.

2,7-Poly-(9-fluorenone) (2,7-PFO) has been introduced as a new electron-deficient polymer in which the withdrawing effect of the carbonyl groups lowers the reduction potential,[334] but there is still a pressing need for electron-deficient (n-type) conjugated polymers and there are only few reports of such polymers.[334,339] The idea was to synthesize

novel conjugated and non-conjugated PIFO polymers containing carbon-nitrogen linkages as electron-deficient polymers *via* palladium-catalyzed aryl amination.

Carbazole derivatives are widely used as hole-transporting materials between the emitting layer and the anode to balance the charge injection.[357] Carbazole units were incorporated into the polymer backbone to obtain new poly(imino carbazole)s PICs. These polymers were expected to have lower oxidation potentials, lower HOMO energy levels than those of carbazole-fluorene copolymer[361] and fluorene homopolymer,[361] i.e have a better hole-transporting (p-type) ability.

In spite of the strong interest in both quinones and n-type conducting polymers, poly(quinone)s serving as n-type conductors along the polymer main chains have received much less attention[198] presumably due to difficulty in preparing such poly(quinone)s by the usual methods e.g. organometallic dehalogenation polycondensation.[199,200]

Obviously, the carbonyl groups in the PIK polymers are good targets for nucleophilic addition. Here it was intended to transform PIKs into their corresponding poly(imino alcohol)s PIAlcos as an intermediate towards synthesizing poly(quinone diimine)s. PIAlcos containing di-tertiary alcohols were considered as new low band-gap polymer materials. This encouraged us to carry out the elimination reactions of the latter polymers to synthesize poly(quinone diimine)s (Scheme 2.1-2).
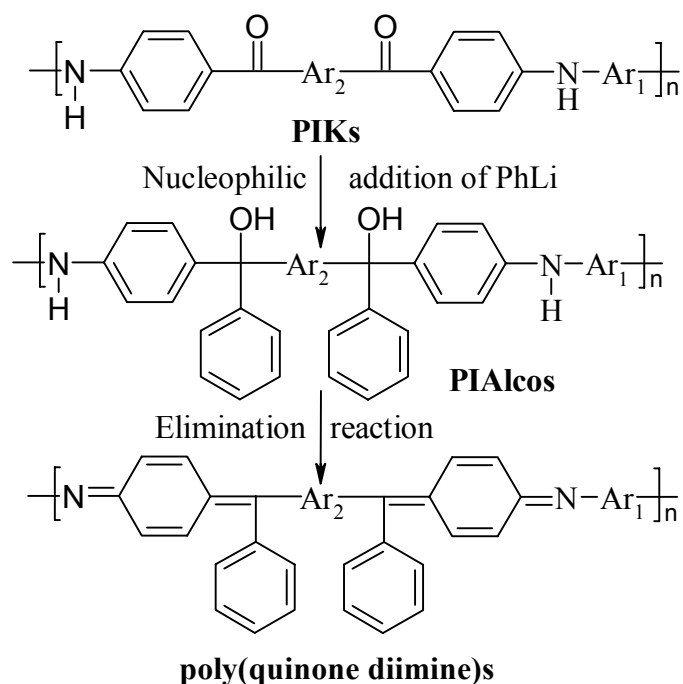
Scheme 2.1-2: From PEKs to poly(quinone diimine)s.

2.2 Objectives

➢ ***The main objective of this dissertation*** is to develop a synthetic route to synthesize novel soluble polymer catagories *via* palladium catalyzed amination polycondensation based on various bromo and various amine compounds. Developing new reaction conditions for the standard Hartwig-Buchwald reaction is the central part of the present work. The synthetic variables to be studied here are including reaction temperature and concentration, catalytic ligands, and the nature of the halogen containing monomers. The work is performed to synthesize the following new polymer materials:

  ➢ Poly(imino ketone)s (PIKs) as new high-performance polymers *via* palladium-
     catalyzed aryl amination

  ➢ Polymers containing an azobenzene group in the main chain by palladium-catalyzed
     polycondensation.

  ➢ Photoluminescent poly(imino carbazole)s (PICs).

  ➢ Poly(imino fluorenone)s (PIFOs).

  ➢ Photoluminescent polymers containing acridine group in the main chain by
     palladium-catalyzed polycondensation.

➢ Modification of PIKs was performed by grafting on the carbonyl groups to synthesize new poly(imino alcohol)s.

  Further, the approach includes:

  ➢ Study of protonation reaction of the ring nitrogen of PIAcs.

  ➢ Study of photoinduced and thermal cis-trans-isomerization.

  ➢ Study of protonation reaction of the azobenzene of polymers containing an
     azobenzene group in the main chain.

➢ The possible hydrogen bonding interactions were studied experimentally by FT-IR spectroscopy.

➢ The new synthetic polymers were characterized by different methods. Fourier transform infrared spectroscopy (FT-IR), nuclear magnetic resonance spectroscopy (NMR), elemental analysis, gel permeation chromatography (GPC), UV-vis absorption spectra, photoluminescence spectra (PL), intrinsic viscosity, thermogravimetric analysis (TGA), differential scanning calorimetry (DSC), wide-angle X-ray diffraction, dynamic mechanical analysis (DMA), dielectric spectroscopy, and cyclic voltammetry (CV) were utilized.

CHAPTER III

RESULTS AND DISCUSSION

Part 1

3.1 Poly(imino ketone)s (PIKs) as new high-performance polymers
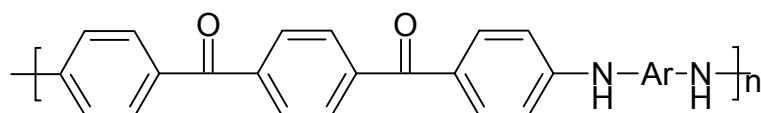
Synthesis of 1,4-bis(4-halobenzoyl)benzene as monomers:

1,4-Bis(4-chlorobenzoyl)benzene (**5**) and 1,4-bis(4-fluorobenzoyl)benzene (**6**) were synthesized by aromatic electrophilic substitution *via* Friedel-Crafts acyaltion of terephthaloyl chloride with chlorobenzene and fluorobenzene, respectively, in the presence of AlCl$_3$ as a catalyst according to literature procedures.[201-202] 1,4-Bis(4-bromobenzoyl)benzene (**7**) was synthesized according to a modified literature procedure (Scheme 3.1-1).[203]

In the aluminum chloride catalyzed Friedel-Crafts reaction the end products are frequently aromatic ketones. Since these may complex with the aluminum chloride there will be a competition for the latter between the products and the carbonyl-containing reactants. Thus, the complexing behavior of ketones may affect the course of the Friedel-Crafts reaction. In general, Friedel-Crafts acylation gives a 1:1 complex of AlCl$_3$ and the carbonyl group formed.[204-208] Therefore, an excess of AlCl$_3$ relative to the carbonyl groups formed should be used to catalyze the reaction.
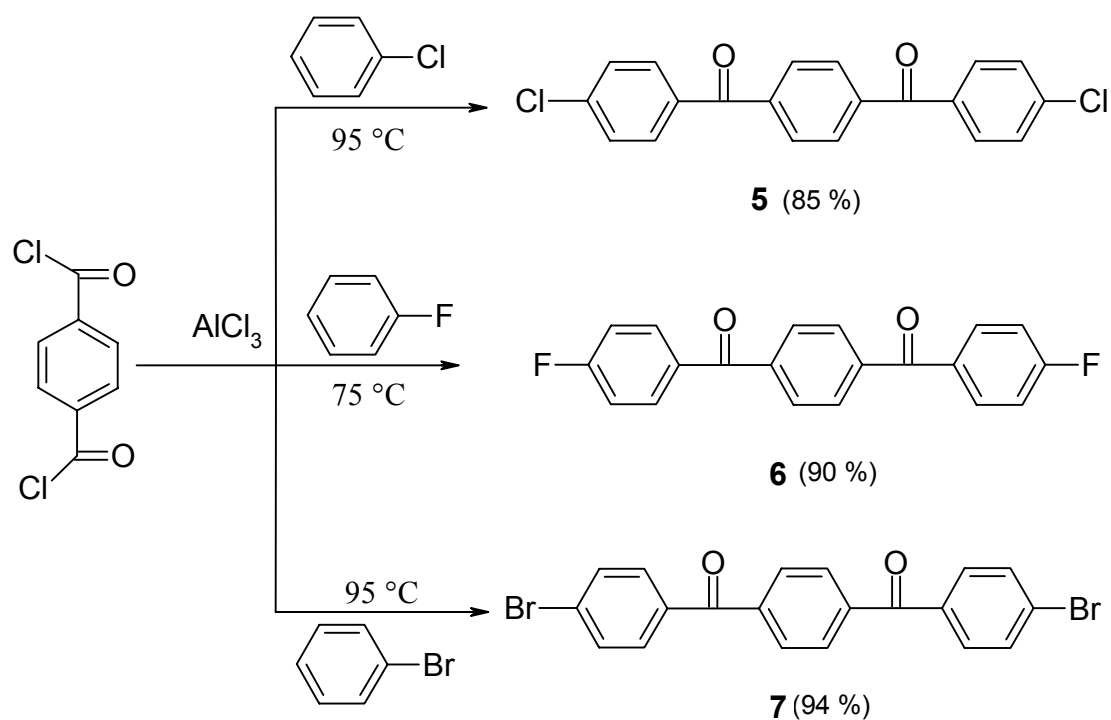
Scheme 3.1-1: Synthesis of 1,4-bis(4-halobenzoyl)benzene.

A similar Friedel-Craft acylation reaction was employed to synthesize 1,3-bis(4-bromobenzoyl -5- *tert*.-butyl)benzene (**9**) (Scheme 3.1-2).
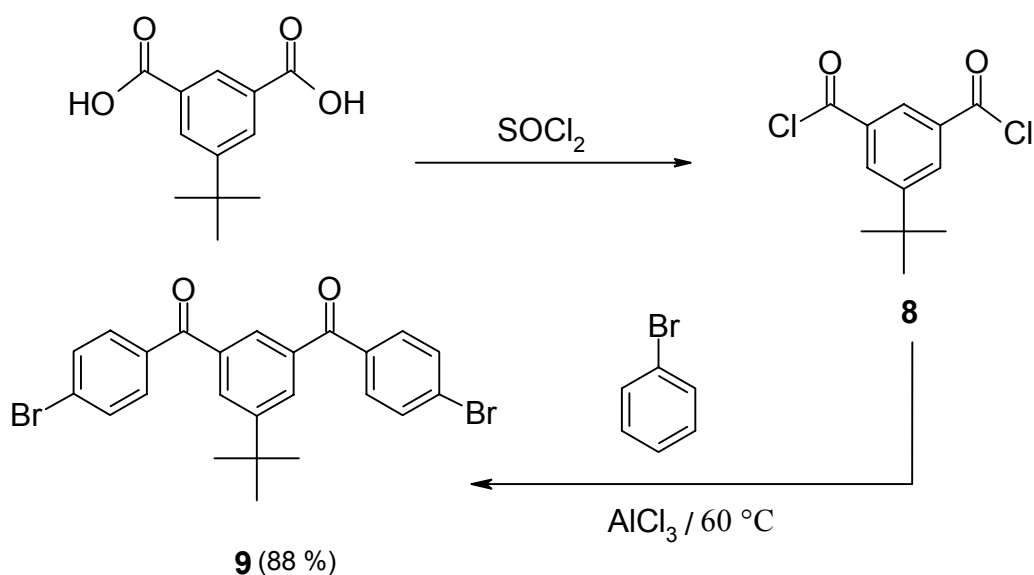
Scheme 3.1-2: Synthesis of 1,3-bis(4-bromobenzoyl -5- *tert*.-butyl)benzene.

The structures of these monomers **5**, **6**, **7**, and **9** were confirmed by their spectral and analytical data.

Synthesis of 4,4´-bis(4-anilinobenzoyl)benzene (10) as a model compound:

The accepted mechanism[196e] of the Pd-catalyzed amination involves oxidative addition of the aromatic halides to a palladium (0) species to form an arylene palladium (II) halide. By inductive effect or by resonance, this step should be favored for an arylene bromide substituted with an electron withdrawing group in the ortho-or para-position. To investigate the potential of the amination reaction for a polycondensation process, 4,4´-bis(4-anilinobenzoyl)benzene (**10**) was synthesized as a model compound by a palladium-catalyzed amination of 1,4-bis(4-bromobenzoyl)benzene (**7**) with aniline as a primary aromatic amine using NaO*t*-Bu as a base and BINAP (**1**) (Figure 3.1-6) as a ligand (Scheme 3.1-3).
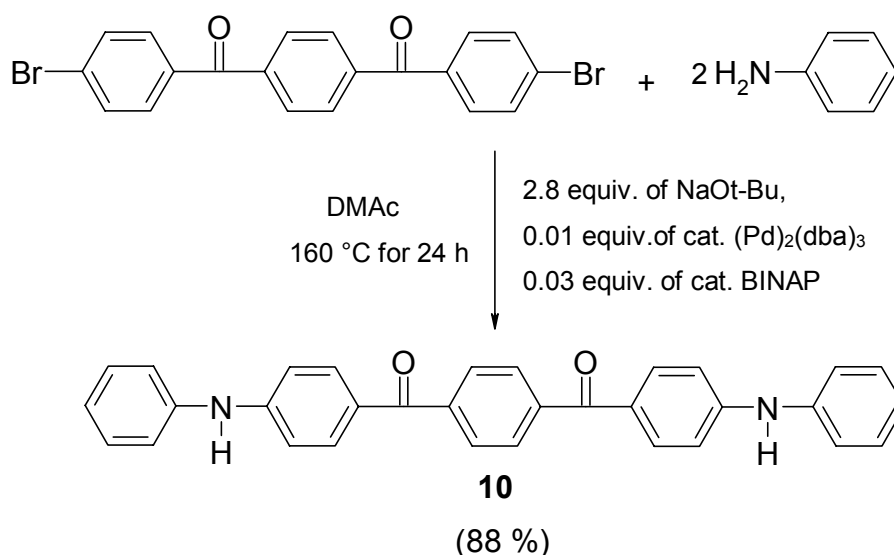
Scheme 3.1-3: Synthesis of model compound **10**.

The isolated yield was 88 % after column chromatography, while there were no minor undesired products detected by ^{1}H and ^{13}C-NMR spectroscopy, (FD[+]) mass spectra or thin-layer chromatography. The structure was confirmed by mass (FD[+]), ^{1}H and ^{13}C-NMR spectroscopy, FT-IR, U.V and elemental analysis and they all show an agreement with the proposed structure. ^{1}H and ^{13}C-NMR spectroscopic results are summarized in Table 3.1-1. In the ^{13}C-NMR spectrum of **10**, the resonance of the carbon of carbonyl group is strongly deshielded ^{13}C nuclei, therefore, it presents downfield while the other 10 carbons of the aromatic rings present upfield are in agreement with the predicted structure (**10**) (Figure 3.1-1).
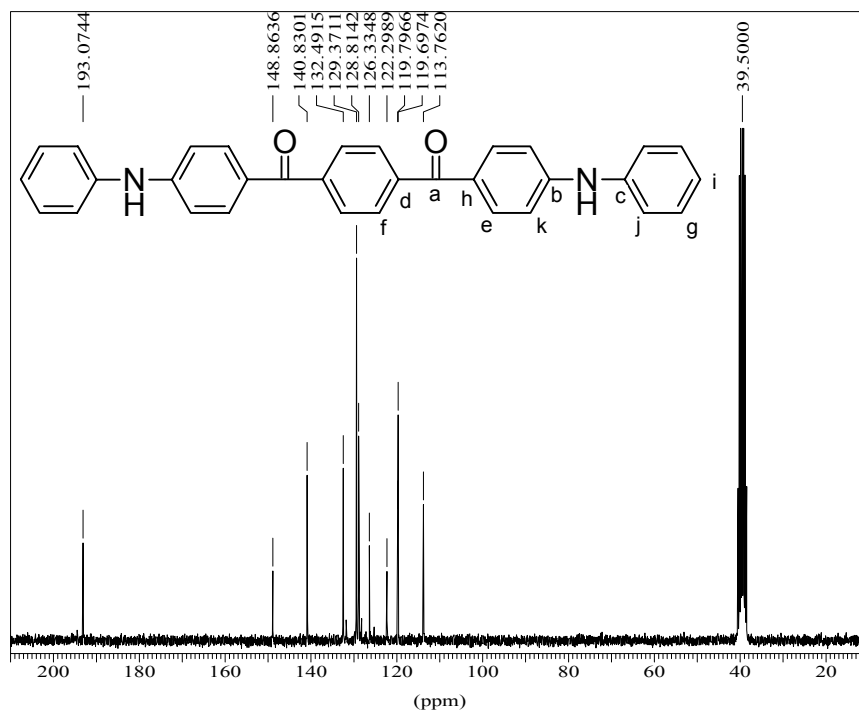
Figure 3.1-1: ^{13}C-NMR (62.5 MHz) spectrum of model compound **10** recorded in DMSO-d_6
at 293K (signal assignement in Table 3.1-1).

Table 3.1-1: ^{1}H-NMR (250 MHz) and ^{13}C-NMR (62.5 MHz) recorded in DMSO-d_6 at 293K
for 4,4´-bis(4-anilinobenzoyl)benzene (**10**).

^{1}H-NMR			^{13}C-NMR	
Proton	δ(ppm)	Coupling	C-Atom	δ(ppm)
NH	8.77	s	a	193.1
1	7.56	s	b	148.9
			c	140.8
2	7.50	d	d	132.5
3	7.13	t	e	129.4
4	7.03	d	f	128.8
			g	126.3
5	6.93	d	h	122.3
6	6.80	t	i	119.8
			j	119.7
			k	113.8

38

The UV-vis absorption spectrum of model compound **10** illustrates two broad absorption bands. The high energy band centered at 296 nm is assigned to the electronic $\pi{\rightarrow}\pi*$-transition of the aniline rings. A similar $\pi{\rightarrow}\pi*$-transition of the aniline rings was reported.[209] The low energy band centered at 368 nm is assigned to the electronic $n{\rightarrow}\pi*$-transition which is well-known for the carbonyl groups.[210] The latter band is not assumed to be the intramolecular charge-transfer (ICT) band because of the low wavelength (λ_{max} = 368 nm), and the high molar extinction coefficient (ε_{368} = 40 400 L. mol^{-1}. cm^{-1}) (Figure 3.1-2). However, ICT band of compound **20** (Part 6, p.147) was observed (λ_{max}= 600 nm, ε_{600}= 6 080 L. mol^{-1}. cm^{-1}) (Figure 3.6-11).
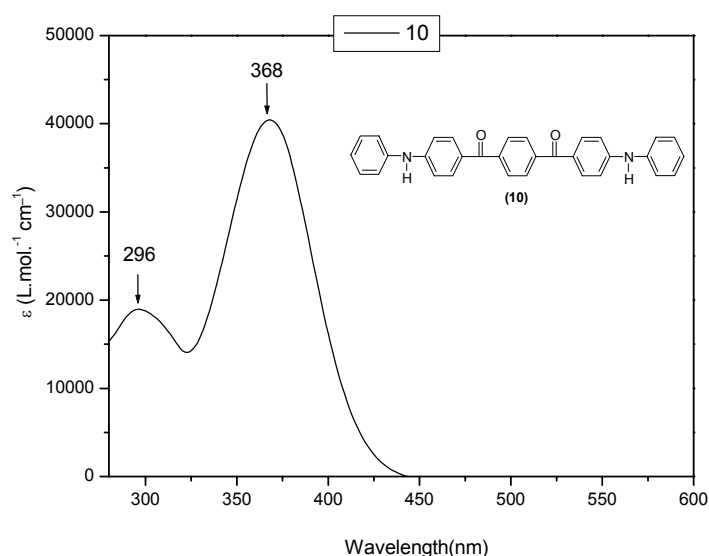
Figure 3.1-2: UV-vis absorption spectrum of model compound **10** (2 x 10^{-5} M in CHCl$_3$).

Synthesis of PIKs:

Reactions of electron-poor aromatic halides and electron-rich amines give the highest yields in the amination protocol.[211] Thus, one attempted the polycondensation of 1,4-bis(4-bromobenzoyl)benzene (**7**) and 1,3-bis(4-bromobenzoyl-5-*tert*.-butyl)benzene (**9**) as electron-poor arylene bromides with a series of electron-rich primary aromatic diamines. The results of the Pd-catalyzed polycondensation of these aromatic bromides with different aromatic diamines are listed in Table 3.1-2. Two methods were developed for the synthesis of poly(imino ketone)s (Scheme 3.1-4).

In both methods the combination of Pd$_2$(dba)$_3$ and BINAP was used as an efficient catalyst. In method (a) DMAc was empoyled as a solvent at a temperature of 100 °C for 4 h followed by 165 °C for 20 h. In method (b) diphenyl sulfone (DPS) was applied as a solvent at a temperature of 165 °C for 4 h, then 200 °C for 20 h and lithium chloride was added to
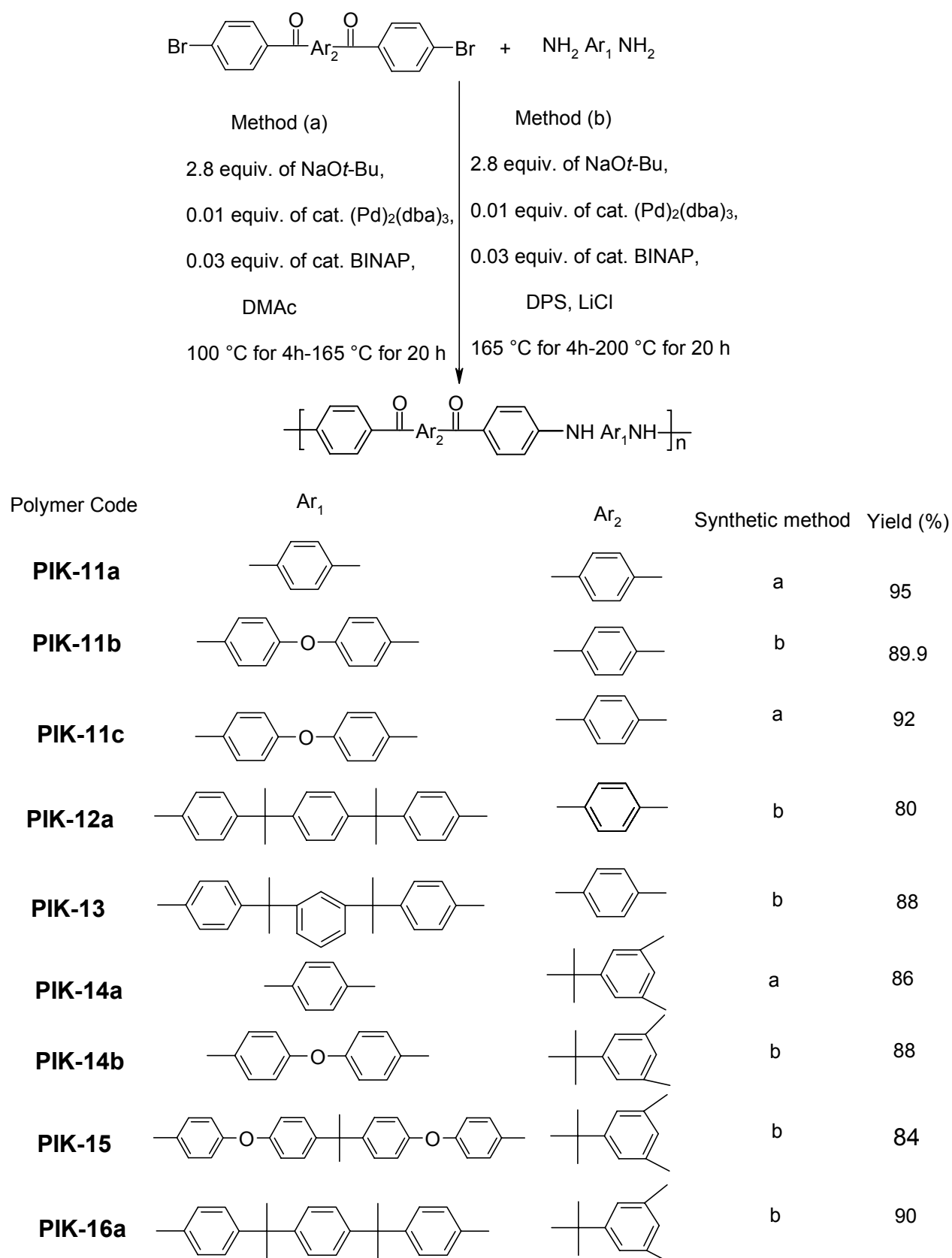
Scheme 3.1-4: Synthesis of poly(imino ketone)s (PIKs) (For molecular weight values see Table 3.1-3).

40

hinder intermolecular and intramolecular hydrogen bonding of the PIK products, and thus increase the solubility. The relative amounts of monomers and DPS were adjusted to maintain a solid content of 30-36 % during the polycondensation process. The reactions of the dibromo monomers **7** and **9** with the arylene diamines having electron donating substituents provided the corresponding PIKs in 80-95 % yields without undesired side products (work up method a or b).

Polymer solubility

When a low molecular weight solute such as sucrose is added to water, the dissolution process takes place immediately. The sugar molecules leave the crystal lattice progressively, disperse in water, and form a solution. But polymer molecules are rather different. They constitute long chains with a large number of segments, forming tightly folded coils which are even entangled to each other. Numerous cohesive and attractive both intra and intermolecular forces hold these coils together, such a dispersion, dipole-dipole interaction, induction, and hydrogen bonding (Figure 3.1-3a).

Based on these features, one may expect noticeable differences in the dissolution behavior shown by polymers. Due to their size, coiled shape, and the attraction forces between them, polymer molecules become dissolved quite slowly than low molecular weight molecules. Billmeyer Jr.[212] (1971) points out that there are two stages involved in this process: in the first place, the polymer swelling, and next the dissolution step itself. When a polymer is added to a given solvent, attraction as well as dispersion forces begin acting between its segments, according to their polarity, chemical characteristics, and solubility parameter. If the polymer-solvent interactions are higher than the polymer-polymer attraction forces, the chain segments start to absorb solvent molecules, increasing the volume of the polymer matrix, and loosening their coiled shape (Figure 3.1-3b). The segments are now "solvated" instead of "aggregated", as they were in the solid state.

The whole "solvation-unfolding-swelling" process takes a long time, and given it is influenced only by the polymer-solvent interactions, stirring plays no role in this case. However, it is desirable to start with finely powdered material, in order to expose more of their area for polymer-solvent interactions. When crystalline, hydrogen bonded or highly crosslinked substances are involved, where polymer-polymer interactions are strong enough, the process does stop at this first stage, giving a swollen gel as a result. If on the contrary, the

polymer-solvent interactions are still strongly enough, the "solvation-unfolding-swelling" process will continue until all segments are solvated. Thus, the whole loose coil will diffuse out of the swollen polymer, dispersing into a solution. At this stage, the disintegration of the swollen mass can be favored by stirring, which increases the rate of dissolution. However, once all the chain segments have been dispersed in the solvent phase, they still retain their coiled conformation, yet they are now unfolded, fully solvated, and with solvent molecules filling the empty space between the loosen segments. Hence, the polymer coil, along with solvent molecules held within, adopts a spheric or ellipsoid form, occupying a volume known as hydrodynamic volume of the polymer coil (Figure 3.1-3c).

a) Polymer molecules in the solid state just after being added to a solvent

b) First step: a swollen gel in solvent
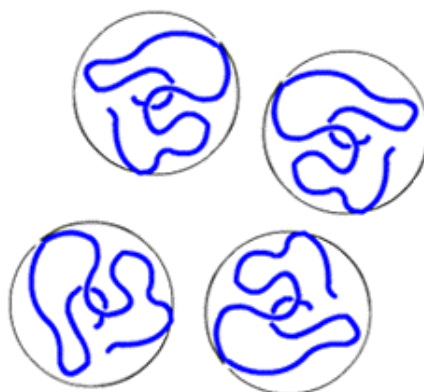
c) Second step: solvated polymer molecules dispersed into a solution

Figure 3.1-3: Schematic representation of the dissolution process for polymer molecules.

The particular behavior shown by polymer molecules, explains the high viscosity of polymer solutions. Solvent and low molecular weight solutes have comparable molecular size, and the solute does not swell when dissolving. Since molecular mobility is not restricted, and therefore, intermolecular friction does not increase drastically, the viscosity of the solvent and the solution are similar. But the molecular size of polymer solutes is much bigger than that of the solvent. In the dissolution process such molecules swell appreciably, restricting their mobility, and consequently the intermolecular friction increases. The solution in these cases, becomes highly viscous.

Solubility of PIK polymers:

Polymer solubility was qualitatively determined by the dissolution of 5 mg of solid polymers in 1 ml of organic solvent, and this mixture was then left for 24 h at room temperature (Table 3.1-2). The polymers showed a different solubility behavior in different organic solvents. The complete dissolution time for a certain polymer in different solvents depended on the solvent quality and the molecular weight of the polymer. When a solid polymer powder was mixed with the solvent, the complete dissolution time defined as the time needed for the solid to disappear completely (similar work was reported in the literature)[213], decreased in the following order:

(THF) > DMF > NMP >DMAc).
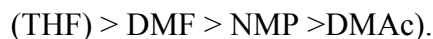
For instance, polymer 12a dissolved in DMAc within 20 min., whereas polymer 16a required 16 h. Thus, PIK polymers showed greatly improved solubility in comparison with the corresponding polyaramides.

The polymers **PIKs-11b**, **11c**, **12**, **13**, **15**, and **16a** could be dissolved in aprotic solvents, such as N-methylpyrrolidinone (NMP), N, N-dimethylacetamide (DMAc), dimethylsulfoxide (DMSO) and dimethylformamide (DMF), while only swelling was observed in other common organic solvents such as chloroform and dichloromethane, and in other organic solvents, such as methanol and ethanol the polymers **PIKs-11b**, **11c**, **12**, **13**, **15**, and **16a** could not be dissolved or swollen. Therefore, common organic solvents with low boiling points, such as dichloromethane, chloroform, methanol and ethanol could not be employed to dissolve PIK polymers.

Table 3.1- 2: Solubility behavior of poly(imino ketone)s. [a]

PIKs	DMAc	DMSO	DMF	NMP	THF	MeOH or EtOH	CHCl$_3$	CH$_2$Cl$_2$
11a	±	±	±	±	±	--	-S	-S
11b	++ 5 M	++ 5 M	++ 5 M	++ at once	++ 4 h	--	--	--
11c	++ 10 M	++ 10 M	++ 10 M	++ at once	--	--	--	--
12a	++ 20 M	±	±	++ 30 M	++ ≈ 4 h	--	--	--
13	++ 30 M	++ ≈ 4 h	++ 4 h	++ 30 M	++ ≈1 h	--	±	±
14a	--	--	±	--	--	--	-S	-S
14b	++	++	++	++	±	--	-S	-S
15	++ 5 h	++ 6 h	++ 5 h	++ 20 h	++ ≈ 3 h	--	--	--
16a	++ ≈ 16 h	± ≈ 48 h	++ ≈ 24 h	++ ≈ 20 h	±	--	-S	-S

[a] Solubility was measured at polymer concentration, 5 mg. ml^{-1} by the mixing of 5 mg of polymer with 1 ml of solvent, followed by stirring for 24 h; ++ indicates that the solid polymer was completely dissolved in the solvent to afford a homogeneous solution at room temperature; ± indicates that the solid polymer could be partially soluble at room temperature; -- indicates that the solid polymer could not be dissolved or swollen in the solvent; -S indicates that the solid polymer could be swell at room temperature.

The molecular weights of the **PIK** polymers were measured by GPC (calibrated by polystyrene standards). The M_n values are in the range of 11 100-85 900 and the M_w values in the range of 19 500-474 500. The polydispersities vary from 1.7 up to 6.7 (Table 3.1-3). Especially, with increasing molecular weights the polydispersity increases drastically.[214]

Table 3.1-3: Characterization of PIKs: (GPC, intrinsic viscosity, and yield).

Polymer Code	$\overline{M}_n$ [a]	$\overline{M}_w$ [a]	$\overline{M}_w / \overline{M}_n$ [b]	DP[c]	Yield (%)	$[\eta]^d_{dl/g}$
PIK-11a	_	_	_	_ e	95	_e
PIK-11b	12200	25300	2.1	25	89.9	0.18
PIK-11c	11100	74100	6.7	23	92	0.16
PIK-12a	15000	26300	1.8	24	80	0.19
PIK-13	11700	19500	1.7	18	88	0.17 [f]
PIK-14a	_	_	_	_ e	86	_e
PIK-14b	44200	295200	6.7	82	88	0.42
PIK-15	37000	139300	3.8	49	84	0.249
PIK-16a	85900	474500	5.5	126	90	0.685

a) By GPC (Calibrated by polystyrene standards); b) Polydispersity index; c) Degree of polymerization determined from number average molecular weight; d) [η] Intrinsic viscosity measured at 25 °C in DMF; e) Not measured due to poor solubility; (f) Measured at 25 °C in THF.

The elemental analysis of the polymers showed that in all cases the determined carbon and nitrogen contents were lower than the calculated ones. This can be explained by the hygroscopic nature of the imino groups of these polymers. The uptake of water was in the range of 1.4-7.0 % as calculated from the weight change of the vacuum-dried polymer samples after exposure to air at room temperature for 10-12 h. Therefore, the measured elemental analysis values were corrected by elimination of the amount of absorbed water (Table 3.1-4). Similar to the study performed on hygroscopic polyaramides,[215] the experimental data were then in good agreement with the calculated ones.

Table 3.1-4: Elemental analysis for poly(imino ketone)s.

Polymer Code	Formula (Molecular weight %)[c]	Elemental analysis[a] (%)				Moisture Uptake[b]
			C	H	N	
PIK-11a	$(C_{26}H_{18}N_2O_2)_n$ $(390.44)_n$	Calc. Found Corrected	79.98 76.70 79.46	4.65 4.86 4.69	7.17 6.89 7.14	3.60
PIK-11b	$(C_{32}H_{22}N_2O_3)_n$ $(482.54)_n$	Calc. Found Corrected	79.65 77.52 79.55	4.60 4.73 4.61	5.81 5.67 5.82	2.62
PIK-11c	$(C_{32}H_{22}N_2O_3)_n$ $(482.54)_n$	Calc. Found Corrected	79.65 76.80 79.59	4.60 4.78 4.61	5.81 5.80 6.01	3.63
PIK-12a	$(C_{44}H_{38}N_2O_2)_n$ $(626.79)_n$	Calc. Found Corrected	84.31 83.10 84.28	6.11 6.19 6.10	4.47 4.33 4.39	1.42
PIK-13	$(C_{44}H_{38}N_2O_2)_n$ $(626.79)_n$	Calc. Found Corrected	84.31 82.62 84.19	6.11 6.21 6.08	4.47 4.34 4.43	2.03
PIK-14a	$(C_{30}H_{26}N_2O_2)_n$ $(446.55)_n$	Calc. Found Corrected	80.69 74.83 79.96	5.87 6.23 5.80	6.27 5.86 6.26	6.85
PIK-14b	$(C_{36}H_{30}N_2O_3)_n$ $(538.65)_n$	Calc. Found Corrected	80.27 74.60 79.80	5.61 6.08 5.66	5.20 4.85 5.19	6.97
PIK-15	$(C_{51}H_{44}N_2O_4)_n$ $(748.92)_n$	Calc. Found Corrected	81.79 77.69 81.52	5.92 5.99 5.69	3.74 3.68 3.50	4.93
PIK-16a	$(C_{48}H_{46}N_2O_2)_n$ $(682.91)_n$	Calc. Found Corrected	84.42 79.81 84.36	6.79 7.18 6.77	4.10 3.81 4.03	5.70

[a] For C and N corrected value = found value × (100 % + moisture uptake %); For H corrected value = found value × (100 % - moisture uptake %); [b] Moisture uptake (%) = $(W-W_0) / W_0 \times 100$ %; W is the weight of polymer sample after standing at room temperature; W_0 is the weight of polymer sample after drying in vacuum at 100 °C for 10 h; [c] In g. mol^{-1}.

Intermolecular and intramolecular hydrogen bonding

Owing to the importance of the hydrogen bonding in nature, an enormous amount of research has been directed at the phenomenon of hydrogen bonding. [216-218] The structure and properties of the condensed phases are strongly dependent on weak interactions such as hydrogen bonding and van der Waals bonding.

One of the more striking consequences of hydrogen bonding appears in the vibrational spectrum. The band which corresponds to the stretch of the A-H bond shifts to lower frequency, is intensified, and undergoes a concomitant broadening. In a quantitative sense, it has been possible to establish a nice correlation between the red shift and the strengh of the hydrogen bond.[216,219] It also appeared that the magnitude of the intermolecular H-bond stretching frequency was directly related to the strength of the H-bond.

The presence of hydrogen bonding in a polymeric material significantly determines its morphological and structural properties. The dynamic behavior of hydrogen bonding, the specific interactions, depend on the system conditions, particularly temperature and the presence of other components that are able to interact in a similar manner. The description given by Pauling describes the interaction of a hydrogen atom is attracted by rather strong forces to two atoms instead of only one, under certain circumstances, so that it may be considered to be acting as a bond between them. This is called a hydrogen bond".[220] A hydrogen atom in an A-H system, in a linear conformation can hydrogen bond to another atom of the same molecule of the same species or a different molecule, A-H···B. The actual position of the hydrogen atom depends on atoms A and B as well as on their electronegativity and size.

It is the hydrogen bonding ability that often gives rise to the crystalline character of polymers; this interaction is opposing the need to lower entropy that allows the polymer chains to align and display crystalline characteristics. In a linear conformation, the regularity can be greatest and allow maximum hydrogen bonding interactions, giving minimum energy. The characteristics of hydrogen bonding allow polymers to form stable intermolecular hydrogen bonds.

Hydrogen bonding interactions are crucial in establishing a molecular network in solution and in the solid state. When both the distance between the heavy atoms fell within the sum of their van der Waals radii compiled by Bondi [221] and the angle defined by the two heavy atoms and

hydrogen (donor atom-H-acceptor atom) were larger than 90° they were accounted as hydrogen bonds.[222] The possible hydrogen bonding interactions were studied experimentally (FT-IR spectroscopy can be an important research tool). Hydrogen bonding interactions of polymers were measured by FT-IR peak shifts.[220]

Intermolecular and intramolecular hydrogen bonding of PIKs

Hydrogen bonding interactions of polymers have frequently been studied by FT-IR spectroscopy.[220,223] Therefore, FT-IR-spectra of all PIKs (KBr pellets) were recorded giving results in good agreement with the proposed structure. The characteristic absorptions for carbonyl groups γ(C = O) appeared between 1631 and 1663 cm^{-1} and for aromatic amino groups γ(NH) between 3318 and 3422 cm^{-1} (Table 3.1-5). Obviously, due to hydrogen bonding a significant broadening and lowering of the absorption frequency of the bands (γ(C = O), γ(NH)) are observed.[224] This effect is known to be a function of the degree and strength of the hydrogen bonding.[225,226] This clearly indicates that N-H...O = C interactions within the same molecule (intramolecular hydrogen bonding) or from neighboring molecules. Intermolecular hydrogen bonding is very likely as the solubility of all polymers is limited but can be drastically improved by the addition of lithium chloride known to break hydrogen bonds.[1] This confirms our assumption that these polymers may be considered as analogous materials to polyaramides. Comparing the frequencies of the N-H-bond of the crystalline model compound **10** (3341 cm^{-1}) with those observed in the polymers **(PIK-12a**, **13**, **14a**, **14b**, **15**, and **16a**: 3377, 3360, 3348, 3384, 3422, and 3364 cm^{-1}) a shift to higher frequencies is observed. This suggests that the hydrogen bonding in PIKs is weaker than in the crystalline model compound.

On the other hand, the frequencies of the N-H-bond of polymers **(PIK-11a**, **11b** and **11c:** 3318, 3322 and 3320 cm^{-1} respectively) were shifted to lower frequencies than frequency of the N-H-bond of their corresponding model compound therefore, the hydrogen bonding in PIKs **(PIK-11a**, **11b**, and **11c**) is weaker than in the crystalline model compound.
The possible intermolecular hydrogen bonding is expected to control the intermolecular backbone-backbone distance within the sheet between adjacent chains (cf. Figure 3.1-23). Therefore, wide-angle X-ray diffractogram was performed in this part of the work. In fact we do not know the number of hydrogen bonds per repeating units. Although good results can be derived from experimentally obtained FT-IR spectra, a lot of questions still remain open, such as (i) the geometric parameters (position, length, angles) of the hydrogen bonds, and the type of H-donor carbon and (ii) the geometric arrangements of the interacting molecules. Modeling

the intermolecular interactions e.g., by semiempirical quantum chemical methods, is expected to give answers to the first question and may give additional support for conclusions drawn form experimental data.

From above, one can conclude that polymers **PIK-12a**, **13**, **14a**, **14b**, **15**, and **16a** have weaker hydrogen bonding than their corresponding crystalline model compound **10**. This is due to the disorder of the polymer system which does not help the hydrogen bonding. However, polymers **PIK-11a**, **11b**, and **11c**, despite their semicrystalline nature, they have stronger hydrogen bonding than their corresponding crystalline model. Similar studies were reported in the literature.[225,226]

Table 3.1-5: FT-IR spectra of PIKs.

Polymer code	γNH^a	$\gamma C=O^a$	$\gamma C- N^a$	$\gamma C-H$ aliphatic	$\gamma C-H$ aromatic
PIK-11a	3318	1631	1312	………	3024
PIK-11b	3322	1635	1314	………	3045
PIK-11c	3320	1638	1316	………	3030
PIK-12a	3377	1642	1308	2962	3024
PIK-13	3360	1644	1307	2961	3028
PIK-14a	3348	1646	1310	2957	3054
PIK-14b	3384	1644	1327	2955	3034
PIK-15	3422	1663	1330	2963	3029
PIK-16a	3364	1646	1328	2962	3028

a) FT-IR (KBr, pellet).

Attempted dissociation and reassociation of hydrogen bonding of PIKs

FT-IR was recorded at 25 °C (curve-a) and at elevated temperature in a nitrogen atmosphere as shown in Figure 3.1-4. The selected sample of polymer **PIK-13** was heated to 100 °C and FT-IR was recorded (curve-b), then gradually cooled to room temperature, then the sample was heated to 200 °C and FT-IR was recorded (curve-c). From curves a, b, and c it was found that the dissociation of hydrogen bonds had not taken place, therefore, from room temperature up to 200 °C hydrogen bonds is stable. The suitable elevated temperature should be over 200 °C at which the dissociation of the hydrogen bonds will be taken place and then gradually cooled to room temperature the broken hydrogen bonds will be reformed. Since there is no way to go over 200 °C, the dissociation of the hydrogen bonds was not recorded.
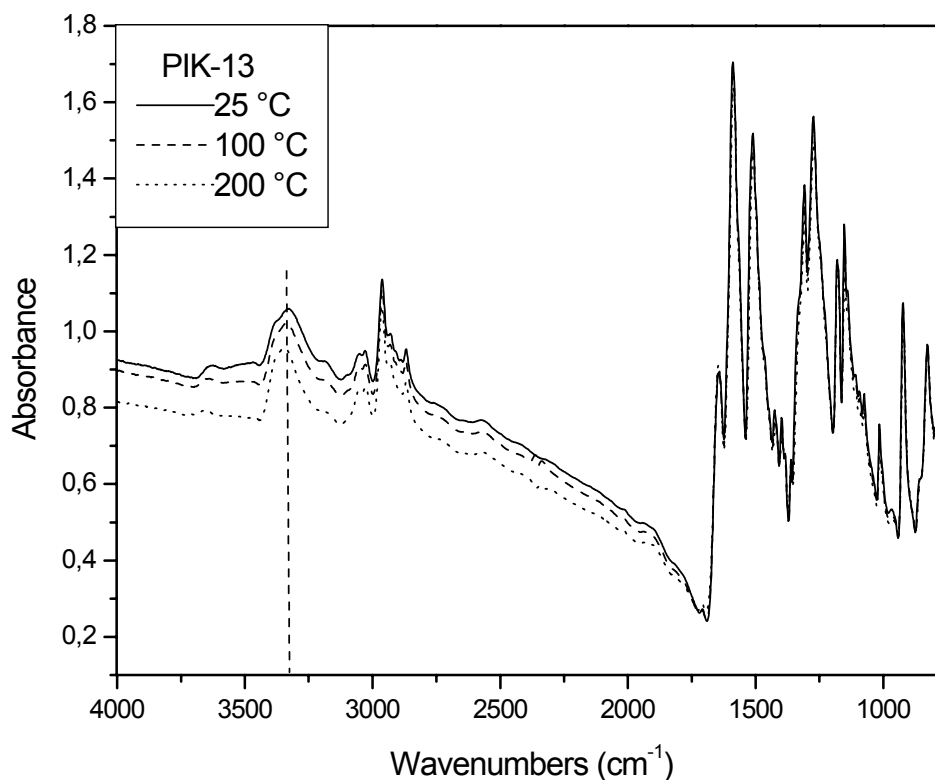
Figure 3.1-4: FT-IR at high temperature of polymer **PIK-13**.

^{1}H-NMR of PIKs:

^{1}H-NMR (700 MHz) spectra of all soluble polymers were recorded. As an example the spectrum of **PIK-13** is shown in Figure 3.1-5 (DMSO-d_6 at 100 °C). Protons of the imino groups are at 8.78 ppm. Two doublets at 7.66 and 7.05 ppm were attributed to the aromatic protons H_1 and H_2 and one singlet at the upfield region at 1.55 ppm were assigned to the aliphatic protons of methyl groups derived from the polymer repeating unit. Peaks at 7.94, 7.66, 7.05, 6.80, 6.44, 4.71 and 1.48 ppm have chemical shifts characteristic of $H_1^{'}$, $H_2^{'}$, $H_3^{'}$, $H_4^{'}$, $H_5^{'}$, NH_2 and CH_3 of the amine protons known by comparing them with the chemical shifts of the ^{1}H-NMR of the diamine monomer. These peaks were assigned to the aromatic and aliphatic protons of minute amounts of the terminal amine unit of polymer **13**.

From this spectrum we can conclude that polymer **PIK-13** contains a low concentration of amino end-groups (resonances at 6.4 ppm). The concentration corresponds to less than 5-mol percent end groups per repetition unit. Bromine end groups are not detectable, but, they can not be excluded as they are expected in the same region as the resonances of the
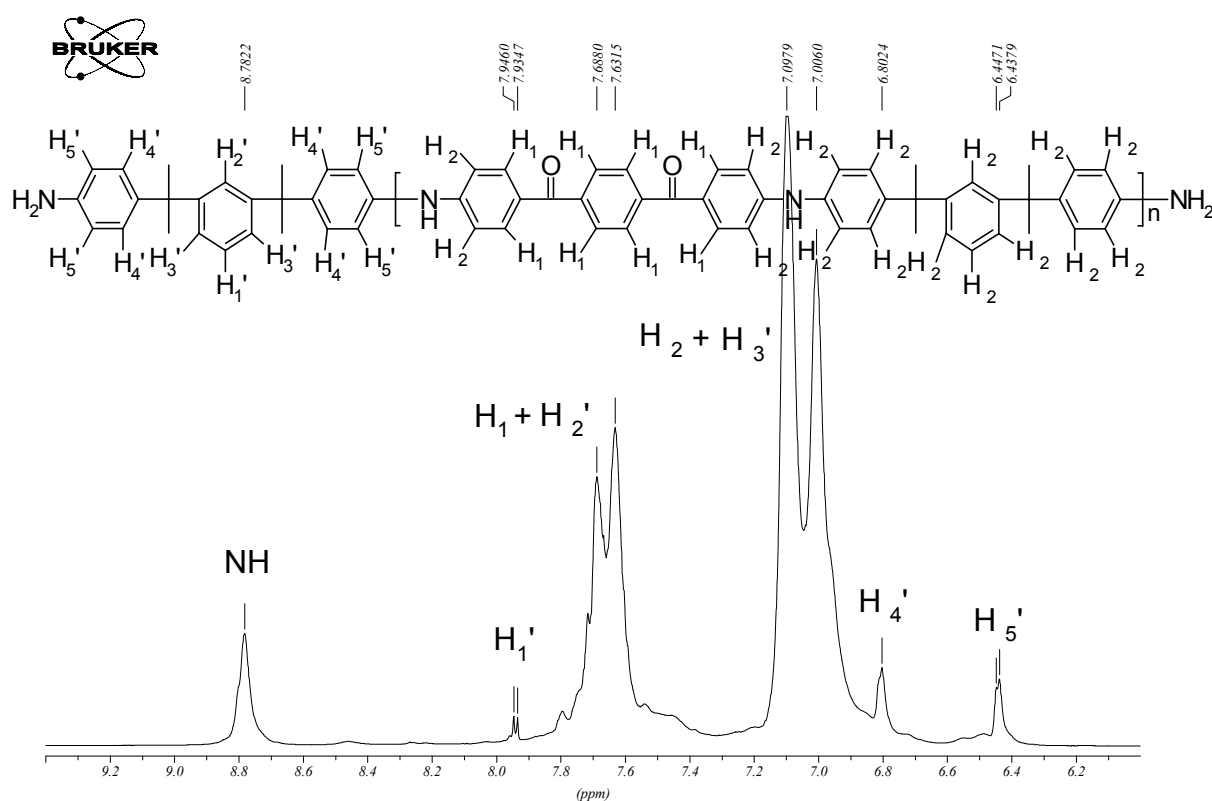
Figure 3.1-5: ^{1}H-NMR (700 MHz) spectrum of polymer **PIK-13** recorded in DMSO-d_6 at 373K.

51

proton H_1. As the concentration of end groups in polymer **PIK-13** is very low the corresponding ^{13}C-NMR signals were not detectable.

The end groups were only detected in case of polymer **PIK-13**, as shown from the ^{1}H-NMR spectrum (Figure 3.1-5). Remarkably, no end groups were detected in the case of the higher molecular weight PIKs. In the previous case, the presence of the end goups could be due to incomplete reaction between the diamine and dibromo monomers (Figure 3.1-5).

The influences of concentration and temperature on the molecular weight of PIKs:

During the synthesis of polymer **PIK-15**, the effect of concentration and temperature on the molecular weight could be followed. Upon increasing the temperature from 100 °C to 165 °C and the concentration form 18 % to 24 % respectively, M_w increased from 4 000 to 10 000 and M_n from 1 000 to 7 000, while upon increasing the concentration form 24 % to 36 % at temperature 165 °C, M_w increased from 11 000 to 42 000 and M_n from 7 000 to 10 000. A temperature of 165 °C and a concentration of 36 % are more suitable for the palladium-catalyzed polycondensation to produce polymer **PIK-15** with higher molecular weight (Table 3.1-6).

Table 3.1-6: Different experimental conditions for the polycondensation of 2,2-bis[4-(4-aminophenoxy)-phenyl]propane with 1,3-bis(4-bromobenzoyl-5-*tert*.-butyl)benzene to form polymer **PIK-15**.

Run	Temp °C	Monomer Conc.(%)	Solubility	Yield (%)	$\overline{M_w}$	$\overline{M_n}$	$\overline{M_W}/\overline{M_n}$	DP
1	100	18	DMF, DMAc,THF	92	4000	1000	4	1.3
2	100	36	DMF, DMAc,THF	90	10000	2000	5	2.6
3	165	24	DMF, DMAc,THF	98	11000	7000	1.6	9
4	165	30	Swelling in DMF, DMAc,THF	95	-	-	-	-
5	165	36	Swelling in DMF, DMAc,THF	96	-	-	-	-
6	100–165	36	DMF,DMAc,THF	96	42000	10000	4.2	13

The influences of the ligand on the polycondensation process:

To test which ligand would be most suitable for the polycondensation process to form PIKs, we attempted the amination of 1,3-bis(4-bromobenzoyl-5-*tert*.-butyl)benzene (**9**) with 4,4´-

(1,4-phenylenediisopropylidine)bisaniline in diphenylsulfone using different ligands from **1** to **4** (Figure 3.1-6) (Table 3.1-7).
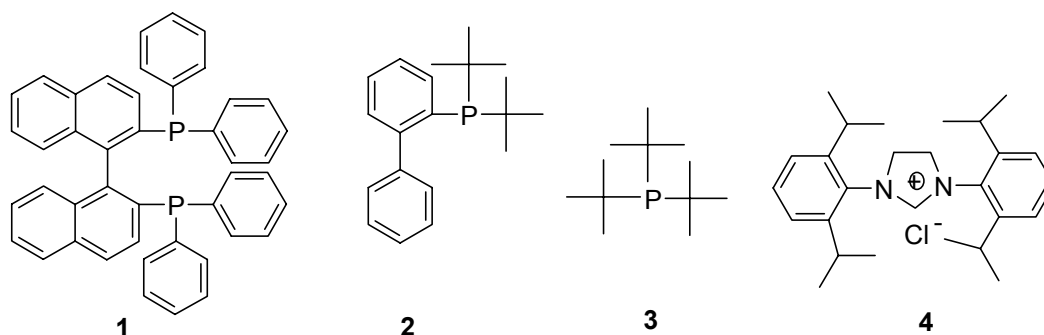
Figure 3.1-6: Complex ligands of the catalyst applied in the Buchwald-Hartwig reaction (**1**: BINAP; **2**: Di-*t*-butylphosphinobiphenyl; **3**: P(*t*-Bu)$_3$; **4**: 1,3-Bis(2,6-diisopropylphenyl)imidaz-olium chloride)

It appears that ligand **1** gives better yield, higher molecular weight and lower polydispersity of the polymer than ligand **2** and that both are superior to **3** and **4**.

Table 3.1-7 Pd-Catalyzed polycondensation of 1,3-bis(4-bromobenzoyl-5-*tert*.-butyl)benzene (**9**) with 4,4´-(1,4-phenylenediisopropylidine)bisaniline using different ligands.[a]

Run	Polymer code	Ligand[b]	Yield[c] (%)	M_n[d]	M_w[d]	DP[f]	M_w/M_n[g]
1	**PIK-16a**	**1**	90	85900	474500	126	5.5
2	**PIK-16b**	**2**	80.9	28000	142000	41	5.1
3	**PIK-16c**	**3**	78	5000	59000	7	8.5
4	**PIK-16d**	**4**	73	5000	52000	7	9.6
5[e]	-	-	0	-	-	-	-

a) The polycondensation of electron-poor 1,3-bis(4-bromobenzoyl-5-*tert*.-butyl)benzene.(4 mmol) was carried out in the presence of Pd$_2$ (dba)$_3$ (0.12 mmol), ligand (P/ Pd ratio = 3/1), and NaO-*t*-Bu (11.2 mmol) in diphenyl sulfone at 165 °C for 4h and at 200 °C for 24 h; b) **1**: BINAP; **2**: Di-*t*-butylphosphinobiphenyl; **3**: P(*t*-Bu)$_3$; **4**: 1,3-Bis(2,6-diisopropylphenyl)imidaz-olium chloride; c) Reprecipitated Polymer; d) Calibrated by GPC (DMF) polystyrene standards; e) No catalyst was added; f) Degree of polymerization determined from number average molecular weight; g) Polydispersity index.

The reactivity of the halogen containing monomers in the polycondensation process:

The reactivity of the halogen containing monomers (**5-7**) was studied during the polycondensation process to form polymer **PIK-12a** (Table 3.1-8). The reaction employing 1,4-bis(4-bromobenzoyl) benzene (**7**) gave polymer **PIK-12a** in better yield and higher molecular weight than 1,4-bis(4-chlorobenzoyl)benzene (**5**) while 1,4-bis(4-fluorobenzoyl) benzene (**6**) is totally unreactive.

So in these reactions, there is a strong dependence of the reactivity upon the halogen atoms used in the diketone monomer. Reactivity decreases strongly with increasing electronegativity of the halogen atoms, so that polymer **12a** with the high molecular weight can only be achieved from the dibromo monomer **7**. It is known that for aryl amination the reactivity decreases strongly with increasing electronegativity of the halogen atoms and oxidative addition is rate limiting,[196e] therefore, dibromo monomer **7** is more favored than dichloro monomer **5** while difluoro monomer **6** is sluggish.

Table 3.1-8: Pd-Catalyzed polycondensation of different 1,4-bis(4-halobenzoyl)benzenes with 4,4-(1,4-phenylenediisopropylidine)bisaniline.[a]

Run	Polymer code	R	Yield[b](%)	M_n[c]	M_w[c]	M_w/M_n[d]	DP
1	**PIK-12a**	Br	80	15000	26300	1.8	24
2	**PIK-12b**	Cl	76.6	11000	16000	1.5	17
3	-	F	0	-	-	-	-

1- a) The polycondensation of electron-poor 1,4-bis(4-halobenzoyl)benzene (4.0 mmol) was carried out in the presence of Pd_2 (dba)$_3$ (0.12 mmol), ligand (BINAP) (P/Pd ratio = 3/1); and NaO-*t*-Bu (11.2 mmol) in diphenyl sulfone at 165 °C for 4 h and at 200 °C for 24 h;

b) Reprecipitated polymer; c) Calibrated by GPC (DMF) polystyrene standards;

d) Polydispersity index.

Viscosity measurements

In order to get more information about the moecular weight of the polymer obtained, their intrinsic viscosities have been determined and compared. All viscosity measurements were carried out in N, N-dimethyformamide or tetrahydrofuran at 25 °C, using a Cannon-Ubbelodhe type viscometer. The determined intrinsic viscosities are in the range of 0.16-0.685 dl/g (Table 3.1-3). The intrinsic viscosities of polymers **PIK-11a**, and **14a** were not measured due to their poor solubility in the known organic solvents.
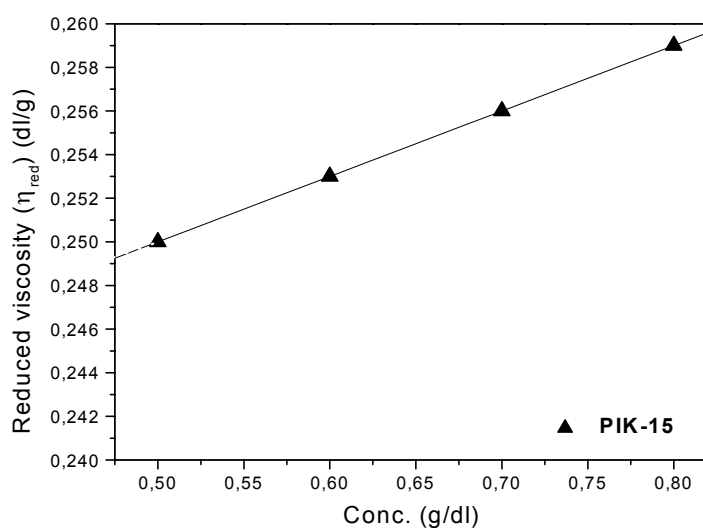
Figure 3.1-7: Determination of intrinsic viscosity of polymer **PIK-15** in DMF at 25 °C.
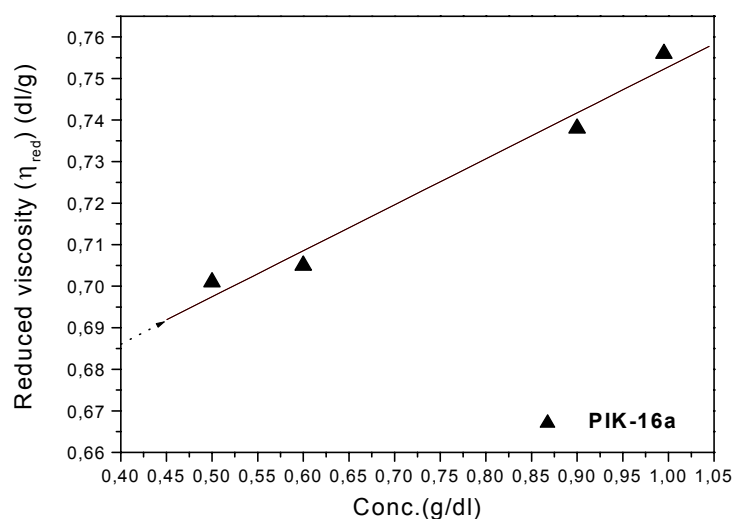
Figure 3.1-8: Determination of intrinsic viscosity of polymer **PIK-16a** in DMF at 25 °C.

Not surprisingly, it can be clearly seen from Figures 3.1-7, 3.1-8 that with increasing the molecular weight of the polymer determined from GPC measurements the intrinsic viscosity of the polymer increases. The intrinsic viscosity $[\eta]$ of polymer 16a is 0.685 dl. g^{-1} which is higher than that of polymer **PIK-15** (0.249 dl. g^{-1}) (Figures 3.1-7 and 3.1-8). Consequently, the intrinsic viscosity $[\eta]$ of PIKs are lower than those of the higher molecular weight PEKs[229] and those of aromatic polyamides.[230]

Thermal behavior of PIKs

A standard test for assessing weight loss, and thus the thermal stability of a material, is dynamic or isothermal thermogravimertic analysis (TGA). In this test, the percent weight loss is recorded as a function of the temperature of the material. All PIKs showed high thermal stability and a high char yield in nitrogen at 600 °C. Typical TGA traces in air and in nitrogen are shown in Figure 3.1-9 for polymer **PIK-12a** and **13**. The thermal stability was evaluated by a 5 % weight loss (Table 3.1-9). TGA curves revealed that the polymers were thermally stable up to 323-494 °C.
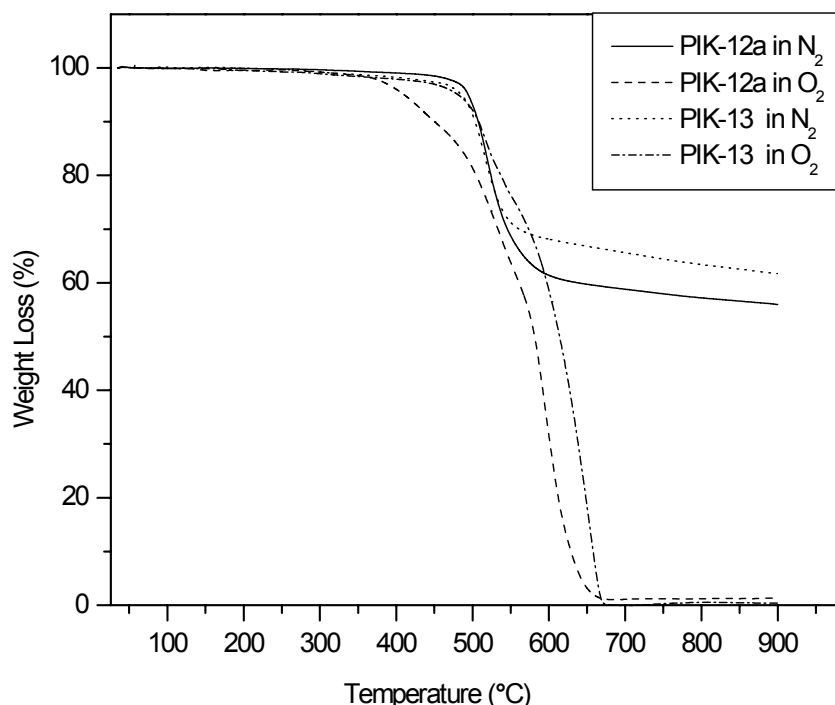
Figure 3.1-9: TGA of the polymers **PIK -12a** and **13** (in N_2, and in O_2 10 °C/min).

The 50 % weight loss of the polymers took place at over 900 °C for polymers **PIK-11a**, **12a**, **13**, **14a** and **15** in nitrogen and for polymer **PIK-11b** and **14b** in both air and nitrogen. Char yield is an easy and important measurement which correlates to the ability to sustain combustion.[227] The maximum char yield at 600 °C was obtained for polymer **PIK-11a** (83 %) and the minimum was obtained for polymer **PIK-16a** (54 %) in nitrogen.

By comparing for example the TGA thermograms of **PIK-12a** and **13** (Figure 3.1-9), it was observed that in air a 50 % weight loss of those polymers took place at 580 °C and at 610 °C respectively, but in nitrogen the 50 % weight loss was not observed up to 900 °C. In air the char yield at 600 °C was 34 % and 59 % respectively but in nitrogen the char yield at 600 °C was 61 % and 68 %.

Differential scanning calorimetry (DSC) of PIKs up to 250 °C showed a single T_g, and the absence of a melting temperature suggested an amorphous polymer structure (Figure 3.1-10). All polymers show high T_gs ranging from 202 to 227 °C, being comparable with the T_gs of modified polyterephthalamides bearing pendent groups connected to the polymer backbone with ester linkages,[228] only polymer **PIK-13** gave in a lower T_g at 154 °C (Table 3.1-9). The T_gs are higher than those of the related PEKs which range from 129 to 167 °C,[229] and lower than those of aromatic polyamides which amount to 292-319 °C.[230] This can be explained by the hydrogen bonding in PIKs which is weaker than that in polyamides while PEKs have no hydrogen bonding.
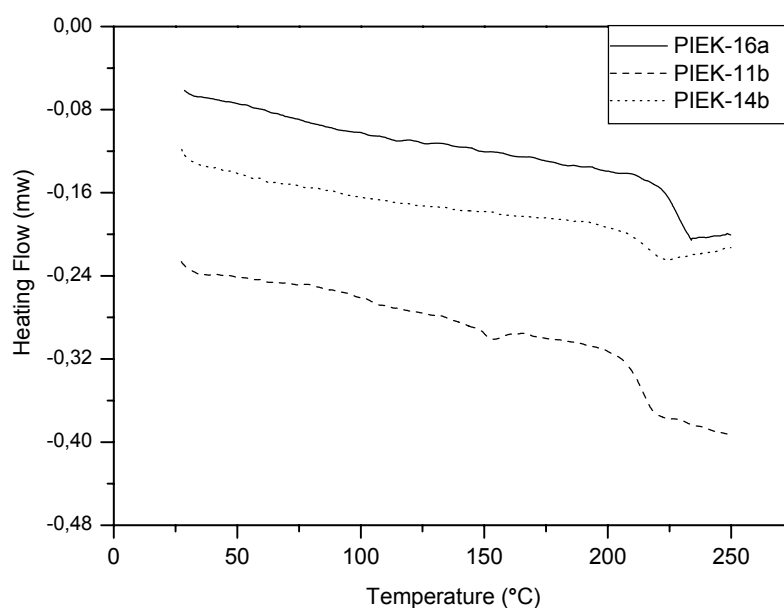
Figure 3.1-10: DSC of PIKs (in N₂, 10 °C/min, second scan).

Table 3.1-9: Thermal behavior of PIKs.

Polymer code	O_2 / N_2	$^aT_5$	$^bT_{10}$	$^cT_{50}$	$^dW_{500}$	$^eW_{600}$	Char yield at 600 °C^f	T_g Midpoint^g
PIK-11a	O_2	323	345	353	95	97	3	-^{h}
	N_2	482	538	>900	6	17	83	
PIK-11b	O_2	435	516	>900	8	22	78	212
	N_2	494	534	>900	6	22	78	
PIK-12a	O_2	407	444	582	19	66	34	220
	N_2	494	507	>900	7	39	61	
PIK-13	O_2	478	507	613	8	41	59	154
	N_2	485	502	>900	9	32	68	
PIK-14a	O_2	335	337	344	94	98	2	-^{h}
	N_2	387	461	>900	17	29	71	
PIK-14b	O_2	365	426	>900	21	30	70	215
	N_2	363	425	>900	23	32	68	
PIK-15	O_2	356	413	567	26	64	36	202
	N_2	328	391	>900	30	40	60	
PIK-16a	O_2	370	461	715	22	47	53	227
	N_2	366	458	742	23	46	54	

a) T_5: Temperature of 5 % weight loss; b) T_{10}: Temperature of 10 % weight loss; c) T_{50}: Temperature of 50 % weight loss; d) W_{500}: weight loss at 500 °C, determined from TGA curve; e) W_{600}: weight loss at 600 °C, determined from TGA curve; f) The remaining of the polymer at 600 °C; g) From the second heating traces of DSC measurements conducted with a heating rate of 10 °C min^{-1} in nitrogen; h) Not detected up to 250 °C.

The relation between thermal behavior, glass transition temperatures (T_gs) and molecular weights of PIKs (PIKs-16a, b, c, and d)

The thermal stability of **PIKs-16a**, **b**, **c**, and **d**) in nitrogen atmosphere was determined by TGA. Thermal stability was evaluated by a 5 % weight loss at the minimum temperature (Figure 3.1-11). TAG revealed that the polymers were stable up to 366-465 °C without any weight loss. The 50 % weight losses of the polymers fell between 740 and > 900 °C (Table 3.1-10). The decomposition of the polymer probably occurred through pyrolytic cleavage of the aliphatic C–C-bond first. The maximum char yield at 600 °C was obtained for polymer

PIK-16d (82 %) and the minimum was obtained for polymer **PIK-16a** (54 %). It was observed that the char yield at very high temperature (600 °C), in nitrogen, can be seen as a direct result of the polymer structure, containing thermodynamically stable chemical bonds. The implication of the thermodynamic stability of the bonds in poly(imino ketone)s is that it will take a large input of energy (high temperature) to dissociate any of the bonds (induce thermal degradation).

The 5 %, 50 % weight loss temperatures in addition to the high char yields at 600 °C in nitrogen suggested that thermal degradation in nitrogen was significantly enhanced in case of polymer **PIK-16a** over **PIKs-16b**, **c**, and **d**. Therefore, **PIKs-16b**, **c**, and **d** were more thermally stable than polymer **PIK-16a**, despite their low molecular weight. These high thermal stabilities were probably attributed to the cross-linking reaction of the amine end groups with the carbonyl groups of the main repeating unit to form fused polycyclic aromatic materials. Which is consistent with the result of TGA thermogram. Since the polymer materials became degraded and insoluble after being heated to 900 °C in the TGA measurements. There were no further spectroscopic proof could be obtained. Some cases of cross-linking reaction of the amino groups with the carbonyl groups reported in the literature.[231] One can conclude that the thermal stability of **PIKs-16a**, **b**, **c**, and **d** was molecular weight dependent.
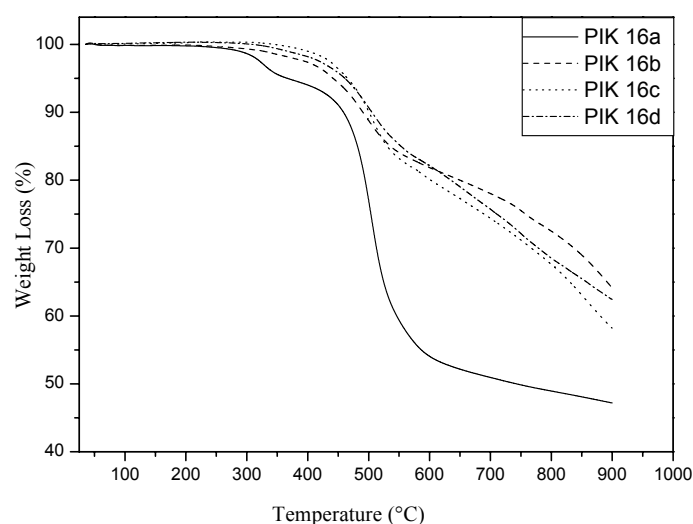
Figure 3.1-11: Dynamic TGA of **PIKs-16a**, **b**, **c**, and **d**.

(in N$_2$, and in O$_2$ 10 °C/min).

Differential scanning calorimetry (DSC) of PIKs from 20 °C up to 250-300 °C showed a single T$_g$ Figure 3.1-12). The absence of melting temperature suggested an amorphous

59

polymer structure (cf. Figure 3.1-21). The glass transition temperatures of these copolymers are listed in Table 3.1-10. They are all in the similar high level with T_gs ranging from 211 to 252 °C, being comparable with the T_gs of modified polyterephthalamides bearing pendent groups connected to the polymer backbone with ester linkages.[232] However, they are higher than those of the related PEKs which ranged from 129 to 167 °C,[229] and lower than those of aromatic polyamides ranged from 292-319 °C.[230] This could be explained by the hydrogen bonding in PIKs which is weaker than that of polyamides while PEKs have no hydrogen bonding. Generally, the glass transition temperature (transition between regions in which the polymer is relatively stiff below T_g and relatively rubbery above T_g) is affected by the molecular weight of the bulk polymer. The highest T_g was 227 °C which observed for the highest molecular weight **PIK-16a**. While the lowest T_g was 211 °C which observed for the lowest molecular weight **PIK-16d**. Therefore, the glass transition temperatures of **PIKs-16a**, **b**, and **d** are affected by the molecular weight of the bulk polymer. Except **PIK-16c** which has low molecular weight and showed a broad, highly exothermic peak centered at 252 °C. One can conclude that increased molecular weight causes increases in the glass transition temperature. This could probably be attributed to the presence of low molecular weight polymers which act as a plasticizer between the chains of the high molecular weight polymer. Which is confirmed by the GPC (polystyrene standards) results of **PIK-16a** with the highest molecular weight and the lowest polydispersity (M_n= 85 900, M_w = 474 500, M_w/M_n = 5.5) (Table 3.1-10).
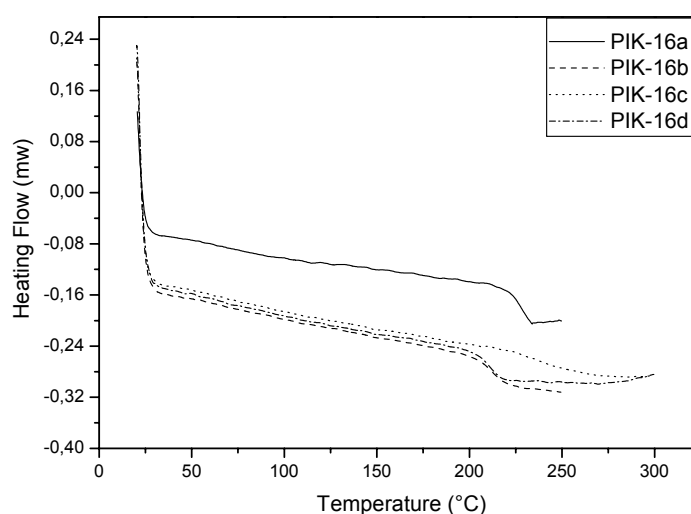
Figure 3.1-12: DSC of **PIKs-16a**, **b**, **c**, and **d**.

(in N_2, 10 °C/min, second scan).

Table 3.1-10: Thermal behavior of **PIKs-16a**, **b**, **c**, and **d**.

Polymer code	M_n^h	M_w^h	DP^i	$^aT_5$	$^bT_{10}$	$^cT_{50}$	$^dW_{500}$	$^eW_{600}$	Char yield at 600 °C^f	T_g Midpoint^g
PIK-16a	85900	474500	126	366	458	740	23	46	54	227
PIK-16b	28000	142000	41	441	490	>900	11	19	81	212
PIK-16c	5000	59000	7	465	500	>900	10	20	80	252
PIK-16d	5000	52000	7	462	500	>900	10	18	82	211

a) T_5: Temperature of 5 % weight loss; b) T_{10}: Temperature of 10 weight loss. C) T_{50}: Temperature of 50 % weight loss; d) W_{500}: weight loss at 500 °C, determined from TGA curve; e) W_{600}: weight loss at 600 °C, determined from TGA curve; f) The remaining of the polymer at 600 °C; g) From the second heating traces of DSC measurements conducted with a heating rate of 10 °C min^{-1} in nitrogen; h) Calibrated by GPC (DMF) polystyrene standards; i) Degree of polymerization determined from number average molecular weight.

After PIKs exhibited excellent thermal stability and low dielectric constant it is of great interest to examine the dynamic mechanical analysis which is one of the most essential requirements of high-performance polymers. To get information on segmental mobility of the polymer chains, elastic, and viscous properties of the PIKs materials the following thermo-mechanical behavior is necessary to be studied.

Thermo-mechanical behavior

The purpose is to achieve good dynamic mechanical analysis which can be used to analyze both elastic and viscous material response simultaneously. Materials respond to the applied strain or stress by dissipating energy in the form of heat (viscous dissipation), storing the energy elastically, or through a combination of these two mechanisms. Several quantities can be calculated from these measurements. The elastic modulus G' (related to the material's ability to store energy elastically). Similarly, the loss modulus G''or E'' (related to the material's ability to dissipate stress through heat). The ratio of these moduli (G'' / G') is defined as tan d, and indicates the relative degree of viscous to elastic dissipation, or damping, of the material. Viscoelastic materials, however, under most conditions show some characteristics of both elastic and viscous behavior. To characterize such materials accurately, both types of response, elastic and viscous must be measured for the polymer material.

The mechanical behavior of the polymers has been examined by means of dynamic mechanical testing performed at various temperatures and various frequencies with a small amplitude sinusoidal deformation.[233] An example of the mechanical behavior determined for polymer **PIK-15** is shown in Figure 3.1-13a. The results indicate that the polymer exhibits a spectrum of viscoelastic properties characteristic for linear amorphous entangled polymers. The two relaxation processes: (1) segmental relaxation at high frequencies detected as the cross-points of the storage (G') and loss (G'') modulae on the frequency scale and (2) chain relaxation at low frequencies (not visible) are controlling the behavior.

These relaxations separate three states characteristic for amorphous polymers: (1) the glassy state with the high value of the elastic modulus (G'~1GPa) at high frequencies, (2) the intermediate rubbery state with the modulus of the order of 1 MPa (the low frequency part of (Figure 3.1-13a) and (3) the flow regime at low frequencies with G' << G'' both varying with frequency in a characteristic way (not visible).[234] The insert in Figure 3.1-13a shows the temperature dependence of the segmental relaxation time which indicates that the relaxation time slows down to nearly 100 s when the polymer is approaching the glass transition temperature (T_g) from higher temperatures. In the presented example, the rubbery plateau is very well developed and extends over many orders of magnitide of the frequency scale indicating a high molecular weight of polymer **PIK-15** (M_n = 37 000, M_w = 139 300). The terminal relaxation and the flow range are not seen in the present data, because the high T_g and the high molecular weight of this polymer shift the detection range of such a behavior to very high temperatures (above 250 °C).

For another specially prepared polymer **PIK-12a** having lower molecular weight the flow regime can be observed in the accessible temperature range but in such a case the rubbry state and the corresponding G' plateau are not so well developed indicating a low molecular weight of polymer **PIK-12a** (M_n = 15 000, M_w = 26 300) (Figure 3.1-13b).
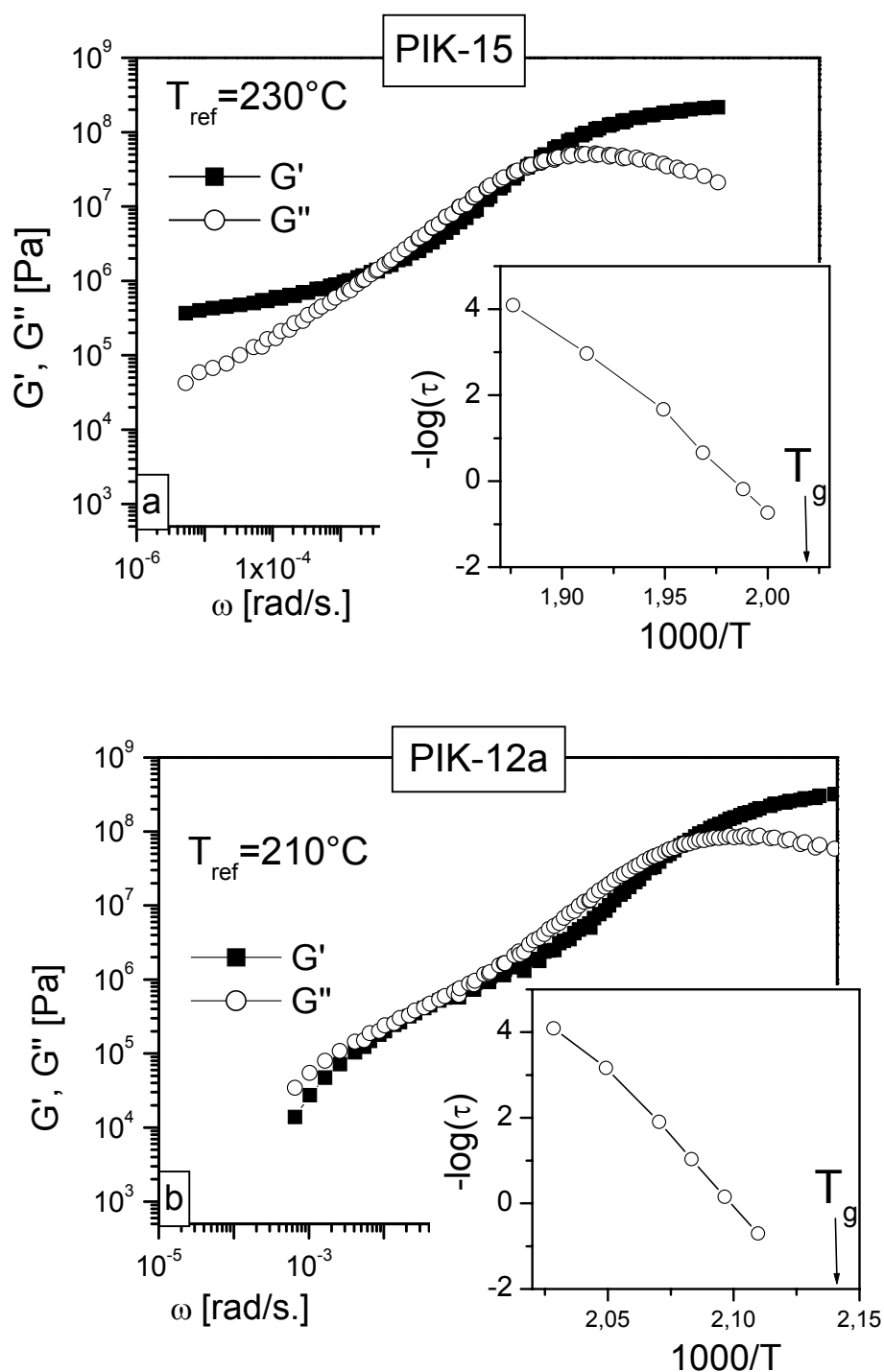
Figure 3.1-13a and b: The mechanical behavior of polymer **PIK-15** and **PIK-12a** as determined by means of the dynamic small amplitude shear deformation with various deformation frequencies and at various temperatures. The properties are represented by frequency dependencies of the real (G') and imaginary (G'') components of the complex shear modulus (master curves at the reference temperature of 230 and 210 °C respectively). The insert shows the temperature dependence of the segmental relaxation time.

The determined dielectric spectroscopy has shown relaxations corresponding to the segmental motion in the polymers as well as processes which can be atributed to charge carrier mobilities. Which result in conductivities reaching at high tempertaures values of the order of 10^{-9} S/cm. Clearly, that the segmental relaxations in both dielectric spectroscopy and the mechanical behavior are found to be comparable for polymers **PIK-12a** and **PIK-13**. This figured out from the comparison of dielectric and mechanical moduli for polymers **PIK-12a** and **PIK-13** at the reference temperature T = 210 ^{o}C (Figure 3.1-14a and b respectively).

Summarizing the first results one can conclude that PIKs can be considered as a new class of high-performance polymers. They exhibit high T_gs (T_g >140 °C) and excellent thermal stability (T_D>320 °C) combined with good mechanical properties (storage (G') and loss (G'') modulae < 10^8-10^9 and extended rubber plateau) comparable to polyaramides or PEK.[235] Furthermore, the chemical stability should be higher as for polyaramides as hydrolyzable amide linkages are absent.
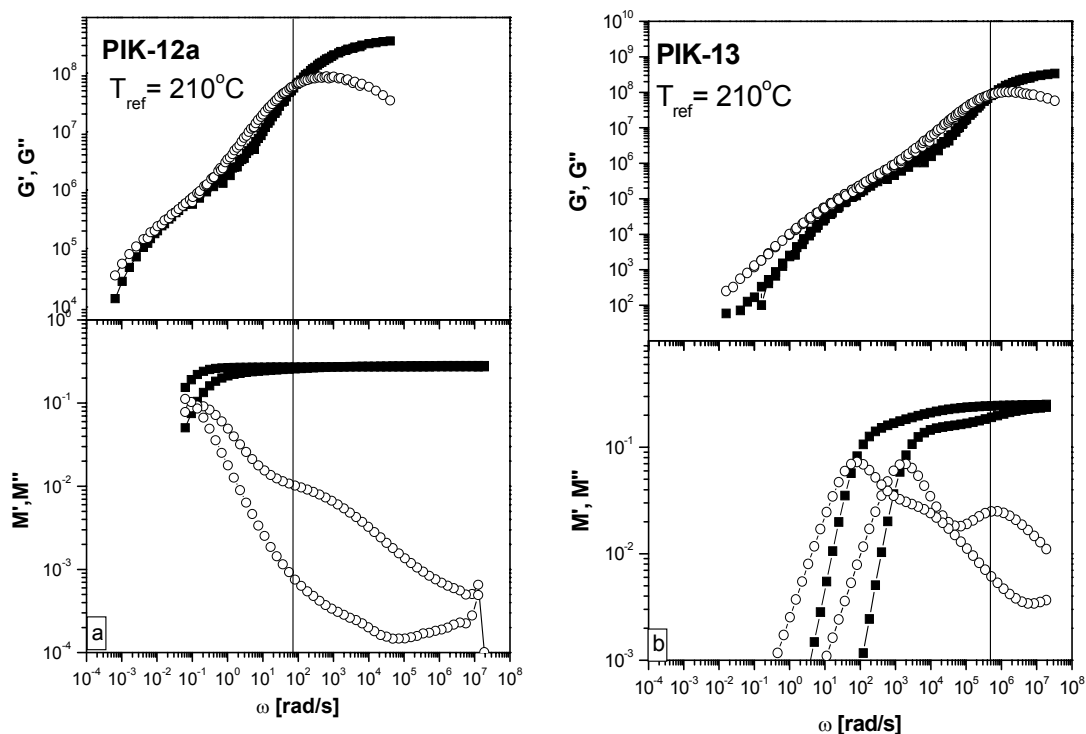
Figure 3.1-14a,b: Comparison of dielectric and mechanical moduli for polymers **PIK-12a** and **PIK-13** at the reference temperature T = 210 ^{o}C.

Dielectric spectroscopy of PIKs:

Microelectronics are important to technologies for both energy and defense applications. Further, the development of commercially available microelectronics for defense applications is becoming increasingly important.[236] A low dielectric constant is required for reduced power consumption in high frequency devices, reduced crosstalk between metallic interconnects, and reduced circuit RC time constants. The reduction in time constants is necessary for increased speed and functionality on a chip. We are currently attracting a considerable research interest toward developing thermally stable polymer material with a low dielectric constant.

The complex dielectric permitivity (ε^* given by the equation $\varepsilon^* = \varepsilon' + \varepsilon''$ where ε' is the real component of the dielectric constant and ε'' is the imaginary component of the dielectric constant, has been measured as a function of frequency at constant temperature. The dielectric loss tangent is defined by $\tan\delta = \varepsilon'' / \varepsilon'$ and was determined as a function of frequency.

The dielectric constant ε' and dielectric loss tangent of polymers **PIKs-11b**, **12a**, and **13** are displayed from 10^{-2} to 10^{6} Hz. Figures 3.1-15a-c presents the dependence of real dielectric constant values (ε') on frequency. The frequency dependencies are typical for all the tested polymers at 25 °C. By increasing the frequency from 10^{-2} to 10^{-6} there is no change in ε' appeared, therefore, the dielectric constant remains constant within a wide range of frequencies at 25 °C. The dielectric loss tangent values are small due to the small values of ε'' of complex permittivity. The dielectric constants for all the polymers at 1 Hz, 100 Hz, 1 KHz and 1 MHz are listed in Table 3.1-11. The values at 1 MHz are in the range 2.71–3.08. These low values of the dielectric constant are very similar to those reported for related polyphenylquinoxalines[237] and are even lower than that of "H Film", polyimide kapton film a polyimide which is prepared from pyromellitic dianhydride and 4,4`-diaminodiphenylether which is one of the most preferred high-performance dielectrics in microelectronic applications having a dielectric constant of 3.5[238] (Table 3.1-12) (Figure 3.1-16). In addition to the low values of the dielectric constants, PIKs have low and adequate glass transition temperatures (T_gs) over kapton and this may make them easily processable. That qualifies the present PIK polymers as potential candidates for use in high-temperature processing of high-speed integrated circuits. The values in Table 3.1-11 also show that more flexible meta-linked diamine systems give lower ε' than the corresponding para-linked systems. Some have speculated that this factor is related to the free volume of the polymer[239] since a meta-

substituted system should have a higher degree of entropy. Furthermore, the presence of an oxy bridge in PIK polymers might result in lower ε' values than the presence of a carbonyl bridge in PIK polymers. The oxy bridge effect is well-known in the literature in case of polyimides.[240]

Poly(imino ketone)s might be introduced into electronics packaging as dielectric materials in order to decrease packaging delays, meaning that signal delays caused by the interaction of the electrical signal with the dielectric medium of the packaging would be reduced. PIKs might be chosen for this role primarily because of their good thermal stability, low T_gs, comparatively low and consistent dielectric constants in comparison with polyimides.[241,242]

Outlook

PIKs showed two advantages over Kapton, one is the low and consistent dielectric constants and the second is the low and adequate glass transition temperatures (T_gs). Recently, considerable attention has been focused on photosensitive polyimides because they can be patterned by exposure to UV light, which thus reduces the number of required processing steps,[243] therefore, synthesizing photosensitive PIKs might be reseult in an interesting dielectric material.

Table 3.1-11: Dielectric constant at selected frequencies and different temperatures for PIKs (**samples: PIKs-11b**, **PIK-12a**, and **PIK-13**) calculated from the dielecric spectra data sheet.

Polymer Code	Frequency (Rad/S)	$\varepsilon^{'}$ at 25 °C	$\varepsilon^{'}$ at 100 °C	$\varepsilon^{'}$ at 200 °C	$\varepsilon^{'}$ at 230 °C	$\varepsilon^{'}$ at 260 °C	$\varepsilon^{'}$ at 300 °C
PIK-11b	1 Hz	2.78	2.86	3.45	3.77	5.80	3.89
	100 Hz	2.78	2.85	3.25	3.39	4.14	_c
	1 KHz	2.78	2.85	3.23	3.34	3.89	_c
	1 MHz	2.78	2.85	3.21	3.31	3.56	3.89
PIK-12a	1 Hz	3.08	3.17	3.75	5.27	_c	_c
	100 Hz	3.08	3.50	3.57	4.36	_c	_c
	1 KHz	3.07	3.50	3.52	3.98	4.63	5.10
	1 MHz	3.07	3.50	3.48	3.63	3.80	4.40
PIK-13	1 Hz	2.72	2.85	_c	_c	_c	_c
	100 Hz	2.72	2.83	_c	_c	_c	_c
	1 KHz	2.71	2.83	6.30	7.00	6.80	6.30
	1 MHz	2.71	2.82	4.10	5.05	5.50	5.42

C: Conductivity process begins.
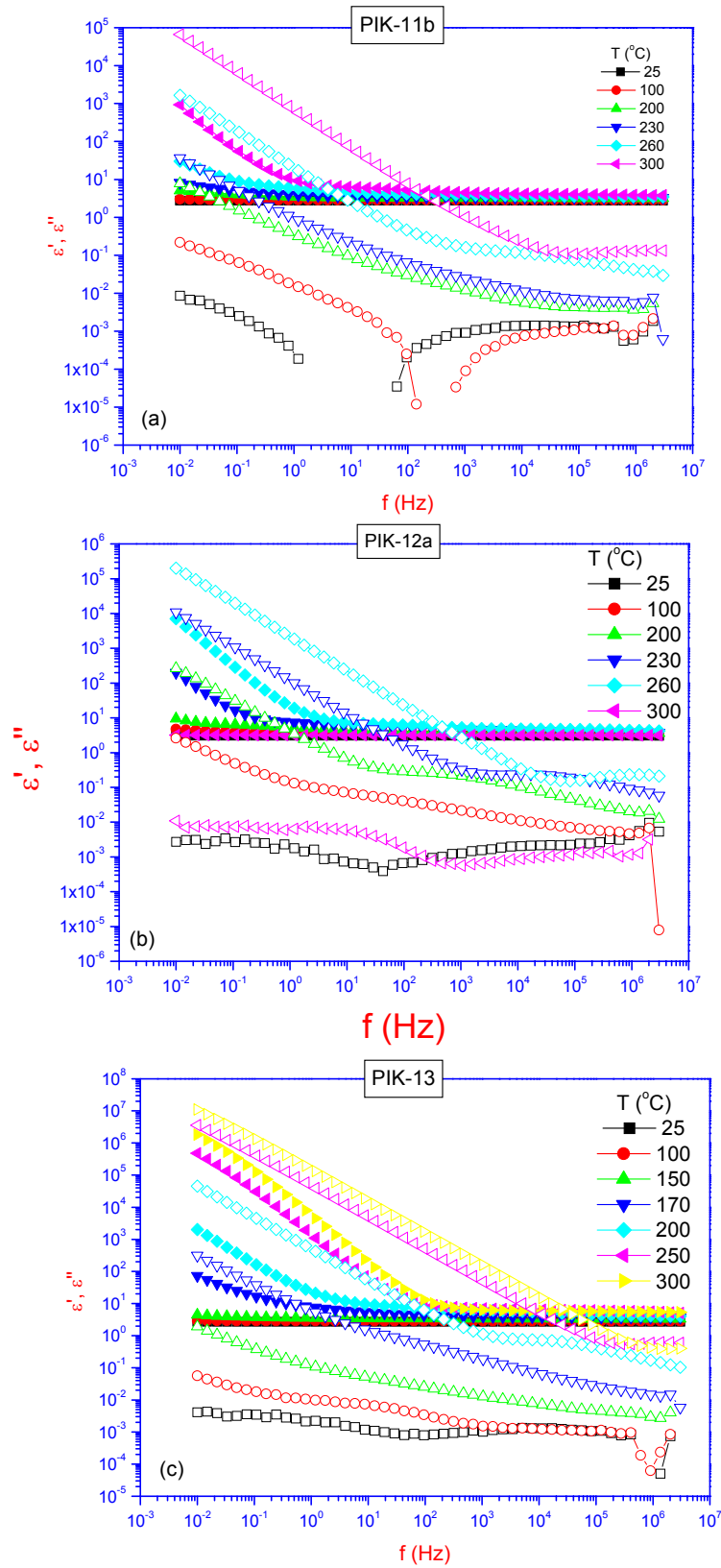
Figure 3.1-15a-c: Dependence of dielectric constant (ε') and dielectric loss (ε'') vs. frequency at different temperatures of **PIKs-11b**, **PIK-12a**, and **PIK-13**.

Table 3.1-12: The values of dielectric constant of the tested PIK polymers were in the range
of 2.71- 3.08.

Polymer Code	Glass transition temperature °C	Dielectric constant at 25 °C 1 MHz
Kapton[238]	385 °C	3.5
PIK-11b	212 °C	2.78
PIK-12a	220 °C	3.07
PIK-13	154 °C	2.71
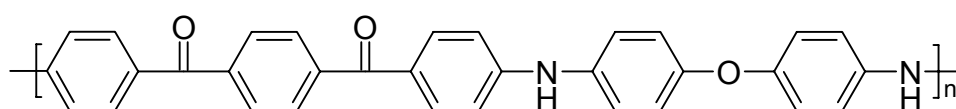
PIK-11b
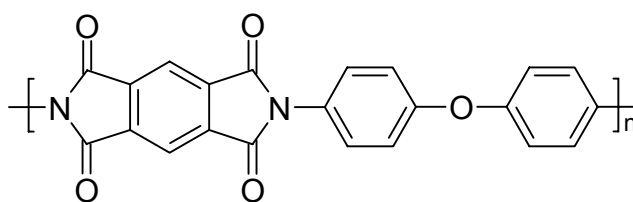
Kapton

Figure 3.1-16.

X-Ray techniques

X-ray diffraction is a good means of determining the degree of crystallinity or the amorphous nature of the polymer according to the diffraction pattern. X-rays are generated when a high energy beam of electrons strikes a target. The incident electrons either radiate X-ray photons as they are rapidly decelerated (Bremsstrahlung- `braking radiation') or eject electrons from the innermost shells of the target atoms. In the former case the X-rays have a range of wavelengths; in the latter case electronic rearrangement within the target atoms results in the emission of X-rays of wavelengths characteristic of the target material.

X-rays are scattered by variations in electron density. Where the electron clouds are ordered with respect to each other the scattered X-rays can interfere according to the Bragg condition to produce a diffraction pattern characteristic of the ordering. Bragg's Law states:

$$n\lambda = 2d. \sin \theta \qquad \qquad \text{(equation 1)}$$

where

λ is the X-ray wavelength

d is the spacing between the atomic planes

θ is the angle between the X-ray beam and the atomic plane
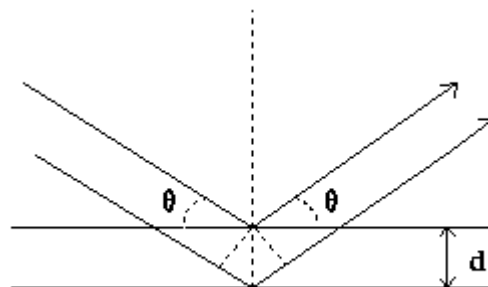
Figure 3.1-17: X-ray reflection from atomic planes.

Constructive interference occurs for integer values of n. By measuring for a known wavelength the Bragg spacing d can be determined.

X-ray diffraction can be used as a means of estimating the degree of crystallinity by separating the components of a diffraction pattern due to crystalline and amorphous regions. This estimate may well differ, however, from an estimate obtained by a different technique such as density measurements, due partly to a contribution to the amorphous halo by diffuse scattering from crystalline regions.[244] If a purely amorphous specimen of a crystallisable polymer can be prepared, and the crystalline reflections do not interefere with the amorphous halo, then the scattered intensity is assumed to be simply the sum of the scattered intensities from the crystalline and amorphous regions and the degree of crystallinity can be calculated from their relative magnitude.

Wide-angle diffraction (WAXD) is able to access correspondingly smaller features such as chain packing in crystalline regions. On the smallest scale, the technique is sensitive to correlations between nearest neighbors in polymer chains and to correlations in the distances separating chains. It is therefore possible to investigate both tacticity and conformation as well as orientation in drawn polymer fibres. If, for example, an amorphous polymer is cold drawn, the typical diffuse halo can develop increased intensity in the diffuse halo perpendicular to the draw direction and reduced intensity elsewhere (Figure 3.1-18). This is due to the molecular orientation conferring a degree of order in the material.

A semicrystalline polymer will typically exhibit an amorphous halo and several sharp concentric rings associated with the randomly oriented crystalline regions. If such a polymer is uniaxially oriented the X-ray diffraction pattern-called a fibre pattern will develop symmetrically spaced high intensity spots and arcs characteristic of regular features in the crystalline regions.
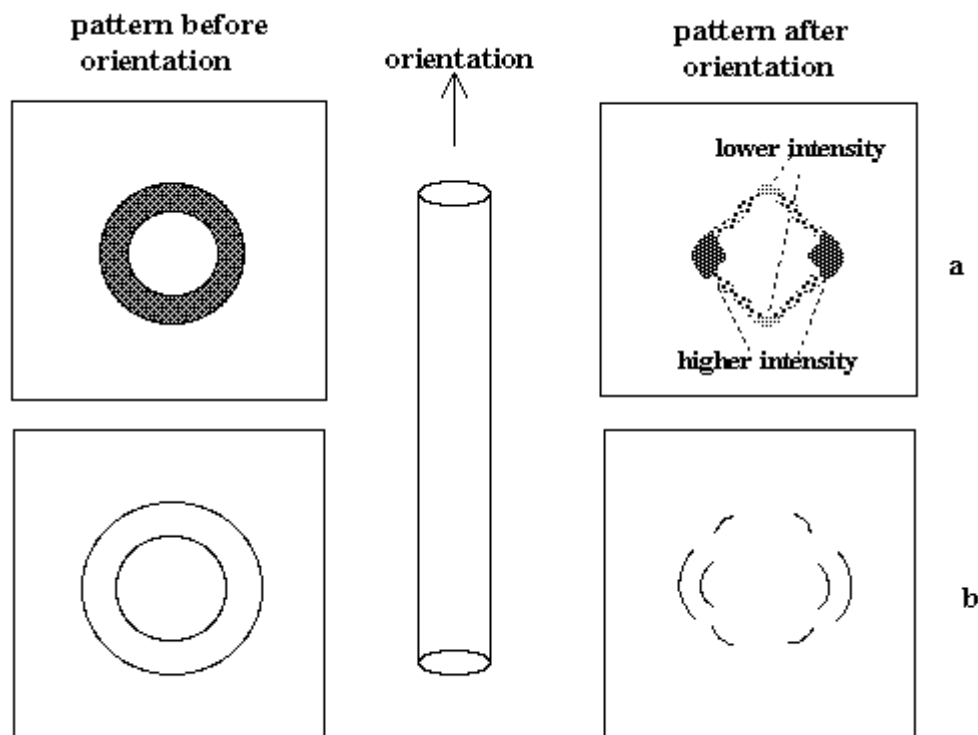
Figure 3.1-18: Effect of orientation on a) the amorphous halo and b) concentric ring pattern.

To obtain fibre patterns of a uniaxially oriented polymer, a number of fibres must be stacked to give a sufficient scattered intensity. Notice in Figure 3.1-18 that sharp arcs are not present on the meridian. In order to obtain information about spatial correlations in this direction the specimen must be tilted so that the deformation axis is not perpendicular to the plane containing the incident and scattered X-ray beam. Patterns are generated over a range of such inclination angles to give a complete picture of the orientation state of the polymer. More complex orientation states e.g. biaxial, require many experiments exploring diffraction as a function of variation in the azimuthal angle as well as the angle of inclination. This 3-d mapping is known as a pole figure. In small angle X-ray scattering (SAXS) fluctuations in electron density over dimensions of typically 3-40 nm contribute to the diffraction patterns.

Thus the long period of crystalline lamellae can be investigated along with information on the initial stages of crazing and microporosity in fibres. The electron density is different not only for crystalline and amorphous regions, but also in microvoids within the polymer. The small angle diffuse scattering is equivalent to the sum of scattering from many large, irregularly spaced particles. In synthetic fibres this diffuse scattering is due, primarily, to microvoids.[244]

As the scattering angle is inversely proportional to the correlating distance, an oriented specimen results in an elongation of the diffuse small angle scatter perpendicular to the orientation direction; in many spun synthetic fibres this effect is due mostly to elongation and orientation of the microvoids. One way of confirming that the diffuse patterns is due to microvoids is to perform a series of SAXS experiments on swollen specimens.

Instrumentation:

X-rays are usually generated in a vacuum from energetic electrons which strike a cooled anode (at Daresbury a synchrotron radiation source provides X-rays). Part of the energy of the electrons is converted into X-rays. A copper anode results in two characteristic X-ray wavelengths K_α and K_β. Unwanted wavelengths can be filtered out by the use of, for example, Ni foil which isolates a CuK_α. Wavelength selection before or after diffraction by the specimen can be made *via* crystal monochromators which are also governed by the Bragg condition. Detection of X-rays is by use of either proportional or scintillation counters (Figure 3.1-19). Both produce electrical pulses and a pulse height analyser can be used to discard unwanted signals and thus lower the background. X-ray diffraction patterns can be recorded on ``photographic" film.
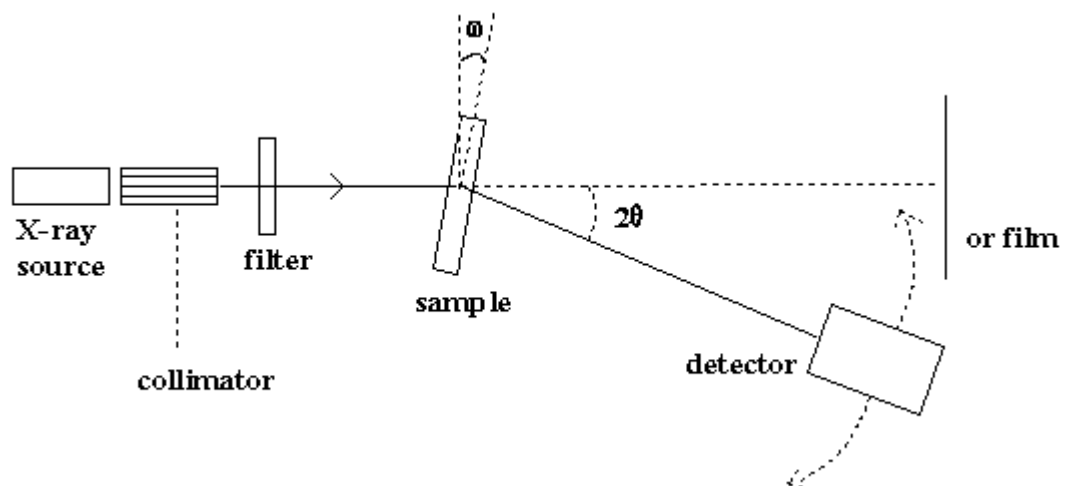
Figure 3.1-19: Schematic of an X-ray experiment
Output is in the form of intensity versus angle.

Wide-angle X-ray diffraction of PIKs

The wide-angle X-ray diffraction patterns of all the polymers over the 2θ range of 5-35° are shown in Figures 3.1-20 and 3.1-21. The diffraction arising from the crystallites is observed which showed crystalline pattern of polymers **PIK-11a**, **11b**, and **11c** at 12.2°, 18.5°, 24.5°, 29.5°, 12.8°, 18.3°, 23.2°, 12.6°, 18.4°, 23.9°, and 29.5°, respectively (Figure 3.1-20). This may be attributed to the existance of the rigid p-diiminophenylene or p-diiminodiphenyl ether segments in their polymer backbones and at the same time the absence of bulky groups such as *tert*. butyl or isopropylidene groups, leading to a better packing of the polymer chains.

However, only the broad halo arising from the amorphous region of polymers (**PIK-12a**, **13**, **14a**, **14b**, **15**, and **16a**) is observed at 17.8°, 18.1°, 17.2°, 18.4°, 16.8°, and 17.2°, respectively (Figure 3.1-21). All polymers despite the presence of the rigid secondary amine ring, revealed essentially amorphous patterns. Obviously, the bulky *tert*. butyl and/or isopropylidene groups hindered chain packing and reduced the level of ordering, thus leading to the amorphous nature of the polymer. The amorphous nature of these polymers was also reflected in their good solubility.

By comparing WAXD of both PIKs and poly(ether ketone)s (PEKs), the latter polymers exhibited semicrystalline behavior and no amorphous behavior was detected.[245-247] We can conclude that insertion of *tert*. butyl group and/or isopropylidene groups into the repeating units of the polymers **PIKs-12a**, **13**, **14a**, **14b**, **15**, and **16a** resulted in a significant increase of the amorphous nature of the polymer. However, the absence of these groups and at the same time the presence of the rigid secondary amine rings in the backbone of polymers **PIKs-11b**, and **11c** showed a significant increase of the crystalline nature of them. This is despite the presence of a kinked ether group which is known to induce loose chain packing.[248]

In order to get an idea about possible intermolecular order in the material, wide and small angle X-ray scattering experiments have been performed using in both cases 2D intensity recording systems (Bruker) and a CuKα radiation (λ=0.154 nm). The scattered intensity distribution vs. the scattering vector ($s = 2\sin\theta/\lambda$, where 2θ is the scattering angle) for the **PIK-11a** sample is shown in Figure 3.1-22. The intensity has been averaged over the azimuthal angle. The diffractogram indicates a clear ordering within the sample which can be considered as a mesophase with some intra-and intermolecular correlations indicated by the four intensity maxima detected.

74

Oriented **PIK-11a** material would allow distinction of intramolecular distance correlations in relation to the polymer orientation. Unfortunately, it was not possible to obtain a macroscopically oriented **PIK-11a** material by a plastic flow at high temperatures attempted up to 250°C using a miniextruder.[249] This is due to the hardness of the pressurized **PIK-11a** sample which indicates a high stability of the solid state until high temperature. Nevertheless, a scheme of an idealized local arrangement of the polymers can be suggested. It takes into account estimated intra-and intermolecular dimensions on one hand and the correlation distances determined form the scattering on the other hand. Such a structural scheme is presented in Figure 3.1-22 and suggests a kind of molecular sheets with locally aligned polymer backbones kept in the well correlated distances by the hydrogen bonding. In such structure two dominant correlation distances can be distinguished. The first is the intramolecular distance correlation between the neighboring phenylene rings along the backbone especially in the extended backbone conformation. The phenylene-phenylene repeat distance can be estimated as being of the order of 0.5 nm when typical bond lengths and angles are assumed. This correlates well with the reflection **C** in the scattered intensity distribution. The values of the correlation distances are given in Table 3.1-13. The second well distinguishable correlation is the intermolecular backbone-backbone distance correlation within the sheet which should be controlled by the hydrogen bonding between adjacent chains. The structurally estimated distance between the backbones for the structure presented in Figure 3.1-23 should be 0.725 nm which perfectly correlates with weak but distinct reflection **A** seen in Figure 3.1-22. The reflection **B** in the scattering pattern is exactly in a double distance on the s coordinates as **A** and can be considered as a second order one but related to the same correlation period as **A**. The last reflection, **D**, corresponds to the distance of nearly 0.3 nm and can be attributed to the correlation distance between the sheets. The small angle X- ray scattering detected was intensive but did not indicate any characteristic correlation distances and is attributed as coming mainly from the porosity of **PIK-11a** powder.

Table 3.1-13: Parameters of the scattering intensity maxima in the diffraction pattern shown in Figure 3.1-22. (positions of the peaks and corresponding correlation distances are given).

Intensity peak	s_{max} [nm^{-1}]	$d=1/s_{max}$ [nm]	d-expected [nm]
A (1)	1.37	0.730	0.725
B (2)	2.77		
C	2.08	0.48	0.5
D	3.31	0.30	0.30
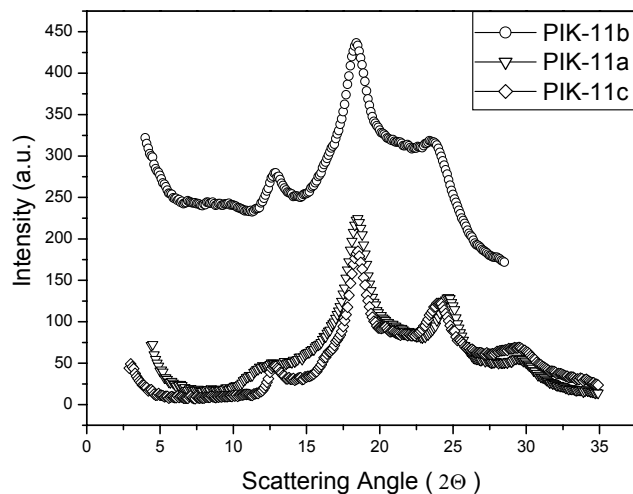
Figure 3.1-20: Wide-angle X-ray diffractograms intensity vs Bragg angle graph for powders of polymers **PIKs-11c**, **PIK-11a**, and **PIK-11b**.
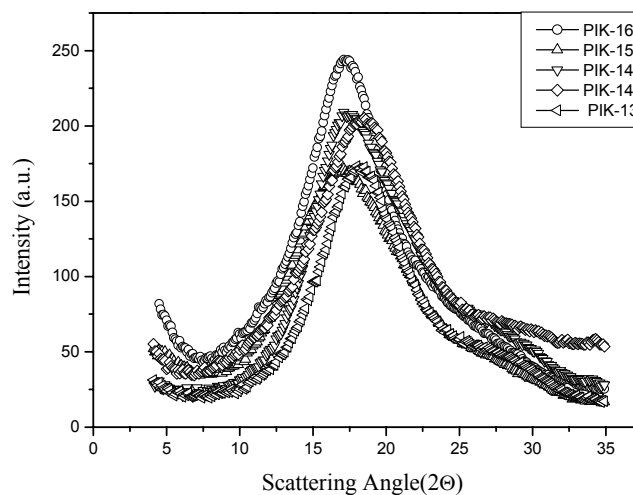
Figure 3.1-21: Wide-angle X-ray diffractograms intensity vs Bragg angle graph for powders of polymers **PIKs-13**, **PIK-14a**, **PIK-14b**, **PIK-15**, and **PIK-16a**.
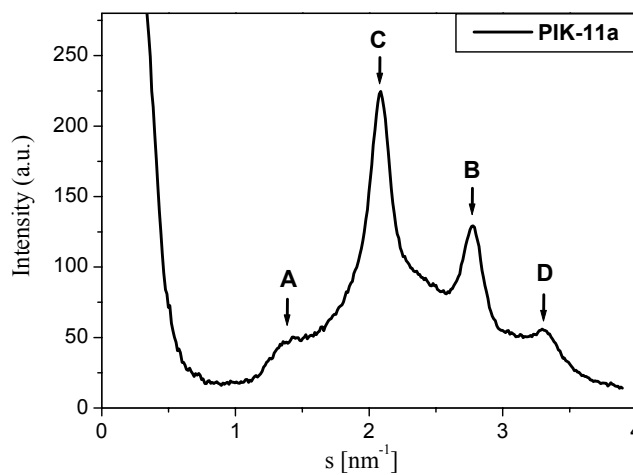
Figure 3.1-22: Wide-angle X-ray diffractogram intensity vs the scattering vector for **PIK-11a**.
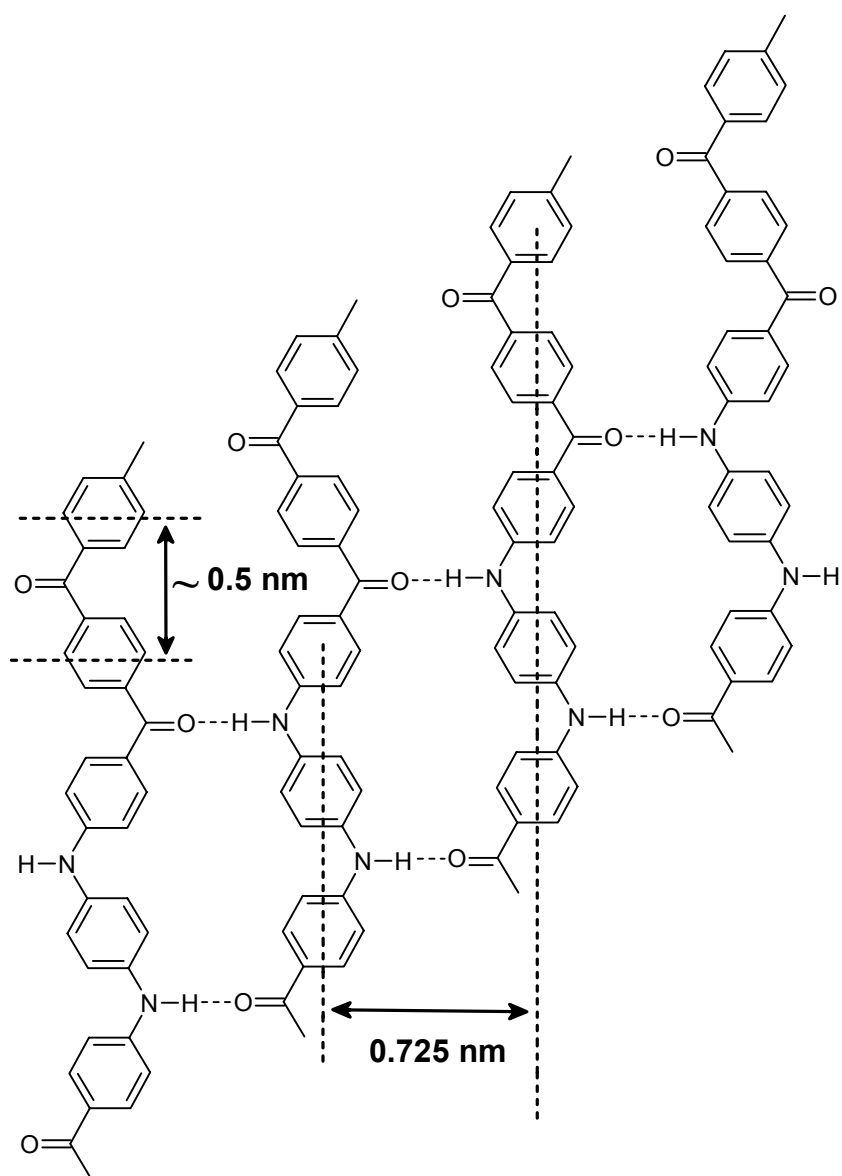
Figure 3.1-23: A parallel conformation suggested arrangement of **PIK-11a** backbone and
related distances.

Conclusions:

Soluble poly(imino ketone)s with high molecular weights have been obtained by a Pd-catalyzed polycondensation (Buchwald-Hartwig reaction) of aromatic dibromides and aromatic amines. Various poly(imino ketone)s were synthesized by using different monomers. Four different ligands were used successfully in the Pd-catalyzed process of which the Pd/BINAP system was found to be the most effective catalyst, producing the highest yield and highest molecular weight polymers. These polymers may be considered as an analog to polyaramides since hydrogen bonding is observed by broadening of the associated imino group (NH) vibrational bands, while the solubility is enhanced. On the other hand due to the incorporated benzophenone and ether moieties one can expect similarities to polyetherketones (high Young modulus, low entanglement molecular weight).[250] All these expectations are already confirmed by initial mechanical and TGA measurements indicating that PIKs can be considered as a new class of high-performance polymers with a good mechanical behavior and high thermal stability. These investigations are presently extended and are supported by dielectric spectroscopy. The values of the dielectric constants at 1 MHz were in the range 2.71–3.08. These low values of the dielectric constant are very similar to those reported for related polyphenylquinoxalines[237] and are even lower than that of "H Film", polyimide kapton films, a polyimide which is prepared from pyromellitic dianhydride and 4,4`-diaminodiphenylether which is one of the most preferred high-performance dielectrics in microelectronic applications having a dielectric constant of 3.5[238] (Table 3.1-12). In addition to the low values of the dielectric constants, PIKs have low and adequate glass transition temperatures (T_gs) over kapton and this may make them to be easily processable.

One major advantage in comparison to the established PEKs and polyaramides is already obvious. In comparison to PEKs one can use cheaper monomers e.g. chloro- or bromofunctionalized aromatic ketones instead of the corresponding difluoro compounds. Also the synthesis of „activated" intermediates, as is the case for the preparation of polyaramides by converting the aromatic esters to e.g. acid chlorides, is avoided. Furthermore, many diamines and dibromo compounds are readily available giving a fast access to numerous new polymers with optimized properties such as thermal stability, mechanical behavior or solubility. The amorphous polymer structure of **PIK-12a**, **13**, **14a**, **14b**, **15**, and **16a** was proven by DSC up to 250 °C, showed a single T_g, and the absence of a melting temperature suggested their amorphous polymer structure. The DSC results were supported by wide-angle

X-ray measurements to prove the amorphous (**PIK-12a**, **13**, **14a**, **14b**, **15**, and **16a**) and the semicrystalline (**PIK-11a**, **11b**, and **11c)** polymer structure.

It was proven by X-ray patterns that insertion of one *tert*. butyl group only or with isopropylidene groups into the repeating units of the polymers **PIKs-12a**, **13**, **14a**, **14b**, **15**, and **16a** resulted in a significant increase of the amorphous nature of the polymer. However, polymers **PIKs-11c**, **11a**, and **11b** despite the presence of a kinked ether group in the polymer backbone, showed a significant increase of the crystalline nature of the polymer. This is quite clear because of the absence of any of the bulky *tert*. butyl, isopropylidene groups and at the same time the presence of the rigid secondary amine rings in the polymer backbone.

The improvement in solubility behavior of PIKs could probably be attributed to the combined effects of the pendant *tert*. butyl group only or with either two isopropylidene groups in the polymer backbone, thus, good solubility was obtained.

CHAPTER III

RESULTS AND DISCUSSION

Part 2

3.2 Novel poly(imino alcohol)s (PIAlco)s
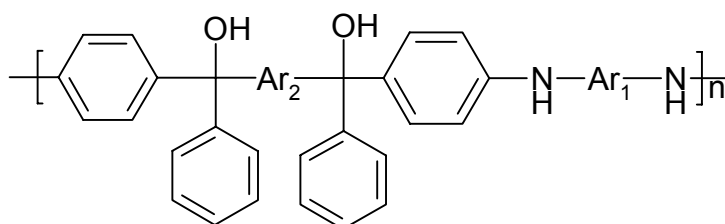
The keto group is one of the most powerful functional groups in organic synthesis. It is quite obvious, that one might also apply its enormous potential in polymer synthesis. Ketones can be involved directly in the formation of the polymer, either as an active site as, e.g. in the formation of poly(phenlene vinylenes) *via* Wittig reactions or as an activating group, e.g. for the nucleophilic aromatic substitution in the preparation of aromatic polyethers. Once introduced into the polymer, the carbonyl function offers a wide range of possibilities for further modification and tuning of the polymer properties. This approach is outlind herein by several examples including the synthesis of poly(imino ketone).

Grafting is by far the most important process for chemical modification of known polymers.[251] Graft copolymers are not only interesting on their own because of their physical properties and morphology, but they have also been applied as compatibilizers, coatings, surface modifiers, and adhesives.[252] Their attractivity stems from an easy access and from the broad range of possible comonomers, which allow for considerable tunability of the polymer properties.

Most of the graft copolymers are prepared by a grafting-from process wherein the grafting is initiated by a thermal[253] or radiation induced[254] radical formation on the polymer backbone. While these methods are inappropriate for the synthesis of well-defined copolymers for principle reasons,[255] it should be possible to control molecular architecture by using the method of anionic deactivation.[256] It was reported that a living anionic polymer was reacted with electrophilic functions of another polymer backbone.[257] This procedure is very efficient and reliable, because the high reactivity of carbanions guarantees a maximum grafting. Accordingly, side chains can be attached in a straightforward fashion. Moreover, the

graft copolymer, the backbone, and the grafts can be characterized separately, allowing determination of the individual molecular weights and thus of the composition of the copolymer.[258] Even though the distribution of grafts along the backbone is random, one should be able to control the average number of grafts by varying the stoichiometry of the nucleophile. Grafting of living anions to poly(ether ether ketone ketone)s was reported.[257]

It is also clear that carbanions due to their high nucleophilicity can attack carbonyl groups. So it is the aim to transfer this idea to poly(imino ketone)s to produce poly(imino alcohol)s. The latter is an intermediate to achieve the main goal of synthesizing poly(quinone diimine)s (cf. part 3, P. 96) for studying thermal stability, mechanical, and electrical properties. In this process approximately 100 % of the carbonyl groups can be converted and a high yield could be achieved. The effect of grafting on the thermal properties of the copolymers wil be discussed.

Synthesis of di-tertiary alcohol 1,4-bis(4-anilino-α-hydroxy-benzhydryl)benzene (11):
Both of the two carbonyl groups of 4,4′-bis(4-anilinobenzoyl)benzene (**10**) were attacked by phenyllithium as a carbanion with a high nucleophilicity to afford the di-tertiary alcohol 1,4-
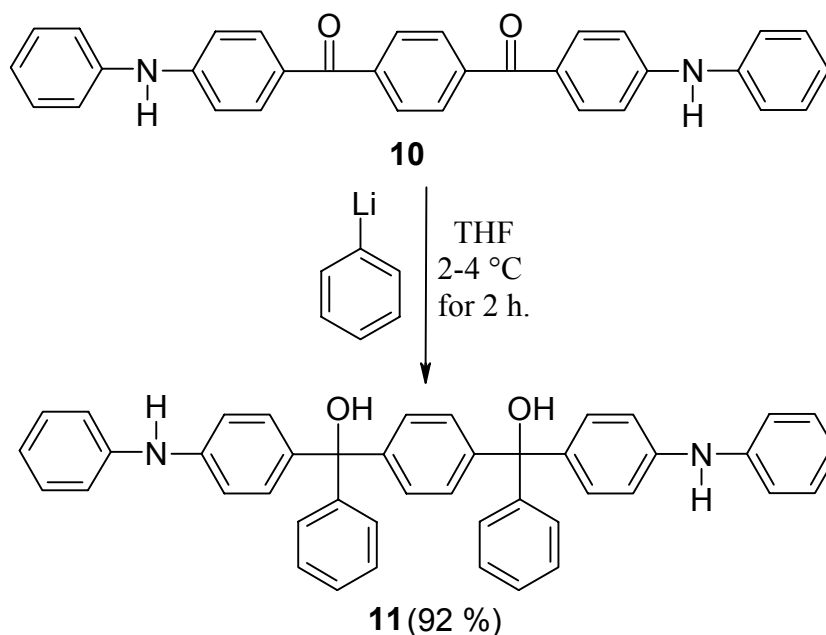
Scheme 3.2-1: Synthesis of ditertiary alcohol 1,4-bis(4-anilino-α-hydroxy-benzhydryl)benzene.

bis(4-anilino-α-hydroxy-benzhydryl)benzene (**11**) in 92 % yield. The structure was confirmed by mass (FD[+]), ^{1}H-NMR spectroscopy, FT-IR, U.V and elemental analysis and all methods

showed the agreement with the proposed structure. In particular, the ^{1}H-NMR spectrum of (**11**), which is shown in Figure 3.2-1, is in agreement with the predicted structure of (**11**).
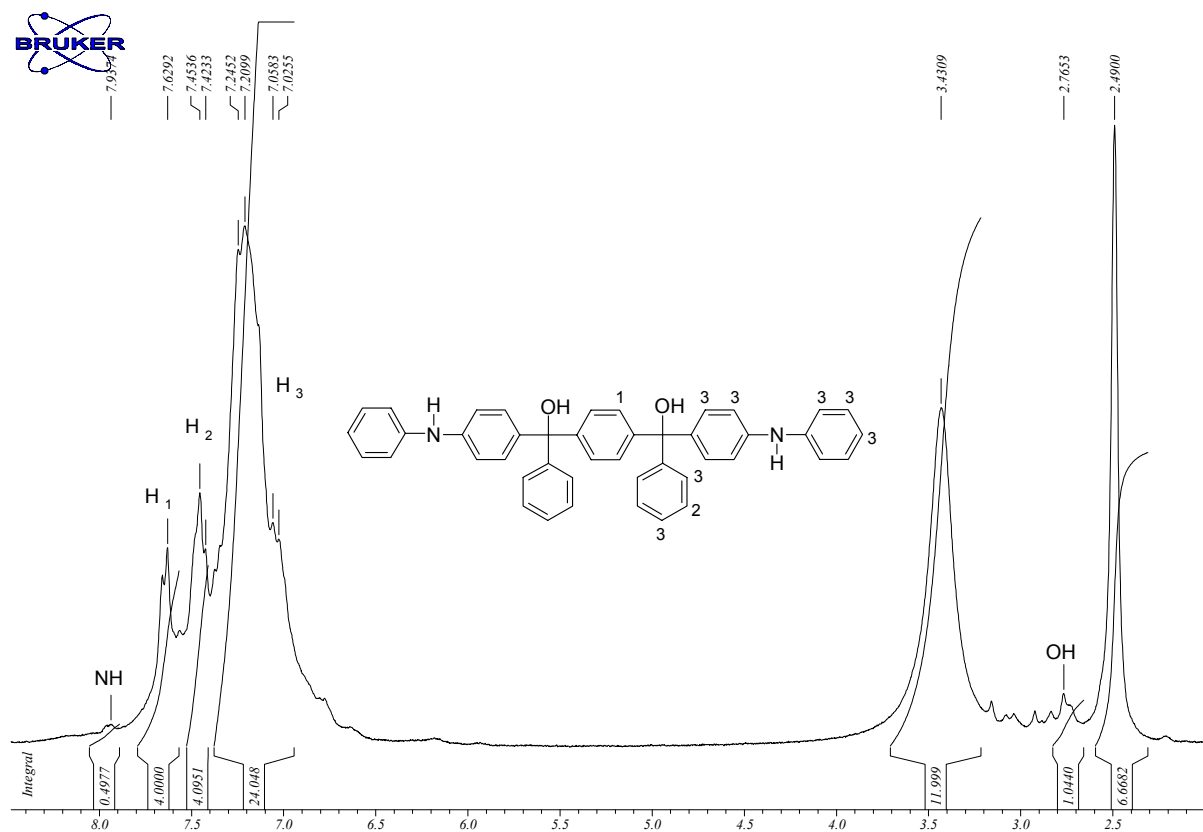
Figure 3.2-1: ^{1}H-NMR (250 MHz) spectrum of compound **11** recorded in DMSO-d_6.

FT-IR spectrum of compound **11** showed the absence of the carbonyl groups γ(C = O), the presence of the hydroxy groups γ(OH) appeared at 3550 cm^{-1} and imino groups γ(NH) appeared at 3390 cm^{-1} (Figure 3.4-2).
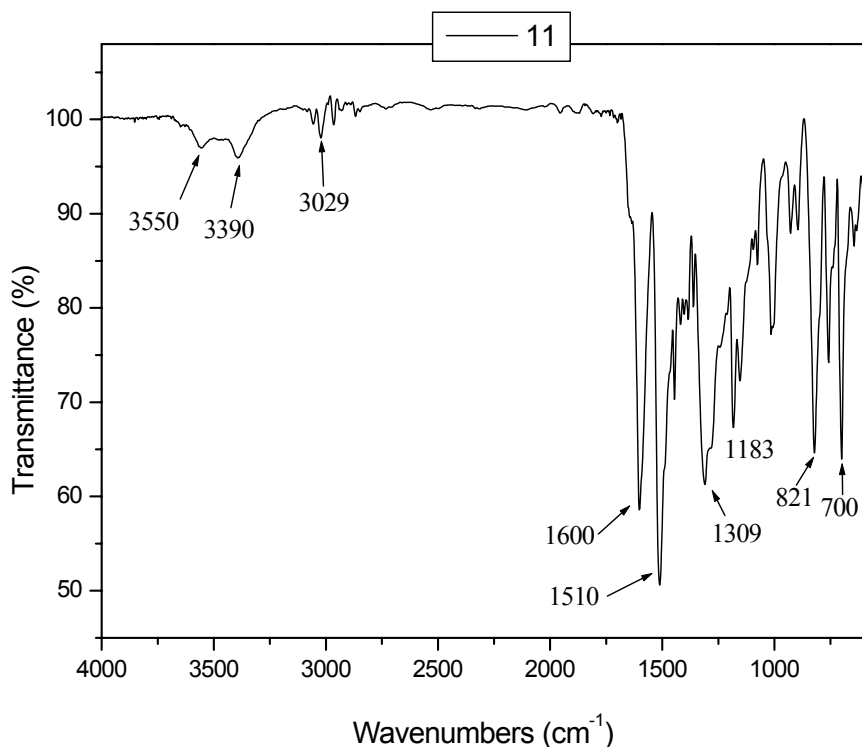
Figure 3.2-2: FT-IR spectrum of compound **11**.

From the FT-IR spectrum there is no detected reaction between phenyllithium and both of the two imino groups in 4,4ʹ-bis(4-anilinobenzoyl)benzene (**11**) (Figure 3.2-2). From the above one can conclude that by using 4.0 mmol of phenyllithium to react with 2.0 mmol of 4,4ʹ-bis(4-anilinobenzoyl)benzene the only possible reaction is the nucleophilic attack on the two carbonyl groups.

Figure 3.2-3 shows UV-vis absorption spectra of compounds **10** and **11**. Two broad absorption bands, one at 296 nm and the other at 368 nm, were detected for compound **10** while, only a broad absorption band at 364 nm for compound **11** could be recorded. Compound **10** has lower ε-value than compound **11** (ε_{368} = 40 400 L. mol^{-1}. cm^{-1}, ε_{364} = 55 000 L. mol^{-1}. cm^{-1}, respectively). This is due to the presence of the π-system containing donor-acceptor substituents in compound **10**. This effect is similar to that reported in the literature for the thermotropic dyes based on amino-substituted perylendicarboximides.[259]
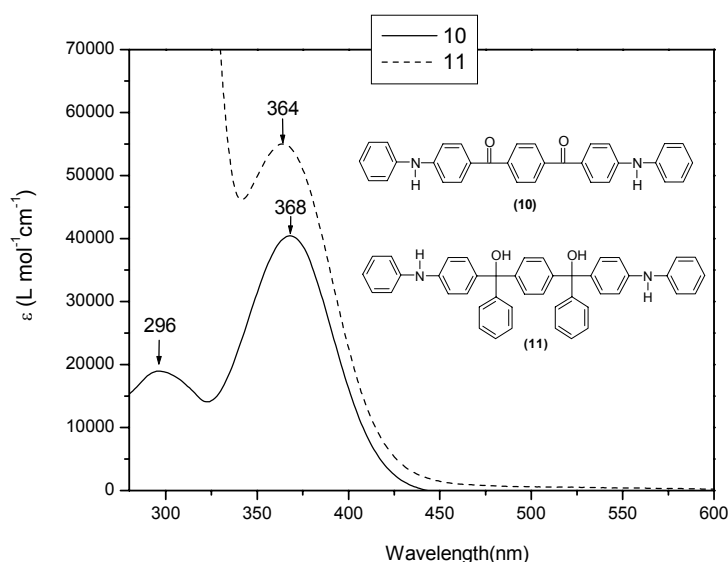
Figure 3.2-3: UV-vis absorption spectra of compounds **10** and **11** (2×10^{-5} M in CHCl$_3$).

Nucleophilic addition of phenyllithium to PIKs

The carbonyl group appeared as an ideal target because of its high reactivity, which provides selective addition under formation of tertiary alcohols. Therefore, we chose poly(imino ketone)s PIKs as polymers for anion deactivation. Since satisfactory results were obtained from the reaction of phenyllithium and compound **10** to afford compound **11**, the synthesis of PIAlco polymers using this new synthetic route was attempted to produce poly(imino alcohol)s. In all cases phenyllithium was used in 2:1 molar ratio to the PIKs

It was found in the course of the grafting reaction that the para-derivatives **PIK-11b**, **12a**, and the meta-derivatives **PIK-13**, **14b**, **15**, and **16a** are suitable for the desired reaction. It is important to note that the poly(imino ketone)s **PIK-11b**, **12a**, **13**, **14b**, **15**, and **16a** are quantitatively transformed into the poly(imino alcohol)s **PIAlco-11b**, **12a**, **13**, **14b**, **15**, and **16a** (Scheme 3.2-2). 100 % conversion of the carbonyl groups to alcohols was already achieved and no carbonyl groups remain as demonstrated by FT-IR spectra (Figures 3.2-4). While, in case of **PIK-11a** and **14a**, no conversion was detected at all this may be due to the poor solubility of **PIK-11a** and **14a**, therefore, their corresponding poly(imino alcohol)s were not obtained (Scheme 3.2-2).

Scheme 3.2-2: Synthesis of poly(imino alcohol)s.

Solubility behavior of PIAlcos

Except polymer **PIAlco-13**, all the **PIAlcos** showed poor solubility in all the known organic solvents, therefore, **PIAlco** polymers could not be dissolved or swollen in polar aprotic solvents, such as N-methylpyrrolidinone (NMP), dimethylacetamide (DMAc), dimethylsulfoxide (DMSO) and dimethylformamide (DMF) or in common organic solvents, such as THF, methanol, acetone, dichloromethane and chloroform, at room or high tempertaure or by any dissolution means.

Since most **PIAlcos** showed poor solubility, the molecular weights were measured only for the soluble polymer **PIAlco-13** of the PIAlco polymers by GPC (calibrated by polystyrene standards). The M_n value was 16 400 and the M_w value was 34 500 while the molecular weight of the corresponding **PIK-13** was 11 000 for M_n and 19 000 for M_w. The increasing of M_n value can be explained by attaching two phenyl rings per every repeating unit. However, this increasing of M_n value is slightly higher than expected. This is due to the polymer functionality which changed the hydrodynamic radius and influenced the elution time during the GPC measurement. Consequently, no degradation has occurred as a result of the addition of phenyllithium to PIKs.

FT-IR spectroscopy of PIAlcos

The structure of the **PIAlco** polymers were also confirmed by FT-IR. In all cases, the absence of the carbonyl groups γ(C = O), the presence of the hydroxy groups γ(OH) appeared between 3540 and 3550 cm^{-1} and imino groups γ(NH) appeared between 3394 and 3405 cm^{-1} were detected. Figure 3.2-4 showed the FT-IR spectrum of polymer **PIAlco-13.**
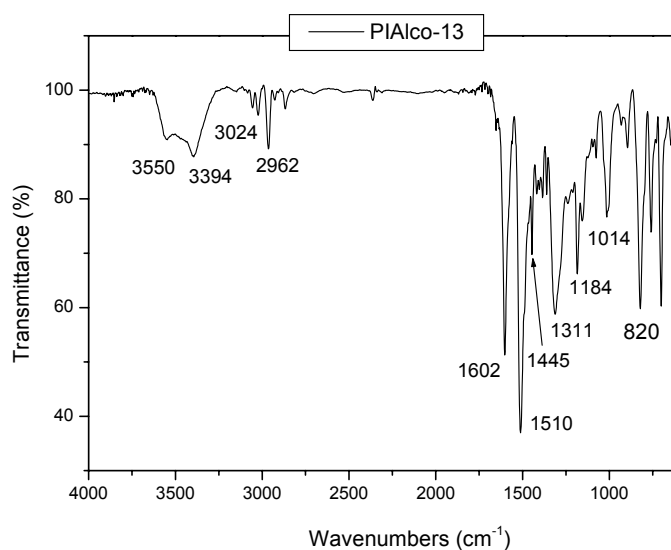
Figure 3.2-4: FT-IR spectrum of polymer **PIAlco-13**.
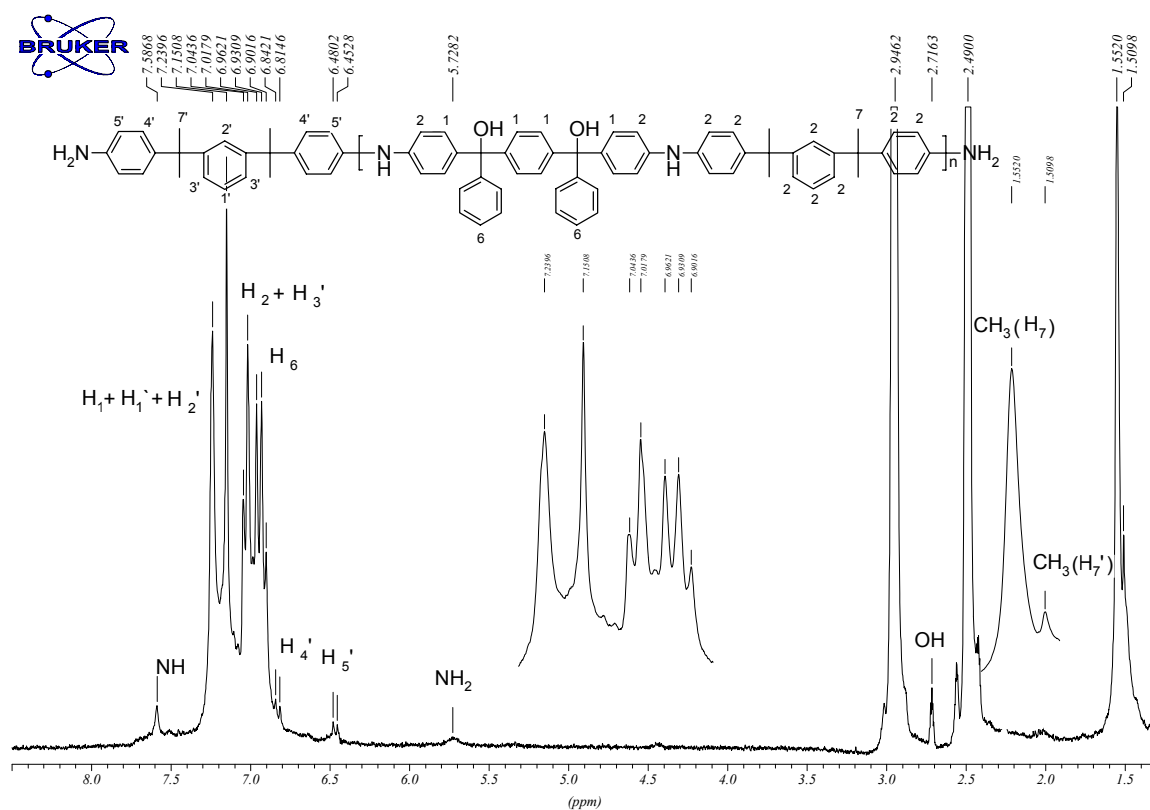
Figure 3.2-5: ^{1}H-NMR (300 MHz) spectrum of polymer **PIAlco-13** recorded in DMSO-d_6 at 373K.

Except polymer **PIAlco-13**, all the PIAlcos are insoluble in both polar aprotic solvents and common organic solvents, therefore, they remained largely uncharacterised. The ^{1}H-NMR spectrum of polymer **PIAlco-13** which is shown in Figure 3.2-5, was recorded in diluted DMSO-d_6 solution to achieve a good resolution of the ^{1}H-NMR peaks. Protons of the imino groups appear at the downfield region at 7.58 ppm. The intensity of this peak is lower than expected due to the hydrogen exchange taking place between the NH groups from the polymer and water present in DMSO-d_6. Two doublets and a multiplet at 7.19, 7.02 and 6.96-6.90 ppm were attributed to the aromatic protons H_1, H_2 and H_6 and two singlets at the upfield region at 2.71 and 1.55 ppm were assigned to the OH and the aliphatic protons of methyl groups derived from the polymer repeating unit. Peaks at 7.19, 7.19, 7.02, 6.82, 6.46, 5.72 and 1.51 ppm have chemical shifts characteristic of H_1`, $H_2$`, H_3`, $H_4$`, H_5`, NH_2 and CH_3 of the amine protons and these peaks were logically assigned to the aromatic and aliphatic protons of minute amounts of the terminal amine unit of polymer **PIAlco-13**.

The FT-IR spectrum of the poly(imino alcohol) **PIAlco-13** shows that there is no complete reaction between phenyllithium and the imino groups in the **PIK-13** (Figure 3.2-5), while by comparing the ^{1}H-NMR spectra before and after the nucleophilic reaction there is no suggestion of a partial reaction between phenyllithium and any of the two imino groups in some repeating units. From the above we can conclude that by using 4.0 mmol of phenyllithium to react with 2.0 mmol of PIKs the only possible reaction is the nucleophilic attack on the carbonyl groups

Thermal behavior of PIAlcos

Typical TGA traces in air and in nitrogen are demonstrated in Figure 3.2-6 for polymer **PIAlco-13** and **PIK-13**. The thermal stability was evaluated by a 5 % weight loss at the minimum temperature (Table 3.2-1). TGA curves revealed that the polymers were thermally stable up to 346 °C. The 50 % weight loss of the polymer took place at over 900 °C in nitrogen and 829 °C in air. The char yield at 600 °C was 58 % and 61 % in air and nitrogen.
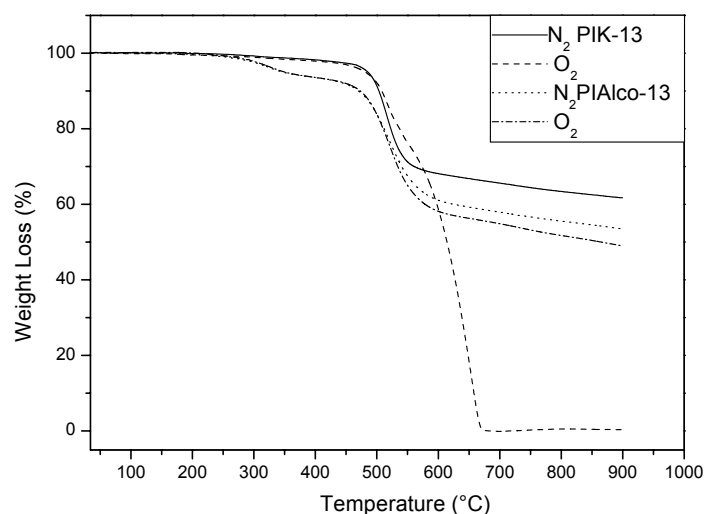
Figure 3.2-6: Comparison of the dynamic TGA of the copolymers **PIK-13** and **PIAlco-13**.
(in N_2, and in O_2, 10°C/min.).

By comparing the TGA thermograms in air and nitrogen for polymers **PIAlco-13** and **PIK-13** (Figure 3.2-6), it was observed that in air the 50 % weight loss of those polymers took place at 829 °C and at 613 °C respectively, but in nitrogen the 50 % weight loss was not observed up to 900 °C. In air the char yield at 600 °C was 58 % and 59 % respectively, but in

nitrogen the char yield at 600 °C was 61 % and 68 % respectively. The 50 % weight loss temperatures in addition to the high char yields at 600 °C in both air and nitrogen suggested that thermal degradation in air was significantly enhanced with respect to nitrogen. By comparing the thermal stability of polymer poly(imino alcohol) **PIAlco-13** and the corresponding **PIK-13** it was found that **PIAlco-13** was thermally stable up to 346 °C but **PIK-13** was thermally stable up to 478 °C. Therefore, **PIAlco-13** is less thermally stable than **PIK-13**.

Differential scanning calorimetry (DSC) of polymer **PIAlco-13** up to 250 °C showed a single T_g, suggesting a homogeneous amorphous copolymer structure. A representative DSC thermogram of the copolymers is illustrated in Figure 3.2-7. The glass transition temperatures of this copolymers **PIAlco-13** is 184 °C being lower than that of the corresponding polymer **PIK-13** which is 154 °C.
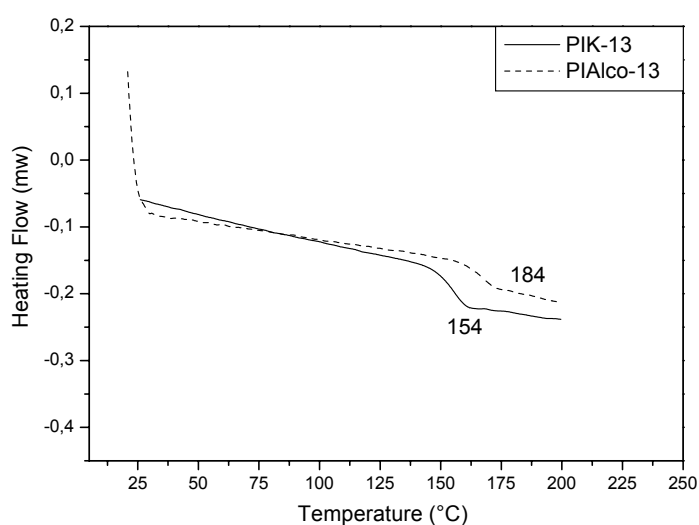
Figure 3.2-7: Comparison of DSC of **PIAlco-13** and **PIK-13**.

(in N_2, 10 °C/min)

The second heating scans were taken into consideration.

Table 3.2-1: Thermal behavior of **PIK-13** and **PIAlco-13**.

Polymer code	O_2 / N_2	$^aT_5$	$^bT_{10}$	$^cT_{50}$	$^dW_{500}$	$^eW_{600}$	Char yield at 600 °C^f	T_g Midpoint^g
PIAlco-13	O_2	350	464	829	17	42	58	184
	N_2	346	470	> 900	17	39	61	
PIK-13	O_2	478	507	613	8	41	59	154
	N_2	485	502	>900	9	32	68	

a) T_5: Temperature of 5 % weight loss; b) T_{10}: Temperature of 10 % weight loss; c) T_{50}: Temperature of 50 % weight loss; d) W_{500}: weight loss at 500 °C, determined from TGA curve; e) W_{600}: weight loss at 600 °C, determined from TGA curve; f) The remaining of the polymer at 600 °C; g) From the second heating traces of DSC measurements conducted with a heating rate of 10 °C min^{-1} in nitrogen.

Wide-angle X-ray diffraction

The wide-angle X-ray diffraction patterns of the polymer **PIAlco-13** over the 2θ range of 3-35° are shown in Figure 3.2-8. Polymer **PIAlco-13** revealed an essentially amorphous patterns. This may be attributed to the fact that the regularity of the repeating units in the polymer is disrupted by the different appearing orders of the imino and phenyl groups, thus leading to no chain packing of the polymer (Figure 3.2-8). Only the broad halo arising from the amorphous region is observed. By comparing the wide-angle X-ray of poly(imino oalcohol) **PIAlco-13** with wide-angle X-ray of the corresponding poly(imino ketone) **PIK-13**, it was observed that both of them showed only the broad amorphous halo without any crystalline pattern (Figure 3.2-8)
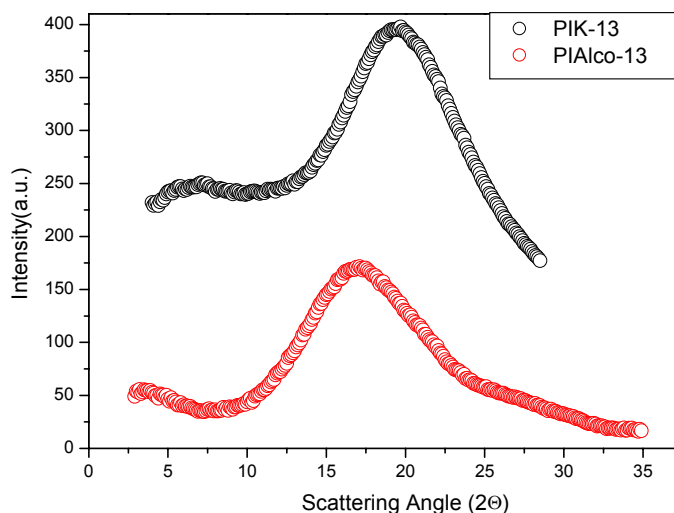
Figure 3.2-8: Wide-angle X-ray diffractograms intensity vs Bragg angle graph for powders of polymers **PIK-13** and **PIAlco-13**.

Dynamic mechanical measurements of PIAlco-13 and PIK-13.

We wanted to study the effect of the hydrogen bonding on the mobility of polymer chains in polymer **PIK-13** and **PIAlco-13** and the reason behind the higher T_g value in case of **PIAlco-13** than **PIK-13**.

Temperature dependencies of the real, G', and imaginary, G'', parts of the complex shear modulus were determined at a constant deformation frequency of 10 rad/s. under continuous cooling or heating of samples with the rate of 2 °C/min. The dependencies are

used to characterize the properties within a broad temperature range above the glass transition.

Figure 3.2-9 shows the thermo-mechanical characteristics of the two polymers. According to both the DSC and the mechanical measurements both polymers have glass transitions observed as specific heat steps and as the cross-points of G' and G'' at nearly the G'' maxima, respectively. The glass transition temperatures determined from the middle points of the specific heat steps are 154 °C and 184 °C for polymers **PIAlco-13** and **PIK-13**, respectively. They are slightly lower than the temperatures at which G' and G'' cross each other (compare Figures 3.2-9a and b). Different results from different experimental conditions such as temperature variation rate and the deformation rate were obtained. The difference in T_g is related to differences of the mobility of polymer segments and this can be well recognized from the master curves shown in Figure 3.2-10 and representing the frequency dependencies of G' and G'' at the reference temperature T = 210 °C, taken as an example. The difference in segmental mobility is temperature dependent and is characterized by temperature dependencies of the segmental relaxation times shown in Figure 3.2-11a. The dependencies can be described by the Vogel-Fulcher-Tamman relation.[260]

$$\log\tau = A + \frac{B}{T - T_\infty}$$

with the parameters given in Table 3.2-2. Fitted dependencies are shown in Figure 3.2-11a by solid lines. In comparison with the corresponding DSC results (Figure 3.2-11b), it can be noticed that in both examined cases the segmental relaxation times reach values of nearly 1000 seconds at the glass transition temperature determined in the above described way.

Table 3.2-2.

Sample	A	B[K]	T_∞ [K]
PIK-13	-9.6	311.8	402.0
PIAlco-13	-13.56	848.5	406.1

The hydrogen bonding in the sample **PIAlco-13** has a stronger effect on the mobility of polymer chains. This is reflected by the behavior of G' and G'' at higher temperatures (Figure 3.2-9a) and the related behavior at low frequencies (Figure 3.2-10). Whereas the sample **PIK-13** shows in this range a weak indication of polymer chain related relaxation and a terminal flow, the polymer **PIK-13** has an almost horizontal plateau of G' which extends to the highest temperatures and the lowest frequency measured. The behavior of the **PIK-13** sample is

typical for a polymer melt with linear chains shorter than the length necessary to create entanglements.[260,261] The other polymer **PIAlco-13** is structurally similar and without any specific interactions should show similar behavior as the first one. The plateau in the G' modulus at the level of approximately 0.5 MPa can be regarded as indication of cross-linking which in this case can be attributed to the hydrogen bonding connecting the relatively short polymers to a continuous network.[233] The behavior of this system at the lowest frequencies suggests an existence of a very slow relaxation within the network but a precise determination of it becomes impossible because of the lower thermal stability of this sample as indicated by the TGA traces shown in Figure 3.2-9c.
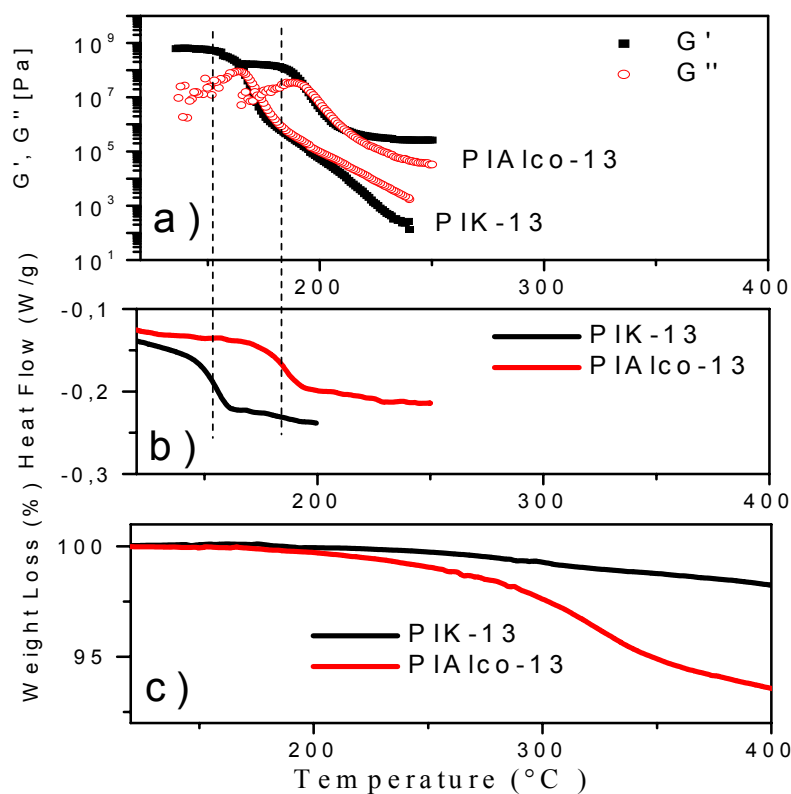
Figure 3.2-9: Temperature dependencies of (a) G' and G' determined in an isochronal dynamic mechanical measurement with the frequency of 10 rad/s., (b) the heat flow traces determined by means of the DSC under heating with the rate of 10K/min and (c) the weight loss determined in TGA experiments during heating with the rate of 10K/min.
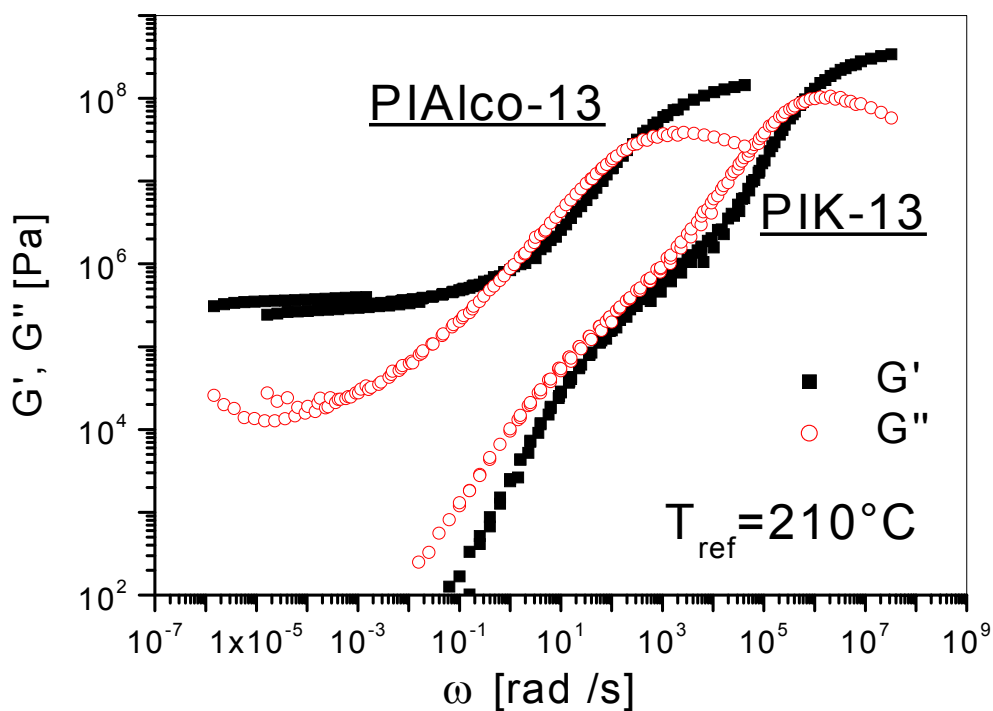
Figure 3.2-10: Dependencies of G' and G'' vs. frequency (master curves) for the two samples considered at the same reference temperature (T_{ref}).
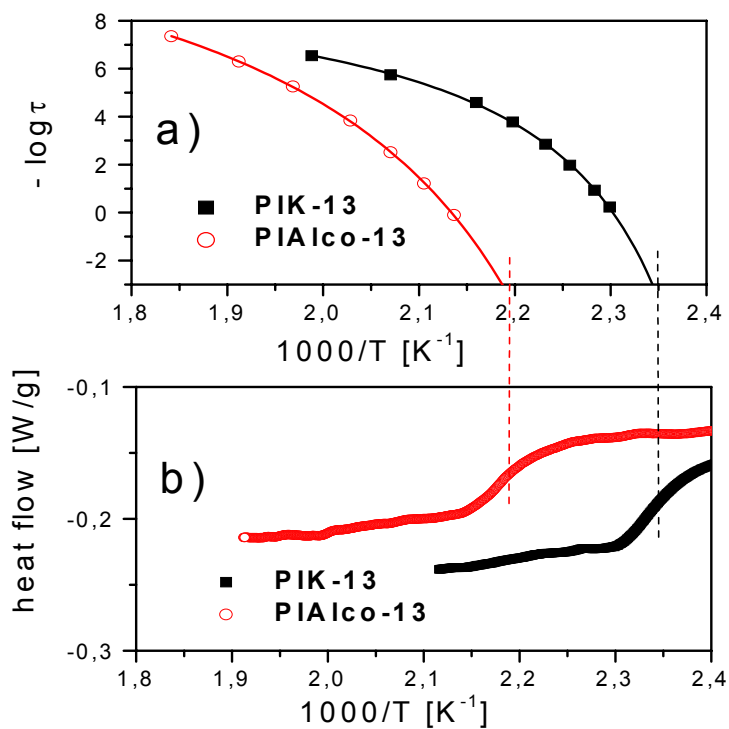
Figure 3.2-11: Temperature dependencies of the segmental relaxation times (a) with the corresponding DSC traces (b). The solid lines in (a) represent the VFT fits. The vertical dashed lines indicate the glass transition temperatures determined on the bases of the DSC traces in (b).

Conclusions:

Achieving poly(imino alcohol)s is an important step toward synthesizing poly(quinone diimine)s. Nucleophilic addition of phenyllithium to PIKs results in poly(imino alcohol)s PIAlcos with less thermal stability and slightly higher glass transition temperature than their corresponding PIKs. In this process approximately 100 % of the carbonyl groups can be converted and a high yield could be achieved. Upon the transformation of PIKs into PIAlcos, there were no change in polymer nature which remain amorphous as detected by wide-angle X-ray. Although **PIAlco-13** has the same chain length as **PIK-13**, the hydrogen bonding in the **PIAlco-13** has a stronger effect on the mobility of the polymer chains than that of **PIK-13**. This can be attributed to the hydrogen bonding connecting the short chains of **PIAlco-13** to a continuous network.[233] This was also seen as a reason behind the higher T_g value in case of **PIAlco-13** than **PIK-13**. Which could be proven by dynamic mechanical analysis of **PIAlco-13** and **PIK-13**.

CHAPTER III

RESULTS AND DISCUSSION

Part 3

3.3 Poly(quinone diimine)s *via* elimination reaction
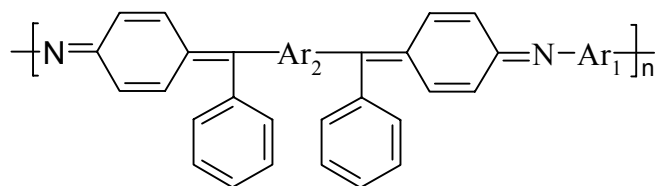
The redox behavior of quinones has attracted the strong interest of chemists for many years, and a number of papers have been published on the synthesis and properties of quinones,[262] On the other hand, electron accepting polymers have been the subject of recent interest because of their redox behavior as well as their conducting and optical properties.[263] However, in spite of the strong interest in both the quinones and electron accepting polymers, poly(quinone)s with the extended conjugation along the polymer main chains have received much less attention[264] presumably due to difficulty in preparing such poly(quinone)s by the usual methods. Among the reported preparative methods of n-type conducting polymers is the organometallic dehalogenation polycondensation.[265,266]

In the previous part of this chapter poly(imino alcohol)s containing tertiary alcohol groups have been synthesized. In the present work we aim at the acid catalyzed dehydration of alcohols in order to transform the poly(imino alcohol)s containing the di-tertiary alcohol group into their corresponding poly(quinone diimine)s as an attractive new structure.

96

Synthesis of 1,4-bis{(4-benzylidene-cyclohexa-2,5-dienylidene)-anilino}benzene (12):

In the presence of trifluoromethanesulfonic acid, di-tertiary alcohol 1,4'-bis{(phenyl-(4-anilinophenyl)methanol)}benzene (**11**) undergoes an elimination reaction to form 1,4-bis{(4-benzylidene-cyclohexa-2,5-dienylidene)-anilino}benzene (**12**) (Scheme 3.3-1). The resulting compound **12** was extracted with chloroform as a deep purple solution. The latter organic solution was washed with water, evaporated and dried in vacuo. The isolated yield was 92 % as a deep purple powder.
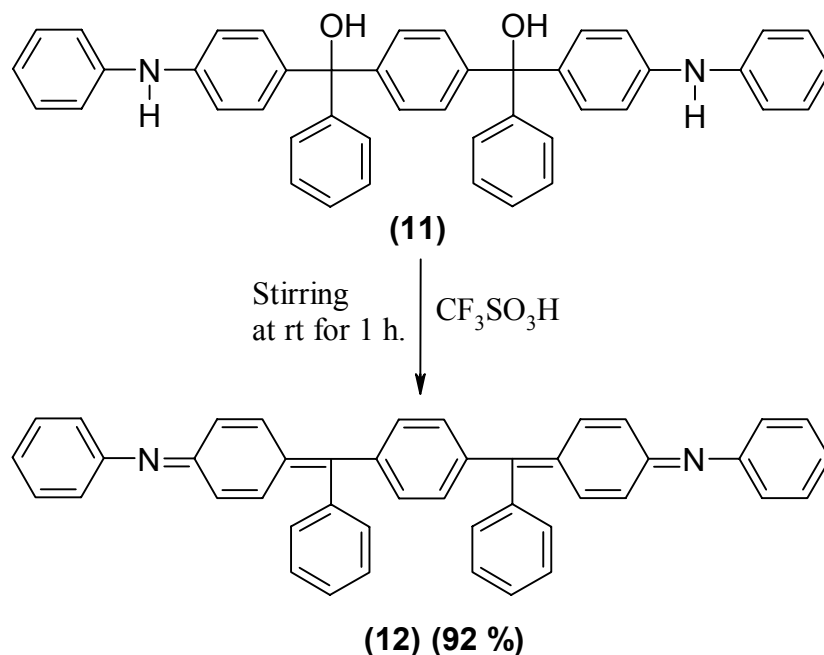
Scheme 3.3-1: Synthesis of 1,4-bis{(4-benzylidene-cyclohexa-2,5-dienylidene)-anilino}benzene (**12**).

Mechanism of the elimination reaction:

The mechanism of the elimination reaction can be summarized in the following steps:

1- In the first step of this reaction, the alcohol is protonated to make the OH a leaving group (**I**).

2- In the second step, two moles of water are removed to generate the di-tertiary bicarbocation (**II**).

3- In the third step, the bicarbocation is stabilized by resonance to give the most stable bicarbocation intermediate (**III**).
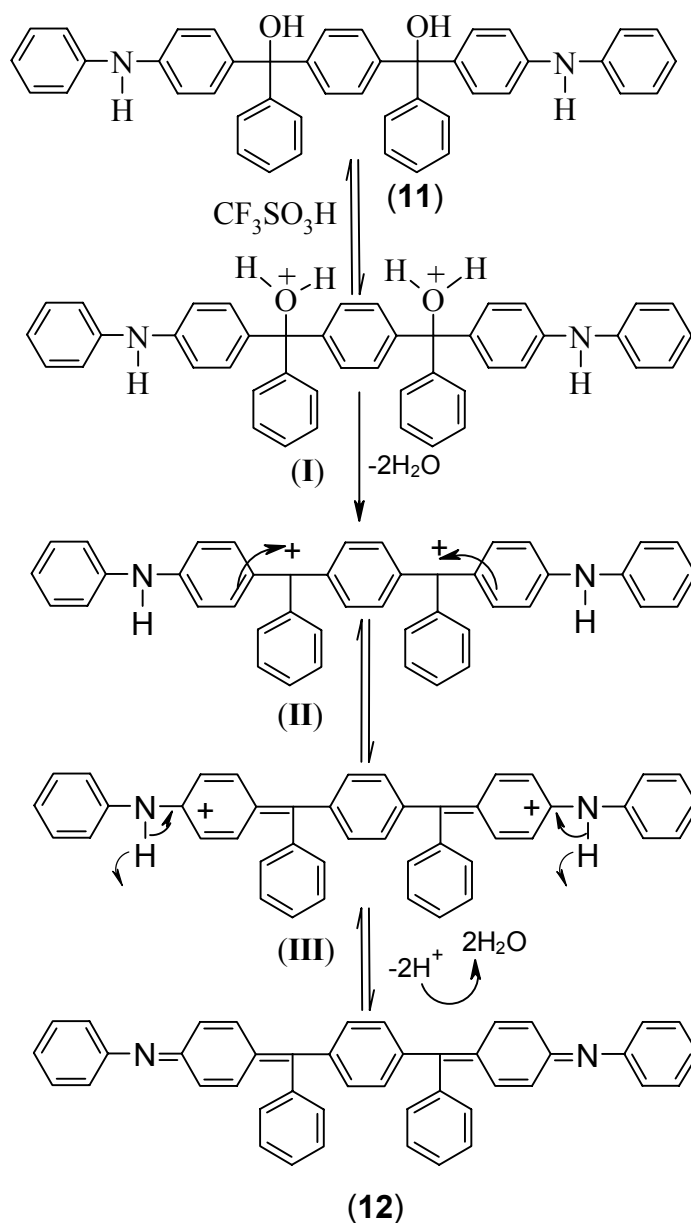
Figure 3.3-1: Trifluoromethanesulfonic acid catalyzed dehydration of 1,4´-bis{(phenyl-(4-anilinophenyl)methanol)}benzene (**11**).

98

4- In the fourth step, the most stable bicarbocation looses two protons from two nitrogen atoms to form the final product 4-bis{(4-benzylidene-cyclohexa-2,5-dienylidene)-anilino}benzene (**12**).

FT-IR spectrum of 1,4-bis{(4-benzylidene-cyclohexa-2,5-dienylidene)-anilino}benzene (12):

Figure 3.3-2 shows the FT-IR spectrum of **12**. By comparing the FT-IR before (compound **11**) and after the elimination reaction (compound **12**), the absence of hydroxy groups γ(OH) at 3550 cm^{-1} and imino groups γ(NH) at 3390 cm^{-1} was detected in the FT-IR spectrum of compound **12**. The spectrum corresponds to the proposed structure **12**, displaying a vibrational peak at 1616 cm^{-1} assigned to the stretch of the quinoid (Q) ring and a peak at 1590 cm^{-1} assigned to the stretch of the benzenoid (B) ring, according to results reported previously for oligo and polyaniline.[267,274] The intensity of these two bands relative to each other are of great interest. In Figure 3.3-2 the benzenoid (B) band has higher intensity than the
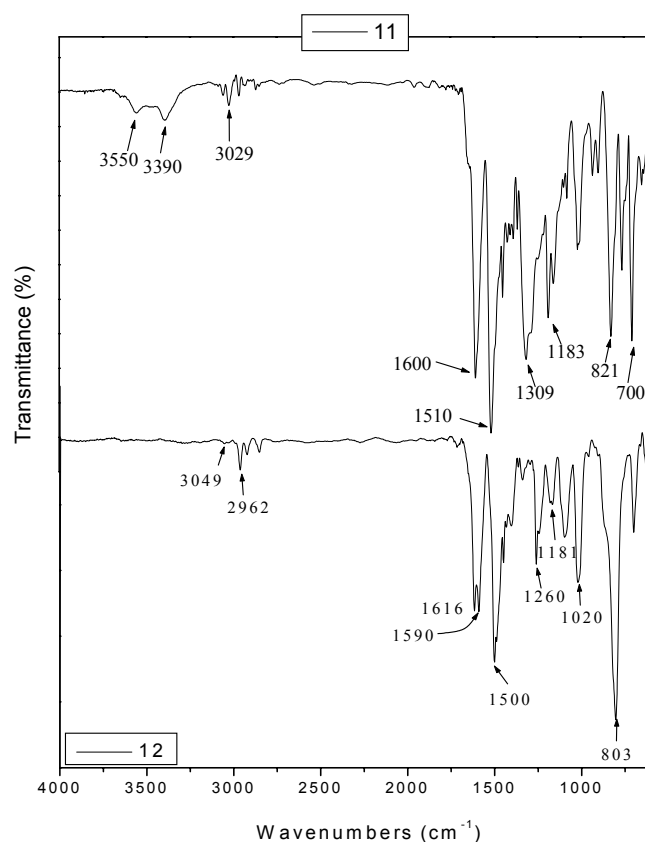
Figure 3.3-2: Comparison of FT-IR spectra of compounds **11** and **12** (KBr pellet).

quinoid (Q) band, indicating that the backbone of compound **12** contains higher populations of benzenoid (B=5) than quinoid (Q=2) rings. The presence of the quinoid ring is also suggested by the peak at 1181 cm^{-1} which could be due to the electronic absorption of the C=Q=N. This band is higher than 1167 cm^{-1}, which is characteristic of the electronic-like absorption of the N=Q=N vibration.[268,269]

UV-vis spectrum of 1,4-bis{(4-benzylidene-cyclohexa-2,5-dienylidene)-anilino}benzene (12):

The first peak at 350 nm in the spectrum of **12** in Figure 3.3-3 can be assigned to the electronic π→π*-transition of the phenyl rings in the compound backbone, while the secondary feature at 500 nm is an excitonic absorption deriving from the quinoid rings in compound **12** according to similar reported results of the quinoid rings in oligo and polyaniline.[270,271]
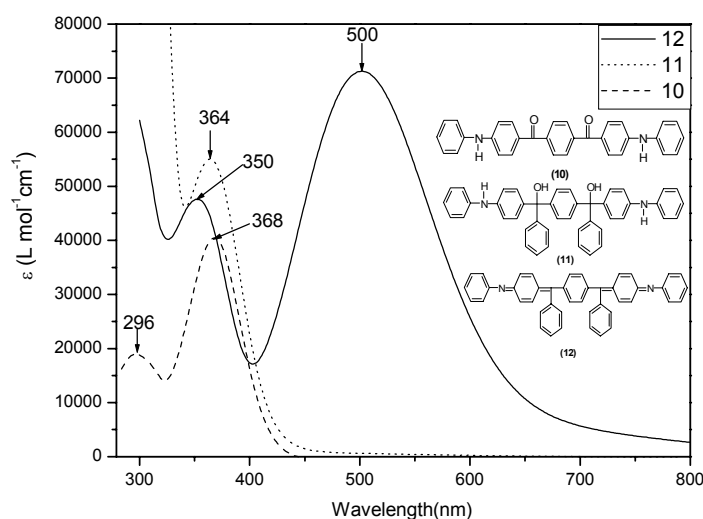
Figure 3.3-3: Comparison of UV-vis absorption spectra of compounds **10** (yellow color), **11** (colorless), and **12** (deep purple color) (2 x 10^{-5} M in CHCl$_3$).

^{1}H-NMR of 1,4-bis{(4-benzylidene-cyclohexa-2,5-dienylidene)-anilino}benzene (12):

In the ^{1}H-NMR spectrum of compound **12** which was recorded in DMSO-d_6 at room temperature the spectrum is divided into three regions (Figure 3.3-4). The down field region contains four aromatic protons H$_1$ at 7.47 ppm. The second represents twenty aromatic protons H$_2$ at 7.25-7.12. The third region at 7.05-6.94 corresponds to eight olefinic protons H$_3$. An agreement with the proposed structure **12** is supported by the ^{1}H-NMR spectrum peaks and FT-IR. Moreover, the quinoid linkage is supported by the presence of the well-known[270,271] quinoid excitonic absorption at 500 nm in the UV-vis spectrum of compound **12**. However, ^{13}C-NMR could not be well detected most probably due to the weak stability of

compound **12** in long time measurements. One can not figure out the reason behind the weak stability of compound **12**.
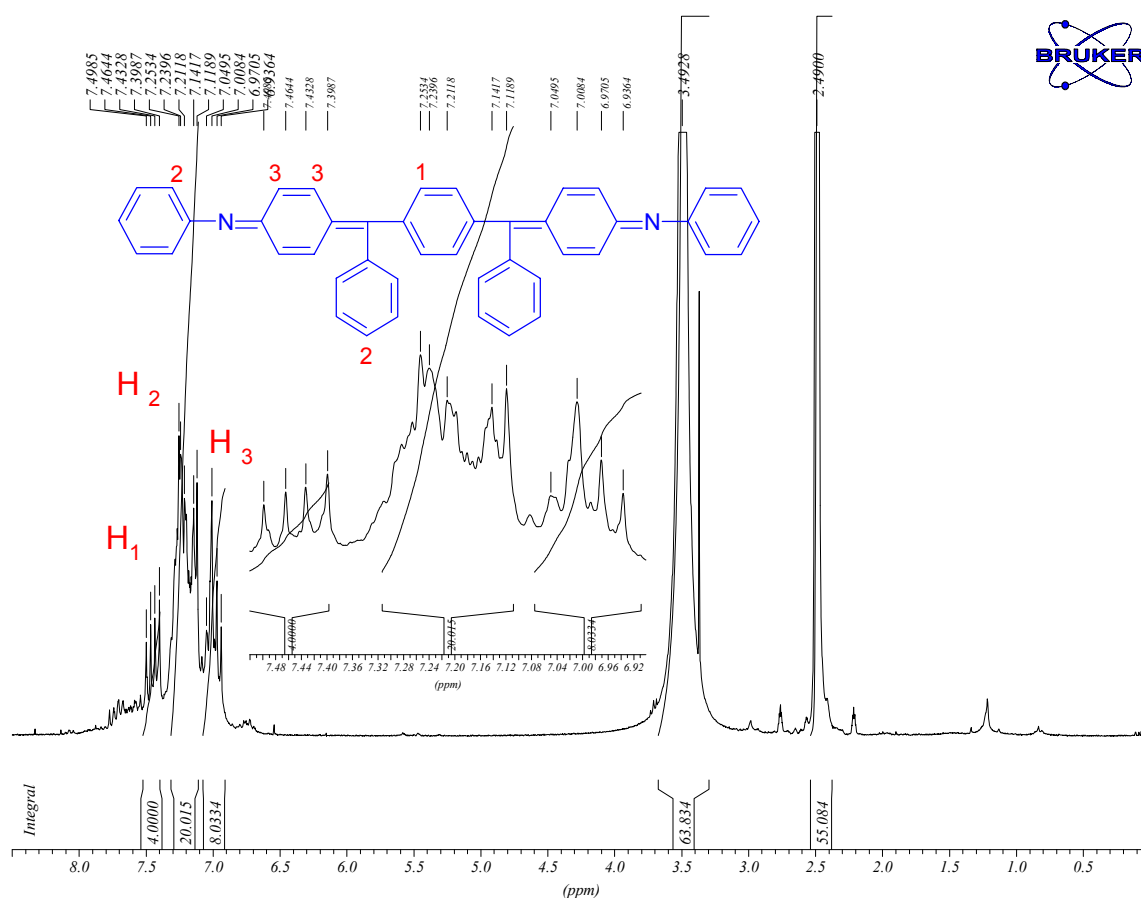
Figure 3.3-4: ^{1}H-NMR (250 MHz, 293K) spectrum of of 1,4-bis{(4-benzylidene-cyclohexa-2,5-dienylidene)-anilino}benzene (**12**) recorded in DMSO-d_6.

Photochromism of 1,4-bis{(4-benzylidene-cyclohexa-2,5-dienylidene)-anilino}benzene (12):

Photochromism is the reversible transformation by photoirradiation of a chemical species between two forms that have different absorption spectra. During the photoisomerization, not only the absorption spectra but also various physicochemical properties change, such as the refractive index, dielectric constant, oxidation/reduction potential and geometrical structure.[272] These changes can be applied to various photonic devices, such as erasable optical memory media and photo-optical switch components.[273,282]

It is found in the detection of the UV-spectrum of compound **12** after exposure to ultraviolet light (λ =365 nm) for different periods that a very obvious photochromism appears

in the liquid state (Figure 3.3-5). Thereby, the intensities of the 500 and 350 bands decrease. This decrease may be due to E-Z-isomerization which leads to a conformational transition of
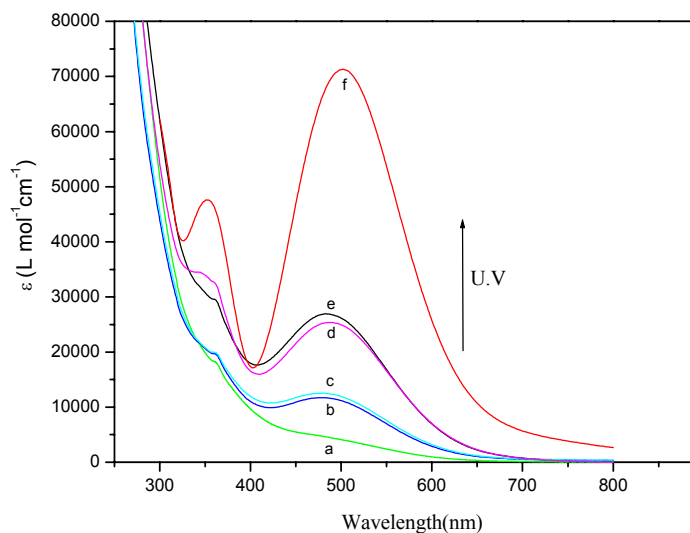
Figure 3.3-5: Changes in UV-vis spectrum of compound **12** with increasing irradiation time (2 x 10^{-5} M in CHCl$_3$): (a) 0 M, (b) 30 M, (c) 60 M, (d) 90 M, (e) 120 M, (f) over night.

the conjugated backbone from a highly conjugated (coplanar or nearly planar, deep purple color E-isomer) form under UV to a non-conjugated conformational structure (non planar, colorless Z-isomer) in the dark (Figure 3.3-6). These optical effects are reversible. This kind of E-Z-isomerization has been reported for oligoaniline N, N`-diphenyl-2,5-cyclohexadiene-1,4-diimine (Figure 3.3-6).[274,275] Moreover, MacDiarmid has pointed out recently that conformational changes could play a major role in determining the properties of an important conducting polymer, polyaniline.[276] For instance, E-Z isomerization might be at play when it is used as a chemical sensor.[276a]

On the basis of these observations, one can conclude that the synthesis produces coplanar E-conformer rather than nonplanar Z-conformer. Although the reported calculation of the total energy values indicate that both the Z-(minority) and E-(majority) conformers ought to coexist in case of oligoanilines and polyanilines.[274] There is no proof that a portion of Z-isomer can coexist. It is unclear at this point why the synthesis produces overwhelmingly the E- rather than Z-isomer.

Figure 3.3-6: E-Z-isomerization of N, N`-diphenyl-2,5-cyclohexadiene-1,4-diimine[274,275]

and 1,4- bis{(4-benzylidene-cyclohexa-2,5-dienylidene)-anilino}benzene (**12**)

Applications of photochromic compounds

The main field of the applications of photochromic compounds is a light-sensitive medium for recording, multiplying, storing, and processing optical information. In view of the fact that information will be transmitted and processed on the optical medium, the development of compounds used for storing of information, optical driving, non-linear optical appliances and others has emphasized significance.[277]

More recently applications have been proposed for use in photoswitching of protein activity,[279,280] as chromophores in 3-D optical data storage,[281] as a means to photocontrol ion

permeation through biological membranes, and photochemical erasable memory.[280,282] Photochromric materials are now anticipated as a promising candidate for erasable memory media of the next generation.

Michler's ketone and 1,4-bis{(4-benzylidene-cyclohexa-2,5-dienylidene)-anilino}benzene (12):

Michler's ketone is well known diaryl ketone.[283] The carbonyl component of Michler's ketone reacted with dimethylaniline analogously to form the substituted triphenyl methane which transformed into carbocation compound. The firstly formed carbocation in this case is stable in acidic and neutral solution and in the crystal structure (crystal violet).[283] In our case the formation of the most stable bicarbocation (**III**) (p. 98, Figure 3.3-1) as took place also in case of the synthesis of Michler's ketone carbocation (**II**) (Scheme 3.3-2). The nitrogen attached with proton in (**III**) is different than nitrogen attached with methyl in (**II**). Therefore, for compound (**III**), it is favored to lose that proton to form the final compound **12** and for (**II**) to use the nitrogen atom lone pair of electron to form the final crystal violet compound.
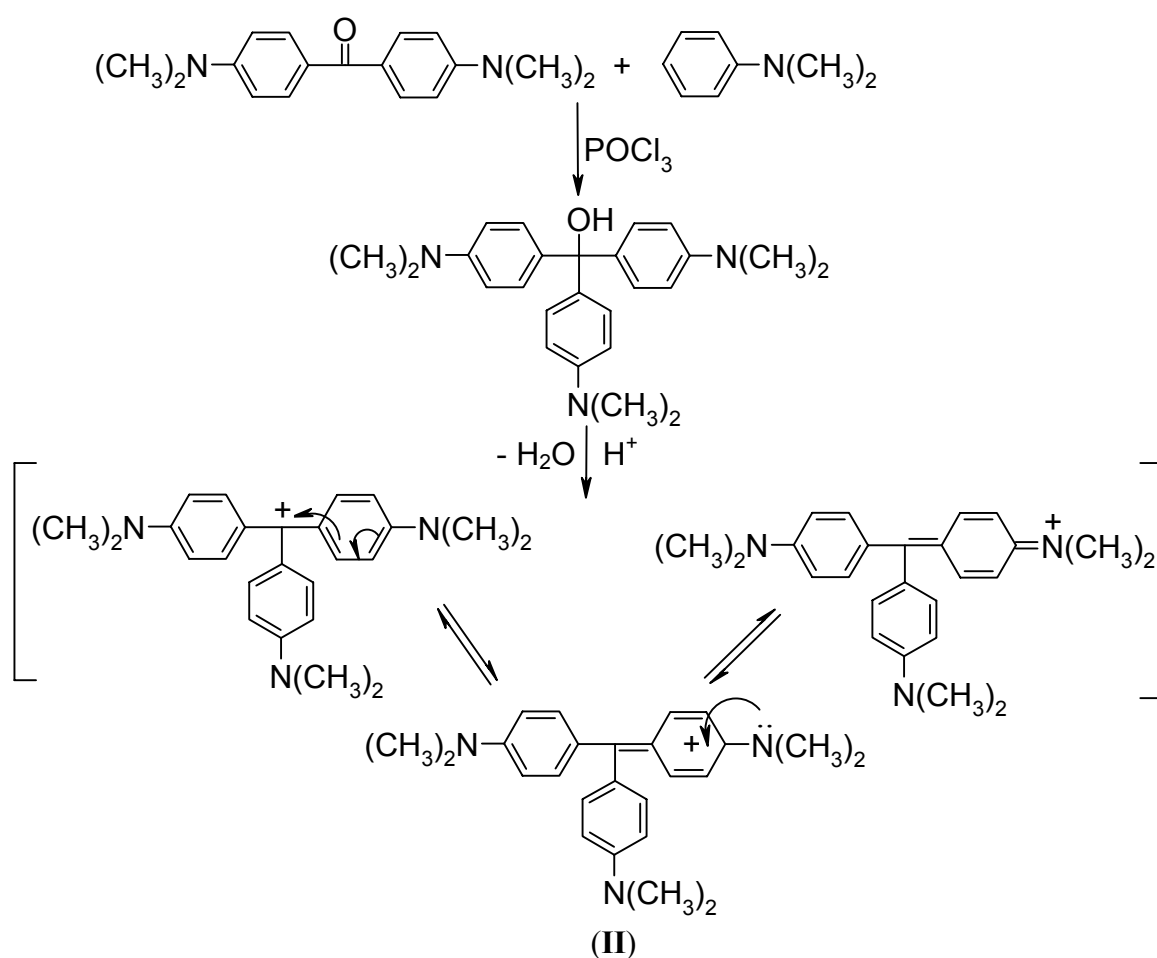
Scheme 3.3-2: Synthesis of Michler's ketone carbocation (**II**).

104

Attempts to synthesize poly(quinone diimine)s *via* elimination reaction:

After the model reaction has been performed the synthesis of poly(quinone diimine)s is attempted. Trifluoromethanesulfonic acid (99 %) hydrochloric acid (37 %), glacial acetic acid (99.5-100%), and acetic acid (20 %) as different acidic conditions were employed to catalyze the dehydration of poly(imino alcohol) **PIAlco-13** in attempts at synthesizing its corresponding poly(quinone diimine) (Scheme 3.3-3). The obtained results were analyzed by GPC (Table 3.3-1). These results showed a strong decrease of both number average molecular weight and weight average molecular weight of the obtained materials. However, the use of glacial acetic acid (99.5-100%) gave $M_n = 400$, and $M_w = 670$ while the use of acetic acid (20 %) gave $M_n = 3\ 500$, and $M_w = 12\ 000$ (runs 3 and 4 in Table 3.3-1). This revealed that the degradation process depended on the strength of acidic condition. One concludes that poly(imino alcohol) **PIAlco-13** undergoes degradation instead of the elimination reaction.

These results are unexpected in view of the stability of compound **12** toward different strength of acidic conditions. No possible explanation has been figured out concerning the sensitivity of the backbone of poly(imino alcohol)s towards acidic conditions. However, this degradation may be avoided by carrying out the elimination reactions under basic conditions.
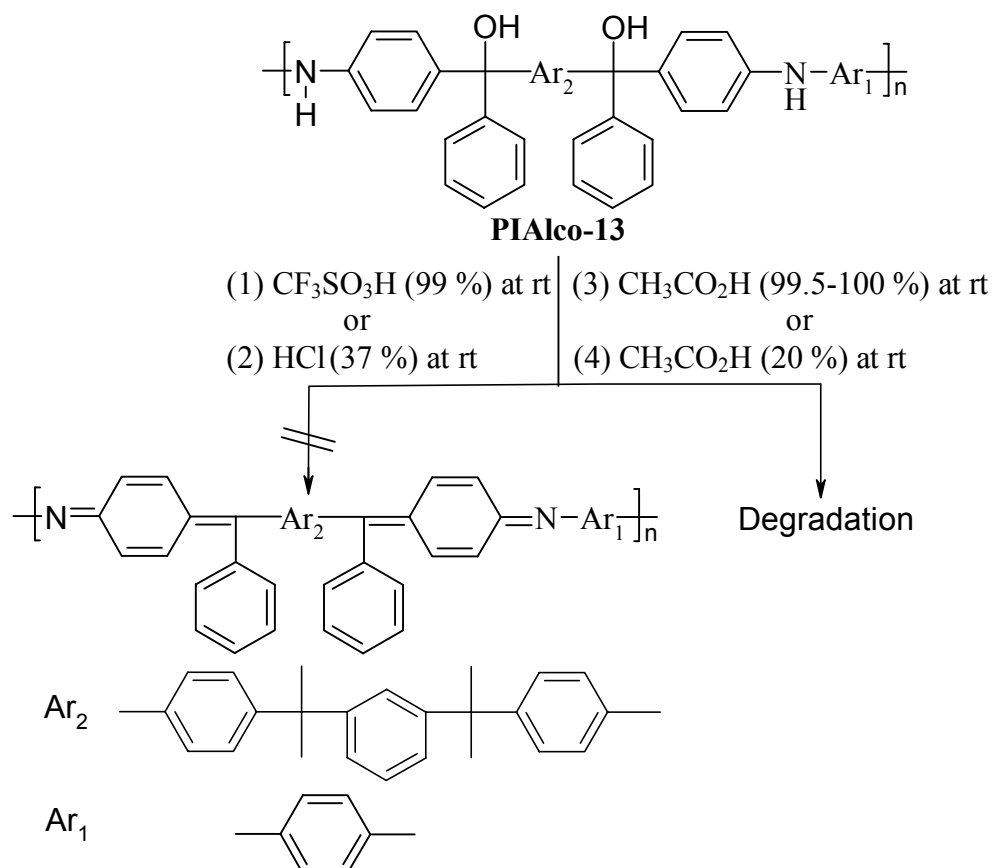
Scheme 3.3-3: Attempts towards synthesis of poly(quinone diimine)s *via* elimination reaction.

105

Table 3.3-1: GPC results of the elimination reactions:

Run	Acid	M_n of PIAlco-13	M_w of PIAlco-13	M_n	M_w
1	CF_3SO_3H (99 %)	16 400	34 500	1 000	2 000
2	HCl (37 %)	16 400	34 500	1500	5300
3	CH_3CO_2H (99.5-100 %)	16 400	34 500	400	670
4	CH_3CO_2H (20 %)	16 400	34 500	3500	12 000

Conclusions:

1,4-Bis{(4-benzylidene-cyclohexa-2,5-dienylidene)-anilino}benzene   (**12**)   has   been synthesized *via* elimination reaction. Attempts have been carried out to synthesize poly(quinone diimine)s from poly(imino alcohol)s. GPC results suggested that there are high decrease in both number average molecular weight and weight average molecular weight of the obtained materials. Which means that the poly(imino alcohol)s degrade instead of undergoing the elimination reaction. Despite compound **12** was achieved under acidic condition by a high yield, poly(imino alcohol)s exhibit a high degree of degradation of the polymer backbone. However, this degradation may be avoided by carrying out the elimination reactions under basic conditions.

CHAPTER III

RESULTS AND DISCUSSION

Part 4

3.4 Novel Poly(imino acridine)s (PIAcs)
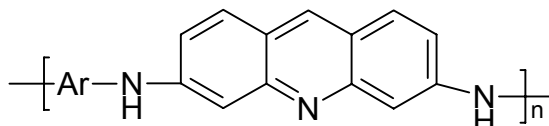
Photoactive polymers have important applications in photolithography, xerography, photocuring of paints and resins, and solar energy conversion systems.[284] These photoactive polymers can be synthesized either by covalently linking photoactive guest molecules to the backbone of a polymer or by copolymerizing a suitable acrylic or vinylic derivative of the photoactive molecule. The copolymerization strategy is, however, more appropriate since this enables us to tailor make the polymer of required property by suitable choice of comonomers and their compositions.

Polymers containing photosensitizers have been investigated for potential use in electron and energy transfers.[285,286] Meanwhile, 3,6-diaminoacridine (proflavine) has been extensively studied as photosensitizer for photoinduced hydrogen evolution from water.[287] However, there have been few reports on the preparation[288] and photoactivities[288c] of polymers containing the proflavine structure.

On this basis, it is aimed at synthesizing new polymers containing acridine units in the main chain by palladium-catalyzed polycondensation of aryl dibromides with 3,6-diaminoacridine to report the results of synthesizing and preliminary photosensitizing of the polymers. The absorption properties of this copolymer are expected to be dependent on the acidity of the medium as it can exist in neutral and singly protonated forms in solution. The expected excited singlet and triplet state properties of the different two forms were investigated by photoluminescence.

Synthesis of proflavine, 3,6-diaminoacridine as a monomer

Proflavine, 3,6-diaminoacridine free base (**14**), was prepared from 3,6-diaminoacridine hydrochloride (**13**) (Aldrich Chemical Co.) by neutralization with a sodium hydroxide solution at 0 °C under an argon atmosphere as shown in Scheme 3.4-1. The chemical structure of the 3,6-diaminoacridine free base was established by elemental and spectral analyses. ^{1}H-NMR spectroscopy is shown in Figure 3.4-1.
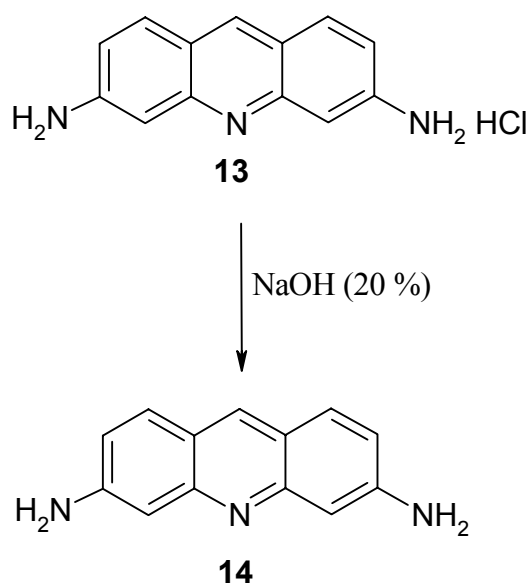
Scheme 3.4-1: Synthesis of proflavine, 3,6-diaminoacridine.
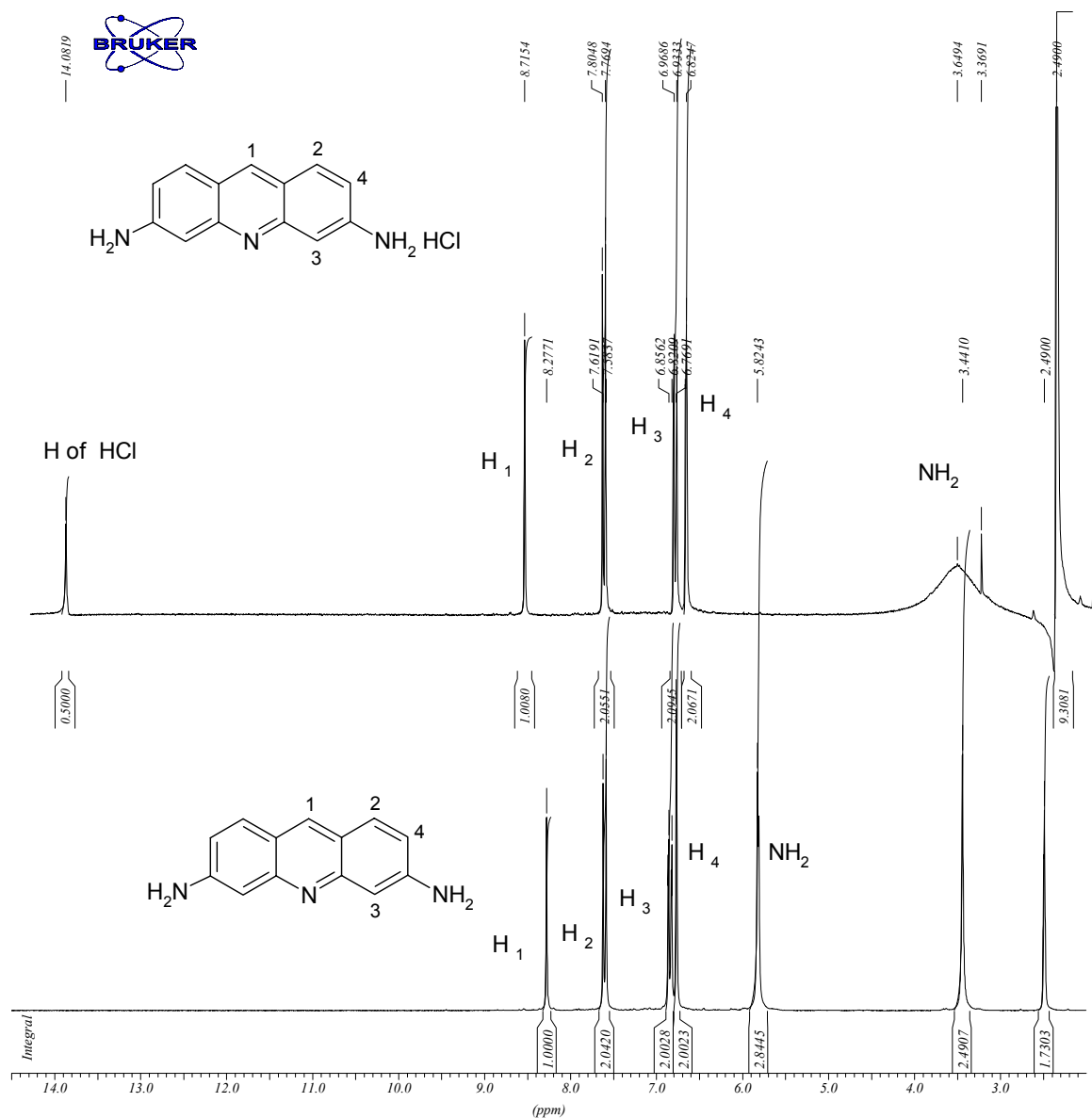
Figure 3.4-1.

Synthesis of poly(imino acridine)s.

The proflavine, 3,6-diaminoacridine free base was then coupled with different arylene dibromides *via* palladium-catalyzed amination polycondensation to afford poly(imino acridine)s having an acridine group in the main chain in 82 %-91 % yields without undesired side products as shown in Scheme 3.4-2.

Table 3.4-2 summarizes the results of the Pd-catalyzed of 4,4´-dibromobenzophenone or 4,4´-dibromodiphenylether, and 4,4´-dibromodiphenyl, with proflavine, 3,6-diaminoacridine free base using the combination of $Pd_2(dba)_3$ and BINAP as an efficient catalytic system for the Pd-catalyzed polycondensation.

$$Br\ Ar_1\ Br\quad +\quad NH_2\ Ar_2\ NH_2$$

2.8 equiv. of NaOt-Bu,

0.01 equiv. of cat. (Pd)$_2$(dba)$_3$,

0.03 equiv. of cat. BINAP,

DMAc

100 °C for 6h-165 °C for 10h

$$\left[\!- Ar_1\ NH\ Ar_2\ NH\ -\!\right]_n$$

Polymer Code	Ar$_1$	Ar$_2$
PIAc-1		
PIAc-2		
PIAc-3		
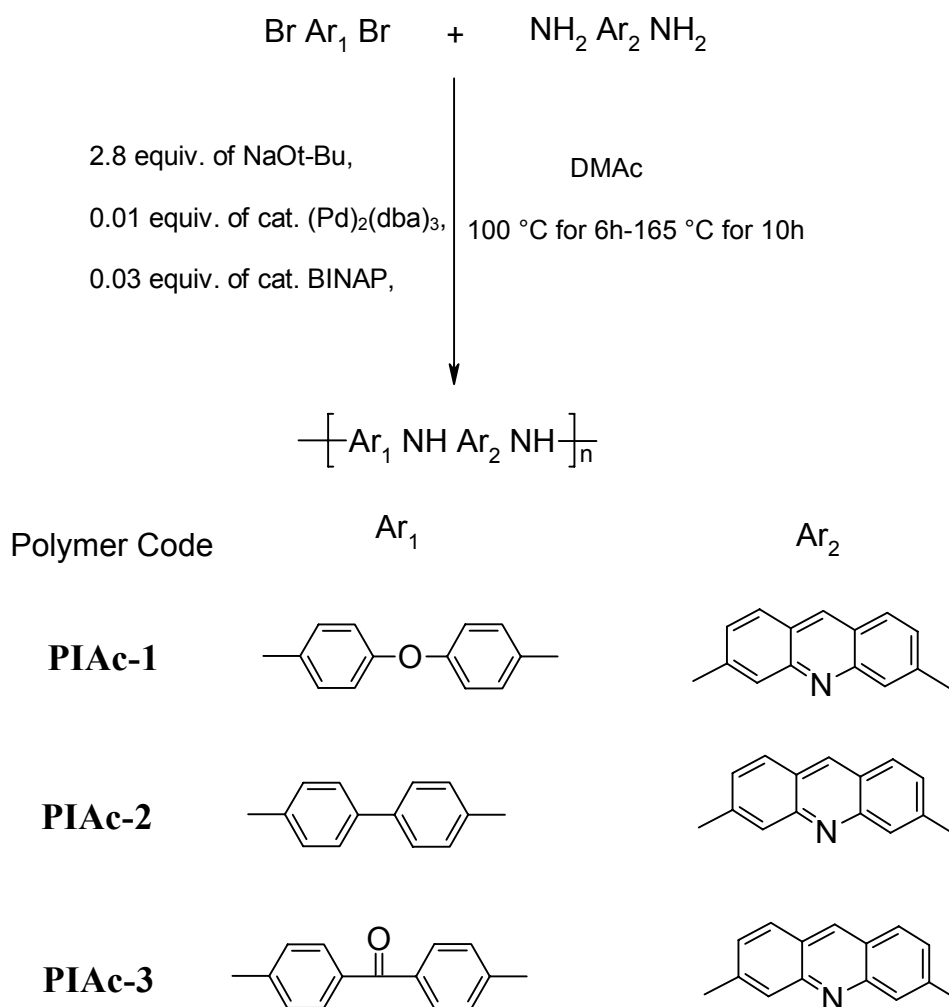
Scheme 3.4-2: Synthesis of poly(imino acridine)s.

Polymer solubility:

The polymers showed different solubility behaviors in different organic solvents. Polymer solubility was qualitatively determined by the dissolution of 5 mg of solid polymers in 1 ml of organic solvent, at room temperature (Table 3.4-1). The polymers could be easily soluble in strong aprotic solvents, such as dimethylacetamide (DMAc) and dimethylsulfoxide (DMSO) while it is partially soluble in dimethylformamide (DMF) and completely insoluble in common organic solvents, such as THF, methanol, acetone, dichloromethane, and could be swell at room tempertaure in chloroform.

All PIAc polymers showed improved solubility in acids such as formic acid in comparison with PIKs. This improvement in solubility probably could be attributed to the presence of the lone pair of electrons on the ring nitrogen which should promote the solubilization of the polymer in acidic solvents (formic acid) to give blood red solution.[289]

Table 3.4-1: Solubility behavior of poly(imino acridine)s.[a]

Polymers	DMAc	DMSO	DMF	THF	CH$_3$OH Acetone	CHCl$_3$	CH$_2$Cl$_2$	HCO$_2$H
PIAc-1	++	++	++	--	--	-S	--	++
PIAc-2	++	++	±	--	--	-S	--	++
PIAc-3	++	++	±	--	--	-S	--	++

[a] Solubility was measured at polymer concentration, 5 mg. ml^{-1} by the mixing of 5 mg of polymer with 1 ml of solvent, followed by stirring; ++ indicates that the solid polymer was completely dissolved in the solvent to afford a homogeneous solution at room temperature; ± indicates that the solid polymer could be partially soluble at room temperature; -- indicates that the solid polymer could not be dissolved or swollen in the solvent; -S indicates that the solid polymer could be swell at room temperature.

The molecular weights of the PIAcs were measured by GPC (calibrated by polystyrene standards). The M$_n$ values are in the range of 4 500-12 600 and the M$_w$ values in the range of 7 000-75 900. The polydispersities vary from 1.5 up to 6.0 (Table 3.4-2). Especially, with increasing molecular weights the polydispersity increases drastically.[214] Taking into consideration that the values in case of polymers **PIAc-2**, and **PIAc-3** represent only the soluble fraction in DMF (about 70 %, and 50 %) respectively. The molecular weight is expected to be higher than the given values.

Table 3.4-2: Characterization of the polymers: (GPC, Yield, FT-IR).

Polymer Code	$\overline{M}_n$ [a]	$\overline{M}_w$ [a]	$\overline{M}_w / \overline{M}_n$ [b]	DP^c	Yield (%)	γNH^d	$\gamma C=O^d$	$\gamma C- N^d$
PIAc-1	4 500	7 000	1.5	12	82	3384	-	1307
PIAc-2	12 600[e]	75900[e]	6.0	35	90	3391	-	1312
PIAc-3	9 500[f]	15 000	1.6	24	91	3330	1620	1311

a) The soluble fraction in DMF calibrated by GPC polystyrene standards; b) polydispersity index; c) Degree of polymerization determined from number average molecular weight.d) FT-IR (KBr, pellet); f, e) The soluble fraction of the polymer (about 70 %, and 50 %) respectively.

Elemental analysis

In all cases, the elemental analysis of the PIAc polymers showed an agreement with the polymer structure. Despite the hygroscopic nature of the PIK polymers, the PIAc polymers did not show hygroscopic nature (Table 3.4-3).

Table 3.4-3: Elemental analysis for poly(imino acridine)s.

Polymer Code	Formula (Molecular weight %)	Elemental analysis (%)			
			C	H	N
PIAc-1	$(C_{25}H_{17}N_3O)_n$ (375.43)n	Calc. Found	79.98 78.67	4.56 4.54	11.19 10.68
PIAc-2	$(C_{25}H_{17}N_3)_n$ (359.43)n	Calc. Found	83.54 80.88	4.77 5.09	11.69 10.45
PIAc-3	$(C_{26}H_{17}N_3O)_n$ (387.44)n	Calc. Found	80.60 78.42	4.42 4.15	10.85 10.35

^{1}H-NMR spectra of PIAcs

The structure of the PIAc polymers was confirmed by ^{1}H-NMR spectroscopy. The ^{1}H-NMR (250 MHz) spectrum of polymer **PIAc-3** which is shown in Figure 3.4-2, was recorded in DMSO-d_6 at 293K. The spectrum showed a broad peak at 9.34 ppm which was attributed to the protons of the imino groups (NH), a broad singlet at 8.58 ppm was assigned to the acridine proton H_1. Except H_1, all the acridine protons and the aromatic protons H_2 appeared as a doublet at 7.49 ppm. No peak was observed assignable to the NH_2 group form proflavine end groups at $\delta = 5.8$ ppm, and all the peaks in the ^{1}H-NMR spectrum were identified as the protons of acridine, and diimino arylene of the main repeating unit of the polymer backbone.

Therefore, neither amine-terminated PIAcs nor bromide-terminated PIAcs were observed. The molecular weights of PIAcs are limited most probably by formation of cyclic polymers or undetectable cyclic oligomers, and this cyclization has terminated the Pd-catalyzed aryl amination. The synthesis of analogous cyclic oligomers of other polymers have been reported,[290-294] and cyclic oligomers of a poly(aryl ether ketone) PEK have been isolated from a commercial sample.[295]

From ^{1}H-NMR spectra, polymer **PIAc-3** shows a broad band corresponding to the imino group (NH) at 9.34 ppm which is more down field than those of polymer **PIAc-2** at 9.08 ppm and of polymer **PIAc-1** at 8.78 ppm. This high ppm value of (NH) in case of **PIAc-3** could be due to the presence of the carbonyl group in the backbone of polymer **PIAc-3** which contribute to the intermolecular and intramolecular hydrogen bonding. This is strongly supported by comparing the frequencies of the N-H-bond of polymers **PIAc-1**, **PIAc-2**, and **PIAc-3** (3384, 3391, and 3330 cm^{-1} respectively) (cf. Table 3.4-2) where **PIAc-3** with the higher shift to lower frequency than those of **PIAc-1**, and **PIAc-2** is observed. Lowering of the absorption frequency of the γ(NH) is known to be a function of the degree and strength of the hydrogen bonding.[225,226] This suggests that the hydrogen bonding in **PIAc-3** is stronger than in both **PIAc-1**, and **PIAc-2**.
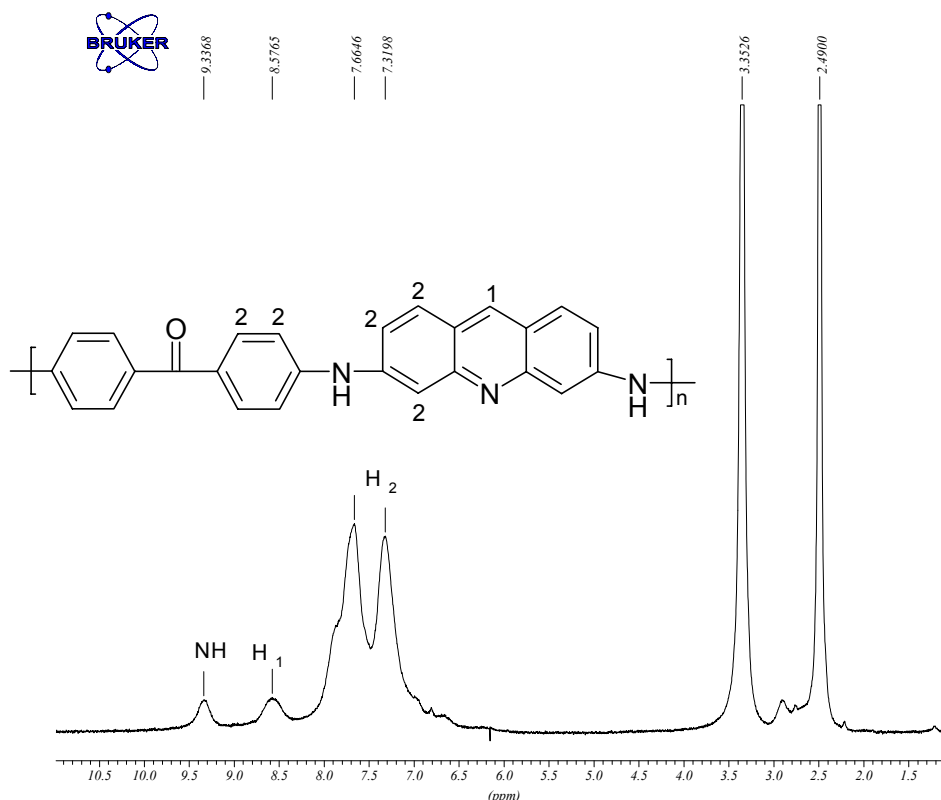
Figure 3.4-2: ^{1}H-NMR (250 MHz) spectrum of polymer **PIAc-3** recorded in DMSO-d_6 at 293K.

FT-IR spectroscopy of PIAcs

The structure of the PIAc polymers were also confirmed by FT-IR and the corresponding γ(NH) shifts were listed in Table 3.4-2. In the FT-IR peak shifts of PIAc polymers, it was observed that the characteristic absorptions for imino groups γ(NH) appeared between 3330 and 3391 cm⁻¹ while in case of PIK polymers, the characteristic absorptions for imino groups γ(NH) appeared between 3318 and 3422 cm⁻¹.

One of the essential requirements of a new polymer material for high temperature applications is thermal stability which makes polymers attractive for potential application. Hence, important informations are needed about the thermal behavior of PIAc polymers, therefore, the following thermal behavior is necessary to be studied.

Thermal behavior of PIAcs:

Typical TGA traces in air and in nitrogen are demonstrated in Figure 3.4-3 for polymers **PIAc-1**, **PIAc-2**, and **PIAc-3**. The thermal stability was evaluated by a 5 % weight loss at the minimum temperature (Table 3.4-4). TGA curves revealed that the polymers were thermally stable up to 360-567 °C only polymer **PIAc-1** shows the poor thermal stability in air and the 5 % weight loss at the minimum temperature at 198 °C.

The 50 % weight loss of the copolymers took place at 441, 414, and 432 °C for polymers **PIAc-1**, **PIAc-2**, and **PIAc-3** respectively in air while they took place over 900 °C in nitrogen. Char yield is an easy and important measurement which correlates to the ability to resist combustion.[296] The maximum char yield at 600 °C was obtained for polymer **PIAc-2** (92 %) and the minimum was obtained for polymer **PIAc-1** (84 %) in nitrogen while the char yield at 600 °C was in the range 0.7-0 % in air.

By comparing the TGA thermograms in air and nitrogen for polymers **PIAc-1**, **PIAc-2**, and **PIAc-3** (Figure 3.4-3), it was observed that in air the 50 % weight loss of those polymers occurs at 441, 414, and 432 °C respectively, but in case of nitrogen the 50 % weight loss was not observed up to 900 °C. In air the char yield at 600 °C was 0 %, 0 %, 0.7 % respectively but in nitrogen the char yield at 600 °C was 84 %, 92 %, and 89 % respectively. The 50 % weight loss temperatures in addition to the high char yields at 600 °C in both air and nitrogen suggested that thermal degradation in air was significantly enhanced over nitrogen atmospher. The PIAc polymers indicated a high thermal stability and a high char yield in nitrogen at 600 °C measured as high as ranging from 84 to 92 %. It was found that the copolymer **PIAc-2** is
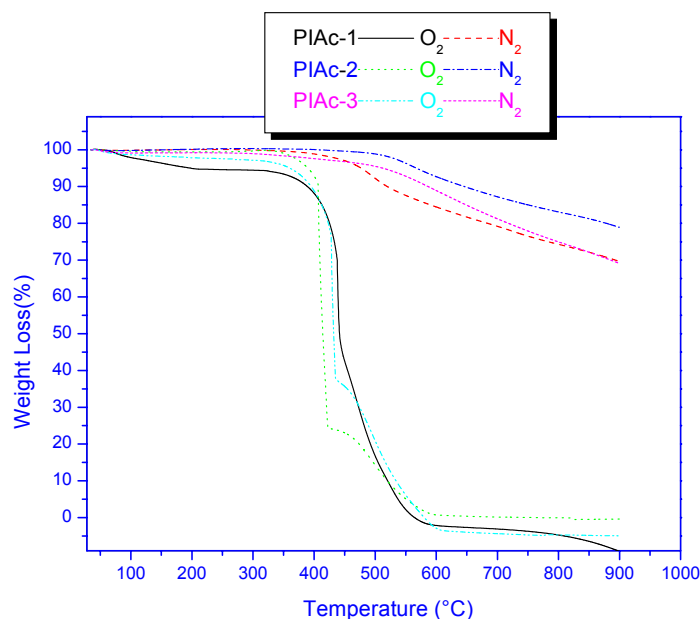
Figure 3.4-3: Dynamic TGA of copolymers **PIAc-1**, **PIAc-2**, and **PIAc-3**

(in N_2, and in O_2, 10 °C/min.).

the most stable PIAcs this can be seen as a direct result of the copolymer structure, involving the extended conjugation of the system which should confer enhanced thermal stability on this polymer over polymers **PIAc-1** and **PIAc-3** that have a less extended aromatic system. The relation between thermal stability and extended conjugation of the polymer system was reported.[289]

Differential scanning calorimetry (DSC) of PIAcs from 20 °C up to 300 °C, T_gs were not detected suggesting T_gs are higher than 300 °C. Although the backbone flexibility of polymer **PIAc-1** resulted from the flexible ether group, the T_g is not detected up to 300 °C. Therefore, one can conclude that the PIAc polymers possess a completely amorphous structure, and no phase transition was observed between 20 °C and 300 °C.

Table 3.4-4: Thermal behavior.

Polymer code	O_2 / N_2	$^aT_5$	$^bT_{10}$	$^cT_{50}$	$^dW_{500}$	$^eW_{600}$	Char yield at 600 °C^f	T_g Midpoint^g
PIAc-1	O_2	198	389	441	84	100	0	$-$ ^{g}
	N_2	477	519	> 900	8	16	84	
PIAc-2	O_2	390	406	414	86	99.3	0.7	$-$ ^{g}
	N_2	567	645	> 900	2	8	92	
PIAc-3	O_2	360	395	432	79	100	0	$-$ ^{g}
	N_2	512	586	> 900	4.5	11	89	

a) T_5: Temperature of 5 % weight loss; b) T_{10}: Temperature of 10 % weight loss; c) T_{50}: Temperature of 50 % weight loss; d) W_{500}: weight loss at 500 °C, determined from TGA curve; e) W_{600}: weight loss at 600 °C, determined from TGA curve; f) The remaining of the polymer at 600 °C; g) Not detected from 20 °C up to 300 °C.

Dynamic mechanical analysis

Since the glass transition temperatures T_gs were not detected from 20 °C up to 300 °C, the dynamic mechanical analysis was not performed.

Wide-angle X-ray diffraction

The powder samples were measured by X-ray wide-angle diffractometry at room temperature. The wide-angle X-ray diffraction patterns of all the polymers over the 2θ range of 5- 35° are shown in Figure 3.4-4. Despite the presence of the rigid p-diiminoacridine segments in the polymer backbones, all of the polymers revealed essentially amorphous patterns. This may be attributed to the fact that the regularity of the repeating units in polymers **PIAc-1**, **2**, and **3** is disrupted by the different appearing orders of the imino and phenyl groups, thus preventing chain packing of the polymer (Figure 3.4-4). The amorphous nature of these polymers was also reflected by their good solubility. Figures 3.4-5, 6, and 7 show the WAXD images of the amorphous halo of polymer PIAcs.
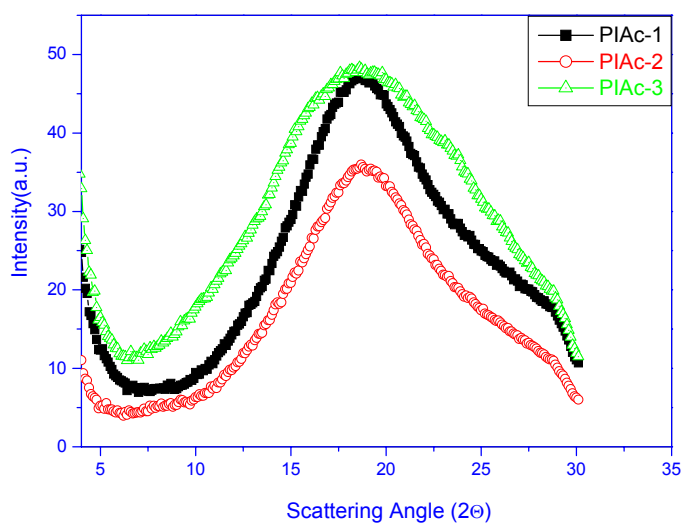
Figure 3.4-4: Wide-angle X-ray diffractograms intensity vs Bragg angle graph for powders of polymers, **PIAc-1**, **PIAc-2**, and **PIAc-3**.

By comparing wide-angle X-ray for PIKs and PIAcs, it was observed that PIAcs showed a broad amorphous halo while **PIKs-11a**, **11b**, and **11c** showed a crystalline pattern (Part 1, Figure 3.1-20). In case of PIKs the crystalline pattern can be attributed to the existance of the rigid p-diiminophenylene or p-diiminodiphenyl ether segments in the polymer backbone and at the same time the absence of any of the bulky *tert.* butyl, or isopropylidene groups, leading to a better packing of the polymer chains.
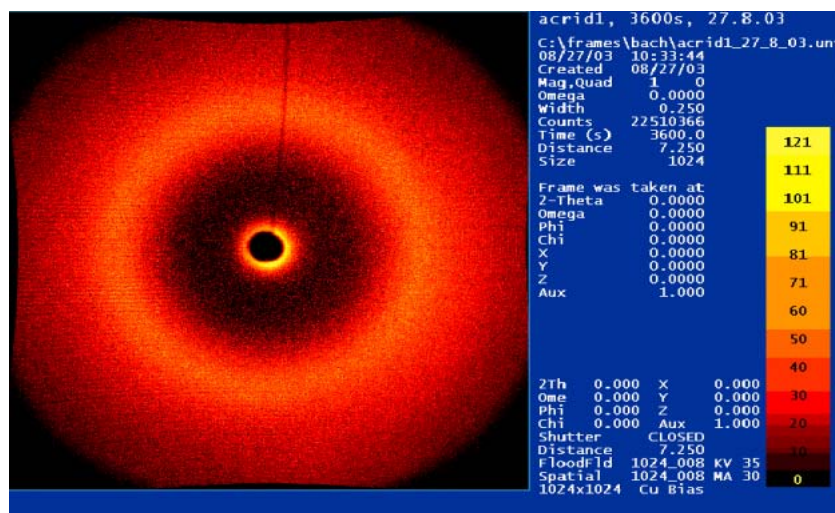
Figrure 3.4-5: WAXD image shows the amorphous halo of polymer **PIAc-1**.
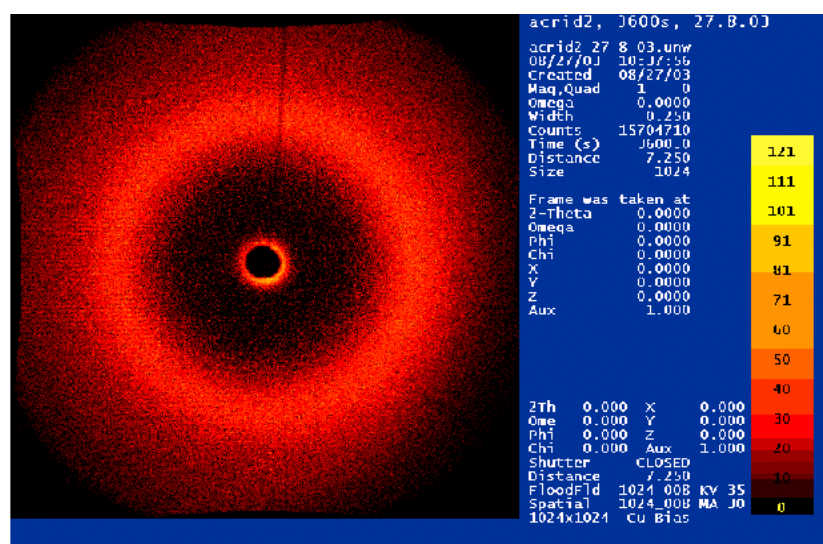
Figrure 3.4-6: WAXD image shows the amorphous halo of polymer **PIAc-2**.
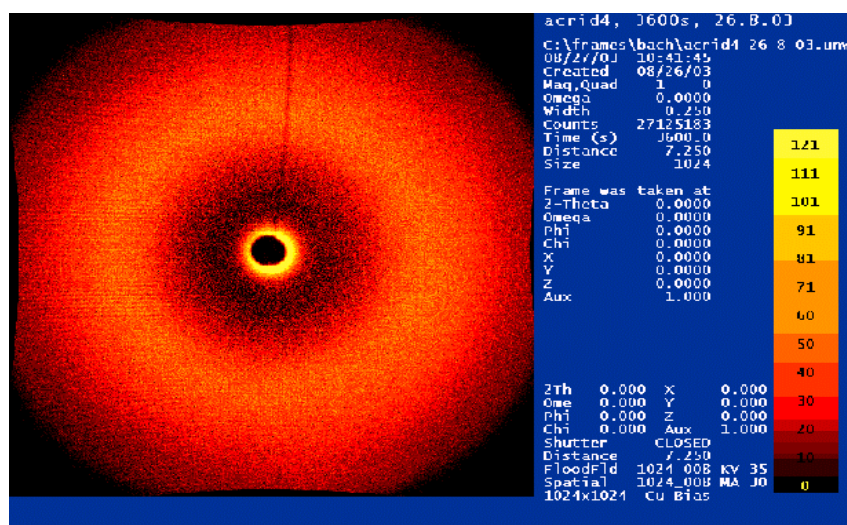
Figrure 3.4-7: WAXD image shows the amorphous halo polymer **PIAc-3**.

118

UV–vis absorption spectra of PIAcs

The absorption spectrum of the neutral form of **PIAc-2** in DMAc (Figure 3.4-8, curve a) shows two major absorption bands of different intensity at 334 and 442 nm. This latter band is similar to the absorption band of neutral proflavine (at 406 nm in DMAc at conc of 2×10^{-5}) with a red shift and is typical of the $\pi \rightarrow \pi^*$-transition of the acridine chromophore.

The absorption properties of the poly(imino acridine) **PIAc-2** are dependent on the acidity of the media. Figure 3.4-8 shows the changes in the absorption spectra of DMAc solutions of polymer **PIAc-2** with increasing concentration of trifluoroacetic acid (TFA). Upon addition of trifluoroacetic acid to this solution, a new band appears at around 500 nm, whereas the two absorption bands at 334 and 442 nm decrease (Figure 3.4-8, curve b, c, and d). These species may be assigned to the singly protonated form of the copolymer (PIAcH$^+$). It has been shown that protonation of proflavine results in the disappearance of the 394 nm band and the formation of a band with a maximum around 444 nm due to the preferential protonation of the
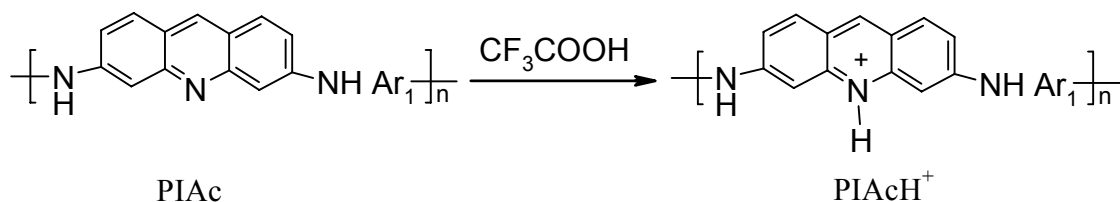
Scheme 3.4-3: Formation of the singly protonated form (PIAcH$^+$) of the PIAc polymers.

intracyclic nitrogen.[297,298] By analogy, the first protonation for PIAcs should occur at the intracyclic nitrogen. The long wavelength transition observed for PIAcH$^+$ can be assigned to the intramolecular charge-transfer transition, where charge transfer occurs from the two imino groups toward the electron-poor acridinium moiety. This transition has a higher wavelength than that observed in the protonated form of proflavine[298] and also in some 9-(aminophenyl)acridinium derivatives.[299] Continued addition of trifluoroacetic acid leads to the complete disappearance of the absorption band at 442 nm, and this is accompanied by the formation of a new band around 500 nm (Figure 3.4-8, curve e). An isosbestic point at 465 nm is also observed which indicates the coexistence of **PIAc-2** and PIAcH$^+$ polymer segments. The spectrum observed under these conditions is assigned to the singly protonated form, PIAcH$^+$. From above, the absorption properties of PIAc polymers were found to be dependent on the acidity of the medium as it can exist in neutral and singly protonated forms in solution (λ_{max} typically red shifts from 442 to 500 nm). A similar red shift in the UV-

spectra has also been observed upon the protonation of poly(p-pyridine vinylene)s (λ_{max} typically red shifts from 410 to 430 nm).[300]
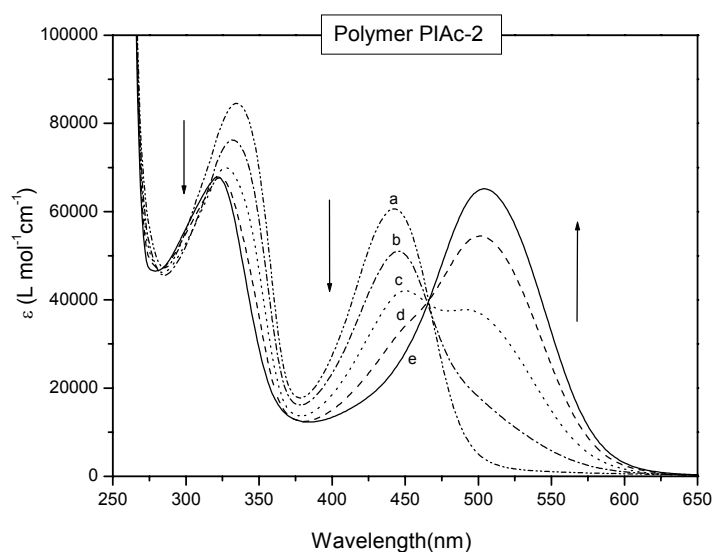
Figure 3.4-8: Changes in the absorption spectra of poly(imino acridine) **PIAc-2** (ca. 2 x10^{-5} M of the acridine unit in DMAc) with increasing concentration of trifluoroacetic acid (TFA) in DMAc. [TFA]: (a) 0, (b) 0.15 x 10^{-5}, (c) 0.4 x10^{-5}, (d) 0.6 x10^{-5}, (e) 2 x 10^{-5} M.
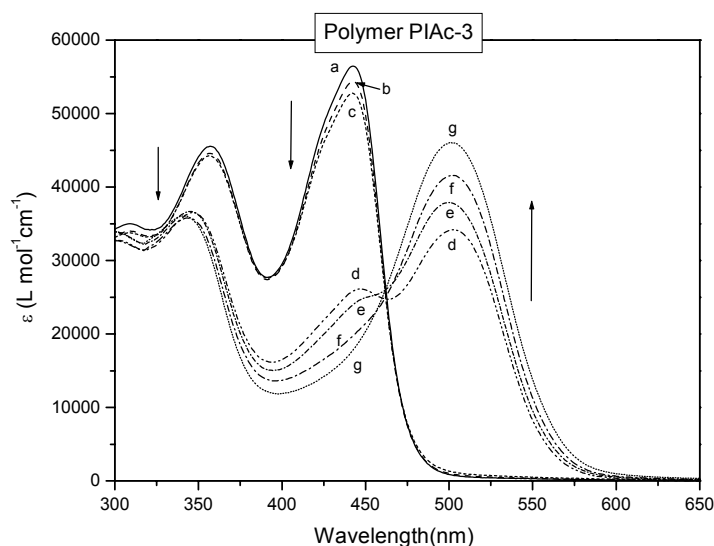
Figure 3.4-9: Changes in the absorption spectra of poly(imino acridine) **PIAc-3** (ca. 2 x 10^{-5} M of the acridine unit in DMAc) with increasing concentration of trifluoroacetic acid (TFA) in DMAc. [TFA]: (a) 0, (b) 0.1 x 10^{-5}, (c) 0.2 x 10^{-5}, (d) 0.8 x 10^{-5}, (e) 1 x 10^{-5} , (f) 2 x 10^{-5}, (g) 3 x 10^{-5} M.

Photoluminescence spectra of PIAcs

The polymers show photoluminescence in DMAc solution when excited at their absorption maximum (Table 3.4-5). The maximum emission wavelength (λ_{em}) ranges from 510 to 610 nm, depending on the structure. The emission spectra of all these species show a broad band with the maxima centered around 510-600 nm, although the absorption maxima of PIAcs is considerably blue shifted compared to that of PIAcH$^+$ (Figure 3.4-10).
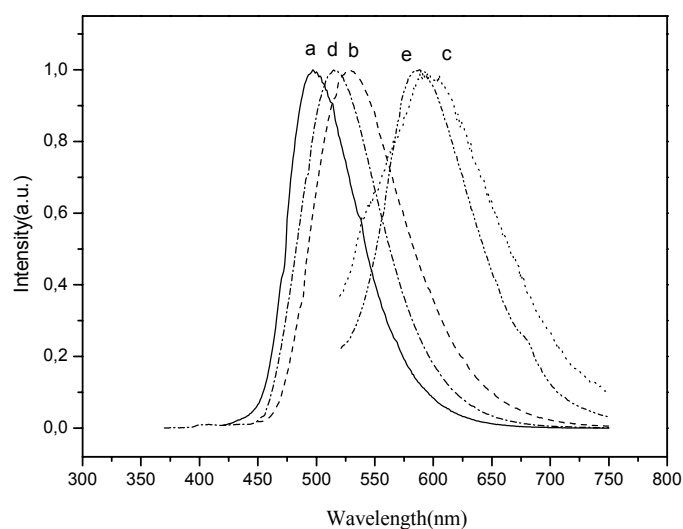
Figure 3.4-10: Emission spectra of photoluminescent poly(imino acridine)s in DMAc at 298K . Emission spectra excited at 406, 442, 500, 357, 341 nm respectively, in DMAc solution.: (a) Proflavine, (b) **PIAc-2** neutral form, (c) **PIAc-2** singly protonated form, (d) **PIAc-3** neutral form, and (e) **PIAc-3** singly protonated form.

The large Stokes' shifts for PIAcs and PIAcH$^+$ suggest that they represent a non-rigid system i.e. the excited and the ground states for these species have different geometries. The excitation spectra, recorded for PIAcs and PIAcH$^+$ species (Figure 3.4-11), are similar to the absorption spectra of the corresponding species. This indicates that the emission does not arise from any trace amounts of the neutral PIAcs which might be present in these solutions. The singly protonated forms of poly(imino acridine)s **PIAc-2** and **PIAc-3** have longer emission maximum (600 and 610 respectively) than their neutral homologues. This red shift in the emission maxima observed with increasing degree of protonation is attributed to the intramolecular charge-transfer transition, where charge transfer occurs from the two imino groups toward the electron-poor acridinium moiety. A similar red shift in the photoluminescence spectra was detected upon the protonation of poly(p-pyridine

vinylene)s.[300] The emission and excitation spectra of the various forms recorded in dimethylacetamide were shown in Figures 3.4-10 and 3.4-11, and these results are summarized in Table 3.4-5. However, the addition of the trifluoroacetic acid (TFA) to the solution of PIAc polymers does not led to a quenching effect in the photoluminescent spectra as was reported for other polymers containing acridine.[297] This is due to the protonation of the proflavine unit. The photoluminescence spectra of PIAcs are a prerequisite for an application in the electronic devices. Further parameters such as the photoluminescent efficiency need to be measured and good film-filming property has to be achieved to determine whether these materials are suitable for application in electronic devices such as LEDs.
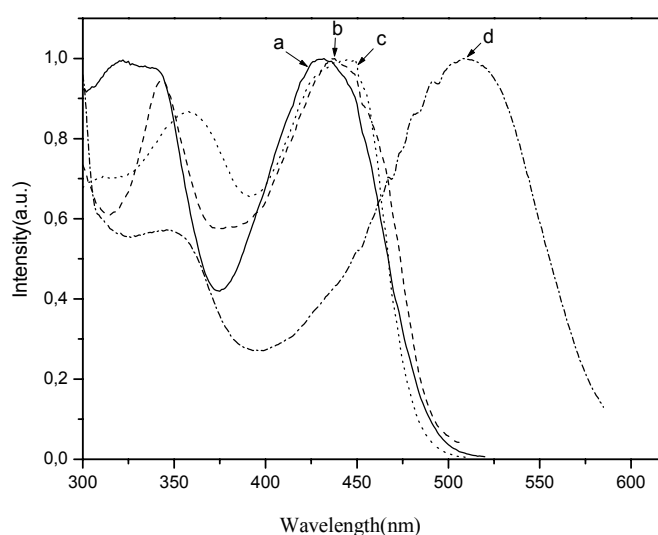
Figure 3.4-11: Excitation spectra of photoluminescent polyiminoacridine in DMAc at 298K. (a) **PIAc-2** neutral form, (b) **PIAc-2** singly protonated form, (c) **PIAc-3** neutral form, and (d) **PIAc-3** singly protonated form.

Table 3.4-5: Maximum UV absorption wavelength, maximum emission wavelength, and photoluminescence Stokes' shifts for the poly(imino acridine)s in DMAc at 298K.

Polymer	λ_{max}^{a} (nm)	λ_{em}^{b} (nm)	Stokes' shifts
Proflavine	406	510	104
PIAc-2	334, 442	530	88
PIAcH^{+}	323, 500	600	100
PIAc-3	357, 442	520	78
PIAcH^{+}	341, 500	610	110

[a]Maximum UV absorption wavelength in DMAc solution, [b]Maximum emission wavelength excited at the absorption maximum 406, 442, 500, 357, 341 nm respectively, in DMAc.

Conclusions:

Poly(imino acridine)s were synthesized *via* palladium-catalyzed amination of aryl dibromides with proflavine, 3,6-diaminoacridine free base. The synthesized polymers were characterized by common spectroscopic methods, gel permeation chromatography (GPC), solubility, thermal behaviour (TGA), differential scanning calorimetry (DSC), UV-vis absorption spectra, and photoluminescence. PIAc polymers were thermally stable in the range of 360-567 °C in nitrogen atmosphere. The absorption spectra of the PIAcs were dependent on the acidity of the media because it can exist in neutral and singly protonated forms in solution. The emission and excitation spectra of the different two forms of the PIAc polymers were investigated by photoluminescence. Moreover, the amorphous nature of the PIAcs was proven by X-ray diffraction. However, T_gs of PIAcs were not detected by DSC. From above one can conclude that insertion of diiminoacridine group into the repeating units of the polymers, **PIAc-1**, **PIAc-2**, and **PIAc-3** resulted in a significant increase of the amorphous nature of the polymer.

The synthesis of PIAc polymers is an important step in the way to convert them into quaternary poly(imino acridinium) salts which might be used as drugs. Our expectations are based on the biological activity such as the bactericidal, algicidal and fungicidal properties of many of these quaternary salts compounds.[301-303]

CHAPTER III

RESULTS AND DISCUSSION

Part 5

3.5 Poly(imino azobenzene)s (PIAzos)
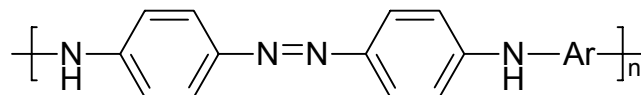
The azobenzene group in a polymer backbone increases the chain stiffness and imparts color to the polymer. Polymers containing azobenzene are expected to be intensively colored because the azo (diazenediyl) linkage, -N=N-, brings the two aromatic rings into conjugation. This gives an extended system of delocalized π-electrons and allows absorption of light in the visible region. These polymers, because of their intense colors and because of their syntheses from relatively inexpensive compounds might be used as dyes.

Photo- and thermolabile polymers revolutionized the modern communication techniques.[304] Large scale reproduction techniques as well as microelectronics would be impossible without polymers which can be structured by light or, more recently, by lasers. Most techniques require a development step in which the latent picture is transformed in the real structure by applying organic solvents, strong bases or acids. More recently, solvent free techniques are favored which prevent swelling of the structures in the solvent (loss of resolution) and are more environmentally friendly. The fast development of the computer techniques with higher structure densities and storage devices of incredible high capacities as well as the aspects of micromechanics and nanotechnogies strongly increase the demand of new polymeric materials with improved property profil adaptable to new imaging techniques.

Azobenzene group is a well-known photosensitive chromophore, which undergoes photoinduced cis-trans isomerization. Owing to the photoactivities, a large number of polymers containing azobenzene groups have attracted interest because of their potential uses in various photonic applications.[304] On the other hand, polymer syntheses using organotransition-metal complexes as catalysts are the subject of recent interest,[305] and various

bond formation processes involving the reaction of two kinds of functional groups catalyzed by organometallic complexes have been applied to the polycondensation reactions of bifunctional organic compounds to give novel poly(arylene)s, aromatic polyesters, polyamides, and the related polymers.[305a,b, 306]

Since the Pd-catalyzed amination reaction offers advantages over the classical methods, which require either activated substrates or severe reaction conditions. The Pd-catalyzed polycondensation could provide various regiodefined polyamines by changing the structure of the aryl dibromides and diamines. Furthermore, a solid-phase synthesis of arylamines *via* the Pd-catalyzed amination of resin-bound aromatic bromides with amines has been reported.[307] These observations prompted us to apply the Pd-catalyzed amination to synthesize polymers containing functional groups in the main chains. Thus, the Pd-catalyzed polycondensation of dibromo compounds with 4,4` diaminoazobenzene to afford polymers (**PIAzo-1-3**) were carried out. These polymers have an azobenzene structure in their main chains and are expected to show photochromic properties similar to those of the reported polymers containing azobenzene groups.[304] Photoinduced cis-trans isomerization behavior of the polymers will be investigated.

Synthesis of 1,4-bis{(4-phenylazo-4`-phenylamino)benzoyl)}benzene (16) as a model compound:

Since model reactions with low molecular weight compounds are extremely useful for better understanding of polymer analogous. Therefore, in studying a new synthetic route for the synthesis of new poly(imino azobenzene)s (PIAzos) *via* diamine and dibromo compounds reaction, the best way to elucidate the processes taking place is by means of model compounds. Careful investigation of the products of the model reaction would provide insights into whether or not there will be side products which will have a negative effect upon the molecular weight or upon the materials properties of the obtained materials in the polymer analogous reaction.

A model compound 1,4-bis{(4-phenylazo-4`-phenylamino)benzoyl)}benzene (**16**) was synthesized by palladium-catalyzed amination of 1,4-bis(4-bromobenzoyl)benzene (**7**) with 4-aminoazobenzene (**15**) as a primary aromatic amine using NaO*t*-Bu as a base and BINAP as a ligand, for comparison with the product of polycondensation. The isolated yield was 83 %, while there were no minor undesired products detected by (FD$^+$) mass spectra or thin-layer

chromatography. The UV-vis absorption spectrum of 1,4-bis{(4-phenylazo-4`-phenylamino)benzoyl)}benzene (**16**) has two broad absorptions. The first absorption is a broad band at 380 nm that is assigned to the electronic $\pi \rightarrow \pi^*$-transition and the second absorption is a shoulder at 430 nm which is assigned to the electronic $n \rightarrow \pi^*$-transition (Table 3.5-4). The first and the second absorption transitions are due to the presence of phenyl and aminoazobenzene rings, respectively.
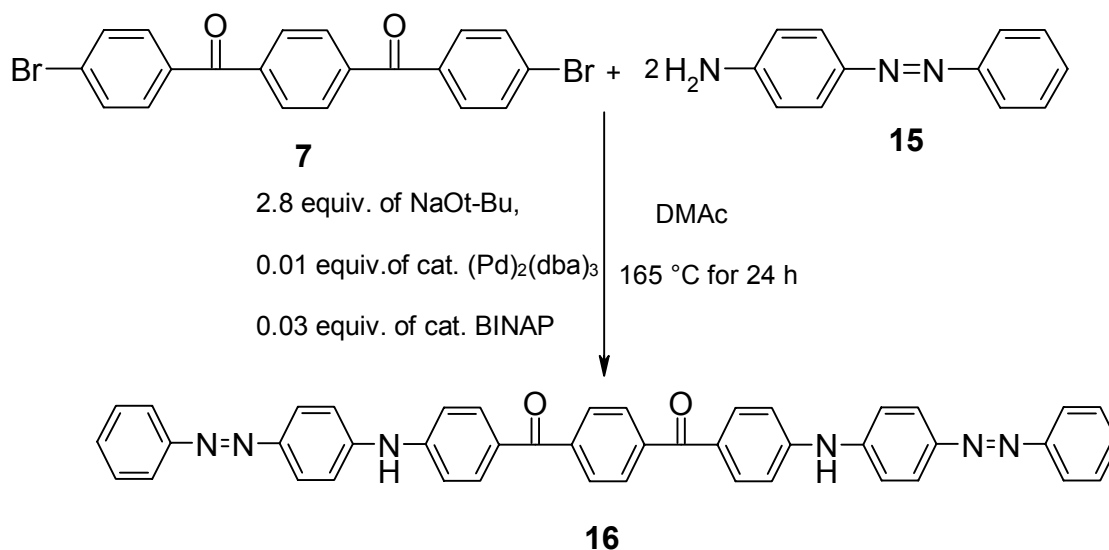
Scheme 3.5-1: Synthesis of 1,4-bis{(4-phenylazo-4`-phenylamino)benzoyl)}benzene (**16**) as a model compound.

Synthesis of poly(imino azobenzene)s (PIAzos)

Recent reports on the Pd-catalyzed aryl amination have demonstrated mechanisms of the reaction and improved catalytic systems.[196] Since satisfactory results were obtained from the model reaction **16**, the synthesis of PIAzo polymers using this new synthetic route was attempted. The model reaction showed that following the diamine / dibromo route PIAzo polymers could be obtained in a single step.

Thus, we planned the Pd-catalyzed polycondensation of 4,4´-dibromobenzophenone or 4,4´-dibromodiphenylether, and 1,4-bis(4-bromobenzoyl)benzene with 4,4` diaminoazobenzene using the combination of Pd₂(dba)₃ and BINAP as an efficient catalytic system for the Pd-catalyzed polycondensation. The results of the Pd-catalyzed polycondensation of these aromatic diamines with different arylene bromides are listed in

Table 3.5-2. The developed method for the synthesis of poly(imino azobenzene)s PIAzo polymers was shown in Scheme 3.5-2.

The reactions of 4,4`-diaminoazobenzene with different arylene bromides provided the corresponding PIAzos in 80-87 % yields without undesired side products.
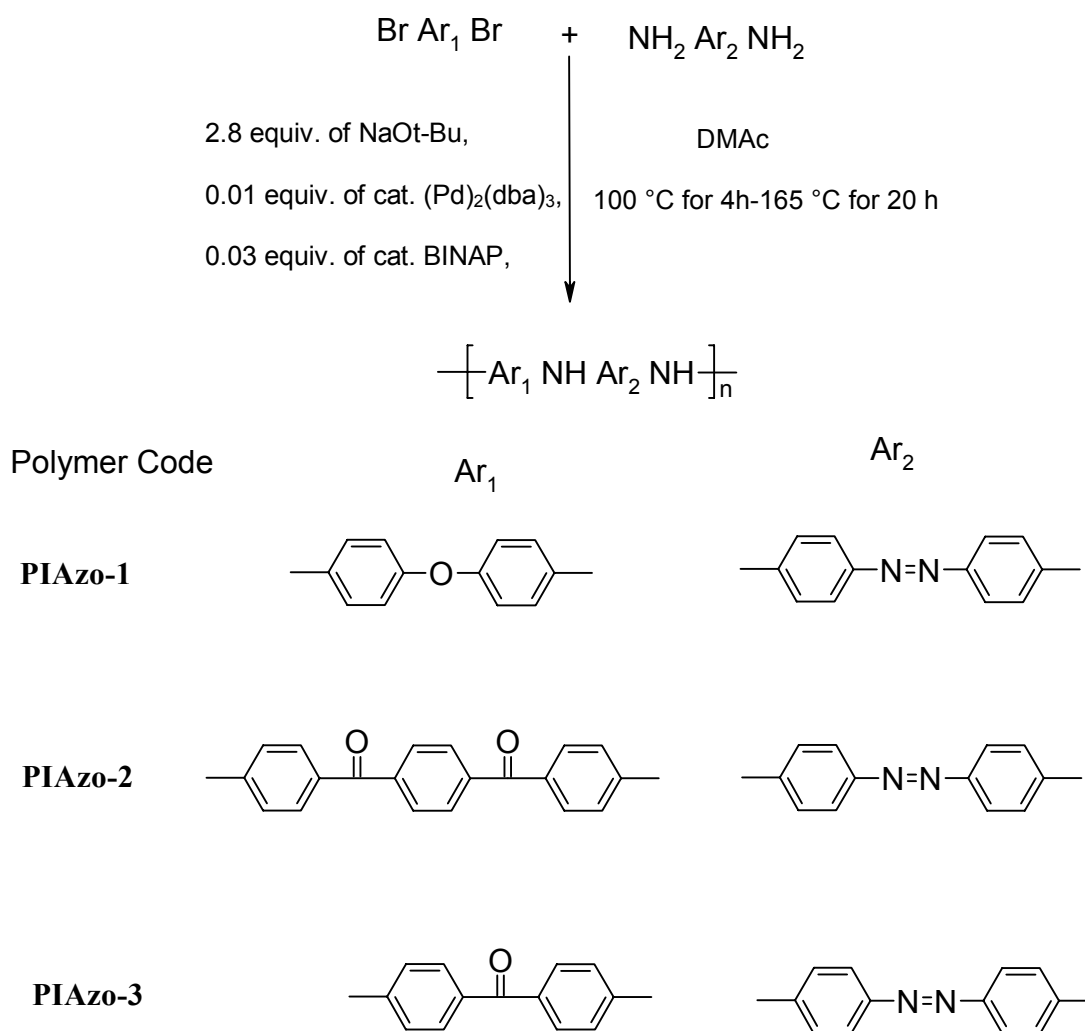
Scheme 3.5-2: Synthesis of poly(imino azobenzene)s PIAzos.

Solubility behavior of PIAzos

The PIAzo polymers showed different solubility in different organic solvents. Polymer solubility was qualitatively determined by the dissolution of 5 mg of solid polymer in 1 mL of organic solvent, and this mixture was then left for 24 h at room temperature, heated or heated using sonication. Polymers **PIAzo-1**, **PIAzo-2**, and **PIAzo-3** could be dissolved in aprotic solvents such as NMP, DMAc, and DMSO while only swelling in other common organic solvents, such as chloroform and dichloromethane (Table 3.4-1). The solid polymer could not be dissolved or swollen in organic solvents, such as methanol and ethanol. Therefore, common organic solvents with low boiling points, such as dichloromethane, chloroform, methanol and ethanol could not be employed to dissolve PIAzo polymers.

Table 3.4-1: Solubility behavior of poly(imino azobenzene).[a]

Polymers	DMAc	DMSO	DMF	NMP	THF	CH$_3$OH EtOH	CHCl$_3$	CH$_2$Cl$_2$
PIAzo-1	++	++	++	++	++	--	-S	--
PIAzo-2	++	++	++	++	±	--	-S	--
PIAzo-3	++	++	++	++	±	--	-S	--

[a] Solubility was measured at polymer concentration, 5 mg. ml^{-1} by the mixing of 5 mg of polymer with 1 ml of solvent, followed by stirring; ++ indicates that the solid polymer was completely dissolved in the solvent to afford a homogeneous solution at room temperature; ± indicates that the solid polymer could be partially soluble at room temperature; -- indicates that the solid polymer could not be dissolved or swollen in the solvent; -S indicates that the solid polymer could be swell at room temperature.

The molecular weights of the PIAzo polymers were measured by GPC (calibrated by polystyrene standards). The molecular weight values M_n are in the range of 7 400-12 900, M_w in the range of 30 000-81 200. GPC analysis revealed that the polydispersities vary from 4.0 up to 6.3. Especially, with increasing molecular weights the polydispersity increases drastically.[214] Table 3.5-2 summarizes the results of the molecular weights of PIAzo polymers.

Table 3.5-2: Characterization of the polymers: (GPC, Yield, FT-IR).

Polymer Code	$\overline{M}_n$ [a]	$\overline{M}_w$ [a]	$\overline{M}_w/\overline{M}_n$ [b]	DP^c	Yield (%)	γNH^d	$\gamma C=O^d$	$\gamma C-N^d$
PIAzo-1	10 900	44 800	4.1	29	82	3389	-	1312
PIAzo-2	7 400	30 000	4.0	15	80	3352	1646	1316
PIAzo-3	12 900	81 200	6.3	33	87	3383	1664	1308

a) Calibrated by GPC polystyrene standards; b) Polydispersity index; c) Degree of polymerization determined from number average molecular weight; d) FT-IR (KBr, pellet).

Elemental analysis of PIAzos

In all cases, the elemental analysis of the PIAzo polymers showed a good agreement with the polymer structure. Obviously, the PIAzo polymers did not show the hygroscopic nature which has been seen for the PIK polymers.

^{1}H-NMR spectra of PIAzos

The ^{1}H-NMR (250 MHz) spectrum of polymer **PIAzo-2** was recorded in diluted solution in DMSO-d_6 at 293K and is shown in Figure 3.5-1. The spectrum revealed a broad peak at 9.42 ppm which was attributed to the protons of the imino groups (NH). The protons of the aromatic ketone H_1 were detected at 7.80 ppm. The protons of azobenzene unit and the aromatic ketone H_2 and H_3 were detected at 7.62 and 7.32 ppm, respectively. The signal of protons H_1-H_3 were figured out from the simulation of polymer **PIFO-4** by the Chem Draw program.[345] Since all the peaks of the ^{1}H- NMR spectrum identified the protons of phenyl and diimino arylene of the main repeating unit of the polymer backbone neither amine-terminated PIAzo polymers nor bromide-terminated PIAzo polymers were observed.
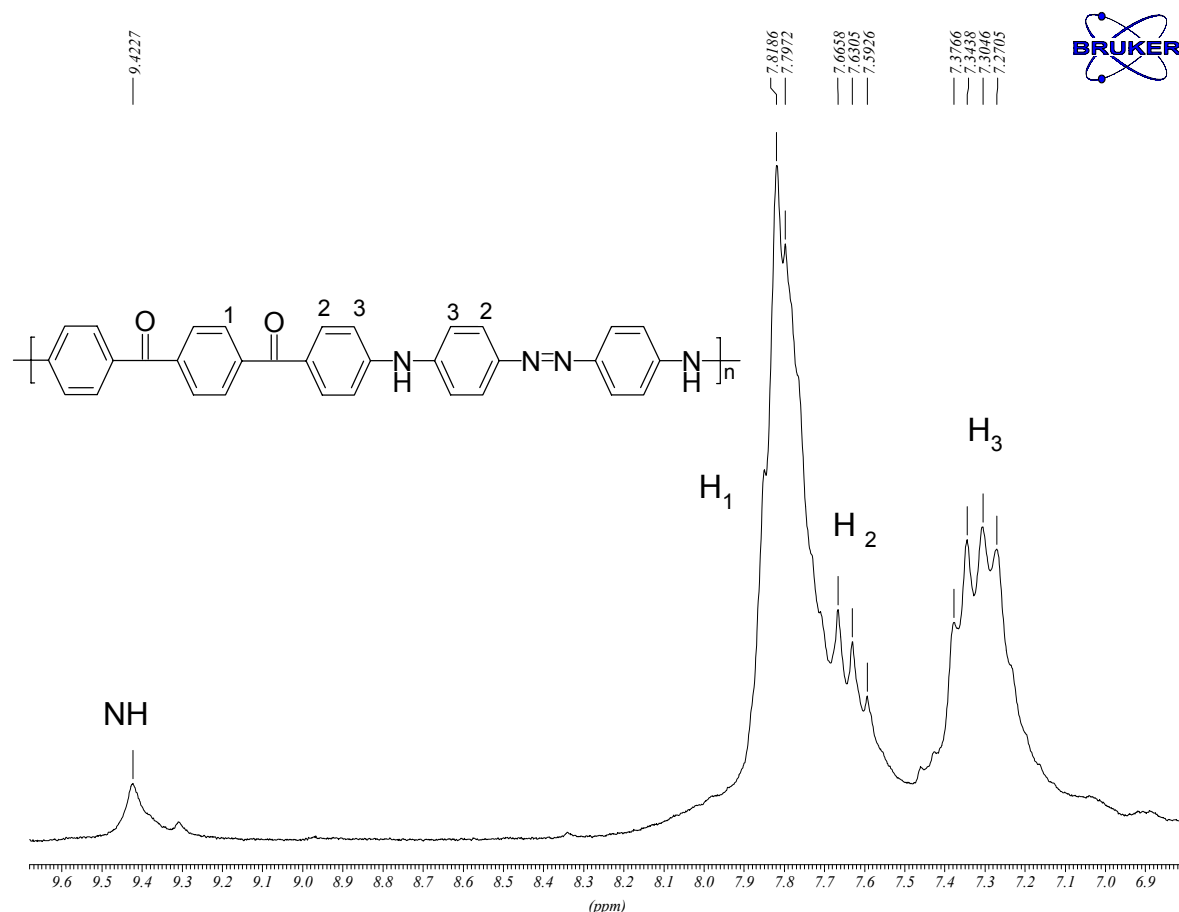
Figure 3.5-1: ^{1}H-NMR (250 MHz) spectrum of polymer **PIAzo-2** recorded in DMSO-d_6 at 293K.

FT-IR spectroscopy of PIAzos

FT-IR spectra were recorded of the all PIAzo polymers in the solid state (KBr pellets) giving results in good agreement with the proposed structure. The characteristic absorptions bands of the imino γ(NH) and carbonyl γ(C = O) groups were detected. The characteristic absorptions for carbonyl groups γ(C = O) appeared between 1646 and 1664 cm^{-1} and characteristic absorption bands for imino groups γ(NH) appeared between 3352 and 3389 cm^{-1}. The assignments of these peaks are listed in Table 3.5-2.

Thermal behavior of PIAzos

Typical TGA traces in air and in nitrogen are demonstrated in Figure 3.5-2 for polymer **PIAzo-2** and **PIAzo-3**. The thermal stability was evaluated by a 5 % weight loss at the minimum temperature (Table 3.5-3). TGA curves revealed that the polymers were thermally stable up to 373-407 °C.

The 50 % weight losse of the polymers took place at over 530-558 °C for polymers **PIAzo-2** and **PIAzo-3** in both air and nitrogen. Char yield is an easy and important measurment which correlates to the ability to sustain combustion.[308] The maximum char yield at 600 °C was obtained for polymer **PIAzo-2** (15 %) and the minimum was obtained for polymer **PIAzo-3** (9 %) in both nitrogen and air.

By comparing the TGA thermograms in air and nitrogen for polymers **PIAzo-2** and **PIAzo-3** (Figure 3.5-2), it was observed that in air the 50 % weight loss of those polymers occurs at 557 and at 530 respectively, which almost the same as in case of nitrogen. In air the char yield at 600 °C was 15 % and 9 % respectively, which is the same as in nitrogen. The 50 % weight losse temperatures in addition to the char yields at 600 °C in both air and nitrogen suggested that thermal degradation in air was not significantly enhanced over the situation in nitrogen. The tested two copolymers indicated a high thermal stability in nitrogen and in air from 373 up to 407 °C.
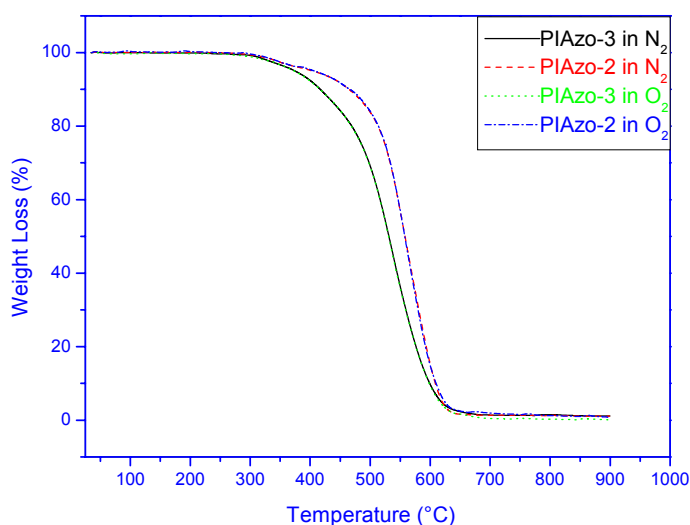
Figure 3.5-2: Dynamic TGA of copolymers **PIAzo-2** and **PIAzo-3**
(in N_2, and in O_2, 10 °C/min.).

Differential scanning calorimetry (DSC) of all the copolymers up to 250 °C showed a single T_g, suggesting a homogeneous amorphous copolymer structure. A representative DSC thermogram of the copolymers is illustrated in Figure 3.5-3. The glass transition temperatures of these copolymers are listed in Table 3.5-3. Polymers **PIAzo-2** and **PIAzo-3** have T_gs 186 and 216 °C respectively, being higher than those of the related PEKs which range from 129 to 167 °C,[229] and are lower than those of aromatic polyamides which range from 292-319 °C.[230] This is due to the hydrogen bonding of polymers **PIAzo-2** and **PIAzo-3** which is weaker than

that of polyamides while PEKs have not. Only polymer **PIAzo-1** has a lower T_g than the other polymers. This is due to the backbone flexibility which results from the flexible ether group.
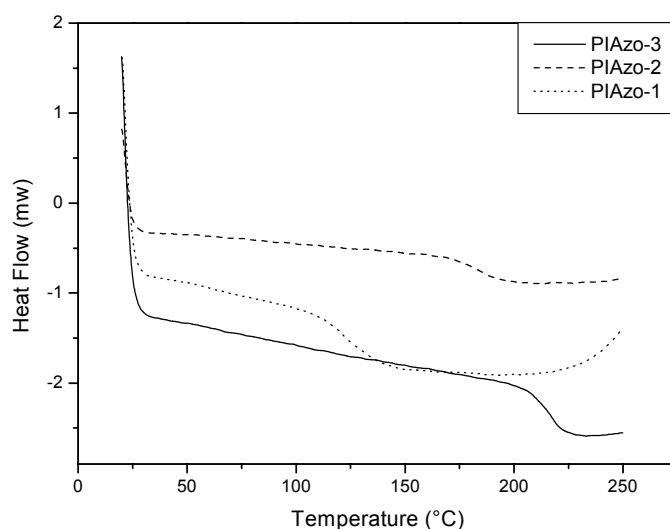
Figure 3.5-3: DSC of PIAzo polymers

(in N_2, 10 °C/min)

The second heating scans were taken into consideration.

Table 3.5-3: Thermal behavior of PIAzos.

Polymer code	O_2 / N_2	$^aT_5$	$^bT_{10}$	$^cT_{50}$	$^dW_{500}$	$^eW_{600}$	Char yield at 600 °C^f	T_g Midpoint^g
PIAzo-2	O_2	407	466	557	16	85	15	185
	N_2	403	464.5	558	16	85	15	
PIAzo-3	O_2	373	416	530	31	91	9	216
	N_2	374	417	531	31	90	10	

a) T_5: Temperature of 5 % weight loss; b) T_{10}: Temperature of 10 % weight loss; c) T_{50}: Temperature of 50 % weight loss; d) W_{500}: weight loss at 500 °C, determined from TGA curve; e) W_{600}: weight loss at 600 °C, determined from TGA curve; f) The remaining of the polymer at 600 °C; g) Midpoint of the second heating traces of DSC measurements conducted with a heating rate of 10 °C min^{-1} in nitrogen.

Wide-angle X-ray diffraction of PIAzos

The wide-angle X-ray diffraction patterns of the PIAzo polymers over the 2θ range of 5-30° are shown in Figure 3.5-4. Despite, the presence of the rigid secondary amine ring in polymers **PIAzo-1**, **2**, and **3**, they revealed essentially amorphous patterns in the solid state (Figure 3.5-4). This may be attributed to the fact that the regularity of the repeating units in polymers **PIAzo-1**, **2**, and **3** is disrupted by the different appearing orders of the imino and carbonyl groups, thus leading to a decreased crystallinity. Moreover, polymer **PIAzo-1** contains a kinked ether group which is known to induce loose chain packing.[248] The amorphous nature of these polymers was reflected in their good solubility.
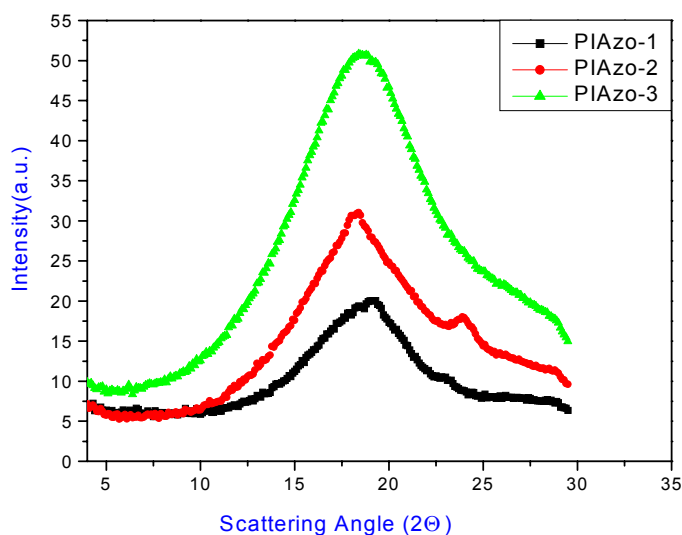
Figure 3.5-4: Wide-angle X-ray diffractograms intensity vs Bragg angle graph for powders of polymers **PIAzo-1**, **PIAzo-2**, and **PIAzo-3**.

Dynamic mechanical analysis of PIAzos

Figure 3.5-6a shows a comparison of the isochronal temperature dependencies of the real, G'; and imaginary, G'', components of the complex shear modulus for polymer **PIK-13**, **PIAzo-2**, and **PIAzo-3** (Figure 3.5-5) with similar monomer size but different constitution which should considerably influence the stiffness of the polymer backbone. It is seen that this variation of constitution increases the temperature of main softening of the polymers. Whereas the polymer **PIK-13** which does not contain "Azo" groups undergoes the softening at the temperature of about 170 °C, the other two samples remain glassy up to high temperatures. Additionally in the two latter polymers **PIAzo-2**, and **PIAzo-3** the softening depends on the proportions between the "Azo" and the flexible fraction in the chains. When the chains contain only one "Azo" and one "Carbonyl" group polymer in case of **PIAzo-3** the softening takes place at a temperature exceeding 250 °C. The softening in the studied polymers **PIK-13**, **PIAzo-2**, and **PIAzo-3** has typical features of a glass transition in amorphous polymers. At the transition the modulus G' drops from nearly 1 GPa level to the level of 1 MPa which is characteristic for the rubbery state of entangled linear polymers. The transition at a given deformation frequency can be considered as taking place at the maximum of G'' which is clearly seen for all samples and should be attributed to the vitrification of the segmental mobility in the polymers. It can be noticed that the G'' maximum is much narrower for the polymer **PIK-13** with the flexible backbone and becomes remarkably broader when the monomer consists of both stiff and flexible fragments (**PIAzo-2**, and **PIAzo-3**) i.e. has a composition which can cause a considerable dynamic heterogeneity. The softening has a calorimetric effect as illustrated in Figure 3.5-6c by means of the DSC traces recorded during heating. The characteristic step in the heat flow trace indicates the glass transitions which change with the varying monomer constitution in the same way as described above i.e. increasing stiffness involves an increase of the glass transition temperature of polymers **PIK-13**, **PIAzo-2**, and **PIAzo-3**. The temperatures determined from the DSC results are given in Table 3.5-3. The differences between the glass transition temperatures determined form the DSC and the softening temperatures seen in the mechanical behavior result from the relatively high deformation frequency used in the mechanical measurements.
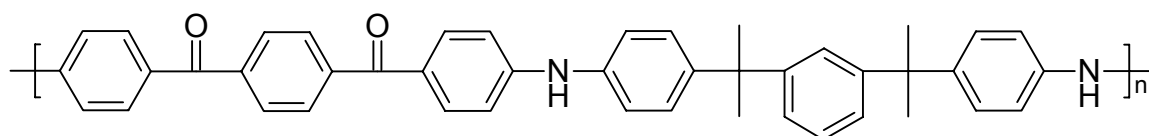
PIK-13
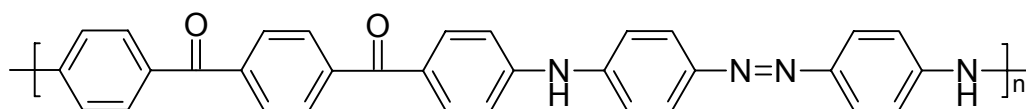
PIAzo-2
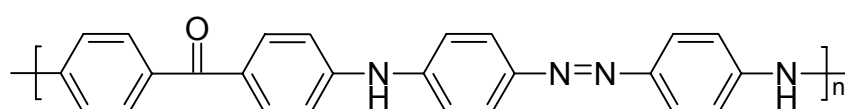
PIAzo-3

Figure 3.5-5.

The behavior of the systems above the glass transitions should be dependent on the terminal flow of the melt and the chain length of the polymers and thus the entanglement if the chains are sufficiently long. For the examined materials the terminal flow is only observed for the most flexible polymer **PIK-13** with the lowest T_g. For the other polymers **PIAzo-2**, and **PIAzo-3**, the high temperature behavior seems to be influenced by the limited thermal stability. They show a rubbery plateau above the glass transition but as the temperature is approaching 300 °C the elastic modulus increases indicating that probably a cross-linking is taking place. At these temperatures the TGA results (Figure 3.5-6c) indicate an onset of the mass loss especially in the samples containing the "Azo" groups (**PIAzo-2**, and **PIAzo-3**). This effect makes an observation of the terminal flow impossible and consequently one can not judge the role of the chain lengths in these polymers for the rheological behavior. For the flexible polymer, **PIK-13** where the terminal flow is observed it is possible to conclude that the chains seem to have lengths slightly below the critical length i.e. the length at which the rheological behavior would be controlled by entanglements.
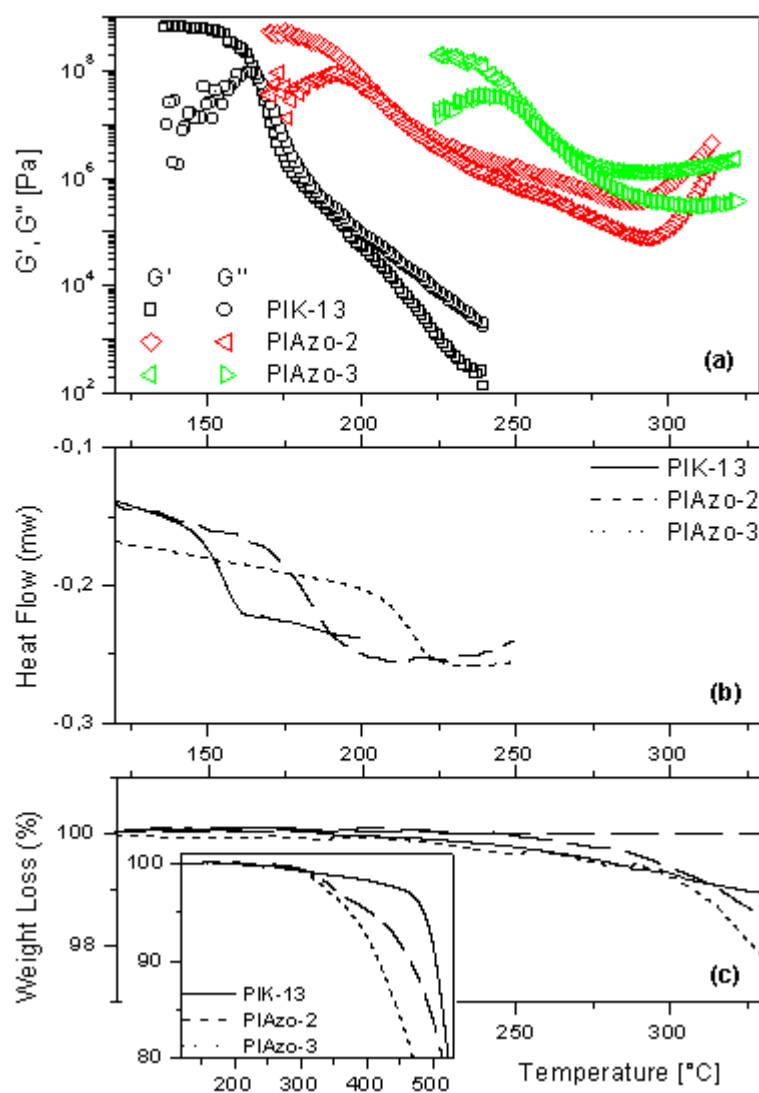
Figure 3.5-6a-c: A comparison of the isochronal temperature dependencies of the real, G';

and imaginary, G'', components of the complex shear modulus for polymer

PIK-13, **PIAzo-2**, and **PIAzo-3**.

UV–vis absorption spectra, photo and thermally induced cis-trans-isomerization

The UV–vis absorption spectrum of polymer **PIAzo-2** in DMF exhibits two absorption peaks at 388 and 452 nm, presumably based on the $\pi{\to}\pi^*$-and $n{\to}\pi^*$-transitions of phenyl and aminoazobenzene units, respectively. The absorption spectrum is essentially the same as those of polymer **PIAzo-3**, two absorption peaks at 386 and 465 nm. However, only one absorption peak at 456 nm was detected for polymer **PIAzo-1** due to the absence of the (C = O) (Figure 3.5-7).
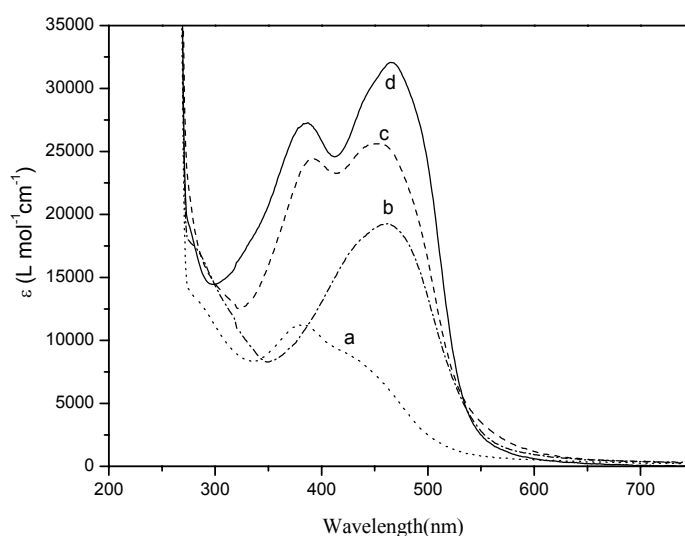
Figure 3.5-7: UV-vis absorption spectra of model compound **16**, polymers **PIAzo-1**, **2** and **3** (conc. 2 x 10^{-5} M in DMF). (a) model compound **16**, (b) polymer **PIAzo-1**, (c) polymer **PIAzo-2**, and (d) polymer **PIAzo-3**.

Before irradiation, polymer **PIAzo-2** exhibited the above two absorption bands at 388 and 452 nm^{-1} (Figure 3.5-9b). After irradiation of **PIAzo-2** by light at about 365 nm, the absorption peak at 388 nm gradually decreased while the absorption peak at 452 nm gradually increased by increasing the irradiation time with two isosbestic points at about 399 and 524 nm. This is attributed to the trans-cis-photoisomerization of the azobenzene moieties in the main chain of **PIAzo-2** polymer backbone (Figure 3.5-9b). The changes in the UV–vis absorption spectra of DMF solutions of polymers **PIAzo-1**, and **PIAzo-3** during irradiation of light at about 365 nm were also recorded (Figures 3.5-9a, and c).

In the thermal isomerization polymer **PIAzo-2**, previously irradiated at about 365 nm, was annealed at 80 °C in the dark. The absorption peak at 388 nm steadily increased while the absorption peak at 452 nm steadily decreased to the starting value before irradiation. This indicates that the cis-trans-isomerization of the azobenzene groups occurred thermally. The changes in the UV–vis absorption spectra of the DMF solutions of 1,4-bis{(4-phenylazo-4`-phenylamino)benzoyl)}benzene (**16**), **PIAzo-1**, and **PIAzo-3** were also observed. In all samples, the photoinduced and thermal cis-trans-isomerization was induced repeatedly. No significant influence of solvents was observed on the azobenzene cis-trans-isomerization (Figures 3.5-9a-c). Both thermal and photoinduced-isomerization processes would occur by in-plane translation of the benzene ring further from the main chain rather than by rotation around the N=N bond (Figure 3.5-8). Similar results have been reported for polymers containing azobenzene groups.[304 c,d]
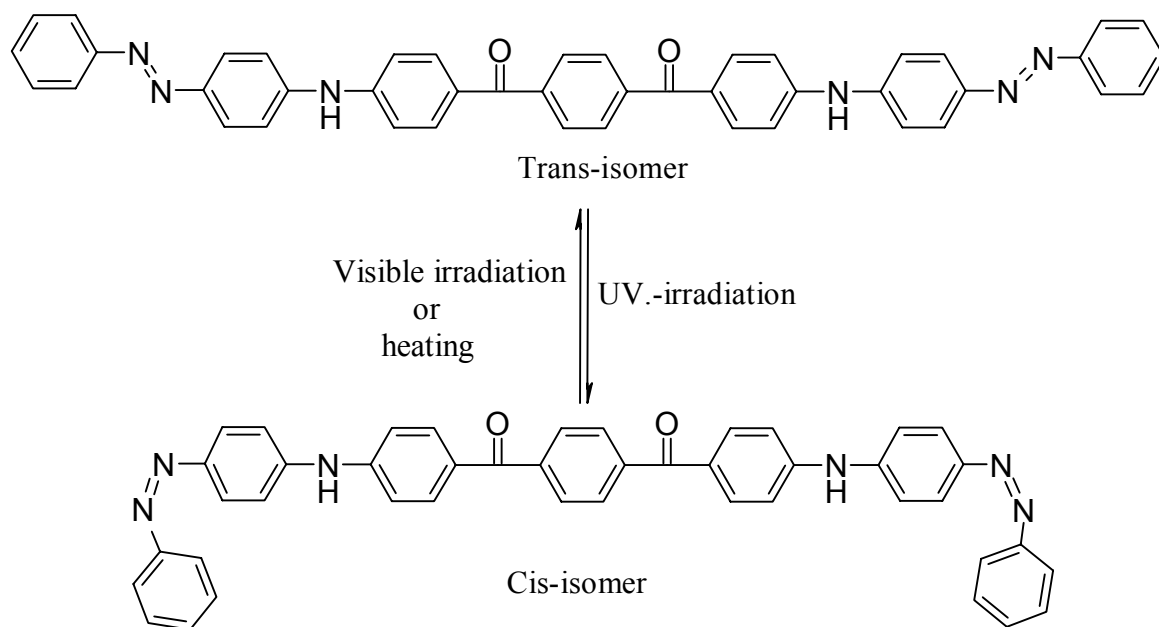
Figure 3.5-8: Photoisomerisation of 1,4-bis{(4-phenylazo-4`-phenylamino)benzoyl)}benzene (**16**).
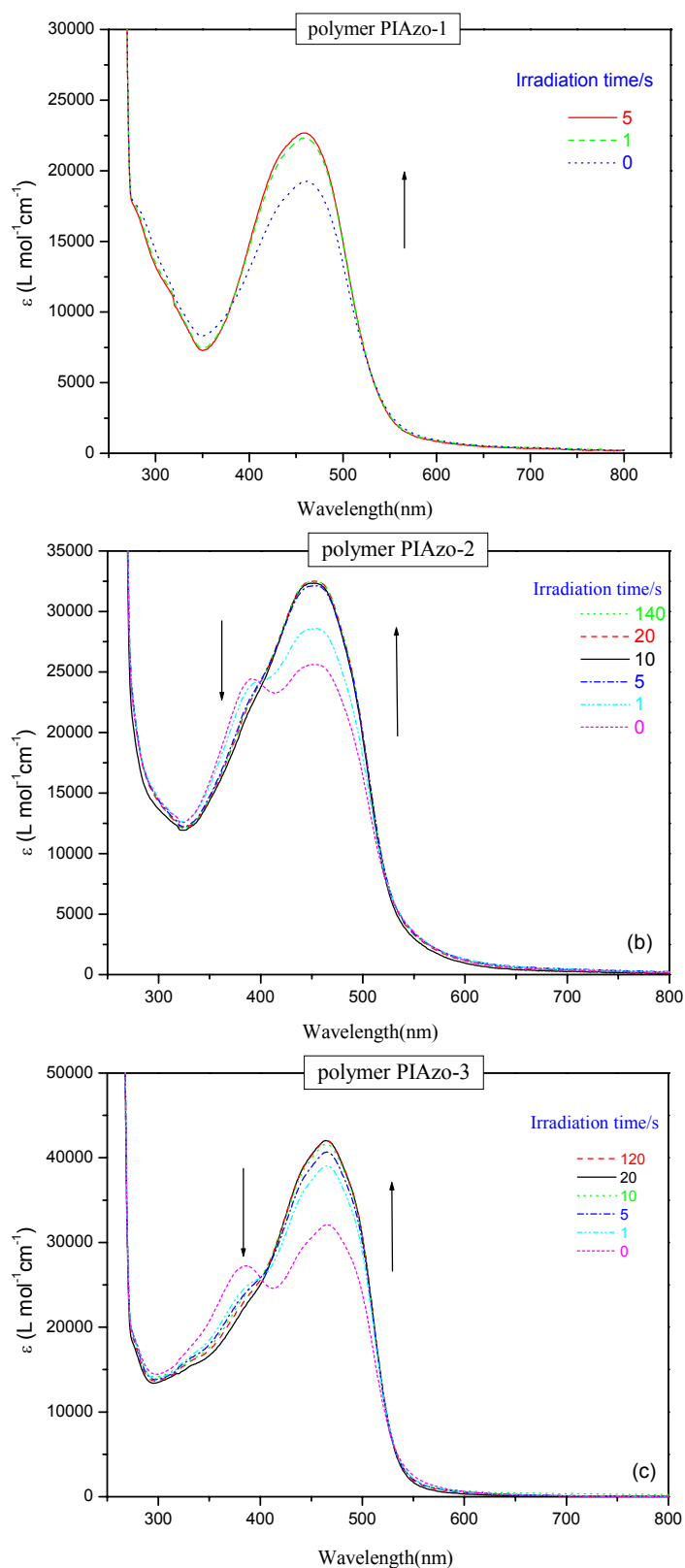
Figures 3.5-9a-c: Changes in the absorption spectra of (a) **PIAzo-1**, (b) **PIAzo-2**, and (c) **PIAzo-3** (ca. 2 x 10^{-5} M of the azobenzene unit in DMF) during irradiation with light at about 365 nm.

Protonation of PIAzos

The absorption properties of the polymers and of the model compound 1,4-bis{(4-phenylazo-4`-phenylamino)benzoyl)}benzene (**16**) are also dependent on the acidity of the media. Figures 3.5-11 and 3.5-12 showed the changes in the absorption spectra of DMF solutions of **PIAzo-2**, and **PIAzo-3** with increasing concentration of CF₃COOH. In Figure 3.5-11, the addition of CF₃COOH led to a decrease of the bands at 388 and 452 nm and an appearance of a new band at 600 nm with no isosbestic points. The absence of the isosbestic points indicates the formation of different reaction products or intermediates as shown below (Figure 3.5-10). DMF solutions of **PIAzo-1** and model compound **16** display similar changes in the absorption spectra upon adding CF₃COOH. The new band at 600 nm may be assigned as the protonated resonating form of aminoazobenzene group expressed by Figure 3.5-10, analogous to that of methyl orange.[309] The complete protonation was monitored by the constancy of the high molar extinction coefficient of the new band at ((λ_{max}= 600 nm, ε_{600} = 34 200 L. mol⁻¹. cm⁻¹). Upon complete protonation, the color of the polymer solution transferred from yellow to blue which differs significantly from other polymer containing azobenzene group where the color transferred from yellow to purple.[310] The blue color is due to the interaction of the positive charge with the extent of the π-electron system in the former. However, the short length of conjugation decreases the interaction of the positive charge with the delocalized π-system in the latter.
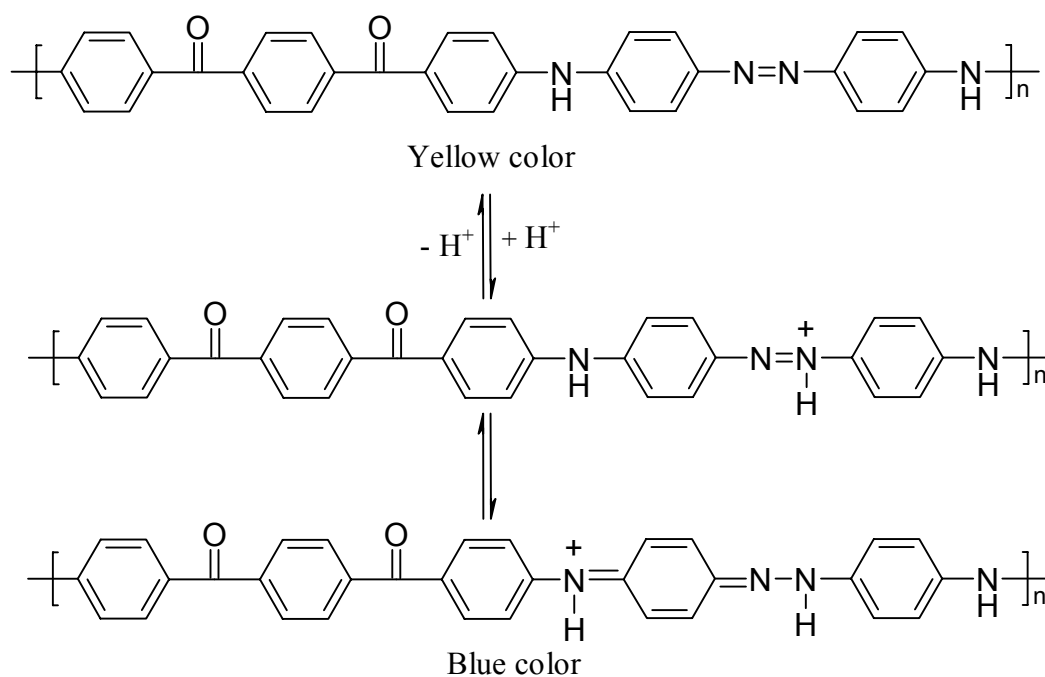
Figure 3.5-10.
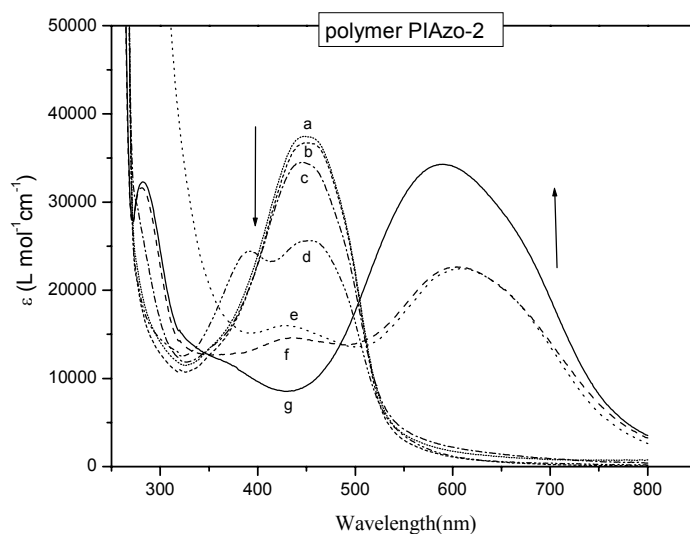
Figure 3.5-11: Changes in the absorption spectra of **PIAzo-2** (ca. $2x10^{-5}$ M of the azobenzene unit in DMF) with increasing concentration of trifluoroacetic acid (TFA). [TFA]: (a) 0, (b) 0.04 x 10^{-1}, (c) 0.2 x 10^{-1}, (d) 1.6 x 10^{-1}, (e) 58.7 x 10^{-1}, (f) 65.3 x 10^{-1}, (g) 78.3 x 10^{-1} mol. l^{-1}.
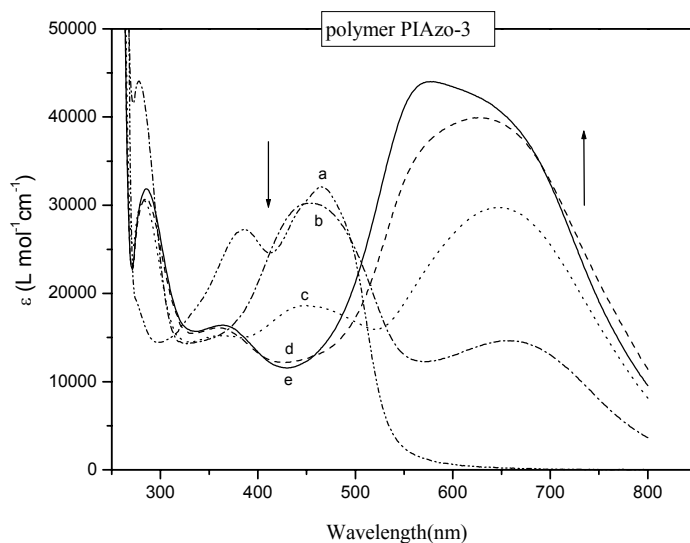
Figure 3.5-12: Changes in the absorption spectra of **PIAzo-3** (ca. $2x10^{-5}$ M of the azobenzene unit in DMF) with increasing concentration of trifluoroacetic acid (TFA) in DMF. [TFA]: (a) 0, (b) 52.2 x 10^{-1}, (c) 58.8 x 10^{-1}, (d) 65.3 x 10^{-1}, (e) 78.3 x 10^{-1} mol. l^{-1}.

Photoluminescence spectra of polymer containing azobenzene group in the main chain

The polymers show photoluminescence in DMF solution when excited at their absorption maximum (Table 3.5-4). The maximum emission wavelength (λ_{em}) ranges from 440 to 550 nm, depending on the starting structures. The emission spectra of all these species show a broad band with the maxima centered around 570-600 nm, although the absorption maxima of polymers **PIAzo-1**, **PIAzo-2**, and **PIAzo-3** are considerably red shifted compared to that of model compound by 100, 80, 110 nm respectively (Figure 3.5-13). The large Stokes' shifts for model compound **16**, polymers **PIAzo-1**, **PIAzo-2**, and **PIAzo-3** were in the range 10, 78, 68, and 85 nm respectively. This revealed that the difference in energy between the excitation and emission maximum is higher in case of the PIAzo polymers than of the model compound **16**. From a practical point of view, the detection of photoluminescent species is of course easier when the Stokes' shift is larger.[311] The excitation spectra, recorded for different species are similar to the absorption spectra of the corresponding species. The emission spectra of the various forms recorded in dimethylformamide were shown in Figure 3.5-13. These results were summarized in Table 3.5-4. In general, the presence of the heavy atoms as substituents of aromatic molecules (e.g Br) results in quenching of the photoluminescence (internal heavy atom effect) because of the increased probability of intersystem crossing.[312] No quenching of the photoluminescence spectra was recorded which may prove that the PIAzo polymers have no bromine end groups. This was confirmed by ^{1}H-NMR (Figure 3.5-1). The emission peaks in the photoluminescence spectra of PIAzos at 520-550 nm are similar to those seen from the other reported polymers.[313]

Table 3.5-4: Maximum UV absorption wavelength, maximum emission wavelength, and photoluminescence Stokes' shifts for the polymer containing an azobenzene group in DMF at 298K.

Polymer	$\lambda_{max}{}^a$ (nm)	$\lambda_{em}{}^b$ (nm)	Stokes' shifts
(**16**)	380, 430	440	10
PIAzo-1	462	540	78
PIAzo-2	388, 452	520	68
PIAzo-3	386, 465	550	85

^{a}Maximum UV absorption wavelength in DMF solution, ^{b}Maximum emission wavelength excited at the absorption maximum 382, 462, 452, and 465 nm respectively, in DMF solution.
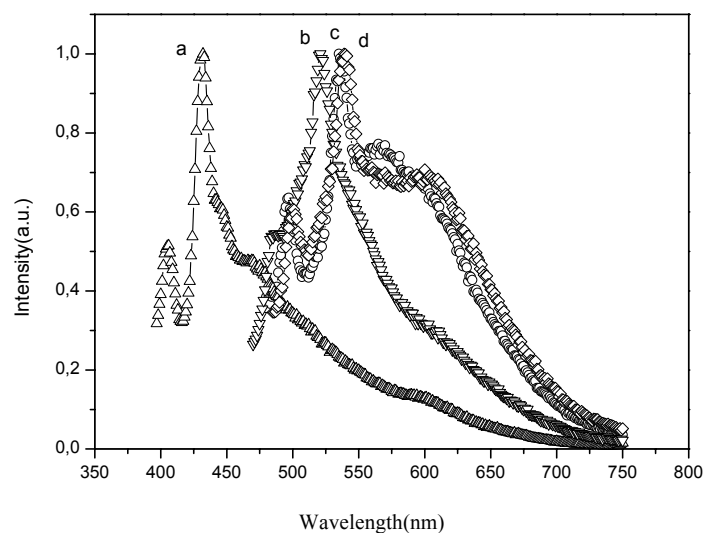
Figure 3.5-13: Emission spectra of photoluminescent polymer containing azobenzene group
in the main chain in DMF at 298K. Emission spectra of model compound and
polymers **PIAzo-1**, **PIAzo-2**, and **PIAzo-3** excited at 382, 462, 452 and 465 nm
respectively, in DMF solution: (a) Model compound **16**, (b) Polymer **PIAzo-2**,
(c) Polymer **PIAzo-1**, and (d) Polymer **PIAzo-3**.

Conclusions

The introduction of aminoazobenzene units into the main chain of the polymer smoothly proceeded in a one-pot procedure *via* the Pd-catalyzed amination. The absorption spectra of PIAzos were dependent on the acidity of media because they can exist in neutral and protonated forms. The obtained polymers exhibited photoinduced and thermal isomerization properties of the azobenzene moieties; however, it appears that the structure of the polymer main chain has no effect on the isomerization behavior. The photoinduced and thermal isomerization behaviors of PIAzos were observed by monitoring the changes in the absorbance (at 388 and 452 nm) with time at constant temperatures with the UV-visible absorption spectrometer.

WAXD revealed that insertion of diiminoazobenzene group into the recurring units of polymers **PIAzo-1**, **2**, and **PIAzo-3** resulted in a significant increase of the amorphous nature of the polymer. This is similar to the insertion of diiminoacridine into the recurring units of PIAzos. In the solid state PIKs showed an increase of ordering which was not detected in case of PIAcs or polymer containing azobenzene group in the main chain as indicated by the X-ray diffractograms. The stiffness of the PIAzo polymers was proven by means of rheological measurements in comparison with flexible PIKs. Due to the presence of the azobenzene group in the PIAzos backbone which imparts an intense red color in addition to resulting from cheap, one-pot and simple chemistry, they might be used as dyes.

Chromic polymers are attracting increasing interest for both fundamental and potential applications,[314-315] particularly in view of their possible exploitation in nonlinear optics and optoelectronics.[316-317] The chromic characteristics of poly(imino azobenzene)s may provide new sensory devices as reported for other polymers containing azobenzene.[310] Moreover, poly(imino azobenzene)s as an optically active polymer are important functionalized materials because of their photoresponsive properties.

CHAPTER III

RESULTS AND DISCUSSION

Part 6

3.6 Novel Poly(imino fluorenone)s (PIFOs)
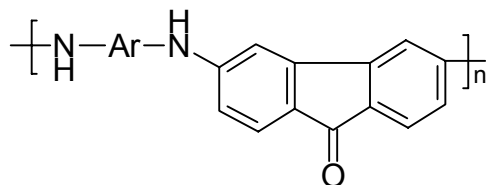
It has become a great challenge to fabricate a light-emitting diode (LED) for a full color display since the polymer LED was introduced in 1990.[318] There have been synthesized a sizable number of polymers emitting blue,[319–322] green [323–325] and red [326–328] light. A large number of light-emitting polymers are listed in the literature.[329] Polymers are attractive since a suitable functional group can be imbedded in the molecule by attaching a chemical group covalently. The solubility of a polymer is easily enhanced by attaching side groups on the polymer chain without disturbing the band gap.[330,331]

A number of fully and partially conjugated polymers have been designed and synthesized to realize efficient blue photoluminescence (PL) and electroluminescence (EL); however, only a limited number of polymers appear promising for use in blue polymer LEDs.[332, 333]

The synthesis of conjugated polymers has developed from a purely structural motivation to providing materials for electrical and optical applications.[334-338] Many such applications are related to the formation and migration of charge. However, there are only few reports on electron-deficient conjugated polymers.[334,339] Characteristic features of these structures are their low-lying conduction bands and their high electron affinity, which would qualify them as candidates for n-type electrical conductors. Typical applications would be conceivable in photovoltaic cells or in multilayer light-emitting diodes (LED). 2,7-Poly-(9-fluorenone) (2,7-PFO) has been introduced as a new electron-deficient polymer in which the withdrawing effect of the carbonyl groups lowers the reduction potential.[334] Our idea is to

synthesize novel conjugated (**PIFO-1** and **2**) and non-conjugated (**PIFO-3**, **4** and **5**) PIFO polymers containing novel carbon-nitrogen linkage as electron-deficient polymers *via* palladium-catalyzed polycondensation. An extensive characterization of the PIFO polymers in terms of gel permeation chromatography (GPC), polymer solubility, thermal behavior (TGA), differential scanning calorimetry (DSC), UV-vis absorption spectra, photoluminescence, dynamic mechanical analysis, and hydrogen bonding will be studied. Moreover, the nature of the polymer will be studied by X-ray diffraction.

Synthesis of 3,6-dibromo-9-fluorenone (19) as a monomer:

3,6-Dibromo-9-fluorenone (**19**) was synthesized from phenanthrenequinone (**17**) using two step reaction according to literature procedures[340,341] after modification. The first step is the aromatic electrophilic substitution *via* bromination reaction using slight excess of bromine in nitrobenzene was at 100 °C to give the brominated 3,6-dibromophenanthrenequinone (**18**). The second step converting of compound **18** into compound **19** by a ring contraction, followed by oxidation using KMnO₄ (Scheme 3.6-1).
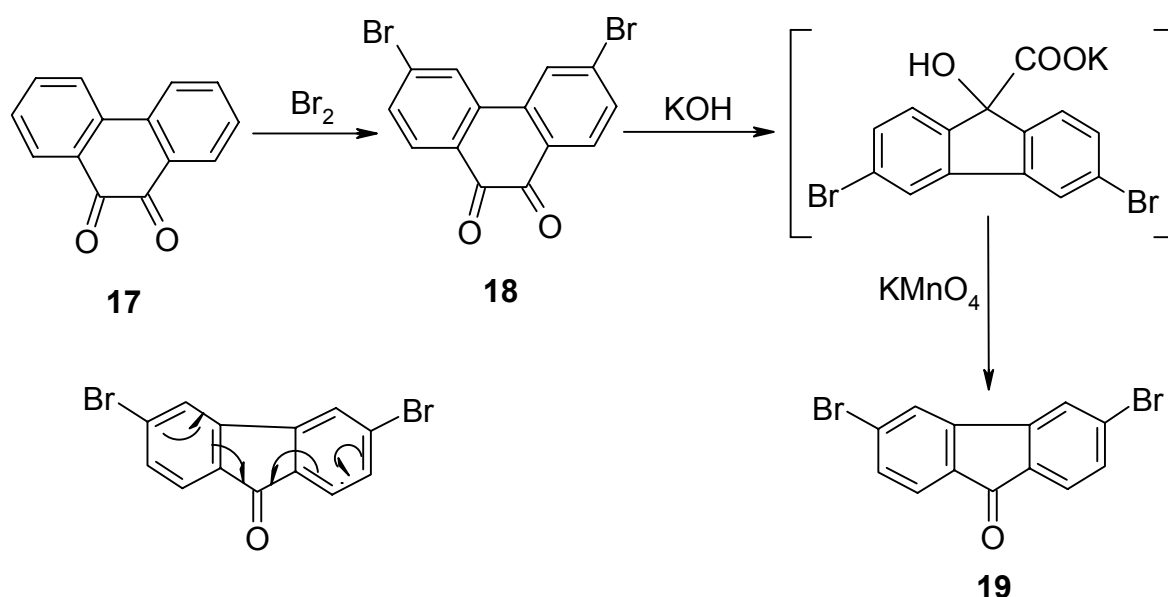
Scheme 3.6-1: Synthesis of 3,6-dibromo-9-fluorenone (**19**) as a monomer.

Synthesis of 3,6-dianilino-9-fluorenone (20) as a model compound

A model compound 3,6-dianilino-9-fluorenone (**20**) was synthesized by palladium-catalyzed amination of 3,6-dibromo-9-fluorenone (**19**) with aniline as a primary aromatic

amine using NaO-*t*-Bu as a base and BINAP as a ligand. The isolated yield was 83 %, while there were no undesired side products detected by (FD$^+$) mass spectra or thin-layer chromatography. Scheme 3.6-2 showed the model compound reaction. The UV-vis absorption spectrum of 3,6-dianilino-9-fluorenone (**20**) has two broad absorptions. The first absorption is a shoulder at 450 nm and the second absorption is a broad band at 600 nm. Since model compound possesses an electron-donating group (imino group) conjugated to an electron-withdrawing group (carbonyl group), this result in a photoinduced intramolecular charge-transfer (ICT).[342] Therefore the long wavelength transition observed for model compound can be assigned to the intramolecular charge-transfer transition (ICT), where charge transfer occurs from the two imino groups toward the electron-poor carbonyl moiety.

Solvatochromism is a typical behavior of compounds containing charge transfer. They exhibit absorption at higher wavelength in polar solvents such as methanol than in non-polar solvents such as benzene. Solvatochromism as a proof of the ICT in the model compound **20** could not be recorded due to its poor solubility in non-polar solvents. This solvatochromism[343] is, however expected to be much smaller for the model compound where solvent interaction is restricted because of the intramolecular hydrogen bond as reported for 1-aminoanthraquinone.[343]
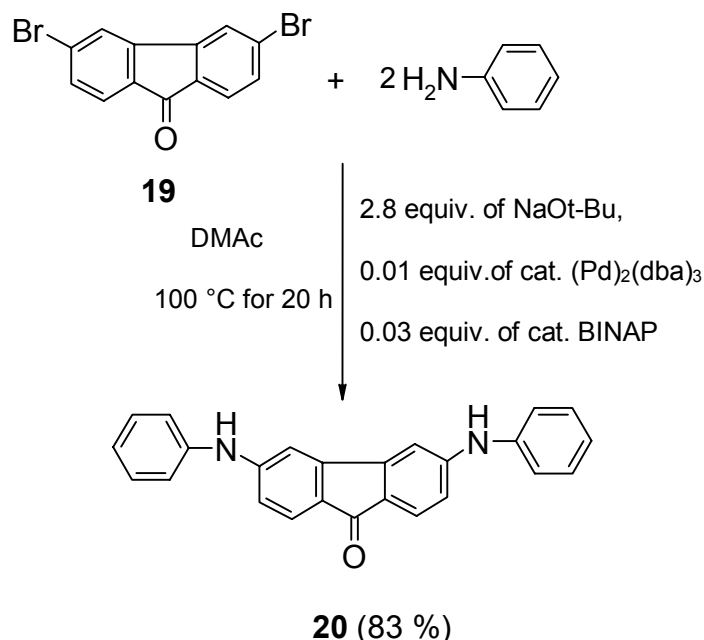
Scheme 3.6-2: Synthesis of 3,6-dianilino-9-fluorenone (**20**) as a model compound.

Synthesis of PIFOs

Since satisfactory results were obtained from the model reaction **20**, the synthesis of PIFOs using this new synthetic route was attempted. The model reaction showed that following diamine / dibromo route PIFO polymers could be obtained in a single step.

Reactions of electron-poor aromatic halides and electron-rich amines give the highest yields in the amination chemistry.[344] Thus, we attempted polycondensation of monomers 3,6-dibromo-9-fluorenone (**19**) as electron-poor arylene bromides with a series of electron-rich primary aromatic diamines. The results of the Pd-catalyzed polycondensation of these aromatic bromides with different diamines are listed in Table 3.6-2.
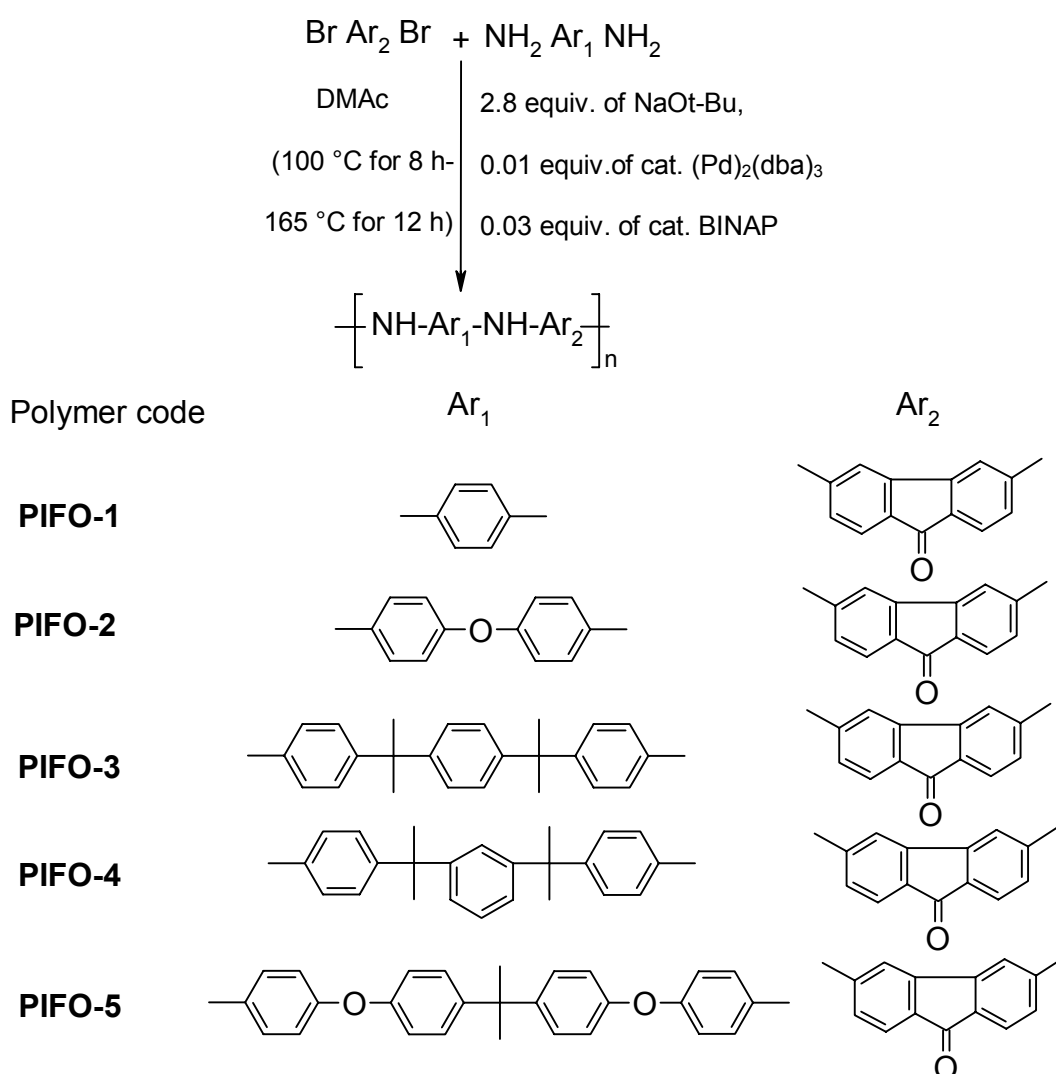
Scheme 3.6-3: Synthesis of novel poly(imino fluorenone)s (PIFOs).

A method was developed for the synthesis of poly(imino fluorenone)s PIFOs (Scheme 3.6-3). The reactions of the dibromo monomer **19** with different arylene diamines having electron donating substituents provided the corresponding PIFOs in 84-93 % yields without undesired side products.

Solubility behavior of PIFOs

The PIFO polymers showed different solubility in different organic solvents. Polymer solubility was qualitatively determined by the dissolution of 5 mg of solid polymer in 1 mL of organic solvent, and this mixture was then left for 24 h at room temperature, heated or heated using sonication. The dissolution process depended on the solvent quality, the molecular weight, and chemical structure of the polymer. Polymers **PIFO-1**, **2**, **3**, **4**, and **5** could be dissolved in aprotic solvents such as NMP, DMAc, and DMSO while only swelling in other common organic solvents, such as chloroform and dichloromethane. Except polymer **PIFO-3**, and **4** which could be dissolved, PIFOs could be patially soluble in DMF by dissolution means. The solid polymer could not be dissolved or swollen in organic solvents, such as methanol and ethanol. Therefore, common organic solvents with low boiling points, such as dichloromethane, chloroform, methanol and ethanol could not be employed to dissolve PIFOs (Table 3.6-1).

Table 3.6-1: Solubility behavior of PIFOs.[a]

Polymers	DMAc	DMSO	DMF	NMP	THF	MeOH EtOH	CHCl$_3$	CH$_2$Cl$_2$
PIFO-1	++	++	±	++	±	--	*-S*	*-S*
PIFO-2	++	++	±	++	±	--	--	--
PIFO- 3	++	++	++	++	±	--	*-S*	*-S*
PIFO-4	++	++	++	++	±	--	*-S*	*-S*
PIFO-5	++	++	±	++	±	--	*-S*	*-S*

[a] Solubility was measured at polymer concentration, 5 mg. ml^{-1} by the mixing of 5 mg of polymer with 1 ml of solvent, followed by stirring; ++ indicates that the solid polymer was completely dissolved in the solvent to afford a homogeneous solution at room temperature or by sonic; ± indicates that the solid polymer could be partially soluble at room temperature, heating and heating using sonication; -- indicates that the solid polymer could not be dissolved or swollen in the solvent; -S indicates that the solid polymer could be swell at room temperature.

Since 2,7-poly(9-fluorenone) (2,7-PFO) and even low-molecular weight oligomers of fluorenone were insoluble materials,[339] the solubility of PIFO polymers (soluble materials) was improved over the 2,7-poly(9-fluorenone) (2,7-PFO) (insoluble material) and even low-molecular weight oligomers of fluorenone.

The molecular weights of the PIFOs were measured by GPC (calibrated by polystyrene standards). The molecular weight values M_n are in the range of 4 500-14 400, M_w in the range of 10 800-83 800. GPC analysis revealed that the polymer polydispersities vary from 2.4 up to 6.4 (Table 3.6-2). Especially, with increasing molecular weights the polydispersity increases drastically.[214] The GPC values in case of polymers **PIFO-1**, **2**, and **5** represent only the soluble fraction in DMF (about 40 %, 60 %, and 75 %, respectively). Therefore the molecular weight of them expected to be higher than the given values.

Table 3.6-2: Characterization of the polymers: (GPC, Yield, FT-IR).

Polymer code	$\overline{M_n}$ [a]	$\overline{M_w}$ [a]	$\overline{M_w}/\overline{M_n}$ [b]	DP[c]	Yield (%)	γNH[d]	γ C=O[d]	γC- N[d]
PIFO-1	4500 [e]	10 800	2.4	15	93	3407	1702	1297
PIFO-2	6 400[f]	32 000	5.0	17	90	3443	1708	1300
PIFO-3	13 200	83 800	6.4	25	86	3436	1709	1297
PIFO-4	14 400	82 000	5.7	27	91	3431	1710	1298
PIFO-5	11200[g]	69 200	6.2	19	84	3430	1705	1301

a) The soluble PIFOs in DMF calibrated by GPC polystyrene standards; b) Polydispersity index; c) Degree of polymerization determined from number average molecular weight; d) FT-IR (KBr, pellet); e, f, g) The soluble fraction in DMF (about 40 %, 60 %, and 75 %, respectively.

Elemental analysis of PIFOs

In all cases, the elemental analysis of PIFOs showed an agreement with the polymer structure. Obviously, the PIFO polymers did not show the hygroscopic nature which has been seen for the PIK polymers (Table 3.6-3).

Table 3.6-3: Elemental analysis for poly(imino flourenone)s.

Polymer Code	Formula (Molecular weight %)	Elemental analysis (%)			
			C	H	N
PIFO-1	$(C_{19}H_{12}N_2O)_n$ $(284.32)_n$	Calc. Found	80.27 78.40	4.25 4.34	9.85 7.04
PIFO-2	$(C_{25}H_{16}N_2O_2)_n$ $(376.41)_n$	Calc. Found	79.77 79.21	4.28 4.40	7.44 5.32
PIFO-3	$(C_{37}H_{32}N_2O)_n$ $(520.67)_n$	Calc. Found	85.35 83.19	6.19 5.46	5.39 4.31
PIFO-4	$(C_{37}H_{32}N_2O)_n$ $(520.67)_n$	Calc. Found	85.35 83.36	6.19 5.25	5.39 4.28
PIFO-5	$(C_{40}H_{30}N_2O_3)_n$ $(586.69)_n$	Calc. Found	81.89 80.56	5.15 6.21	4.77 3.81

^{1}H-NMR spectra of PIFOs

The ^{1}H-NMR (500 MHz) spectrum of polymer **PIFO-4** which is shown in Figure 3.6-1, was recorded in diluted DMSO-d_6 solution at 373K. The spectrum shows a broad peak at 7.09 ppm which was attributed to the protons of the imino groups (NH), the aromatic protons H_1, H_2, H_4, H_5 and H_6 and the fluorenone aromatic proton H_3. Two singlets at 6.86 and 6.49 ppm were attributed to the fluorenone protons H_7 and H_8, respectively. A singlet in the high field region at 1.53 ppm was assigned to the aliphatic protons of methyl groups derived from the polymer repeating unit. The signal of protons H_1-H_8 were figured out from the simulation of polymer **PIFO-4** by the Chem Draw program.[345] Since all the peaks of the ^{1}H-NMR spectrum identified the protons of fluorenone and diimino arylene of the main repeating unit of the polymer backbone, neither amine-terminated PIFOs nor bromo-terminated PIFOs was observed. Thus, one can conclude that the end groups were not detected in case of PIFOs. A low concentration of amino end-groups (resonances at 6.4 ppm) was detected in polymer

PIK-13 (Part 1, Figure 3.1-5, p. 51). This concentration corresponds to less than 5-mol percent end groups per repetition unit.
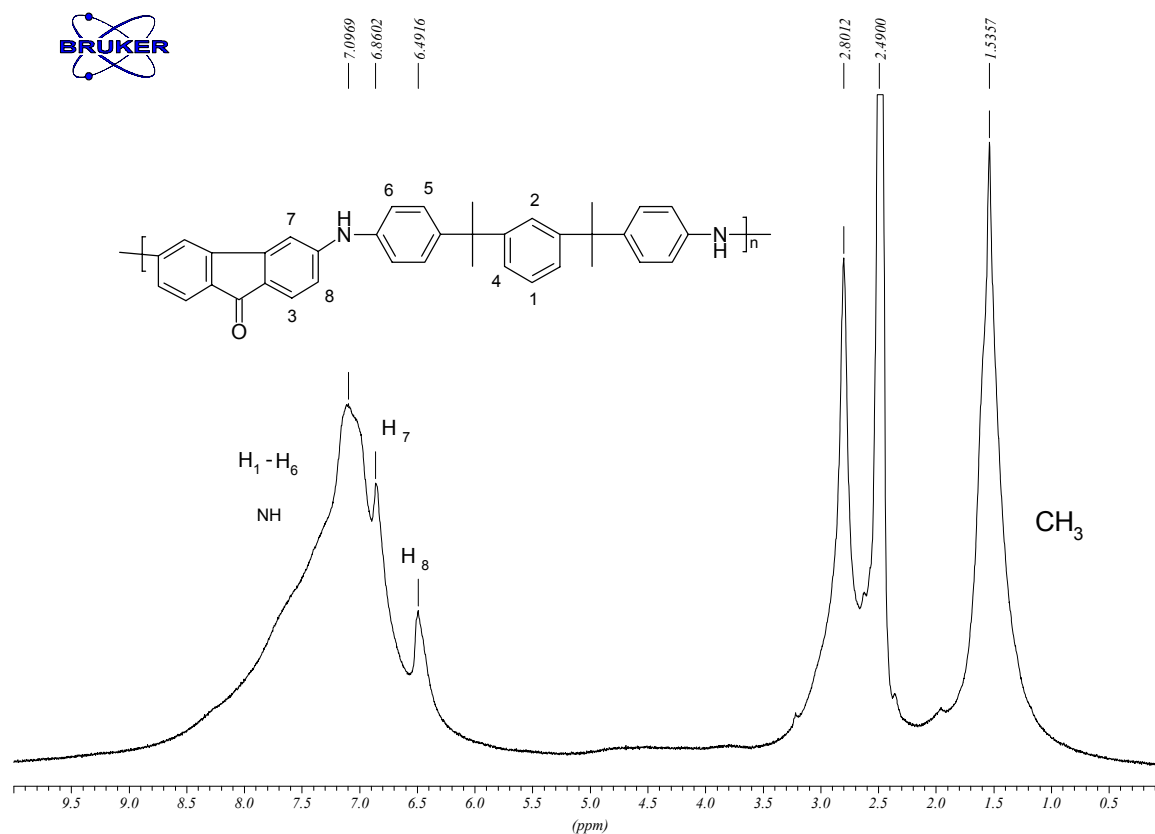
Figure 3.6-1: ^{1}H-NMR (500 MHz) spectrum of **PIFO-4** recorded in DMSO-d_6 at 373 K.

Intermolecular and intramolecular hydrogen bonding of PIFOs

FT-IR spectra of PIFOs were recorded in the solid state (KBr pellets) giving results in good agreement with the proposed structure. The significant broadening and lowering of the absorption bands of the imino groups γ(NH) were detected (Figure 3.6-2). The characteristic absorptions for carbonyl groups γ(C=O) appeared between 1702 and 1710 cm^{-1} and characteristic absorption bands for imino groups γ(NH) appeared between 3407 and 3443 cm^{-1}. The assignment of these peaks are listed in Table 3.6-2.

In the model compound **20** which has lower frequency at 3417 cm^{-1} i.e strong hydrogen bonding, a small shift to lower frequency is observed. From the FT-IR spectra PIFOs are divided into two groups: (1) polymer has lower frequency than its corresponding model compound i.e stronger hydrogen bonding. Thus in polymer **PIFO-1**, the frequency is 3407 cm^{-1}, and the model compound has 3417 cm^{-1}, (2) polymers have higher frequencies i.e weaker hydrogen bonding than their corresponding model compound. Thus in **PIFO-2**, **3**, **4**, and **5**, the frequencies are 3443, 3436, 3431, and 3430 cm^{-1} respectively. Despite the amorphous nature of the polymer **PIFO-1**, it has stronger hydrogen bonding than the corresponding crystalline model compound. Polymers **PIFO-2**, **3**, **4**, and **5** have weaker hydrogen bonding than their corresponding model compound **20** due to the disorder of the system known to disrupt the hydrogen bonding.[346,347]
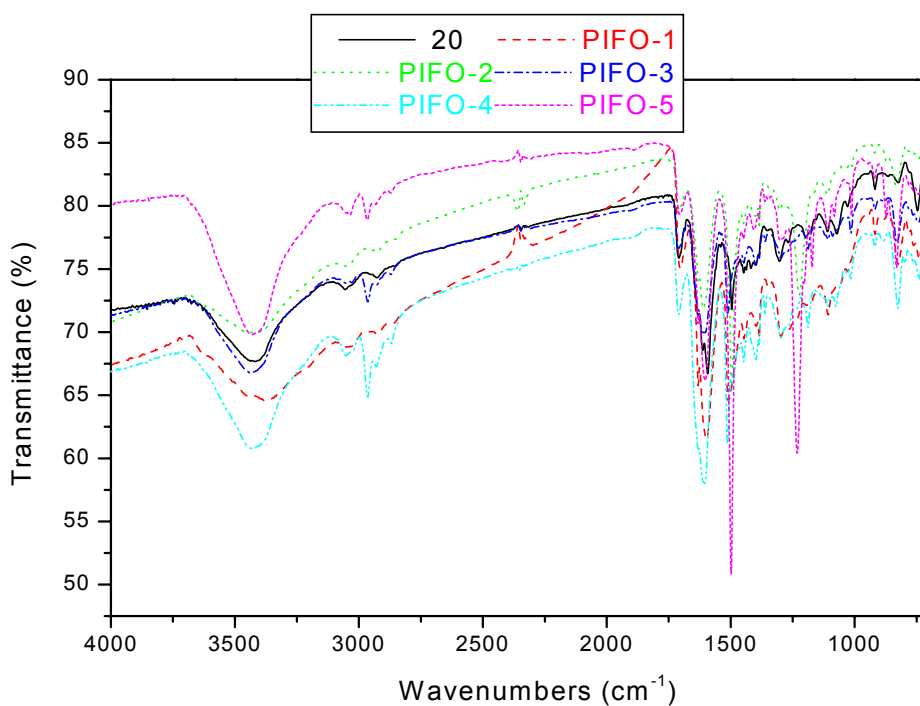
Figure 3.6-2: FT-IR spectra of 3,6-dianilino-9-fluorenone (**20**) and of the poly(imino fluorenone)s (PIFOs) (KBr pellet).

By comparing the FT-IR peak shifts of PIKs[353] and PIFOs (Figure 3.6-2), it was observed that in case of PIK polymers, the characteristic absorptions for imino groups γ(NH) appeared between 3318 and 3422 cm^{-1} while in case of PIFO polymers characteristic absorptions for imino groups γ(NH) appeared between 3407 and 3443 cm^{-1}. Since the

lowering of the frequency tends to be a function of the degree and strength of the hydrogen bonding, the intermolecular and intramolecular hydrogen bonding of PIK polymers are stronger than those of PIFOs. This is possibly due to the number of the carbonyl groups per repeating unit. This proposal is supported by comparing the FT-IR peak shifts of model compound 3,6-dianilino-9-fluorenone (**20**) which has higher frequency at 3417 cm^{-1} and model compound 4,4$^{'}$-bis(4-anilinobenzoyl)benzene (**10**) (Figure 3.6-3) which has lower frequency at 3341 cm^{-1} i.e more stronger hydrogen bonding.
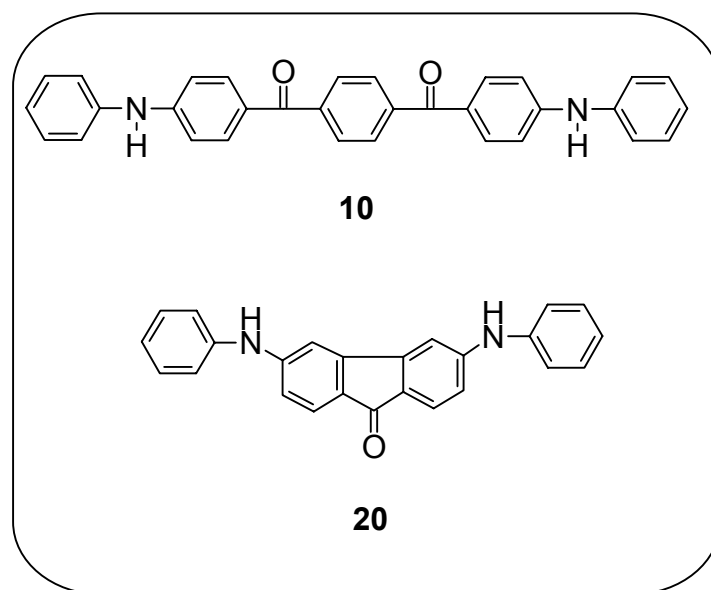
Figure 3.6-3.

Thermal behavior of PIFOs

   Typical TGA traces in air and in nitrogen are demonstrated in Figure 3.6-4 for PIFOs polymers. The thermal stability was evaluated by a 5 % weight loss at the minimum temperature (Table 3.6-4). TGA curves revealed that the polymers were thermally stable up to 305-373 °C in nitrogen. The 50 % weight loss of the polymers took place at different temperature and it was strongly dependent on the condition for instance, it took place at 876, 833 °C in nitrogen, while it took place at 285, 270 °C in air for polymers **PIFO-1** and **2**, respectively. The maximum char yield at 600 °C was obtained for polymer **PIFO-1** (73 %) and the minimum was also obtained for polymer **PIFO-1** (1 %) in nitrogen. Therefore, the maximum char yield at 600 °C was strongly dependent on the condition.

154
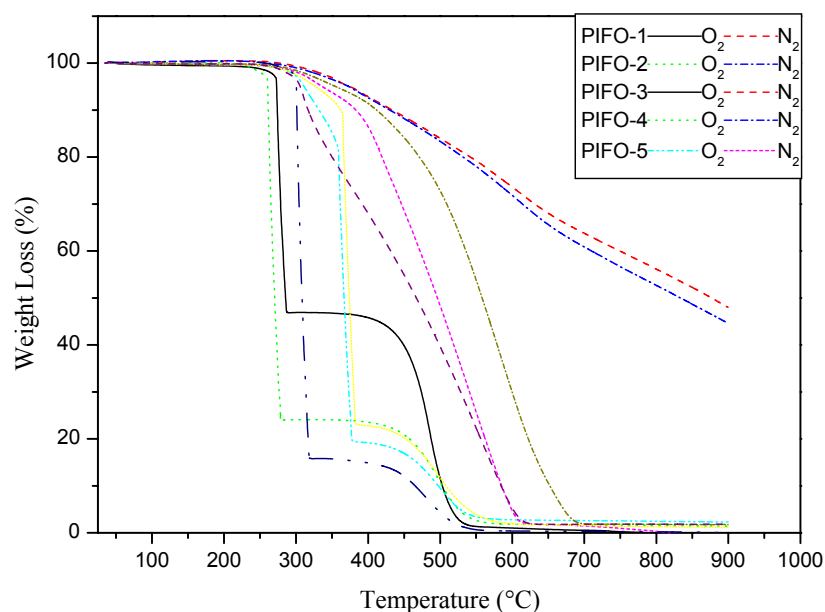
Figure 3.6-4: Dynamic TGA of the copolymers

(in N_2, and in O_2, 10 °C/min).

By comparing the TGA thermograms in air and nitrogen for polymers **PIFO-1**, **2**, **3**, **4**, and **5** (Figure 3.6-4), it was observed that in air the 50 % weight loss of those polymers took place at 285, 270, 366, 374, and 308 °C, respectively, while in nitrogen the 50 % weight loss was observed at 876, 833, 496, 558, and 467 °C, respectively.

In air the char yield showed complete oxidative degradation at 600 °C and it was 1 %, 2 %, 3 %, 2 %, and 2 %, respectively but in nitrogen the char yield at 600 °C was 73 %, 71 %, 5 %, 30 %, and 5 % respectively. The 50 % weight loss temperatures in addition to the high char yields at 600 °C in both air and nitrogen suggested that thermally degradation in air was significantly enhanced over nitrogen. The highest thermally stable PIFOs are **PIFO-1** and **2** in nitrogen. This may be due to the extended conjugation of the system which should confer enhanced thermal stability on these polymers over PIFOs that have a less extended aromatic system.[289] The lowest thermal stable PIFOs in air are **PIFO-1** and **2**; this may be due to the oxidative degradation enhanced by the extended conjugation of the system over the unextended conjugated system of the other PIFOs.

From above it was observed that PIFOs showed less thermal stability and lower char yield in nitrogen at 600 °C than PIKs. This can be clearly demonstrated when comparing the TGA thermograms of PIFOs, to TGA thermograms of PIKs (Table 3.1-9). This may be due to the weaker intermolecular and intramolecular hydrogen bonding of PIFO polymers than those of PIK polymers.

155

Table 3.6-4: Thermal behavior of PIFOs.

Polymer code	O_2 / N_2	$^aT_5$	$^bT_{10}$	$^cT_{50}$	$^dW_{500}$	$^eW_{600}$	Char yield at 600 °C^f	T_g Midpoint^g
PIFO-1	O_2	272	274	285	89	99	1	–
	N_2	373	433	876	17	27	73	
PIFO-2	O_2	260	262	270	90	98	2	–
	N_2	373	430	833	17	29	71	
PIFO-3	O_2	311	332	366	91	97	3	–
	N_2	336	383	496	52	95	5	
PIFO-4	O_2	327	362	374	82	98	2	–
	N_2	355	411	558	27	70	30	
PIFO-5	O_2	300	301	308	96	99	1	–
	N_2	305	316	467	60	95	5	

a) T_5: Temperature of 5 % weight loss; b) T_{10}: Temperature of 10 % weight loss; c) T_{50}: Temperature of 50 % weight loss; d) W_{500}: weight loss at 500 °C, determined from TGA curve; e) W_{600}: weight loss at 600 °C, determined from TGA curve; f) The remaining of the polymer at 600 °C; g) Not detected from 20 °C up to 300 °C.

Differential scanning calorimetry (DSC) of PIFOs was carried out up to 300 °C. The samples were heated at a rate of 10 °C/min under flowing nitrogen gas. While no T_m was detected from the DSC trace of PIFO polymers, none of the PIFOs showed any crystalline behavior. In contrast to PIKs, PIFOs showed no detectable glass transition temperature (T_g) in the range 20-300 °C (Table 3.6-4). This could be explained by the formation of hydrogen bonding between protons of the imino groups and oxygen atoms of the carbonyl groups in PIFOs. In this case the conformation allows interchain interactions, leading to hindrance in the mobility of the polymer chains. Confirmation of this explanation was found in the FT-IR spectra. There is no proof of the occurrence of crosslinking from both TGA and DSC traces. A similar case of a physical cross-linking was already reported in the literature for the amino-

functionalized poly(arylene ether ketone)s.[348] Which confirmed the increased interaction between the polymer chains caused by the hydrogen bonding between the protons of the imino group and the oxygen atom of the carbonyl group, respectively. Figure 3.6-5 showed the relation between galss transition temperatures, architecture and molecular weight of different polymer categories.
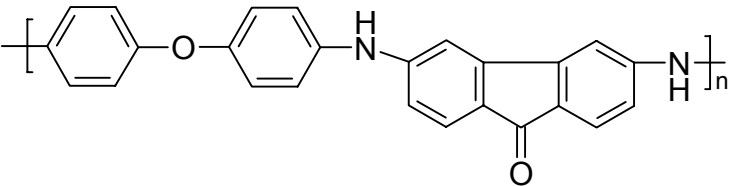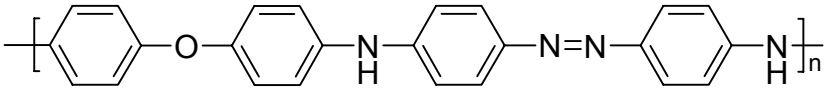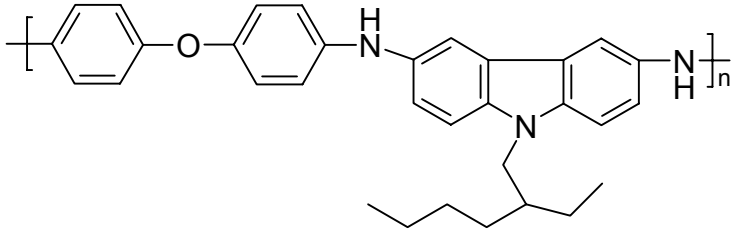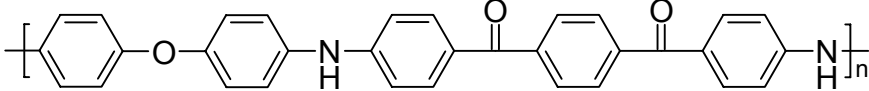
Polymer categories T_g M_n D_p

PIAc-1   higher than 300 °C   4 500   12

PIFO-2   higher than 300 °C 6 400   17

PIAzo-1   126 °C   10 900   29

PIC-1   150 °C   10 000   21

PIK-11b   212 °C   12 200   25

Figure 3.6-5: The relation between glass transition temperatures, the structure and molecular
weight of different polymer categories.

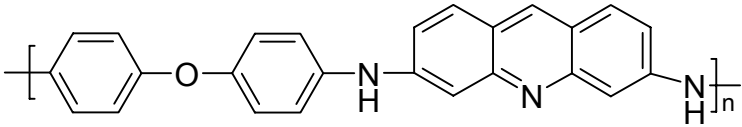**Wide-angle X-ray diffraction of poly(imino fluorenone)s (PIFOs)**

The wide-angle X-ray diffraction patterns of all the polymers over the 2θ range of 5-35° are shown in Figure 3.6-6. All of the poly(imino fluorenone)s (PIFOs) (**PIFO-1-5**) revealed essentially amorphous patterns as broad peaks at 15.8°, 16.7°, 15.7°, 15.0°, and 16.8°, respectively. This may be attributed to the fact that the regularity of the repeating units in polymers **PIFO-1**, **2**, **3**, **4**, and **5** is disrupted by the different appearing orders of the imino and fluorenone units, thus leading to no detectable crystallinity. However, polymers **PIFO-1** and **2**, despite the presence of the rigid secondary amine unit, showed no increased ordering in the solid state as indicated by the X-ray diffractograms (Figure 3.6-6). The amorphous nature of these polymers was reflected in their good solubility in polar aprotic solvents in comparison with the 2,7-poly(9-fluorenone) (2,7-PFO) (insoluble material) and even low-molecular weight oligomers of fluorenone.

In Figures 3.6-7, 8, and 9 any diffraction from crystallites is not observed at all and only the broad halo from the amorphous region is observed in all samples. This was also supported by DSC trace where melting points (T_ms) were not detected.

By comparing wide-angle X-ray for PIKs and PIFOs, it was observed that all PIFOs showed only the broad amorphous halo while PIKs (**PIK-11a** and **PIK-11b**) crystalline patterns as sharp peaks at 12.2°, 18.5°, 24.5°, and 29.5° for polymer **PIK-11a** and 12.8°, 18.3°, and 23.2° for polymer **PIK-11b**, respectively (Figures 3.6-10a-d). In case of PIKs the crystalline pattern can be attributed to the existance of the rigid p-diiminophenylene or p-diiminodiphenyl ether segments in the polymer backbone and at the same time the absence of the bulky groups. On the other hand, in case of PIFOs, the presence of the bulky fluorenone unit which significantly increased the disorder in the chains and caused poor chain packing.[349] In addition, the fluorenone group also decreases the intermolecular force such as hydrogen bonding between the polymer chains, subsequently causing a decrease in crystallinity. Confirmation of this explanation was found in the FT-IR spectra where a clear evidence that the intermolecular and intramolecular hydrogen bonding of PIFOs are weaker than those of PIK polymers was obtained. T_ms of polymer **PIK-11a** and **PIK-11b** were not detected on the DSC trace of the polymers from 20 °C up to 300 °C (Part 1, Table 3.1-9, P. 58).
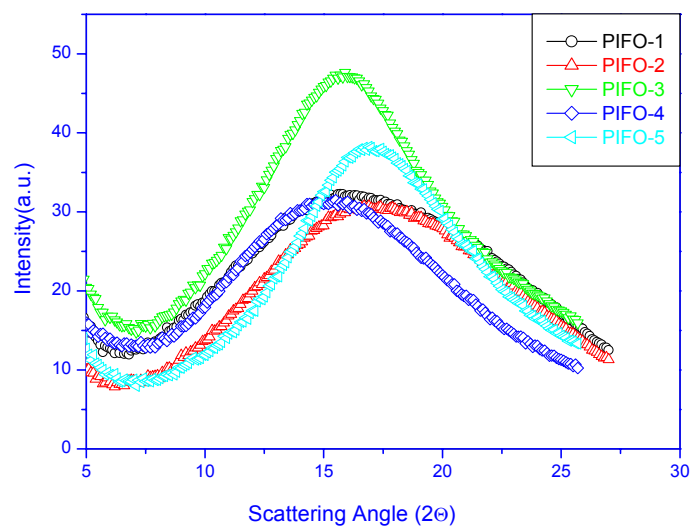
Figure 3.6-6: Wide-angle X-ray diffractograms intensity vs Bragg angle graph for powders of poly(imino fluorenone)s (PIFOs).
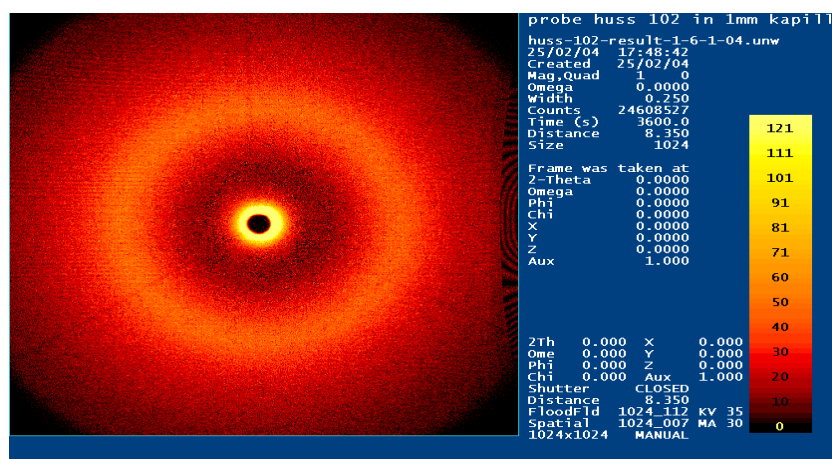
Figure 3.6-7: WAXD image shows the amorphous halo of the copolymer **PIFO-3**.
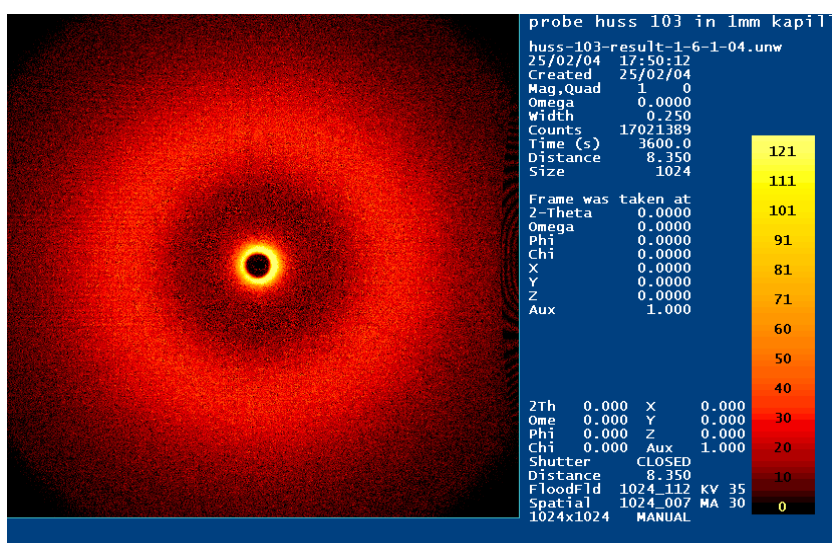
Figure 3.6-8: WAXD image shows the amorphous halo of the copolymer **PIFO-4**.
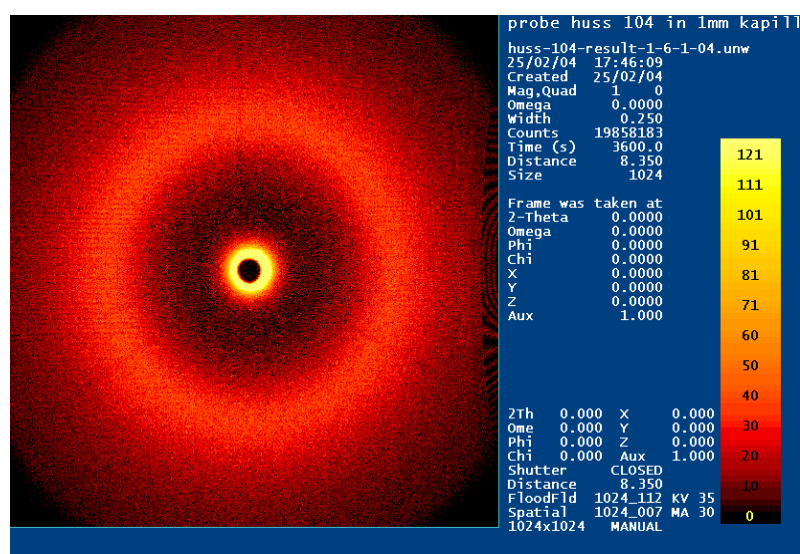
Figure 3.6-9: WAXD image shows the amorphous halo of the copolymer **PIFO-5**.

161
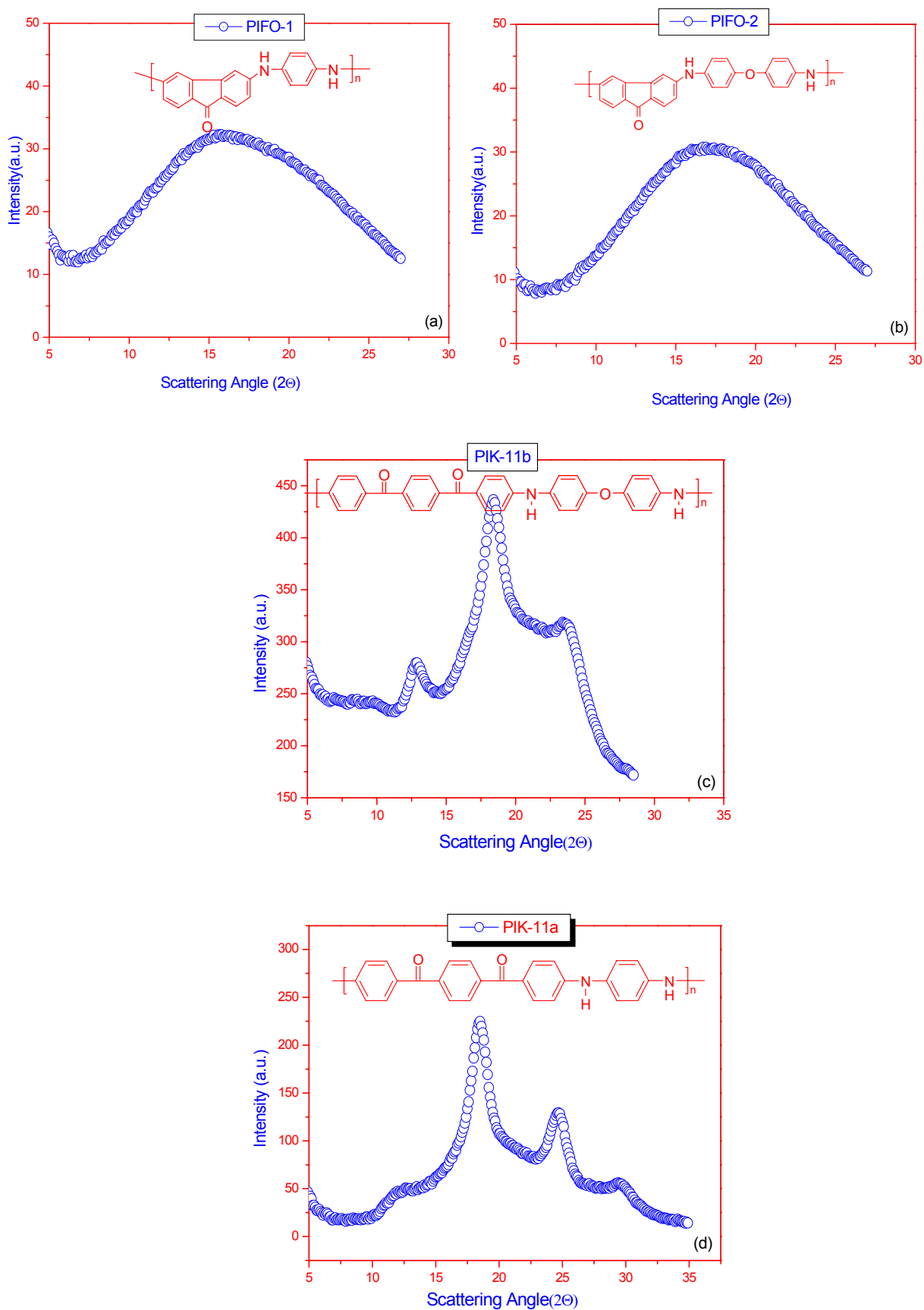
Figure 3.6-10a-d: Wide-angle X-ray diffractograms intensity vs Bragg angle graph of poly(imino fluorenone)s (PIFOs) and poly(imino ketone)s.

U.V absorption spectra of PIFOs

The absorption spectra of polymers **PIFO-3**, **PIFO-4**, and **PIFO-5** (Figure 3.6-11) show a low energy broad absorption band at 600 nm and the second absorption is a shoulder at ~ 450 nm. They are comparable with the absorption spectrum of the model compound **20**. Whereas, in the absorption spectra of **PIFO-1** and **PIFO-2** only a broad absorption band at 450-460 nm of the polymer backbone was observed. Therefore, the absorption spectra of **PIFO-1** and **PIFO-2** differ significantly from that of the model compound. This is due to the increasing different extent of the π-electron system.

By analogy, PIFOs possess electron-donating groups (imino groups) conjugated to an electron-withdrawing groups (carbonyl groups), which results in a photoinduced intramolecular charge-transfer (ICT).[342] Therefore the low energy transition observed for PIFO polymers can be assigned to the intramolecular charge-transfer (ICT), where the charge transfer occurs from the two imino groups toward the electron-poor carbonyl moiety.
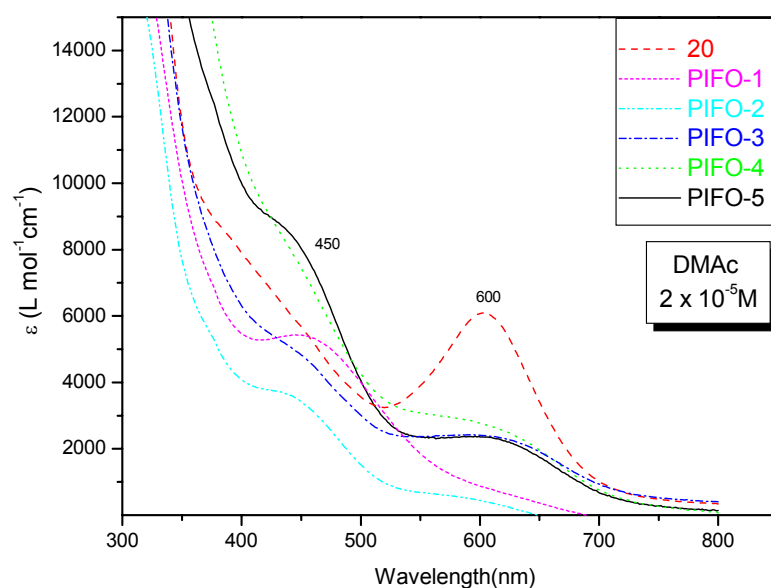
Figure 3.6-11: UV-vis absorption spectra of compound 3,6-dianilino-9-fluorenone (**20**), and of the poly(imino fluorenone)s (PIFOs) in DMAc at room temperature (2 x 10^{-5} M).

The low energy intramolecular charge-transfer band (ICT) in case of **PIFO-3**, **4**, and **5** polymer and the complete disappearance of this band in case of **PIFO-1** and **PIFO-2** band is a consequence of the interaction with the delocalized π-system. Which increased with extended π-delocalization of the polymer backbone of **PIFO-1** and **PIFO-2** result in complete disappearance of the low energy band. This can be clearly demonstrated when comparing the absorption maxima of model compound **20** (600 nm, DMAc), with the absorption maxima of

PIFO-3 (600 nm, DMAc), **PIFO-4** (600 nm, DMAc), **PIFO-5** (600 nm, DMAc), **PIFO-1** (no peak, DMAc) and **PIFO-2** (no peak, DMAc). This effect is similar to that reported in the literature.[339]

By comparing U.V absorption spectra of model compound **20**, PIFO polymer and the reported materials containing 9-fluorenone, it was observed that the absorption maxima of the low energy intramolecular charge-transfer band (ICT) of both model compound **20**, and PIFOs system is shifted toward longer wavelength (red shift-120, 214, and 188 nm) than the absorption maxima of the low energy n→π*-transition band of the carbonyl groups of the reported materials containing 9-fluorenone such as 2,7-poly(9-fluorenone) (**A**) (480nm, film),[339] 9-fluorenone (**B**) (386 nm, ethanol),[350] and the "dimeric" compound 2,2-bi(9-fluorenone) (**C**) (412 nm, CHCl₃),[339] respectively (Figure 3.6-12). This red shift in the new band system is due to the presence of the carbon-nitrogen bond in the 3 and 6 positions which results in an ICT band. Solvatochromism as a proof of the ICT[343] in PIFOs could not be recorded due to their poor solubility in non-polar solvents.
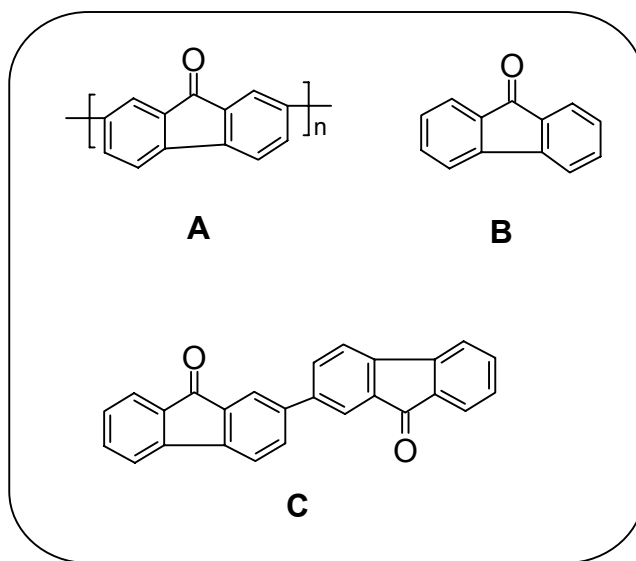
Figure 3.6-12.

Photoluminescence (PL) spectra of PIFOs

The photoluminescence (PL) spectrum of model compound **20** in dimethyl acetamide solution exhibits emission maximum at 518 nm with a strong vibronic peak at 555 nm, on photoexcitation at 450 nm. The photoluminescent spectra of polymers **PIFO-3**, **4** and **5** exhibit emission maximum at 508 nm with a strong vibronic peak at 545 nm, on photoexcitation at 450 nm. The two emission peaks in the photoluminescence (PL) spectra of polymers **PIFO-3**, **4** and **5** are shifted towards shorter wavelength by 10 nm (blue shift-10

nm) than the corresponding emission peaks in photoluminescence (PL) spectrum of model compound **20**.

Meanwhile, polymers **PIFO-1** and **2** have emission maximum at 473 nm as a shoulder and a peak at 510 nm, on photoexcitation at 450 nm. Therefore, they are shifted towards shorter wavelength by 45 nm (blue shift-45 nm) than the corresponding emission peaks in photoluminescence (PL) spectrum of model compound **20** (Figure 3.6-13). The blue shift in the latter case is higher than in the former case as a consequence of increasing the interaction with extended π-delocalization of the polymer backbone of **PIFO-1** and **PIFO-2**. The emission peak in the photoluminescence spectra of PIFOs at 550 nm matches that seen from other polymers containing fluorenone units.[351,352] One possibility is that the band at 520 nm comes from an isolated fluorenone and the 550 nm band from an excimer of fluorenone units. The broadening of the photoluminescence spectra is similar to that of other polymers containing fluorenone.[351,352]
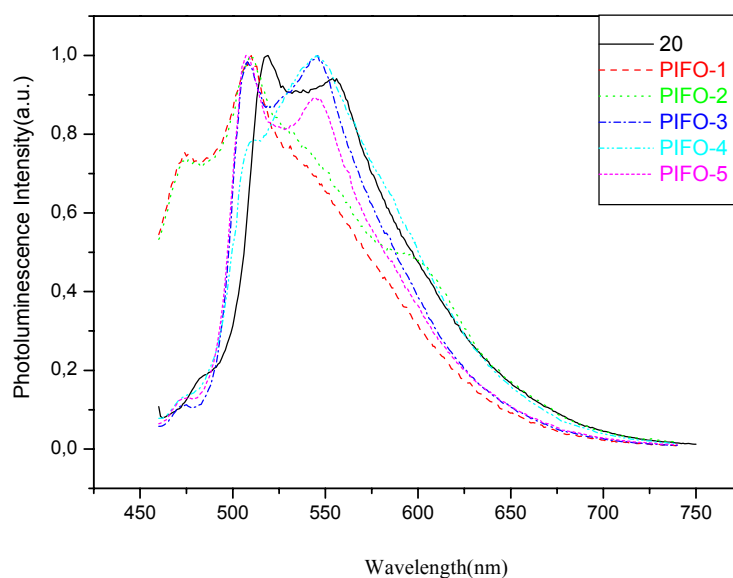
Figure 3.6-13: Photoluminescence spectra of the fluorenone containing polymer (excited at 450 nm, concentration: 2 x 10^{-5} M).

Conclusions:

A series of novel poly(imino fluorenone)s (PIFOs) have been synthesized *via* palladium-catalyzed polycondensation of aromatic dibromoketone (3,6-dibromo-9-fluorenone (**20**)) with various aromatic diamines. The Pd-catalyzed process of which the Pd/BINAP system was found to be the most effective catalyst, producing the highest yield and highest molecular weight polymer in our previous work[353] was used. PIFOs exhibit good thermal stability and high T_gs. The amorphous nature of the polymer was proven by X-ray diffraction where the bulky[354,355] substituent fluorenone unit disturbs dense chain packing of the polymer chain; consequently, the solvent molecules can penetrate easily to solubilize the chain.

None of the two possible side reactions, ketimine formation that involves the reaction between amino and carbonyl groups, or self coupling of the dibromo compound under this basic catalyzed condition, were observed. A clear evidence that the intermolecular and intramolecular hydrogen bonding of PIK polymers are stronger than those of PIFOs was obtained from FT-IR spectra.

Since, there is still a need for electron-deficient (n-type) conjugated polymers and only few reports of these polymers are found,[334,339] PIFO polymers have been synthesized. PIFO polymers as new electron-deficient (n-type) polymers have a unique chemical structure in which the withdrawing effect of the carbonyl groups is expected to lower the reduction potential as it has been observed for the PFO polymer.[334] Consequently, PIFO polymers are interested materials for further investigations to be presented as possible candidates for use as an electron transport layer (n-type) in multilayer LEDs.

CHAPTER III

RESULTS AND DISCUSSION

Part 7

3.7 Synthesis and characterization of poly(imino carbazole)s (PICs)
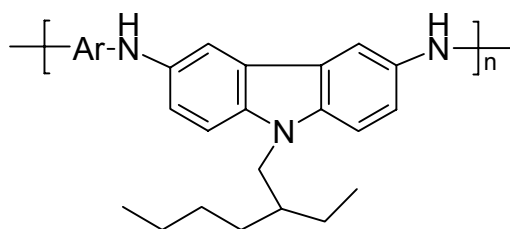
The problem of polyfluorene is its poor hole-transporting abilities.[356] Carbazole derivatives are widely used as hole-transporting materials between the emitting layer and the anode to balance the charge injection.[357] After acridine, azobenzene and fluorenone containing polymers have synthesized, an attempt is now made at synthesizing polymer containing carbazole. In this study, carbazole units are incorporated into the polymer backbone and the photoluminescence of the resulted synthetic polymer is investigated.

Synthesis of PICs

3,6-Diamino-N-(2-ethylhexyl)carbazole (**EHCDN**) was synthesized from carbazole *via* the three-step synthesis according to the reported synthetic procedures.[358] The results of the Pd-catalyzed polycondensation of different aromatic bromides with diamines carbazole are listed in Table 3.7-2. A method was developed for the synthesis of poly(imino carbazole)s (Scheme 3.7-1).

The reactions of 3,6-diamino-N-(2-ethylhexyl)carbazole (**EHCDN)** having electron donating substituents with different arylene dibromides provided the corresponding PICs in 85-90 % yields without undesired side products (work up method a, b or c).

167

Br Ar$_1$ Br   +   NH$_2$ Ar$_2$ NH$_2$

Method a) 100 °C for 20 h | 2.8 equiv. of NaOt-Bu,

Method b) 80 °C for 20 h | 0.01 equiv. of cat. (Pd)$_2$(dba)$_3$,

Method c) 80 °C for 20 h | 0.03 equiv. of cat. BINAP,

LiCl | DMAc

$\left[\text{Ar}_1 \text{ NH Ar}_2 \text{ NH} \right]_n$

Polymer Code	Ar$_1$	Ar$_2$	Method
PIC-1			a
PIC-2, 5			a, c respectively
PIC-3, 6, 8			a, b, c respectively
PIC-4, 7			a, b respectively
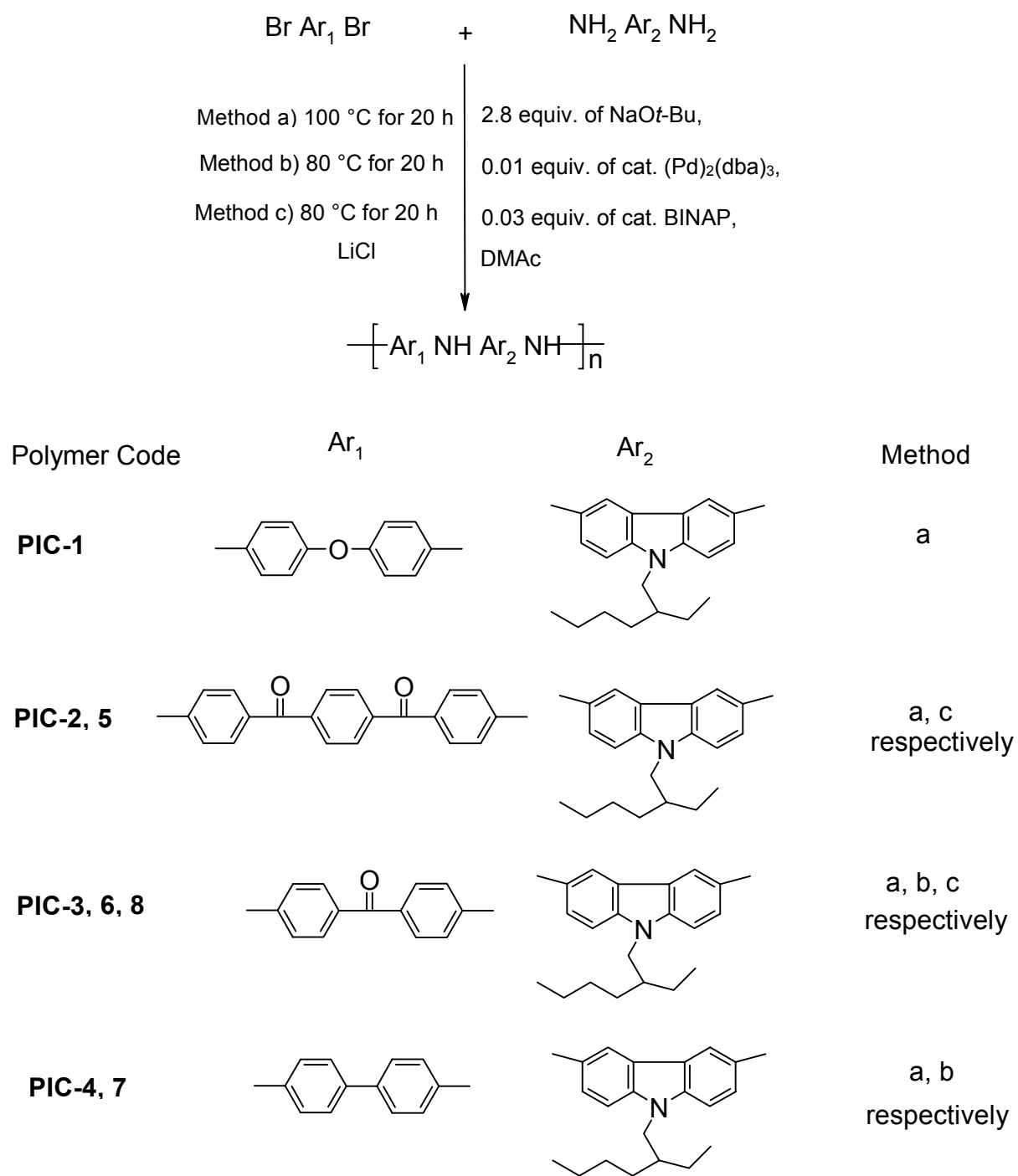
Scheme 3.7-1: Synthesis of poly(imino carbazole)s PICs.

168

Solubility behavior of PICs

The PICs showed different solubility in different organic solvents. The dissolution process depended on the solvent quality, the molecular weight, and chemical structure of the polymer. Polymers **PIC-1**, **5**, **7**, and **8** could be dissolved in aprotic solvents such as NMP, DMAc, and DMSO while only swelling or partially soluble in other common organic solvents, such as chloroform and dichloromethane. Except polymer **PIC-1**, **5**, and **7** which could be dissolved in DMF by dissolution means, **PIC-8** could be partially soluble in DMF. However, **PICs-2**, **3**, **4**, and **6** could not be dissolved or swollen in the known organic solvents, therefore, they are largely uncharacterized (Table 3.7-1). The solid PICs could not be dissolved or swollen in organic solvents, such as methanol and ethanol. Therefore, common organic solvents with low boiling points, such as dichloromethane, chloroform, methanol and ethanol could not be employed to dissolve PICs.

Table 3.7-1: Solubility behavior of poly(imino carbazole)s PICs.[a]

Polymers code	DMAc	DMSO	DMF	THF	NMP	MeOH EtOH	CHCl$_3$	CH$_2$Cl$_2$
PIC-1	++	++	++	±	++	--	±	±
PIC-2	--	--	--	--	--	--	--	--
PIC-3	--	--	--	--	--	--	--	--
PIC-4	--	--	--	--	--	--	--	--
PIC- 5	++	++	++	++	++	--	±	±
PIC- 6	--	--	--	--	--	--	--	--
PIC- 7	++	++	++	++	++	--	-S	-S
PIC- 8	++	++	±	--	++	--	-S	-S

[a] Solubility measured at polymer concentration, 5 mg. ml^{-1} by the mixing of 5 mg of polymer with 1 ml of solvent, followed by stirring; ++ indicates that the solid polymer was completely dissolved in the solvent to afford a homogeneous solution at room temperature or by sonic; ± indicates that the solid polymer could be partially soluble at room temperature; -- indicates that the solid polymer could not be dissolved or swollen in the known organic solvents neither by heating nor by using dissolution means such as sonication; -S indicates that the solid polymer could be swell at room temperature.

The molecular weights of the PICs were measured by GPC (calibrated by polystyrene standards). The molecular weight values M_n are in the range of 8 600-16 600, M_w in the range of 23 000-135 000. GPC analysis revealed that the polymer polydispersities vary from 2.7 up to 8.1 (Table 3.7-2). Especially, with increasing molecular weights the polydispersity increases drastically.[214] The low polydispersity of polymer **PIC-8** is due to its partial solubility in DMF. The GPC values in case of polymer **PIC-8** represent only the soluble fraction in DMF (ca. 35 %). The molecular weights of polymers **PIC-2**, **3**, **4**, and **6** were not measured by GPC because of their poor solubility.

Table 3.7-2: Characterization of PICs: (GPC, Yield, and FT-IR).

Polymer Code	$\overline{M}_n$ [a]	$\overline{M}_w$ [a]	$\overline{M}_w/\overline{M}_n$ [b]	DP[c]	Yield (%)	γNH[d]	$\gamma C=O$[d]	$\gamma C-N$[d]
PIC -1	10 000	72 000	7.2	21	87	3385	-	1305
PIC-2	_	_	_	_[e]	_[g]	3410	1630	1300
PIC-3	_	_	_	_[e]	_[g]	3412	1630	1307
PIC-4	_	_	_	_[e]	_[g]	3394	_	1300
PIC-5	9 800	68 000	6.9	16	88	3415	1630	1310
PIC-6	_	_	_	_[e]	_[g]	3440	1630	1307
PIC-7	16 600	135 000	8.1	36	85	3389	_	1294
PIC-8	8 600[f]	23 000[f]	2.7	17[f]	90	3405	1630	1312

a) The soluble fraction in DMF calibrated by GPC polystyrene standards; b) Polydispersity index; c) Degree of polymerization determined from number average molecular weight; d) FT-IR (KBr, pellet); e) Not measured because of the poor solubility of the polymer; f) Soluble part in DMF (Ca. 35 %); g) Not calculated because of the crude polymer material.

Elemental analysis of PICs

In all cases, the elemental analysis of the PICs showed an agreement with the polymer structure. The low measured values of the carbon content of PIC-polymers may be attributed to the incomplete combustion of the polymer material during the elemental analysis measurements because of their high carbon contents (Table 3.7-3). A similar behavior has observed for carbonaceous materials.[359,360] Obviously, the PIC polymers did not show the hygroscopic nature which has been seen for the PIK polymers (Table 3.7-3).

Table 3.7-3: Elemental analysis for poly(imino carbazole)s (PICs).

Polymer code	Formula (Molecular weight)	Elemental analysis (%)		
			C	H	N
PIC -1	$(C_{32}H_{33}N_3O)_n$ (475.63)$_n$	Calc. Found	80.81 76.81	6.99 6.46	8.83 7.96
PIC -5	$(C_{40}H_{37}N_3O_2)_n$ (591.75)$_n$	Calc. Found	81.19 76.14	6.30 6.41	7.10 7.19
PIC -7	$(C_{32}H_{33}N_3)_n$ (459.63)$_n$	Calc. Found	83.62 81.22	7.24 7.03	9.14 8.55
PIC-8	$(C_{33}H_{33}N_3O)_n$ (487.64)$_n$	Calc. Found	81.28 77.84	6.82 6.52	8.62 8.45

^{1}H-NMR of PICs

The ^{1}H-NMR spectrum shows a peak at 7.71 ppm which was attributed to the protons of the imino groups (NH). Two singlets at 7.37 and 7.20 and a doublet at 6.91 ppm were attributed to the carbazole aromatic protons H_1, H_2 and H_3, respectively. One doublet at 6.91 ppm was attributed to the aromatic protons H_4 and H_5, respectively. Two singlets at the upfield region at 4.14 and 2.01 ppm were assigned to the aliphatic protons H_6 and H_7, respectively. Two doublets at the high upfield region at 1.25 and 0.82 ppm were assigned to the aliphatic protons H_8 and H_9 of methylene and methyl groups derived from the polymer-repeating unit, respectively (Figure 3.7-1 down). Since all the peaks of the ^{1}H-NMR spectrum identified the protons of carbazole and diimino arylene of the main repeating unit of the polymer backbone, therefore, neither amine-terminated PICs nor bromide-terminated PICs was observed. Thus, one can conclude that the end groups were not detected in case of PICs.
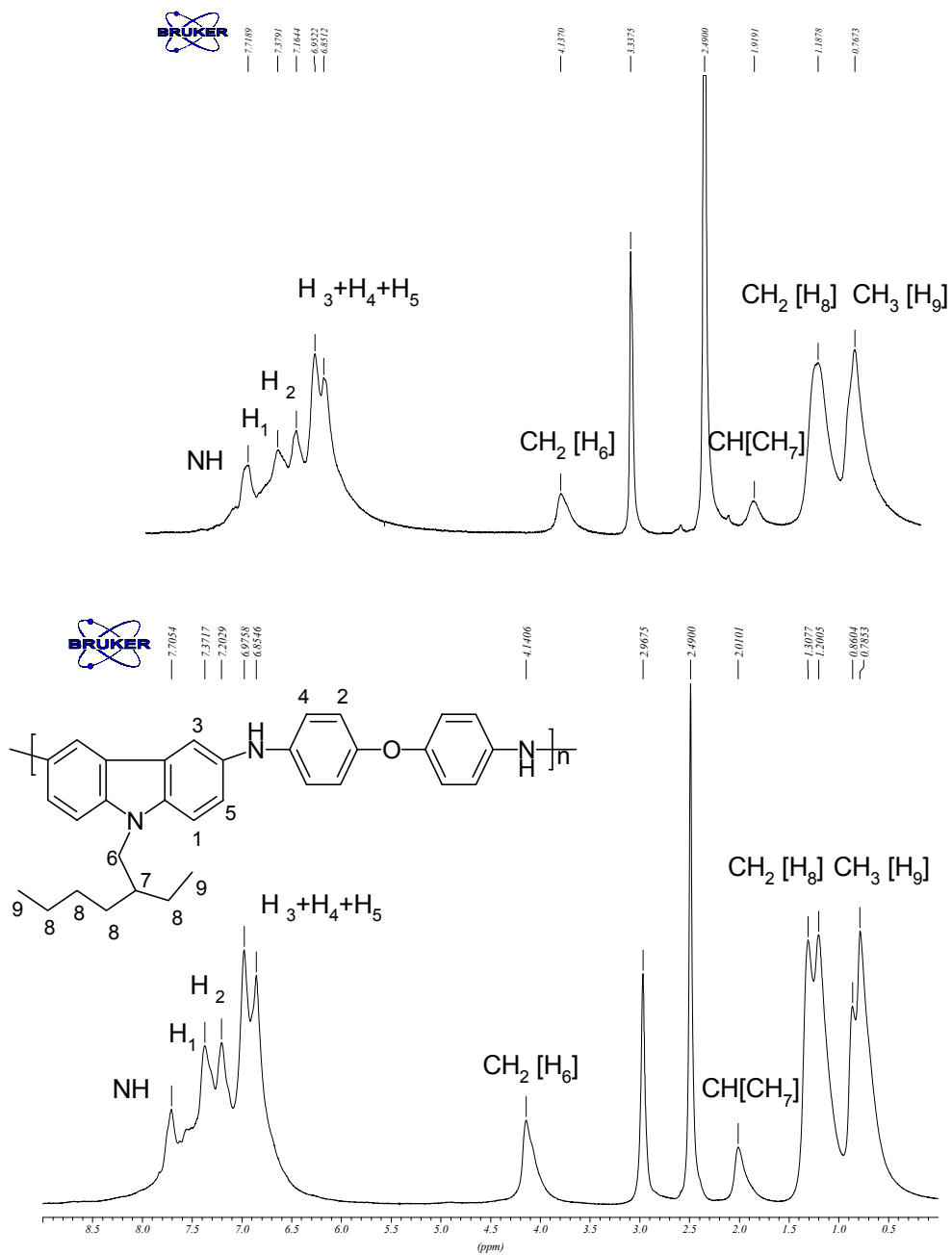
Figure 3.7-1:

^{1}H-NMR spectrum (250 MHz) of polymer **PIC-1** recorded in DMSO-d_6 at 293K (up).

^{1}H-NMR spectrum (700 MHz) of polymer **PIC-1** recorded in DMSO-d_6 at 373K (down).

Thermal behavior of PICs:

TGA of PICs curves revealed that these polymers were thermally stable up to 310-450 °C. The 50 % weight loss of the polymers took place at lower than 900 °C for poly(imino carbazole)s in air while in nitrogen took place at higher than 900 °C. The maximum char yield at 600 °C was obtained for **PIC-7** (77 %) and the minimum was obtained for **PIC-1** (72 %) in nitrogen (Figure 3.7-2 and Table 3.7-4).

By comparing the TGA thermograms in air and nitrogen for PICs, the 50 % weight loss temperatures in addition to the char yields at 600 °C suggested that thermal degradation in air was significantly enhanced over that in nitrogen. From Table 3.7-4, it was observed that **PIC-1** is more stable than **PIC-7** in air while **PIC-7** is more stable than **PIC-1** in N_2. This may be due to the fact that **PIC-7** is the more highly conjugated polymer than **PIC-1**.
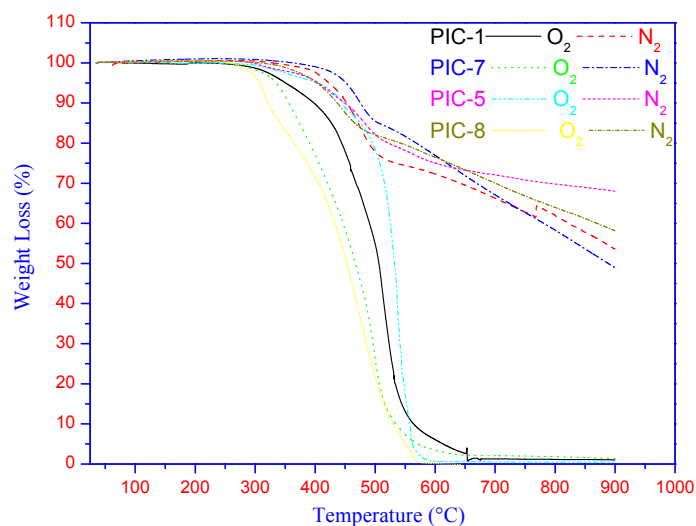
Figure 3.7-2: Dynamic TGA of poly(imino carbazole)s (PICs)

(in N_2, and in O_2, 10 °C/min.).

Differential scanning calorimetry (DSC) of PICs up to 300 °C showed a single T_g and the absence of a melting temperature suggesting an amorphous polymer structure (Figure 3.7-3). Polymers **PIC-1**, **7**, and **5** have T_gs 150, 182 and 230 °C respectively, while the T_g of PIC-8 was over 300 °C (Table 3.7-4). Polymer **PIC-1** has a lower T_g than **PIC-7**. This is due to the backbone flexibility resulting from the flexible ether group. Which has a T_g 126 °C and this may be due to the presence of diiminoazobenzene unit in the polymer backbone, therefore this

173

system is more flexible than other system containing the diiminoacarbazole unit in the polymer backbone.
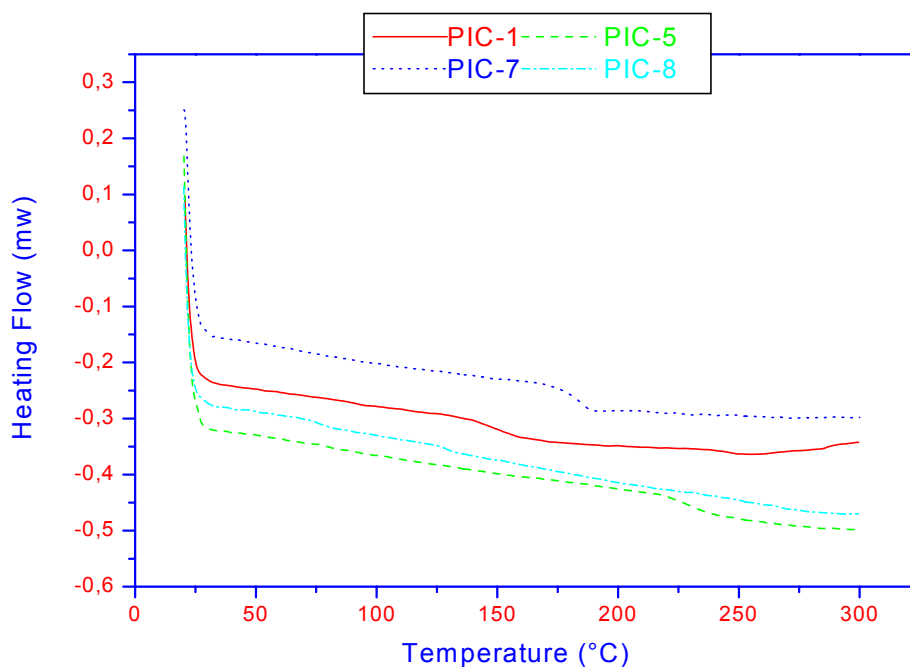
Figure 3.7-3: DSC of PICs (in N_2, 10 °C/min).

The second heating scans were taken into consideration.

By comparing differential scanning calorimetry (DSC) of PICs and PIFOs it was found that in case of PICs the T_gs were in the range 150-230 °C. While in case of PIFOs the T_gs were not detected from 20 °C up to 300 °C. Therefore the PIC system is more flexible than the PIFO system containing the diiminoflourenone unit in the polymer backbone (Figure 3.7-4).

	PICs	PIFOs
Tgs	150-230 °C	higher than 300 °C
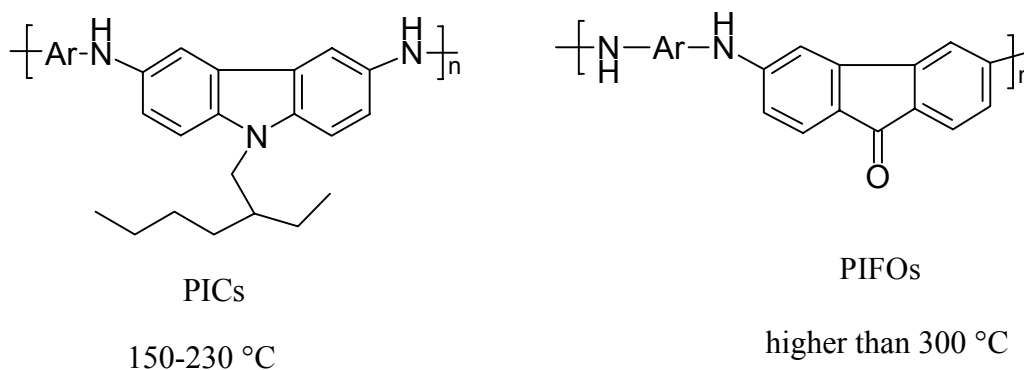
Figure 3.7-4: DSC of poly(imino carbazole)s PICs and poly(imino fluorenone)s PIFOs.

Table 3.7-4: Thermal behavior of PICs.

Polymer code	O_2 / N_2	$^aT_5$	$^bT_{10}$	$^cT_{50}$	$^dW_{500}$	$^eW_{600}$	Char yield at 600 °C^f	T_g Midpoint^g
PIC –1	O_2	350	398	506	46	94	6	150
	N_2	423	452	> 900	22	28	72	
PIC-5	O_2	404	446	532	22	100	0	230
	N_2	405	449	> 900	18	25	75	
PIC-7	O_2	335	356	467	84	97	3	182
	N_2	450	475	> 900	15	23	77	
PIC-8	O_2	310	321	452	79	100	0	
	N_2	403	436	> 900	18	24	76	–

a) T_5: Temperature of 5 % weight loss; b) T_{10}: Temperature of 10 % weight loss; c) T_{50}: Temperature of 50 % weight loss; d) W_{500}: weight loss at 500 °C, determined from TGA curve; e) W_{600}: weight loss at 600 °C, determined from TGA curve; f) The remaining of the polymer at 600 °C; g) Midpoint of the second heating traces of DSC measurements conducted with a heating rate of 10 °C min^{-1} in nitrogen.

Wide-angle X-ray diffraction of PICs

The wide-angle X-ray diffraction patterns of all the polymers over the 2θ range of 5-35° are shown in Figure 3.7-5. All of the poly(imino carbazole)s (**PICs-1**, **5**, **7**, and **8**) revealed essentially amorphous patterns as broad peaks at 19.0°, 18.9°, 19.1°, and 17.7°, respectively. This can be attributed to the fact that the regularity of the repeating units in polymers **PIC-1**, **5**, **7**, and **8** is disrupted by the different appearing orders of the two units of the PICs. This was also supported by DSC trace where melting points (T_ms) were not detected.
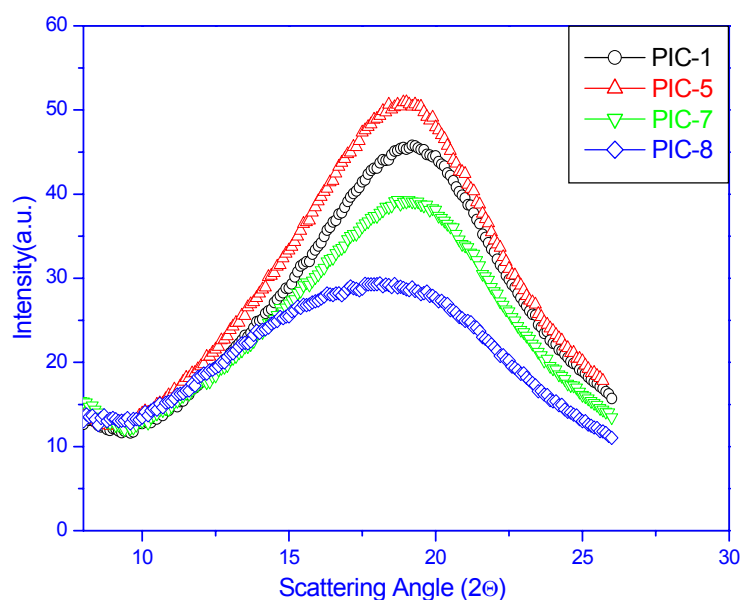
Figure 3.7-5: Wide-angle X-ray diffractograms for polymer powder of PICs.

By comparing wide-angle X-ray for PIKs, PIFOs and PICs, the tested PICs showed the broad amorphous halo while **PIK-11b** showed crystalline patterns as sharp peaks at 12.8°, 18.3°, and 23.2° (Figure 3.7-6c). In case of PIKs the crystalline pattern can be attributed to the existance of the rigid p-diiminodiphenylether segments in the polymer backbone and at the same time the absence of the bulky groups, leading to a better chain packing of polymer **PIK-11b**. On the other hand, in case of PICs and PIFOs, carbazole and fluorenone as bulky units significantly increased the disorder in the chains and caused poor of the chain packing (Figures 3.7-6a, and b). In addition, the fluorenone group also decreases the intermolecular

force such as hydrogen bonding between the polymer chains, subsequently causing a decrease in crystallinity.
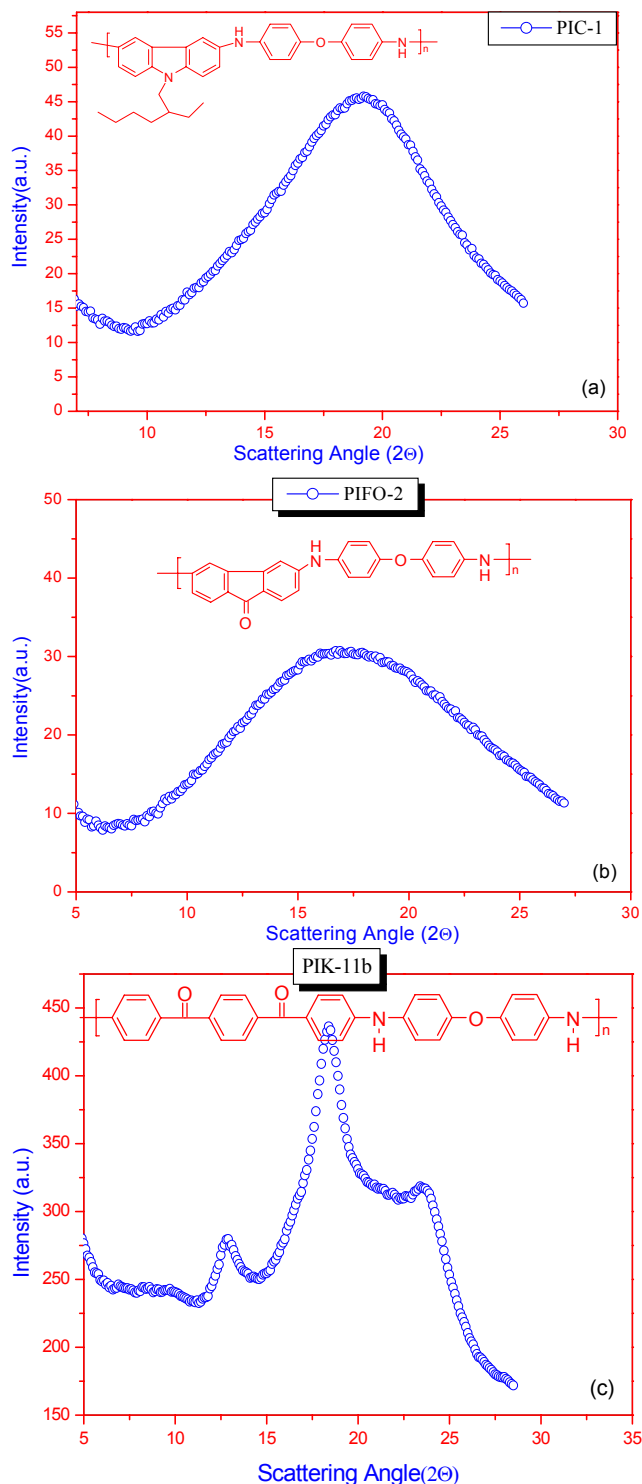
Figures 3.7-6a-c: Wide-angle X-ray diffractograms of a) poly(imino carbazole)s (**PIC-1)**, b) poly(imino fluorenone)s (**PIFO-2**), and c) poly(imino ketone)s (**PIK-11b**).

Optical characterization of PICs

UV-vis absorption spectra of PICs

The UV-vis absorption spectra of diamino carbazole monomer and of the **PIC-1** in DMAc at room temperature are shown in Figures 3.7-7 and these results are summarized in Table 3.7-5. The monomer 3,6-diamino-N-(2-ethylhexyl)carbazole showed two absorption maxima at 290 and 330 nm, characteristic of the carbazole chromophore, and a broad peak at 400 nm due to the π→π*-transition of the diaminocarbazole chromophore. In comparison, the **PIC-1** showed absorption maxima at 280 nm due to the aromatic rings, at 310 nm characteristic of the carbazole chromophore, and a broad peak at 400 nm due to the π→π*-transition of the diiminocarbazole chromophore.

The λ_{max} of polymer **PIC-1** was blue shifted (20, 50, and 30 nm) than those of polymers **PIC-5**, **PIC-7**, and **PIC-8**, respectively. The λ_{max} of **PIC-7** (350 nm) was shorter than that of **PIC-1** (400 nm), indicating that the conjugation length decreases by introducing the biphenyl unit because of the interruption of the linear system by 4,4`-biphenyl relative to **PIC-1**. This is unexpected as observed in the introduction of 3,6-carbazole[361] or 2,8-dibenzothiophene[362] unit into poly(9,9-dialkyl-2,7-fluorene) based polymer. Moreover, this reflects the flexibility role of the kinked ether group in 4,4`-biphenylether unit in the **PIC-1** polymer backbone which induces the system to be in-plane; consequently, the conjugated length increases.
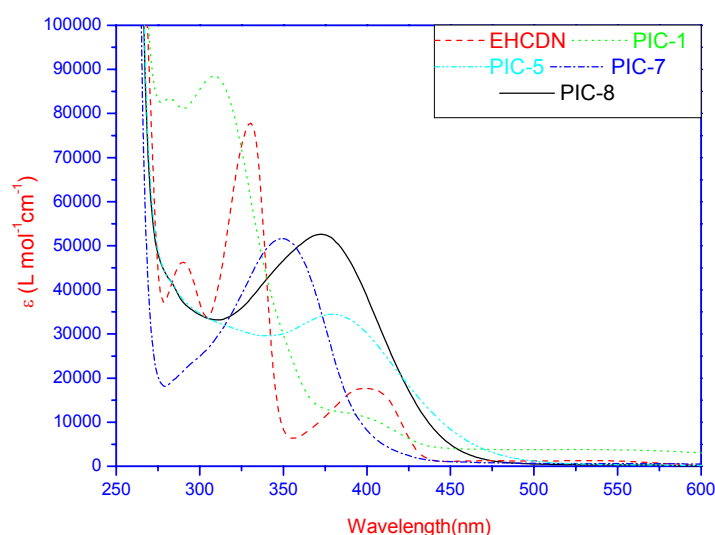
Figures 3.7-7: UV-vis absorption spectra of monomer **EHCDN** and poly(imino carbazole)s PICs in DMAc at room temperature.

Table 3.7-5: Maximum UV absorption wavelength, maximum emission wavelength, and photoluminescence Stokes' shifts for the poly(imino carbazole)s PICs in DMAc at 298 k.

Polymer	λ_{max}^{a} (nm)	λ_{em}^{b} (nm)	Stokes' shifts
CHCDN	290, 330, 400	445	45
PIC –1	280, 310, 400	448	48
PIC –5	380	430	50
PIC –7	350	450	100
PIC -8	370	435	65

[a]Maximum UV-absorption wavelength in DMAc solution, [b]Maximum emission wavelength excited at the absorption maximum 400, 400, 380, 350, and 370 nm respectively, in DMAc solution.

Photoluminescence (PL) spectra

The polymers show photoluminescence in DMAc solution when excited at their absorption maximum (Table 3.7-5). The emission spectra of all PICs species showed a sharp band represent the maximum emission wavelength (λ_{em}) ranges from 430 to 450 nm, depending on the starting structures. The maximum emission of polymer **PIC-7** is red shifted compared to that of polymer **PIC-1**, **PIC-5**, **PIC-8**, and **EHCDN** monomer (Figures 3.7-8). This is unexpected as the introduction of 4,4`-biphenyl or 3,6-carbazole[361] or 2,8-dibenzothiophene[362] units into poly(9,9-dialkyl-2,7-fluorene) based polymers do not cause red shifts of the λ_{em}. The large Stokes' shifts for **EHCDN** monomer, **PIC-1**, **PIC-5**, **PIC-7**, and **PIC-8** suggest that they represent a non-rigid system i.e. the excited and the ground state of the photoluminescence for these species have different geometries. The emission spectra of the various poly(imino carbazole)s (PICs) recorded in dimethylacetamide were shown in Figures 3.7-8, and these results are summarized in Table 3.7-5.
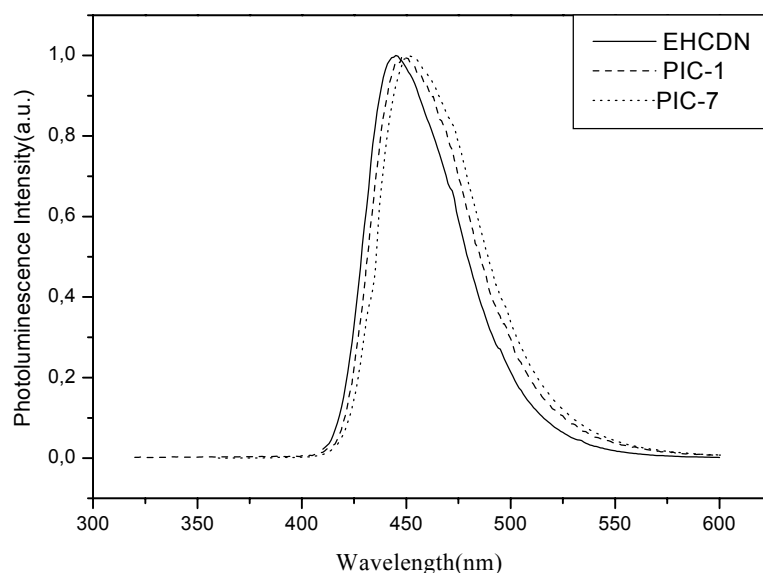
Figures 3.7-8: Photoluminescence spectra of monomer **EHCDN** and carbazole-containing
polymer (excited at 400, 400, and 349 nm, concentration: 2 x 10^{-5} M).

Cyclic voltammetry (CV) of PICs:

The redox behavior of the polymers was investigated by cyclic voltammetry (CV)
with a standard three-electrode electrochemical cell in a 0.10 M tetrabutylammonium
perchlorate solution in DMF at room temperature under nitrogen with a scanning rate of 100
mV/s. A platinum working electrode, counter electrode, and an Fe^{+2}/Fe^{+3} (10^{-3} M in DMF)
reference electrode were used. The anodically scanned cyclic voltammograms are shown in
Figures 3.7-9 and from that the HOMO of **PIC-5** and **PIC-7** was estimated to be -4.95 and -
4.79 ev, respectively. Meanwhile, the cathodic wave was not observed from the tested PIC
polymers beyond the solvent limit therefore the LUMO energy was not estimated. The
oxidation process of **PIC-7** has an onset at 0.44 V (vs Ag/AgCl (10^{-3} M)). The oxidation is
pseudoreversible and gives the corresponding reduction peak at 0.33 V (vs Ag/AgCl (10^{-3}
M)). As shown in Figures 3.7-9, both of the oxidation potential of **PIC-5** (0.63 V (vs
Ag/AgCl (10^{-3} M)) and the corresponding reduction peak at 0.46 V (vs Ag/AgCl (10^{-3} M)) are
higher than those of **PIC-7**. Thus, it is obvious that both the oxidation and reduction potential
of PICs are shifted to low values with increasing degree of polymerization {**PIC-7** (DP = 37),
PIC-5 (DP = 16) (cf. Table 3.7-6)}, i.e. with increasing carbazole content in the backbone of
PICs. This effect of the carbazole content in the polymer backbone has been reported.[361] The
ferrocene electrode potential (Fe^{+2}/Fe^{+3} (10^{-3} M in DMF)) was calibrated to be 0.19 V higher

than $\left(Ag/AgCl \ (10^{-3} \ M)\right)$ and 0.32 V higher than Ag/AgCl (3 M NaCl) electrode. The latter electrode was used to calculate the HOMO and LUMO in case of the introduction of 3,6-carbazole[361] unit into poly(9,9-dialkyl-2,7-fluorene) based polymer. In our case the reference electrode potential is lower than the latter case by 0.13 V. Consequently, the studied PIC polymers exhibited lower oxidation potential values than the latter polymers (0.93, and 0.84, respectively)[361] and also lower than the fluorene homopolymer which has an onset at 1.09 V (vs Ag/Ag$^+$(0.01 M)).[361] Certainly, PIC polymers having lower oxidation potentials and lower energy levels of the HOMO than those of carbazole-fluorene copolymer[361] and fluorene homopolymer,[361] which is a prerequisite for a better hole-transporting (p-type) ability. For this purpose, some information about the hole mobility of the polymer is required. Therefore, the following time of flight measurements has to be performed.
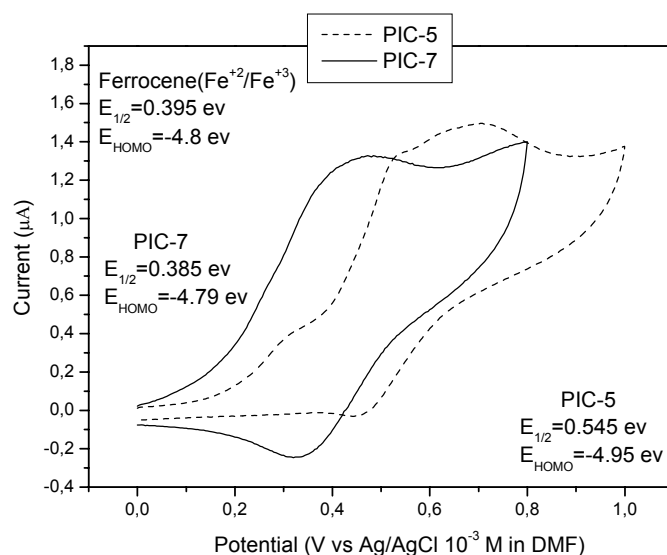
Figures 3.7-9: Cyclic voltammogram of **PIC-5** and **PIC-7** Scan rate: 100 mV/s.

Time of flight (TOF) of charge carrier in PICs:

Figures 3.7-10 and 3.7-11 show typical TOF transients obtained from polymer **PIC-7** at room temperature measured by Dr. S. Balouchev and F. Laquai. Clearly, the TOF transients are highly dispersive. Therefore, it is not possible to measure the hole charge carrier mobility in **PIC-7** using the TOF technique. The dispersive hole transport can be an intrinsic property of the polymer caused by high disorder and/or traps (chemical or physical defects in the polymer structure). The measurements were performed at different electric fields but the shape of the signal (its dispersive character) did not change. Nevertheless, the obtained results

181

represent just a first approximation whether this material can be used as a hole transporting layer (HTL), for instance, in PLEDs. To clarify this question a deeper study of different TOF samples with different device architectures has to be performed as well as measurements on LEDs using **PIC-7** as a HTL between ITO and electroluminescent polymer.
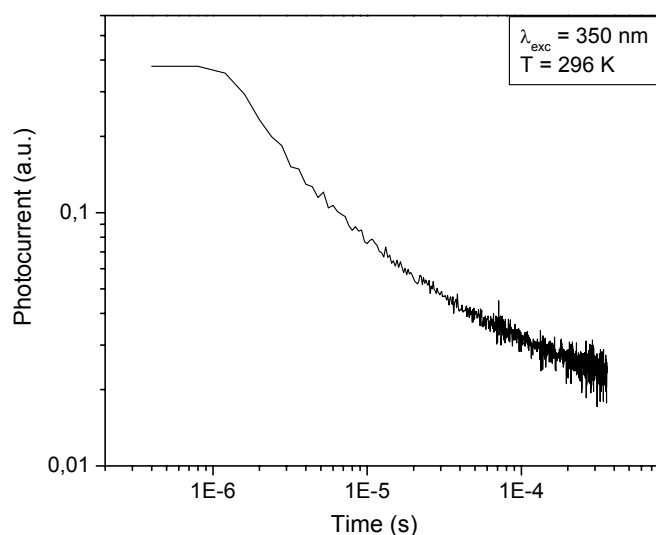
Figures 3.7-10: Typical TOF transient of polymer **PIC-7** in a double logarithmic plot.
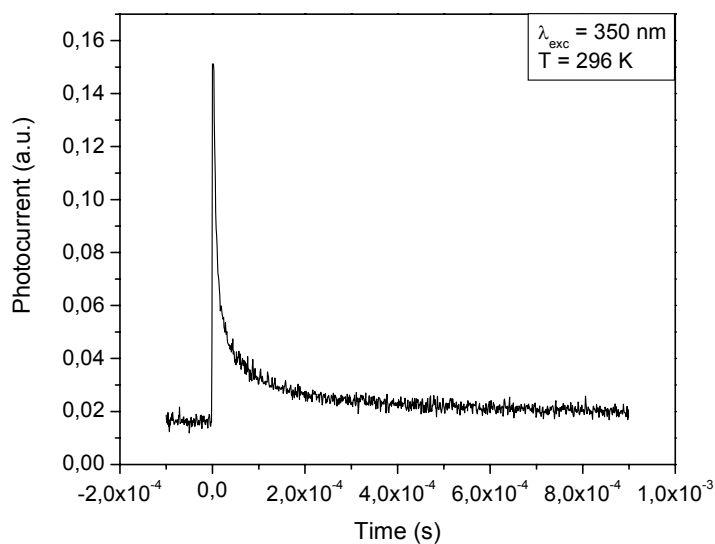
Figures 3.7-11: Typical TOF transient of **PIC-7** in a linear-linear plot.

Conclusions

A series of novel photoluminescent polymers containing carbazole chromophore have been synthesized *via* palladium-catalyzed polycondensation of aromatic diamines (3,6-diamino-N-(2-ethylhexyl)carbazole (**EHCDN)** with various aromatic dibromoketone. The Pd-catalyzed process of which the Pd/BINAP system was found to be the most effective catalyst, producing the highest yield and highest molecular weight polymer in our previous work [353] was used. Three protocols for the synthesis of poly(imino carbazole)s (PICs) have been investigated. Not all the three methods afforded soluble polymer materials. Since, **PICs-1**, **5**, **7**, and **8** showed a good solubility, therefore, they were fully characterized, while **PICs-2**, **3**, **4**, and **6** were an insoluble materials, therefore, they were fully uncharacterized. PIC Polymers obtained by protocol (a) showed a higher molecular weight than those synthesized by protocol (b or c). ^{1}H-NMR spectroscopy showed that there was no amine termini of the initial polymers can be detected. The photoluminescence spectrum of the monomer has also been examined, and photoluminescence emission was detected. Cyclic voltammetry (CV) of PIC polymers were measured. PIC polymers exhibited lower oxidation potentials in the range of 0.44 and 0.63 V lower energy level of the HOMO of the HOMO than those of carbazole-fluorene copolymer[361] and fluorene homopolymer.[361]

4.1. Summary

The goal of the present work was to synthesize and characterize novel N-containing aromatic polymers *via* palladium amination polycondensation. This was inspired by the idea of combining the properties of the high-performance polymers such as PEEKKs, and those of N-containing species such as polyaniline (PANI), poly(aromatic amides) (PAAs), and N-containing simple aromatic compound made by the Buchwald-Hartwig reaction.

The thesis can be summarized in the following main parts:

Part 1. Synthesis of poly(imino ketone)s (PIKs) as new high-performance polymers.

The ability of the halogen containing monomers **5**, **6**, and **7** to undergo Buchwald-Hartwig reaction with a number of diamines was investigated. A series of soluble poly(imino ketone)s (PIKs) with high molecular weights was obtained by a Pd-catalyzed polycondensation (Buchwald-Hartwig reaction) of aromatic dibromides and aromatic diamines. Various poly(imino ketone)s were synthesized using different monomers (Scheme 4-1). The effect of concentration and temperature on the molecular weight of **PIK-15** was determined. A temperature of 165 °C and a concentration of 36 % were optimal for the palladium-catalyzed polycondensation to produce polymer **PIK-15** with high molecular weight. Four different ligands were used successfully and the Pd/BINAP system was found to be the most effective catalyst, producing the highest yield and highest molecular weight polymers. It was found that the reactivity decreases strongly with increasing electronegativity of the halogen atoms so that better yield, and higher molecular weight **PIK-12** was obtained by using 1,4-bis(4-bromobenzoyl)benzene (**7**) rather than 1,4-bis(4-chlorobenzoyl)benzene (**5**) while 1,4-bis(4-fluorobenzoyl)benzene (**6**) was totally unreactive. This may be because the oxidative addition is rate limiting in the catalytic amination cycle (Scheme 1.4-15). These polymers may be considered as analogs to polyaramides since hydrogen bonding is detected by broadening of the associated imino group (NH) vibrational bands. On the other hand due to the incorporated benzophenone and ether moieties one can expect similarities to poly(ether ketone)s (high Young modulus, low entanglement molecular weight). All these expectations were confirmed by mechanical and TGA measurements indicating that PIKs can be considered as a new class of high-performance polymers with good mechanical behavior and high thermal stability. These investigations were extended and supported by dielectric spectroscopy. The values of the dielectric constants at 1 MHz were in the range 2.71–3.08. These low values of the dielectric constant are very similar to those reported for related polyphenylquinoxalines and are even lower than that of "H Film", a polyimide Kapton film.

In addition to the low values of the dielectric constants, PIKs have lower glass transition temperatures (T$_g$s) than Kapton which makes them more easily processable.

One major advantage in comparison with the established PEKs and polyaramides is that one can use cheaper monomers e.g. chloro- or bromofunctionalized aromatic ketones instead of the corresponding difluoro compounds. Also the synthesis of „activated" intermediates, as is the case for the preparation of polyaramides by converting the aromatic esters to e.g. acid chlorides, is avoided. Furthermore, many diamines and dibromo compounds are readily available or easy to synthesize providing rapid access to numerous new polymers with optimized properties such as thermal stability, mechanical behavior or solubility. The amorphous polymer structure of PIKs was proven by DSC and by wide-angle X-ray measurements.

The X-ray diffraction patterns proved that insertion of one *tert*. butyl group or two isopropylidene groups into the recurring units of the polymers **PIKs-12a**, **13**, **14a**, **14b**, **15**, and **16a** resulted in a significant increase of the amorphous nature of the polymer. However, polymers **PIKs-11c**, **11a**, and **11b** showed a significant increase in the crystalline nature of the polymer, despite the presence of a kinked ether group in the polymer backbone. The improvement in solubility behavior of **PIKs** could probably be attributed to the combined effects of the pendant *tert*. butyl group and/or with either two isopropylidene groups in the polymer backbone.

Part 2. Novel poly(imino alcohol)s (PIAlcos) by grafting on the carbonyl groups.

The synthesized PIKs are an ideal target because of the highly reactive carbonyl groups, which allows selective addition to form tertiary alcohols. Therefore, nucleophilic addition of phenyllithium on 4,4`-bis(4-anilinobenzoyl)benzene was carried out to afford 1,4-bis{(phenyl-(4-anilinophenyl)methanol)}benzene in high yield.

A series of poly(imino alcohol)s **PIAlcos** was synthesized by nucleophilic addition of phenyllithium on PIKs. In this process approximately 100 % of the carbonyl groups could be converted and a high yield could be achieved. The obtained polymers showed lower thermal stability and slightly higher glass transition temperatures than those of the corresponding PIKs. PIAlcos are amorphous as detected by wide-angle X-ray diffraction.

Part 3. Poly(quinone diimine) *via* **elimination reaction:**

Elimination reaction of 1,4-bis{(phenyl-(4-anilinophenyl)methanol)}benzene afforded 1,4-bis{(4-benzylidene-cyclohexa-2,5-dienylidene)-anilino}benzene in 92 % yield. The latter compound as a new material with interesting structure exhibited photochromism due to E-Z-isomerization. Attempts were made to synthesize poly(quinone diimine)s from poly(imino alcohol)s *via* elimination reaction under acidic conditions. GPC analysis suggested that the poly(imino alcohol)s degrade instead of undergoing elimination.

Part 4. Synthesis of poly(imino acridine)s (PIAcs).

In this section, the ability of 4,4`-dibromophenylether, 4,4`-dibromobenzophenone and 4,4`-dibromodiphenyl to undergo Buchwald-Hartwig reaction with 3,6-diaminoacridine was investigated. Palladium-catalyzed amination of aryl dibromides with proflavine, 3,6-diaminoacridine free base afforded poly(imino acridine)s having an acridine group in the main chain in good yields. The absorption spectra of the polymers were dependent on the acidity of media because they can exist in neutral and singly protonated forms in solution. PIAc polymers showed strong photoluminescence in DMAc solution. Despite the undetected T_gs of this class of polymers, their amorphous nature was proven by wide-angle X-ray diffraction.

Part 5. Synthesis of polymers containing an azobenzene group in the main chain (PIAzos).

In this part of studies, the ability of 4,4`-dibromophenylether, 1,4-bis(4-bromobenzoyl)benzene, and 4,4`-dibromobenzophenone to undergo Buchwald-Hartwig reaction with 4,4`-diaminoazobenzene was investigated. Since electron-poor dibromo compounds and electron-rich diamines were successfully used in the polycondensation process, reactions of 4,4`-diaminoazobenzene as an electron-deficient diamine with 1,4-bis(4-bromobenzoyl)benzene, and 4,4`-dibromobenzophenone as an electron-deficient dibromo compound were examined and shown to be compatible with the standard Buchwald-Hartwig reaction. On the other hand, the reaction between 4,4`-dibromophenylether as an electron-rich dibromo compound and 4,4`-diaminoazobenzene an electron-deficient diamine was investigated. 4,4`-Dibromophenylether was also found to be compatible with polycondensation process. The reason to select 4,4`-diaminoazobenzene as a diamine was to study the effect of the azobenzene group containing N=N as an electron withdrawing group which is known to have a weaker withdrawing effect than that of the carbonyl group and also

to introduce the azobenzene group into the polymer backbone. The obtained polymers exhibited photoinduced and thermal isomerization properties of the azobenzene moieties; however, it appears that the structure of the polymer main chain has no effect on the isomerization behavior. The photoinduced and thermal isomerization behaviors of the polymer samples were observed by monitoring the changes in the absorbance (at 388 and 452 nm) with time at constant temperatures with the UV-visible absorption spectrometer. The absorption properties of the polymers were also dependent on the acidity of the media.

Dynamic mechanical measurements have been performed and temperature dependencies of the real, G', and imaginary, G'', parts of the complex shear modulus was determined. The effect of the stiffness due to the azobenzene group in the polymer backbone was recorded by dynamic mechanical measurements of **PIAzo-2**, and **3** relative to the **PIK-13** which has a flexible backbone. These tested samples show a rubbery plateau above the glass transition but as the temperature approached 300 °C, the elastic modulus increased indicating that probably a cross-linking taking place. It can be noticed that the G'' maximum is much narrower for the **PIK-13** with the flexible backbone and becomes remarkably broader when the monomer consists of both stiff and flexible fragments (**PIAzo-2**, and **3**) i.e. has a composition which can cause a considerable dynamic heterogeneity. For the examined materials the terminal flow is only observed for the most flexible polymer **PIK-13** with the lowest T_g. A calorimetric effect was also illustrated and showed that increasing stiffness involves an increase of the glass transition temperature.

Part 6. Synthesis of novel poly(imino fluorenone)s (PIFOs).

In part 1 it was found that the Pd-catalyzed process of which the Pd/BINAP system to be the most effective catalyst, producing the highest yield and highest molecular weight polymer. By using these condition, a series of novel poly(imino fluorenone)s (PIFOs) was synthesized *via* palladium-catalyzed polycondensation of aromatic dibromoketone (3,6-dibromo-9-fluorenone (**19**)) with various aromatic diamines.

Part 7. Synthesis of novel photoluminescent poly(imino carbazole)s (PICs).

A series of novel highly photoluminescent polymers containing carbazole chromophore has been synthesized *via* palladium-catalyzed polycondensation of aromatic diamines (3,6-diamino-N-(2-ethylhexyl)carbazole (**EHCDN**) with various aromatic dibromo compounds, namely, 4,4`-dibromophenylether, 1,4-bis(4-bromobenzoyl)benzene, 4,4`dibromobenzophenone, and 4,4`-dibromodiphenyl using three different reaction

conditions. All the tested PICs showed high thermal stability and a high char yield in nitrogen at 600 °C. Cyclic voltammetry (CV) studies showed that the oxidation potential of the PIC polymers decreased as the carbazole content increased in the polymer backbone. PIC polymers exhibited lower oxidation and reduction potentials compared to poly(9,9-dialkyl-2,7-fluorene) based polymers.[361] This may have important implications on chemical tuning hole-transport properties for these materials.

Method (a)

2.8 equiv. of NaO*t*-Bu,

0.01 equiv. of cat. (Pd)₂(dba)₃,

0.03 equiv. of cat. BINAP,

DMAc

100 °C for 4h-165 °C for 20 h

Method (b)

2.8 equiv. of NaO*t*-Bu,

0.01 equiv. of cat. (Pd)₂(dba)₃,

0.03 equiv. of cat. BINAP,

DPS, LiCl

165 °C for 4h-200 °C for 20 h
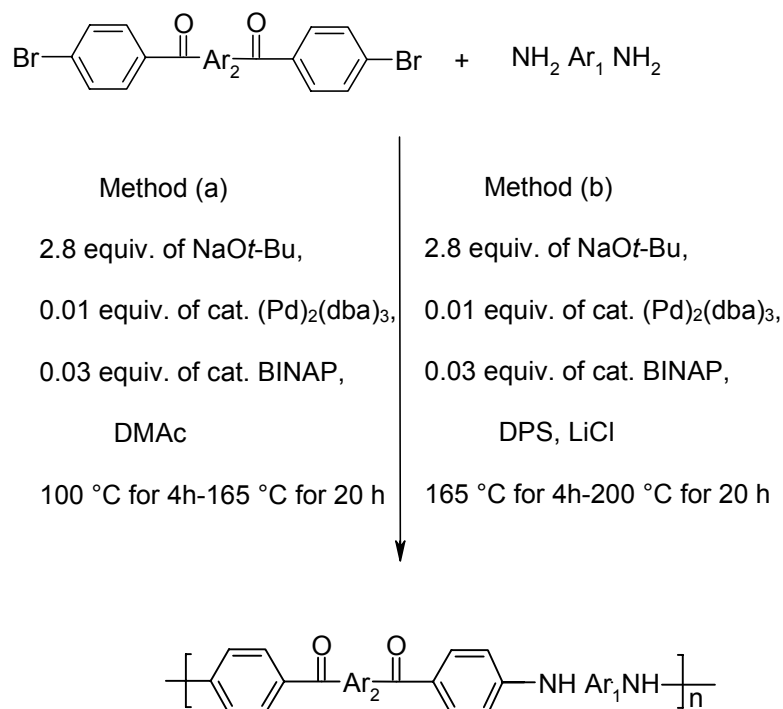
Polymer Code	Ar$_1$	Ar$_2$	Synthetic Method	Yield (%)
PIK-11a			a	95
PIK-11b			b	89.9
PIK-11c			a	92
PIK-12a			b	80
PIK-13			b	88
PIK-14a			a	86
PIK-14b			b	88
PIK-15			b	84
PIK-16a			b	90

Scheme 4-1: Schemes out the reactions involved in the synthesis of poly(imino ketone)s PIKs.

Figure 4-1 provides a reference to the backbone structure of polymers developed in this thesis. The acronyms of the polymers are listed below their structure. For simplicity, these polymers will be described by these acronyms.
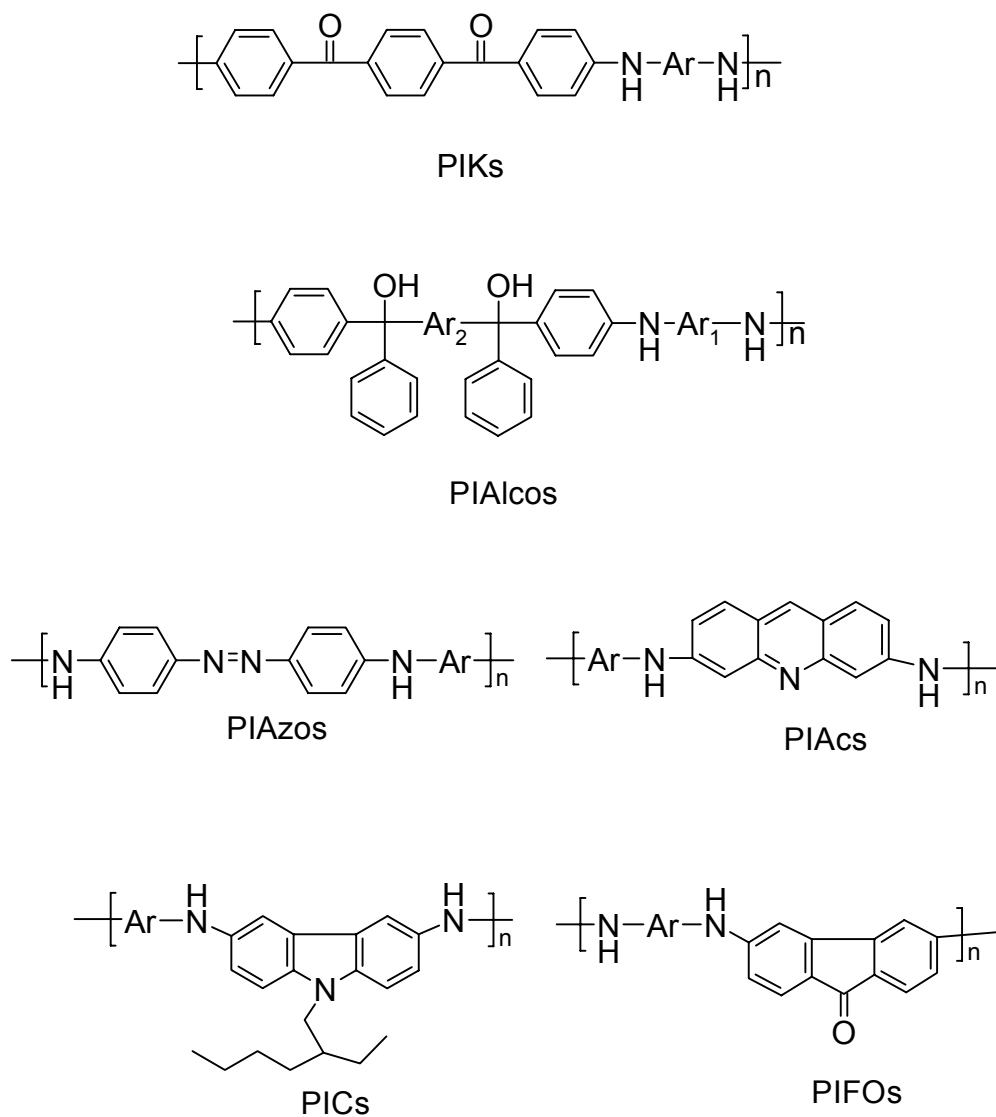
Figure 4-1: Novel structures and corresponding acronyms of polymers developed in this thesis.

Figure 4-2 provides a reference to the backbone structure of model compounds developed in this thesis.
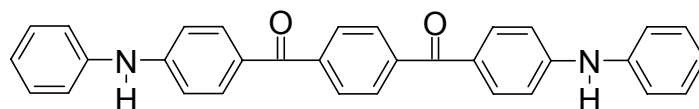
4,4´-Bis(4-anilinobenzoyl)benzene.
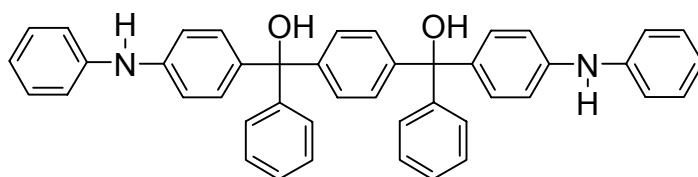
1,4-Bis{(phenyl-(4-anilinophenyl)methanol)}benzene.
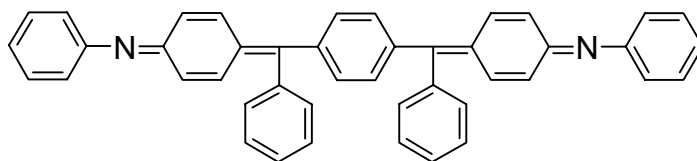
1,4-Bis{(4-benzylidene-cyclohexa-2,5-dienylidene)-anilino}benzene.
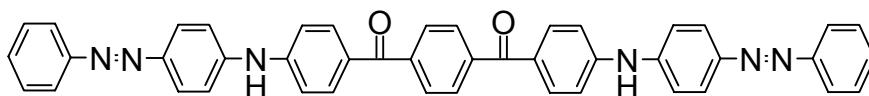
4,4´-Bis(4-aminoazobenzenebenzoyl)benzene.
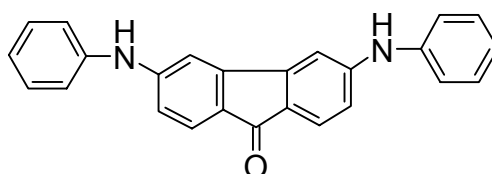
3,6-Dianilino-9-fluorenone.

Figure 4-2: Novel structures of model compounds developed in this thesis.

4.2. Outlook

This work provided the first access to the structurally pure, high molar mass, N-containing polymers *via* palladium-catalyzed polycondensation of various aromatic diamines with various aromatic dibromo compounds. Most of the goals of this dissertation were achieved and good characterization results were obtained.

One major advantage is to use cheap monomers aromatic bromides and aromatic amines. Furthermore, many diamines are readily available or easy to synthesize giving a fast access to numerous new functionalized polymer either by using bromofunctionalized or aminofunctionalized monomers in order to optimize and improve the polymer properties.

The Pd-catalyzed arylation amination reaction is a broadly useful method for the construction of a wide variety of aromatic polymers in a one-pot synthesis. Consequently, the corresponding polymers containing alcohol were constructed. The careful optimization of reaction conditions and reagents, supplemented by a sound mechanistic understanding of both organic and organometallic chemistry was a key to our approach.

The chemical inertness, thermal stability, and low dielectric constant characteristics of the polymer materials make them attractive for advanced technology applications, since aromatic polyelectrolytes containing azobenzene have photoresponsive properties.[363] The Pd-catalyzed system may be used to synthesize these polyelectrolytes in a one-pot reaction. It is anticipated that future studies might not only improve the scope and understanding of this process, but will lead to new types of interesting polymers followed by their new applications by using of Pd-catalyzed cross-coupling reactions.

Our synthesized PIAcs, PIFOs, and PICs need further studies to get important informations about parameters such as the photoluminescence efficiency, film-forming and ability of the charge carrier mobility to determine whether these materials are suitable for application in electronic devices such as LEDs. These investigations clearify the potential application values of our synthesized materials containing the attractive architectures, PIFOs suggested to use as electron-deficient (n-type) and PICs suggested to use as hole-transporting (p-type).

CHAPTER V

EXPERIMENTAL PART

5.0 Characterization methods

Fourier transform infrared spectroscopy (FT-IR)

FT-IR was used to examine the structure of the polymers and to monitor the curing process of the reactive functional group terminated thermosetting imide oligomers. Spectra were obtained with a Nicolet Impact 400 FT-IR spectrometer. In order to monitor the cure, chloroform solutions of oligomers were deposited on KBr plates.

Elemental analyses

Elemental analyses were performed on a Perkin-Elmer Model 2400 CHN analyzer.

U.V

UV-vis absorption spectra were recorded at room temperature on a Perkin-Elmer Lambda 15.

Mass spectroscopy:

FD^+ and EI mass spectra were recorded on a VG Instrument ZAB 2-SE-FPD.

Nuclear magnetic resonance (NMR) spectroscopy.

Proton ^{1}H-NMR and carbon ^{13}C-NMR spectra were recorded using a Bruker AMX250 Hz, Bruker AC300 Hz, and Bruker AMX700 Hz NMR spectrometers in $CDCl_3$, CD_2Cl_2, or DMSO-d_6, depending on the solubility of the material being analyzed. Instrument. ^{1}H and ^{13}C-NMR spectra were referred to tetramethylsilane (TMS) at 0 ppm. NMR spectra were used to determine purity, chemical composition, and figure out the end groups of the synthesized polymers.

Melting point of monomers by capillary methods

The melting points of purified compounds were determined on a Büchi melting point apparatus at a heating rate of no greater than 1 °C/min. Samples were ground before measuring and the formation of a meniscus was identified as the beginning of the melt.

Intrinsic viscosity

Intrinsic viscosities were determined to obtain the molecular weight information of polymers. The measurements were conducted at 25 °C in DMF or THF according to the solubility of the tested polymer, using a Cannon-Ubbelodhe viscometer. The intrinsic viscosity value [η] was obtained by measuring specific viscosity $\eta_{sp} = \eta/\eta_0 - 1$ and reduced viscosity $\eta_{red} = \ln(\eta/\eta_0)$ at four different concentrations, plotting η_{sp}/C versus C and extrapolating to zero concentration.

Gel Permeation Chromatography (GPC)

GPC measurements were used to determine molecular weight and molecularweight distribution information. Chromatographs were obtained on a Waters 150CALC/GPC instrument equipped with a differential refractive index detector and a Viscotek$^®$ Model 100 viscosity detector connected in parallel. NMP (HPLC grade), containing ~0.02M P_2O_5 and filtered through 0.5μm Teflon filter, served as mobile phase. The stationary phase was crosslinked polystyrene gel (Waters μstyragel HT 10^2 Å, 10^3 Å and 10^4 Å, mean particle diameter 10 μm) packed in three (7.8 mm I. D. x 30cm) stainless steel columns. Samples prepared to known concentrations ~4 mg/mL) were dissolved in the mobile phase and filtered through 0.2 μm PTFE disposable filter prior to analysis. The injected sample volume was 200 μL and the flow rate of the mobile phase was 1.0 mL/min. The column compartment, lines and detectors were kept at a temperature of 25 °C during the measurements. Number average molecular weight (M_n), weight average molecular weight (M_w) and polydispersity (M_w / M_n) were determined by universal calibration generated with narrow molecular weight distribution polystyrene standards.[364]

Differential Scanning Calorimetry (DSC)

DSC was used to determine glass transition temperatures of polymers. DSC was conducted on a Perkin-Elmer DSC 7 instrument. Scans were run in nitrogen at a heating rate of 10 °C/min. T_g values were identified as the midpoint of the change in endothermic baseline from the second heat after a quench cool from the first run.

Thermogravimetric analysis (TGA)

Dynamic TGA was performed to access the relative thermal stability of polymers. Thermograms were obtained using a Perkin Elmer TGA 7 thermogravimetric analyzer. Thin film or powder samples of ~10 mg were placed in a platinum pan connected to an electric microbalance. The samples were heated at a rate of 10 °C/min. in air or nitrogen, weight loss of the samples was measured as a function of temperature.

X-Ray Diffraction (WAXD)

WAXD analysis was performed on a Perkin-Elmer PHI 5400 diffractometer employing a MgKα (1253.6 eV) achromatic X-ray source operated at 14 KeV with a total power of 300 watts.

Rheology Measurements

Vacuum dried polymers were used to prepare samples for dynamic mechanical measurements which were prepared by compression molding at a temperature above T_g. Dynamic mechanical measurements have been performed by means of the Rheometrics RMS

800 mechanical spectrometer. Shear deformation has been applied under condition of controlled deformation amplitude, always remaining in the range of the linear viscoelastic response of studied samples. Frequency dependencies of the storage (G') and loss (G'') shear modulus have been measured at various temperatures. The cone-plate of 6 mm diameter has been used. Experiments have been performed under dry nitrogen atmosphere.

Frequency dependencies of G' and G'' measured within the frequency range 0.1 - 100 rad/s. at various temperatures have been used to construct master curves representing a broad range frequency dependencies of these quantities. Only shifts along the frequency scale have been performed. This procedure provided a temperature dependence of shift factors (log a_T vs. T).[260] The low frequency range of the master dependence of G'' (with G''~ϖ, indicating the newtonian flow range) has been used to determine the zero shear viscosity at the reference temperature ($\eta_o(T_{ref}) = G'/\varpi$). Viscosity values related to other temperatures have been determined as $\log \eta_o(T) = \log \eta_o(T_{ref}) + \log a_T$. The relaxation time corresponding to the transition between the newtonian flow range at low frequencies and the glassy range at high frequencies at the reference temperature has been determined as $\tau(T_{ref}) = 1/\varpi_c$, where ϖ_c is the frequency at which the G' and G'' dependencies cross each other.[261] Relaxation times at another temperatures are given by $\log \tau(T) = \log \tau(T_{ref}) + \log a_T$.

Dielectric spectroscopy

The setup for the dielectric measurements consisted of the temperature controlled sample cell and a Novocontrol system composed of an Alpha frequency response analyzer and Quattro temperature controller. The samples were sandwiched between two copper electrodes of diameter 10 mm and had a thickness of 100 μm. The quartz ring spacer was used to control geometry of the samples.

The dielectric measurements were carried out at different temperatures in the range from room temperature to 300 °C for frequencies in the range from 10^{-2} to 10^6 Hz. The complex dielectric permittivity ε*=ε'-iε'', where ε' is the real and ε'' is the imaginary part, is a function of frequency ω and temperature T ε*=ε*(ω, T).

In the analysis the maxima of the imaginary part of the dielectric modulus (M*=1/ε*), that relate to the relaxation times of the dielectric processes, were fitted using well-known Havriliak-Negami equation:

$$\frac{M^*(T,\omega) - M_\infty(T)}{\Delta M(T)} = \frac{1}{\left[1 + (i\omega\tau_{HN}(T))^\alpha\right]^\gamma} \quad (1)$$

where $\tau_{HN}(T)$ is the characteristic relaxation time in this equation. Only the imaginary part of spectra was used in the fitting procedure.

Cyclic Voltammetry (CV):

The cyclic voltammetry experiments were performed on a model 173 potentiostat. The experiments were carried out at room temperature under a purified argon atmosphere. Argon gas was also used to purge all solutions prior to experimentation. The concentration of the electroactive species was 10^{-3} mol/L. Tetrabutylammonium perchlorate (0.1 M) was added as a supporting electrolyte. A platinum electrode was used as a working electrode. Ferrocene was used as an internal standard. The obtained data were processed with the research electrochemistry software M270.

Time of flight technique (TOF):

The polymer (**PIC-7**) was spincoated from a 4 wt.% solution in THF on a precleaned ITO substrate. The polymer film was kept under high vacuum overnight prior to the evaporation of an aluminum layer (100 nm) on top of the polymer film using the shadow mask technique. The sample was attached to a sample holder in a homebuilt cryostate under a dynamic vacuum of 10^{-5} mbar. Excitation of the polymer film was performed at 350 nm with a laser pulse of 8 ns length provided by a Nd:YAG / OPO / SHG laser system. The current transient was monitored by a Tektronix TDS 524A oscilloscope triggered by the laser pulse.

5.1-1 Synthesis of poly(imino ketone)s (PIKs):
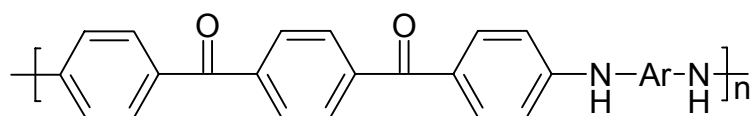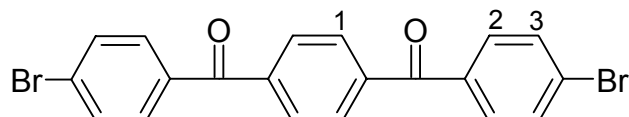

PIKs

5.1.1 Synthesis of dibromo compounds as monomers:

5.1.1.1 Synthesis of 1,4-bis(4-bromobenzoyl)benzene (7):

Synthesized by the following modified procedure:[203]

40 g of anhydrous powdered aluminium chloride (0.3 mol) was added to a stirred solution of 25.4 g of terephthaloyl chloride (0.125 mol) and 255.14 g of bromobenzene (1.63 mol). After an exothermic reaction which raised the temperature to 30 °C the solution was stirred at room temperature for 12 h, then heated at 95 °C for 2 h. After cooling, the solution was poured into cold aqueous hydrochloric acid to precipitate a solid which was isolated by filtration. The cream colored solid was thoroughly washed with water, sodium bicarbonate solution (10 %), and water and then dried at 100 °C in air. The crude product was recrystallized from N, N-dimethylacetamide (DMAc) or toluene to give (**7**) as colorless crystals. Yield: 52.2 g, 94 %. Mp: 274 –275 °C. ^{1}H-NMR (300 MHz, DMSO-d_6, 373K): δ = 7.86 (s, 4H, H-1), 7.76 (d, 4H, H-2, m to Br), 7.73(d, 4H, H-3, o to Br). FD$^+$-MS (m / z): 444.10. FT-IR spectrum (KBr pellet): 840, 843 cm^{-1} (p-disubstituted benzene); 1640 cm^{-1} carbonyl group). U.V. spectrum (CHCl$_3$): λ$_{max}$ 271 nm.

Elemental analysis:

(C$_{20}$H$_{12}$Br$_2$O$_2$)	Calculated:	C, 54.09 %; H, 2.72 %; Br, 35.98 %
(444.12)	Found:	C, 54.00 %; H, 2.70 %; Br, 35.56 %

5.1.1.2 Synthesis of 1,3-bis(4-bromobenzoyl-5-*tert.*-butyl)benzene (9):
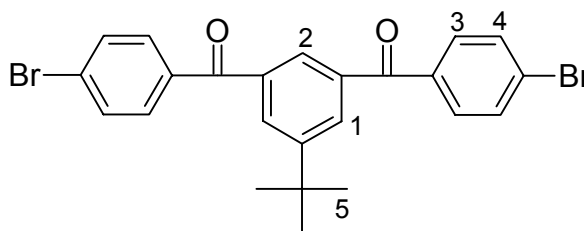
A mixture of 5-*tert.*-butylisophthalic acid (25.0 g, 0.113 mol) and $SOCl_2$ (250 mL) was stirred at reflux for 24 h. The excess $SOCl_2$ was distilled off under vacuum, and the resultant acid chloride was used in the following Friedel-Craft benzoylation without further purification. Bromobenzene (230.6 g, 1.469 mol) was added to the acid chloride, and the solution was cooled in an ice-water bath. Anhydrous aluminium chloride (36.0 g, 0.27 mol) was added slowly such that the temperature did not exceed 5 °C. The obtained red suspension was stirred at room temperature for 16 h and then at 60 °C for 4 h. The reaction mixture was allowed to cool to room temperature and poured into a mixture containing ice-water and concentrated HCl. The pale yellow precipitate was washed with water and sodium bicarbonate solution (10 %) resulting in a colorless solid which was dried in an oven. Two recrystallisations from chloroform/petroleum ether gave (**9**) as colorless crystals. Yield: 49.8 g, 88.2 %. Mp: 167-68 °C. ^{1}H-NMR (250 MHz, CD_2Cl_2, 293K): δ = 8.01 (s, 2H, H-1, *o* to *t*-Bu group), 7.84 (1H, H-2, *p* to *t*-Bu group), 7.65 (d, 4H, H-3), 7.49 (d, 4H, H-4), 1.36 (s, 9H, *t*-Bu group). ^{13}C-NMR (62.5 MHz, CD_2Cl_2, 293K): δ = 195.2, 152.7, 137.6, 136.4, 132.9, 132.1, 131.0, 128.1, 126.4, 35.4, 31.2. FD^+- MS (m / z): 499.60 (molecular peak).

Elemental analysis:

($C_{24}H_{20}Br_2O_2$)	Calculated:	C, 57.63 %; H, 4.03 %; Br, 31.95 %
(500.23)	Found:	C, 57.04 %; H, 3.89 %; Br, 31.62 %

5.1.2 Synthesis of a model compound 4,4´-bis(4-anilinobenzoyl)benzene (10):
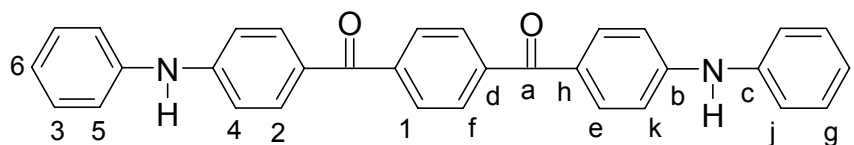
5.1.2.1 Method (A):

An oven-dried resealable Schlenk flask was evacuated and backfilled with argon. The flask was charged with $Pd_2(dba)_3$ (18.3 mg, 0.02 mmol, 2.0 mol %), BINAP (37.4 mg, 0.06 mmol, 6.0 mol %), and NaOt-Bu (538 mg, 5.6 mmol). The flask was evacuated and backfilled with argon and then capped with a rubber septum. DMAc (5 mL), 1,4-bis(4-bromobenzoyl)benzene (7) (888.0 mg, 2.0 mmol), aniline (373.0 mg, 4.0 mmol), and additional DMAc (2 mL) were added through the septum. The flask was fitted with a reflux condenser, and the mixture was heated to 160 °C with stirring for 24 h. The resulting solution was allowed to slowly cool to room temperature and subsequently poured into cold water, filtered through celite and dried. The crude material was purified by flash chromatography on silica gel and recrystallized from toluene to afford (10) as yellow crystals. Yield: 825 mg, 88 %. Mp: 248-50 °C. ^{1}H-NMR (250 MHz, DMSO-d_6, 293K): δ = 8.77 (s, NH); 7.56 (s, 4H, H-6); 7.50 (d, 4H, H-5); 7.13 (t, 4H, H-4); 7.03 (d, 4H, H-3); 6.93 (d, 4H, H-2), 6.80 (t, 2H, H-1). ^{13}C-NMR (62.5 MHz, DMSO-d_6, 293K): δ = 193.1 (C_a), 148.8(C_b), 140.8(C_c), 132.5(C_d), 129.4(C_e), 128.8(C_f), 126.3(C_g), 122.3(C_h), 119.8(C_i), 119.7(C_j), 113.7(C_k). EI-MS (m / z): 468.9 (molecular peak), 467.9, 422.6, 300.3, 285.3, 238.9, 195.8 (100 %), 166.7, 151.0; FT-IR (KBr pellet): γNH at 3341 cm^{-1}; γC=O at 1633 cm^{-1}, γC-H aromatic at 3049 cm^{-1} and C-N at 1338 cm^{-1}; UV recorded in CHCl$_3$ λ$_{max}$ at 296 and 368 nm;

Elemental analysis:

$(C_{32}H_{24}N_2O_2)$ Calculated: C, 82.03 %; H, 5.16 %; N, 5.98 %

(468.55)   Found: C, 81.54 %; H, 5.15 %; N, 5.20 %

5.1.2.2 Method (B):

An oven-dried resealable Schlenk flask was evacuated and backfilled with argon. The flask was charged with $Pd(OAc)_2$ (4.4 mg, 0.02 mmol, 2.0 mol %), di-t-butylphosphinobiphenyl (12.0 mg, 0.04 mmol, 4.0 mol %), and NaOt-Bu (270.0 mg, 2.8 mmol). The flask was evacuated and backfilled with argon and then capped with a rubber septum. DMAc (2 mL), 1,4-bis(4-bromobenzoyl)benzene (7) (444.0 mg, 1.0 mmol), aniline (205.0 mg, 2.2 mmol),

and additional DMAc (2 mL) were added through the septum. The flask was fitted with a reflux condenser, and the mixture was heated to 160 °C with stirring for 24 h. The resulting solution was allowed to slowly cold to room temperature and subsequently poured into cold water, filtered through celite and dried. The crude material was purified by flash chromatography on silica gel and recrystallized from toluene to afford 4,4'-bis(4-anilinobenzoyl)benzene (**10**) as yellow crystals.

5.1.2.3 Method (C):

Under an atmosphere of argon DMAc (3 mL), KOt-Bu (336.0 mg, 3.0 mmol), 1,4-bis(4-bromobenzoyl)benzene (**7**) (444.0 mg, 1.0 mmol), and aniline (205.0 mg, 2.2 mmol) were added in turn to a Schlenk tube charged with $Pd_2(dba)_3$ (18.3 mg, 0.02 mmol), P(t-Bu)$_3$ (25.5 mg, 0.06 mmol, 6.0 mol %), and a magnetic stirring bar. The Schlenk tube was placed in a 160 °C oil bath and stirred for 24 h. The reaction mixture was allowed to cool to room temperature and absorbed directly onto silica gel and purified by flash chromatography (hexane/ethyl acetate (10:1).

5.1.2.4 Method (D):

In a dry box, 1,4-bis(4-bromobenzoyl)benzene (**7**) (444.0 mg, 1.0 mmol), aniline (205.0 mg, 2.2 mmol), Pd(dba)$_2$ or Pd(OAc)$_2$ (0.02 mmol, 4.0 mol %), 1,3-bis(2,6-diisopropylphenyl)imidaz-olium chloride) (12.0 mg, 0.06 mmol, 6.0 mol %), and sodium *tert*-butoxide (270.0 mg, 2.8 mmol) were weighed directly into a screw cap vial. A stir bar was added followed by 2.0-3.0 mL of DMAc The vial was removed from the drybox, evacuated and flushed with argon. The mixture was stirred as rapidly as possible with a magnetic stirring plate at 160 °C. The reaction was monitored by thin-layer chromatography or GC. After the consumption of starting materials, the reaction mixture was adsorbed onto silica gel and purified by chromatography

5.1.3 Synthesis of poly(imino ketone)s (PIKs):
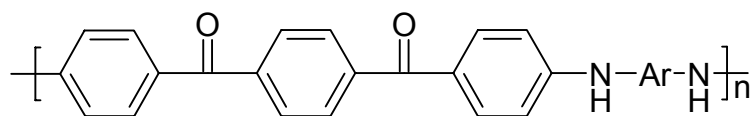
PIKs

5.1.3.1 Method (a):

To a Schlenk flask equipped with magnetic stirrer, an argon outlet, inlet and water cooled condenser, dibromo compound (4.0 mmol), diamine (4.0 mmol), sodium *tert*-butoxide (1.076 g, 11.2 mmol), tris(dibenzylideneacetone)dipalladium(0) (36.6 mg, 0.04 mmol, BINAP (74.8 mg, 0.12 mmol), and dimethylacetamide (6-8 mL) were added. The reaction mixture was evacuated and flushed with high purity argon. This procedure was repeated 5 times. The flask was immersed with continuous stirring in a 100 °C oil bath for 4 h, and in a 165 °C oil bath for 20 h. The resulting polymer solution was allowed to slowly cool to room temperature, filtered and subsequently poured into cold water, filtered, washed with water and methanol, then dried at 100 °C under vacuum.

PIK-11a:
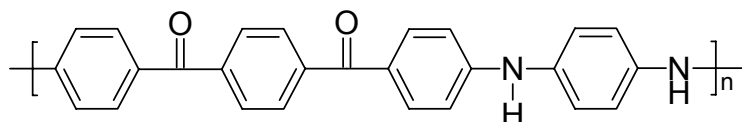
Yield: 740 mg, 95 %; FT-IR (KBr pellet): γNH at 3318 cm^{-1}; γC=O at 1631 cm^{-1}, γC-H aromatic at 3049 cm^{-1} and C-N at 1312 cm^{-1}; ^{1}H-NMR and GPC were not recorded due to the poor solubility of the polymer.

Elemental analysis:

$(C_{26}H_{18}N_2O_2)_n$

$(390.44)_n$			
Calculated	79.98 %	4.65 %	7.17 %
Found	76.70 %	4.86 %	6.89 %
Corrected	79.46 %	4.69 %	7.14 %

Moisture uptake   3.60

Polymer PIK-11c
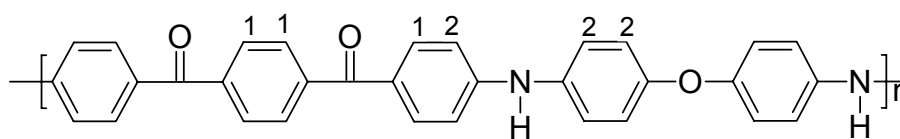
Yield: 888 mg, 92 %; FT-IR (KBr pellet): γNH at 3320 cm^{-1}; γC=O at 1638 cm^{-1}, γC-H aromatic at 3049 cm^{-1} and C-N at 1316 cm^{-1}; ^{1}H-NMR (250 MHz, DMSO-d_6, 293K): δ = 8.93 (s, NH); 7.69 (d, H-1); 7.14 (s, H-2); The molecular weights of the polymer was calibrated by GPC: M_n = 11 100; M_w = 74100; M_w / M_n = 6.7; DP = 23.

$(C_{32}H_{22}N_2O_3)_n$

$(482.54)_n$

	Calculated	79.65 %	4.60 %	5.81 %
	Found	76.80 %	4.78 %	5.80 %
	Corrected	79.59 %	4.61 %	6.01 %

Moisture uptake   3.63

Polymer PIK-14a
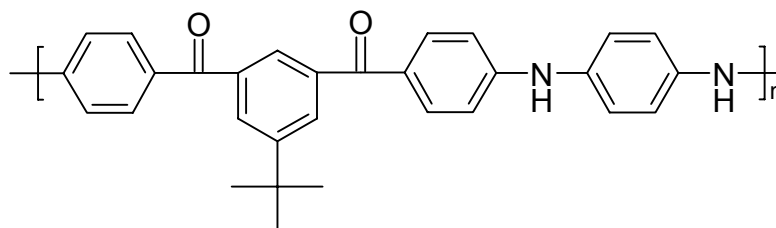
Yield: 768 mg, 86 %; FT-IR (KBr pellet): γNH at 3332 cm^{-1}; γC=O at 1646 cm^{-1}, γC-H aromatic at 3054 cm^{-1}; γC-H aliphatic at 2957 cm^{-1} and C-N at 1310 cm^{-1}; ^{1}H-NMR and GPC were not recorded due to the poor solubility of the polymer.

Elemental analysis:

$(C_{30}H_{26}N_2O_2)_n$

$(446.55)_n$

	Calculated	80.69 %	5.87 %	6.27 %
	Found	74.83 %	6.23 %	5.86 %
	Corrected	79.96 %	5.80 %	6.26 %

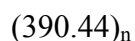Moisture uptake   6.85

5.1.3.2 Method (b):

To a Schlenk flask equipped with magnetic stirrer, an argon outlet, inlet and water cooled condenser, dibromo compound (4.0 mmol), diamine (4.0 mmol), sodium *tert*-butoxide (1.076 g, 11.2 mmol), tris(dibenzylideneacetone)dipalladium(0) (36.6 mg, 0.04 mmol), BINAP (74.8 mg, 0.12 mmol), lithium chloride (0.96-1.4 g), and diphenyl sulfone (7.0-10.0 g) were added. The reaction mixture was evacuated and flushed with high purity argon. This procedure was repeated many times. The flask was immersed with continuous stirring in a 165 °C oil bath for 4 h, and in a 200 °C oil bath for 20 h. The reaction mixture was then cooled to room temperature and grinded into a powder. The product was subsequently washed with acetone to remove the solvent and dissolved in dimethyl formamide, filtered, precipitated by acetone to ensure removal of salts, washed with water many times, then dried at 100 °C under vacuum.

Polymer PIK-11b
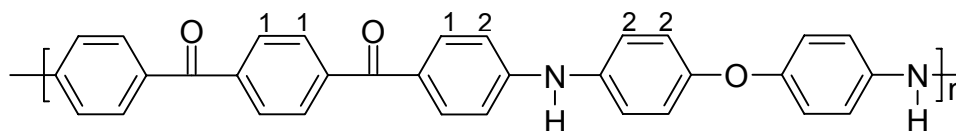

Yield: 867 mg, 89.8 %; FT-IR (KBr pellet): γNH at 3322 cm^{-1}; γC=O at 1635 cm^{-1}, γC-H aromatic at 3045 cm^{-1} and C-N at 1314 cm^{-1}; ^{1}H-NMR (250 MHz, DMSO-d_6, 293K): δ = 8.91 (s, NH); 7.66 (d, H-1); 7.12 (d, H-2). The molecular weights of the polymer was calibrated by GPC: M_n = 12 200; M_w = 25 300; M_w / M_n = 2.1; DP = 25.
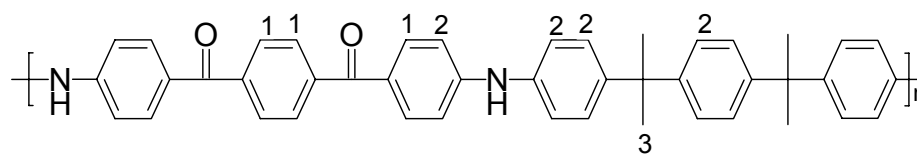
Elemental analysis:

$(C_{32}H_{22}N_2O_3)_n$

(482.54)$_n$			
Calculated	79.65 %	4.60 %	5.81 %
Found	77.52 %	4.73 %	5.67 %
Corrected	79.55 %	4.61 %	5.82 %

Moisture uptake   2.62.

Polymer PIK-12a

Yield: 1002 mg, 80 %; FT-IR (KBr pellet): γNH at 3377 cm^{-1}; γC=O at 1642 cm^{-1}, γC-H aromatic at 3024 cm^{-1}; γC-H aliphatic at 2962 cm^{-1} and C-N at 1308 cm^{-1}; ^{1}H-NMR (700 MHz, DMSO-d_6, 373K): δ = 8.80 (s, NH); 7.66 (d, H$_1$); 7.15 (d, H$_2$); 1.54 (s, isopropylidene group or H$_3$, CH$_3$). The molecular weights of the polymer was calibrated by GPC: M$_n$ = 15 000; M$_w$ = 26 300; M$_w$/M$_n$ = 1.8; DP = 24.

Elemental analysis:

(C$_{44}$H$_{38}$N$_2$O$_2$)$_n$

(626.79)$_n$			
Calculated	84.31 %	6.11 %	4.47 %
Found	83.10 %	6.19 %	4.33 %
Corrected	84.28 %	6.10 %	4.39 %

Moisture uptake   1.42.

Polymer PIK-13
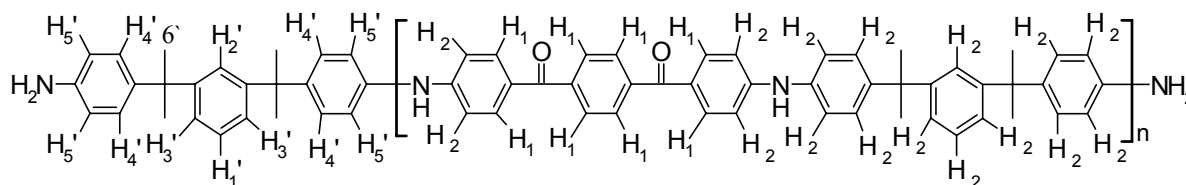
Yield: 1103 mg, 88 %; FT-IR (KBr pellet): γNH at 3360 cm^{-1}; γC=O at 1644 cm^{-1}, γC-H aromatic at 3028 cm^{-1}; γC-H aliphatic at 2961 cm^{-1} and C-N at 1307 cm^{-1}; ^{1}H-NMR (700 MHz, DMSO-d_6, 373K): δ = 8.78 (s, NH); 7.94 (d, H-1`); 7.66 (d, H-1+2`); 7.05 (d, H-2+3`); 6.80 (s, H-4`); 6.44 (d, H-5`); 4.71 (s, NH$_2$); 1.55 (s, isopropylidene group or H-6, CH$_3$); and 1.48 (s, isopropylidene group or H-6`, CH$_3$). The molecular weights of the polymer was calibrated by GPC: M$_n$ = 11 700; M$_w$ = 19 500; M$_w$/M$_n$ = 1.7; DP = 18.

Elemental analysis:
(C$_{44}$H$_{38}$N$_2$O$_2$)$_n$
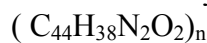
(626.79)$_n$			
Calculated	84.31 %	6.11 %	4.47 %
Found	82.62 %	6.21 %	4.34 %

Corrected   84.19 %   6.08 %   4.43 %

Moisture uptake   2.03.

Polymer PIK-14b.
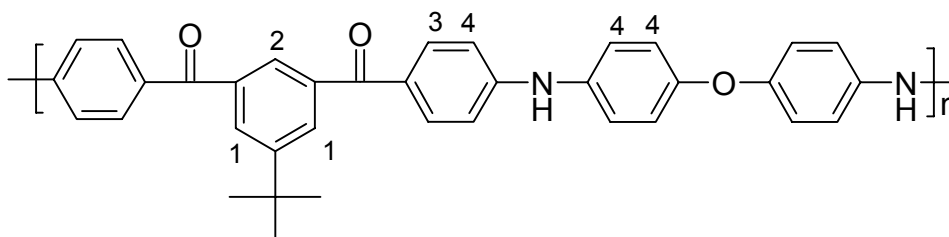
Yield: 948 mg, 88 %; FT-IR (KBr pellet): γNH at 3384 cm^{-1}; γC=O at 1644 cm^{-1}, γC-H aromatic at 3034 cm^{-1}; γC-H aliphatic at 2955 cm^{-1}; C-N at 1328 cm^{-1} and C-N at 1327 cm^{-1}; ^{1}H-NMR (700 MHz, DMSO-d_6, 313K): δ = 8.82 (s, NH); 7.94 (s, H-1); 7.84 (s, H-2); 7.64 (s, H-3); 7.06 (d, H-4) and 1.29 (s, t-Bu group, CH$_3$). The molecular weights of the polymer was calibrated by GPC: M_n = 44 200; M_w = 295 200; M_w / M_n = 6.7; DP = 82.

Elemental analysis:

(C$_{36}$H$_{30}$N$_2$O$_3$)$_n$

(538.64)$_n$ Calculated   80.27 %   5.61 %   5.20 %

                                 Found   74.60 %   6.08 %   4.85 %

   Corrected   79.80 %   5.66 %   5.19 %

Moisture uptake   6.97.

205

Polymer PIK-15
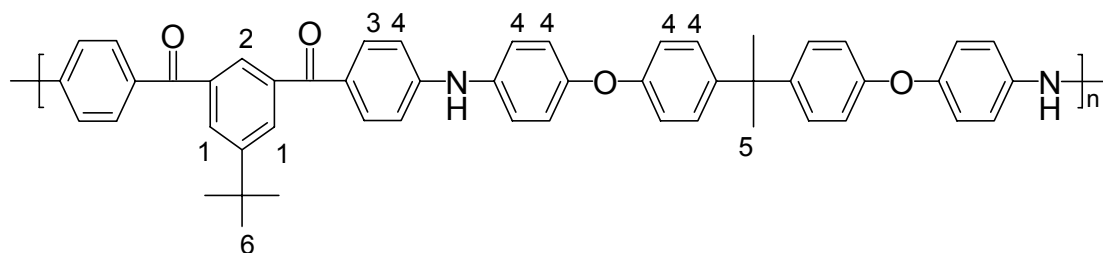
Yield: 1258 mg, 84 %; FT-IR (KBr pellet): γNH at 3422 cm^{-1}; γC=O at 1663 cm^{-1}, γC-H aromatic at 3029 cm^{-1}; γC-H aliphatic at 2963 cm^{-1}; C-N at 1328 cm^{-1} and C-N at 1330 cm^{-1}; ^{1}H-NMR (700 MHz, DMSO-d_6, 373K): δ = 8.82 (s, NH); 7.82 (s, H-1); 7.62 (s, H-2); 7.34 (s, H-3); 6.89 (d, H-4); 1.47(s, isopropylidene group or H-5, CH$_3$) and 1.22 (s, t-Bu group or H-6, CH$_3$). The molecular weights of the polymer was calibrated by GPC: M$_n$ = 37 000; M$_w$ = 139 300; M$_w$ / M$_n$ = 3.8; DP = 49.

Elemental analysis:

(C$_{51}$H$_{44}$N$_2$O$_4$)$_n$

(748.92)$_n$

Calculated	81.79 %	5.92 %	3.74 %
Found	77.69 %	5.99 %	3.68 %
Corrected	81.52 %	5.69 %	3.50 %

Moisture uptake   4.93.

Polymer PIK-16a

Yield: 1229 mg, 90 %; FT-IR (KBr pellet): γNH at 3348 cm^{-1}; γC=O at 1646 cm^{-1}; γC-H aromatic at 3028 cm^{-1}; γC-H aliphatic at 2962 cm^{-1} and C-N at 1328 cm^{-1}; ^{1}H-NMR (700 MHz, DMSO-d_6, 393K): δ = 8.36 (s, NH); 7.85 (s, H-1); 7.62 (s, H-2); 7.06 (broad band, H-3 + H-4); 1.53 (s, isopropylidene group or H-5, CH$_3$) and 1.22 (s, t-Bu group or H-6, CH$_3$). The

molecular weights of the polymer was calibrated by GPC: M_n = 85 900; M_w = 474 500; M_w /

M_n = 5.5; DP = 126.
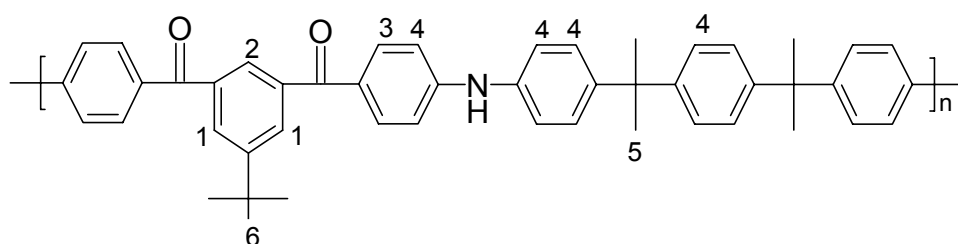
Elemental analysis:

$(C_{48}H_{46}N_2O_2)_n$

$(682.90)_n$
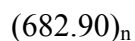
Calculated	84.42 %	6.79 %	4.10 %
Found	79.81 %	7.18 %	3.81 %
Corrected	84.36 %	6.77 %	4.03 %

Moisture uptake   5.70.

5.2 Novel poly(imino alcohol)s PIAlcos by grafting on the carbonyl groups
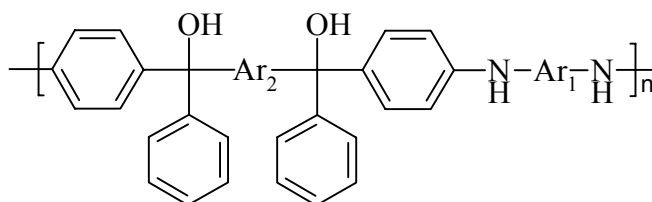
5.2.1 Synthesis of 1,4-bis{(phenyl-(4-anilinophenyl)methanol)}benzene (11):
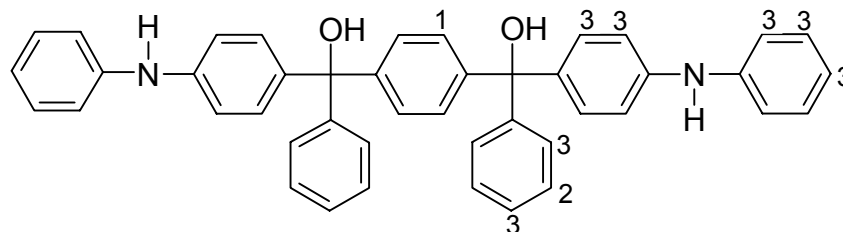
4,4$'$-bis(4-anilinobenzoyl)benzene (**10**) (2.0 mmol, 937.0 mg) was dissolved in 30 mL of distilled THF and cooled to 0 °C. After the addition of 4.0 mmol of phenyllithium (1.8 M in THF), the mixture was stirred for 2 h at 2-4 °C, then quenched by the addition of 5 mL of methanol and filtered. The resulting compound was precipitated by water washed with water several times and dried in vacuo. The solid product was recrystallized from chloroform / petroleum ether (3:1) to afford (**11**) as colorless crystals. Yield: 1150 mg, 92 %. Mp: 93 - 4 °C. ^{1}H-NMR (250 MHz, DMSO-d_6, 293K): δ = 7.94 (s, NH); 7.63 (d, 4H, H-1); 7.43 (d, 4H, H-2); 7.24-7.02 (m, 24H, H-3); 2.76 (s, OH). ^{13}C-NMR (62.5 MHz, DMSO-d_6, 293K): δ = 140.2, 145.7, 147.2, 130.4, 129.9, 128.9, 127.7, 127.6, 127.5, 127.4, 127.0, 126.8, 126.7, 120.0, 80.1. FD$^+$-MS (m / z): 624.0 (molecular peak), FT-IR (KBr pellet): γOH at 3550 cm^{-1};

γNH at 3390 cm^{-1}; C-H aromatic at 3029 cm^{-1} and C-N at 1309 cm^{-1}; UV recorded in CHCl$_3$

λ$_{max}$ at 364 nm.

Elemental analysis:

(C$_{44}$H$_{36}$N$_2$O$_2$)

(624.79)   Calculated: C, 84.59 %; H, 5.81 %; N , 4.48 %

                                        Found: C, 84.38 %; H, 5.68 %; N, 4.29 %

5.2.2 Synthesis of poly(imino alcohol)s PIAlcos:

Nucleophilic addition of phenyllithium to PIKs:

General procedure:

PIK polymer (2.0 mmol) was dissolved in 100 mL of distilled THF and cooled to 0 °C. After the addition of 4.0 mmol of phenyllithium (1.8 M in THF), the mixture was stirred for 2 h at 2-4 °C, then quenched by the addition of 5 mL of methanol and filtered. The precipitated PIAlco was washed with water and methanol and dried at 100 °C in vacuo to afford PIAlco in 90-94 % yield.

PIAlco-13
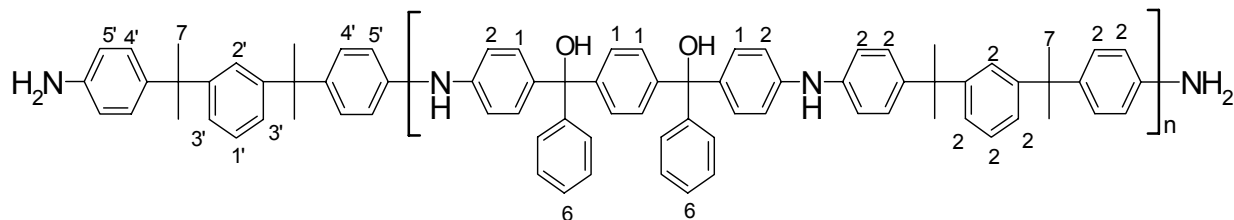
Yield: 1180 mg, 94 %; FT-IR (KBr pellet): γOH at 3551 cm^{-1}; γNH at 3394 cm^{-1}; γC-H aromatic at 3024 cm^{-1}; γC-H aliphatic at 2962 cm^{-1} and C-N at 1311 cm^{-1}; ^{1}H-NMR (300 MHz, DMSO-d_6,): δ = 7.58 (s, NH); 7.19 (d, H-1); 7.02 (d, H-2); 6.96-6.90 (m, H-6); 2.71 (s, OH); 1.55 (s, CH-3); 7.19 (d, H-1`, H-2`); 7.02 (d, H-3`); 6.82 (d, H-4`); 6.46 (d, H-5`); 5.72 (s, NH$_2$); 1.51 (s, CH$_3$). The molecular weights of the polymer was calibrated by GPC: M$_n$ = 16 400; M$_w$ = 34 500; M$_w$ / M$_n$ = 2.1.

Elemental analysis:
(C$_{44}$H$_{38}$N$_2$O$_2$)$_n$

(626.79)$_n$ Calculated: C, 79.98 %; H, 4.56 %; N, 11.19 %

                                    Found: C, 76.79 %; H, 4.22 %; N, 10.88 %

PlAlco-11b
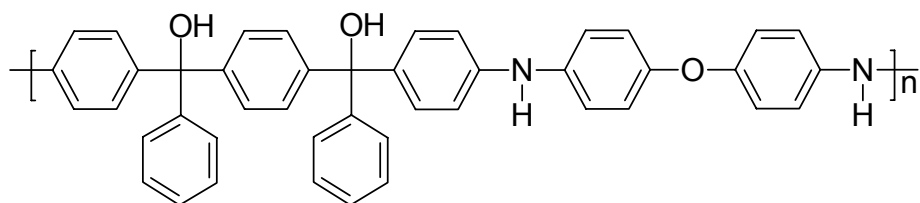
Yield: 1150 mg, 92 %; FT-IR (KBr pellet): γOH at 3541 cm^{-1}; γNH at 3396cm^{-1}; γC-H aromatic at 3026cm^{-1} and C-N at 1310 cm^{-1}; ^{1}H-NMR and GPC were not recorded due to the poor solubility of polymer **PlAlco-11b**.

5.3 Attempts to synthesize poly(quinone diimine)s

5.3.1 Synthesis of 1,4-bis{(4-benzylidene-cyclohexa-2,5-dienylidene)anilino}benzene (12):
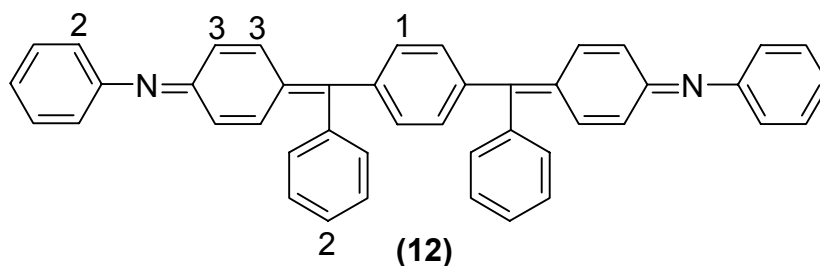
1,4-bis{(phenyl-(4-anilinophenyl)methanol)}benzene (**11**) (1.0 mmol, 624.8 mg) was dissolved in few drops of trifluoromethanesulfonic acid (TFA) and cooled to room temperature. The reaction mixture was stirred for 1 h at room temperature, then water was added dropwisely while cooling in ice bath to avoid the rise of the temperature. The resulting compound was extracted by chloroform as a deep purple color solution. The latter organic solution was washed with water, evaporated and dried in vacuo. The solid product was obtained as a deep purple powder of compound **12**. Yield: 542 mg, 92 %. ^{1}H-NMR (250 MHz, DMSO-d_6, 293K): δ = 7.47-7.44 (4H, H-1); 7.25-7.12 (20H, H-2); 7.05-6.94 (8H, H-3). FD^{+}-MS (m / z): (molecular peak is not recorded), FT-IR (KBr pellet): absence of γOH at 3550 cm^{-1} and γNH at 3390 cm^{-1}; presence of C-H aromatic at 3049 cm^{-1}; 1616 cm^{-1} (N=Q=C); 1590 cm^{-1} benzenoid (B) and C-N at 1260 cm^{-1}; UV recorded in CHCl$_3$ λ$_{max}$ at 350 and 500 nm.

5.3.2 Attempts to synthesize poly(quinone diimine)s:
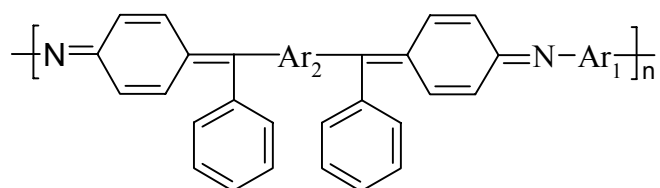
Poly(imino alcohol) **PIAlco-13** (1.0 mmol, 626.8 mg) was dissolved in few drops of trifluoromethanesulfonic acid (TFA, 99 %), or HCl (37 %) or CH_3COOH (99.5-100 %) or CH_3COOH (20 %) and cooled to room temperature. The reaction mixture was stirred for 1 h at room temperature, then water was added dropwisely while cooling in ice bath to avoid the rise of the temperature. The resulting compound was extracted by chloroform. The latter organic solution was washed with water, evaporated, dried in vacuo and GPC analysis was recorded.

GPC results are summarized in the following Table 3.3-1:

Run	Acid	M_n	M_w
1	CF_3SO_3H (99 %)	1 000	2 000
2	HCl (37 %)	1500	5300
3	CH_3CO_2H (99.5-100%)	400	670
4	CH_3CO_2H (20 %)	3500	12000

5.4 Synthesis of poly(imino acridine)s PIAcs:
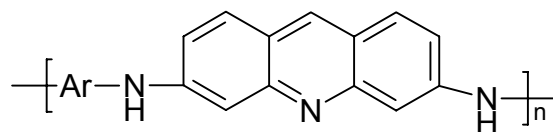
General procedure:

To a 50 mL an oven-dried resealable Schlenk flask equipped with magnetic stirrer, an argon outlet, inlet and water cooled condenser, dibromo compound (4.0 mmol), 3,6-diaminoacridine **(14)** (837.0 mg, 4.0 mmol), sodium *tert*-butoxide (1.076 g, 11.2 mmol), tris(dibenzylideneacetone)dipalladium(0) (36.6 mg, 0.04 mmol, BINAP (74.8 mg, 0.12 mmol), dimethylacetamide (6.5 mL) were added. The reaction mixture was evacuated and flushed with high purity argon. This procedure was repeated several times. The flask was immersed with contineous stirring in a 100 °C oil bath for 6 h, and in a 165 °C oil bath for 10 h. The resulting polymer solution was allowed to slowly cold to room temperature, filtered and subsequently poured into methanol, filtered, washed with methanol several times, then dried at 100 °C under vaccum.

PIAc-1:
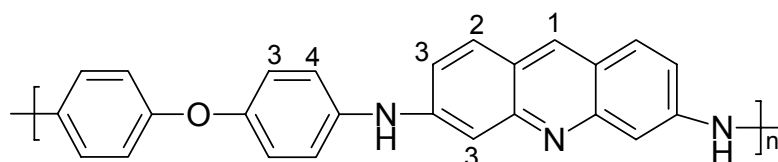
Yield: 1.24 g, 82 %; FT-IR spectrum (cm^{-1}, KBr): 3384 (γNH); 1307 (γC- N); ^{1}H-NMR (250 MHz, DMSO-d_6, 293K): δ = 8.78 (s, NH); 8.48 (s, H-1); 7.81 (s, H-2); 7.19 (d, H-3); 6.68 (s, H-4). The molecular weights of the polymer was calibrated by GPC: M_n = 4 500; M_w = 7 000; M_w / M_n = 1.5; DP = 12.

Elemental analysis:

$(C_{25}H_{17}N_3O)_n$
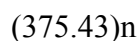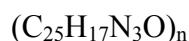
(375.43)n   Calculated: C, 79.98 %; H,4.56 %; N, 11.19 %

                                  Found: C, 78.67 %; H, 4.54 %; N, 10.68 %

PIAc-2:
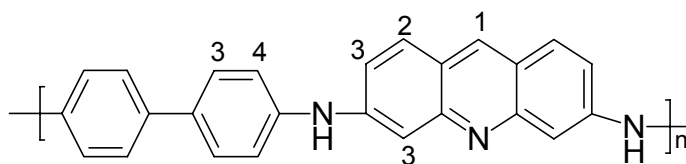
Yield: 1.58 g, 80 %; FT-IR spectrum (cm^{-1}, KBr): 3391 (γNH); 1312 (γC- N); ^{1}H-NMR (250 MHz, DMSO-d_6, 293K): δ = 9.09 (s, NH); 8.52 (s, H-1); 7.82 (s, H-2); 7.39 (d, H-3); 6.85 (s, H-4). The molecular weights of the polymer was calibrated by GPC: M_n = 12 600; M_w = 75900; M_w / M_n = 6.0; DP = 35.

Elemental analysis:

$(C_{25}H_{17}N_3)_n$ Calculated: C, 83.54 %; H, 4.77 %; N, 11.69 %

   $(359.43)_n$ Found: C, 80.88 %; H, 5.09 %; N, 10.45 %

PIAc-3:
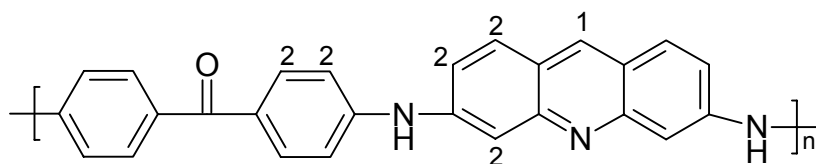
 Yield: 1.36 g, 87 %; FT-IR spectrum (cm^{-1}, KBr): 3330 (γNH) 1620 (γC=O) 1311(γC- N); ^{1}H-NMR (250 MHz, DMSO-d_6, 293K): δ = 9.34 (s, NH); 8.58 (s, H-1); 7.49 (d, H-2). The molecular weights of the polymer was calibrated by GPC: M_n = 9 500, M_w = 15 000, M_w / M_n = 1.6, DP = 24.

Elemental analysis:

     $(C_{26}H_{17}N_3O)_n$

      $(387.44)n$ Calculated: C, 80.60 %; H, 4.42 %; N, 10.85 %

                                 Found: C, 78.42 %; H, 4.15 %; N, 10.35 %

5.5 Synthesis of Synthesis of poly(imino azobenzene)s (PIAzos).
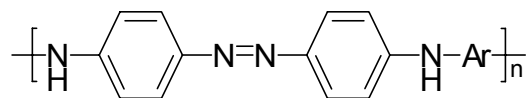
5.5.1 Synthesis of 1,4-bis{(4-phenylazo-4`-phenylamino)benzoyl)}benzene (16) as a model compound.
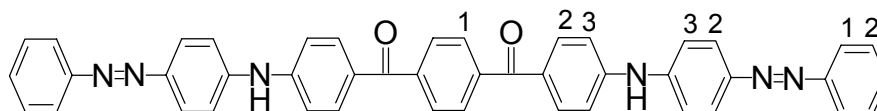
An oven-dried resealable Schlenk flask was evacuated and backfilled with argon. The flask was charged with $Pd_2(dba)_3$ (18.3 mg, 0.02 mmol, 2.0 mol %), BINAP (37.4 mg, 0.06 mmol, 6.0 mol %), and NaOt-Bu (538.0 mg, 5.6 mmol). The flask was evacuated and backfilled with argon and then capped with a rubber septum. DMAc (3 mL), 1,4-bis(4-bromobenzoyl)benzene (7) (888.0 mg, 2.0 mmol), 4-aminoazobenzene (15) (789.0 mg, 4.0 mmol), and additional DMAc (2 mL) were added through the septum. The flask was fitted with a reflux condenser, and the mixture was heated to 165 °C with stirring for 24 h. The resulting solution was allowed to slowly cold to room temperature, filtered and subsequently poured into cold water, filtered through celite and dried. The crude material was purified by recrystallization from chloroform/ methanol to afford (16) as red crystals. Yield: 1120 mg, 83 %. Mp: 192-194 °C. ^{1}H-NMR (250 MHz, DMSO-d_6, 293K): δ = 9.43 (s, NH); 7.79 (s, 8H, H-1); 7.49 (s, 14H, H-2); 7.19 (s, 8H, H-3). FD$^+$-MS (m / z): 676.0 (molecular peak); FT-IR (KBr pellet): γNH at 3351 cm^{-1}; γC=O at 1646 cm^{-1}, γC-H aromatic at 3049 cm^{-1} and C-N at 1338 cm^{-1}; UV recorded in DMF λ$_{max}$ at 378 nm; Anal.Calcd for $C_{44}H_{32}N_6O_2$ (676.78): C, 78.09; H, 4.77; N, 12.42. Found: C, 77.25; H, 4.49; N, 12.16.

5.5.2 Synthesis of poly(imino azobenzene)s (PIAzos).

General procedure:

To a 50 mL an oven-dried resealable Schlenk flask equipped with magnetic stirrer, an argon outlet, inlet and water cooled condenser, dibromo compound (4.0 mmol), 4,4`-diaminoazobenzene (849.0 mg, 4.0 mmol), sodium $tert$-butoxide (1.076g, 11.2 mmol), tris(dibenzylideneacetone)dipalladium(0) (36.6 mg, 0.04 mmol, BINAP (74.8 mg, 0.12 mmol), dimethylacetamide (6.5 mL) were added. The reaction mixture was evacuated and

flushed with high purity argon. This procedure was repeated several times. The flask was immersed with contineous stirring in a 100 °C oil bath for 4 h, and in a 165 °C oil bath for 20 h. The resulting polymer solution was allowed to slowly cold to room temperature, filtered and subsequently poured into cold water, filtered, washed with methanol, then dried at 100 °C under vaccum.

PIAzo-1:
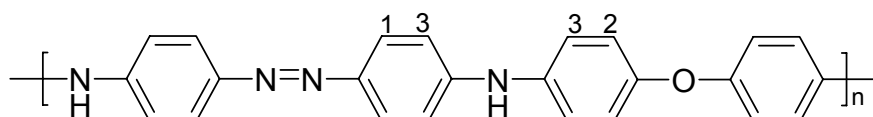
Yield: 1.24g, 82 %; FT-IR spectrum (cm^{-1}, KBr): 3389 (γ NH); 1312 (γC- N); ^{1}H-NMR (250 MHz, DMSO-d_6, 293K): δ = 8.72 (s, NH); 7.72 (d, H-1); 7.58-7.46 (m, H-2); 7.21-7.02 (m, H-3). The molecular weights of the polymer was calibrated by GPC: M_n = 10 900; M_w = 44 800; M_w / M_n = 4.1; DP = 29.

Elemental analysis:

$$(C_{24}H_{18}N_4O)_n \quad \text{calculated:} \quad \text{C, 76.17 %; H, 4.79 %; N, 14.80 %}$$
$$(378.43)_n \quad \quad \text{found:} \quad \text{C, 73.88 %; H, 4.67 %; N, 13.78 %}$$

PIAzo-2:
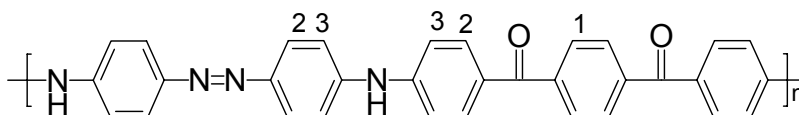
Yield: 1.58 g, 80 %; FT-IR spectrum (cm^{-1}, KBr): 3352 (γ NH); 1646 (γ C=O); 1316 (γC- N); ^{1}H-NMR (250 MHz, DMSO-d_6, 293K): δ = 9.42 (s, NH); 7.80 (d, H-1); 7.62 (t, H-2); 7.37-7.27 (m, H-2). The molecular weights of the polymer was calibrated by GPC: M_n = 7 400, M_w = 30 000, M_w / M_n = 4.0, DP = 15.

Elemental analysis:

$$(C_{32}H_{22}N_4O_2)_n \quad \text{calculated:} \quad \text{C, 77.72 %; H, 4.48 %; N, 11.33 %}$$
$$(494.55)_n \quad \quad \text{found:} \quad \text{C, 73.01 %; H, 4.51 %; N, 10.91 %}$$

PIAzo-3:
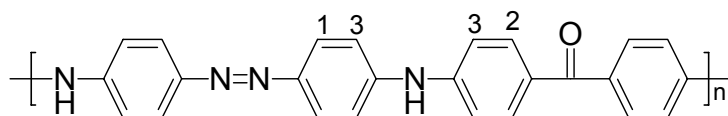
Yield: 1.36 g, 87 %; FT-IR spectrum (cm^{-1}, KBr): 3383 (γ NH); 1664 (γC=O); 1308 (γC- N); ^{1}H-NMR (250 MHz, DMSO-d_6, 293K): δ = 9.28 (s, NH); 7.71 (s, H-1); 7.25 (s, H-2); 6.64 (s, H-3). The molecular weights of the polymer was calibrated by GPC: M_n = 12 900; M_w = 81 200; M_w / M_n = 6.3; DP = 33.

Elemental analysis:

$(C_{25}H_{18}N_4O)_n$ calculated: C, 76.91 %; H, 4.65 %; N, 14.35 %

$(390.44)_n$ found: C, 78.90 %; H, 5.08 %; N, 13.81 %

5.6 Synthesis of novel poly(imino fluorenone)s (PIFOs):

5.6.1 3,6-Dibromophenanthrenequinone (18):
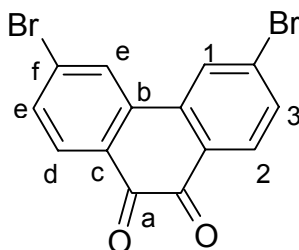
Synthesized by the following modified procedures: [193]

5.6.1.1 Method (a)

A mixture of phenanthrenequinone (**17**) (10.0 g, 48.0 mmol), Br$_2$ (5.1 mL, 100.0 mmol), nitrobenzene (60 mL) was heated to 100 °C. The evolution of HBr gas became intensive after 1 h. The reaction mixture was kept at 100 °C for over night. The evolution of gas became imperceptible after that time and the color of Br$_2$ disappeared from the reaction mixture. On cooling to laboratory temperature followed by cooling in ice clusters of yellow crystals were separated by filtration, washed with ethanol, dried, and recrystallized from ethanol furnished 3,6-dibromophenanthrenequinone (**18**) as yellow needles. Yield: 31.0 g, 83 %. Mp: 287-288 °C, Lit.[340] Mp: 286-287 °C. ^{1}H-NMR (250 MHz, DMSO-d_6, 293K): δ = 8.58 (s, 2H, H$_1$); 7.89 (d, 2H, H$_2$); 7.72 (d, 2H, H$_3$). ^{13}C-NMR (62.5 MHz, DMSO-d_6, 293K): δ = 177.6 (C$_a$), 135.8 (C$_b$), 132.7 (C$_c$), 130.7 (C$_d$), 129.9 (C$_e$), 127.6 (C$_f$). FD^{+}-MS (m / z): 366.0 (molecular peak).

Elemental analysis:

$C_{14}H_6Br_2O_2$

((366.01)   Calculated: C, 45.94 %; H, 1.65 %; Br, 43.66 %

Found: C, 45.78 %; H, 1.68 %; Br, 43.46 %

5.6.1.2 Method (b)

A solution of phenanthrenequinone (**17**) (10.0 g, 48.0 mmol), Br_2 (5.1 mL, 100.0 mmol), nitrobenzene (60 mL) was exposed to sunlight. After 2 h intesive formation of HBr without further heating is observed. After the first intensive reaction is over, the reaction mixture was heated to 100 °C for 5 h. The evolution of gas became imperceptible after that time and the color of Br_2 disappeared from the reaction mixture. On cooling to laboratory temperature followed by cooling in ice clusters of yellow crystals were separated by filtration, washed with ethanol, dried and recrystallized from ethanol furnished 3,6-dibromophenanthrenequinone (**18**) as yellow needles. Yield: 31.0 g, 83 %. Mp: 287-288 °C.

5.6.2 3,6-Dibromo-9-fluorenone (19).
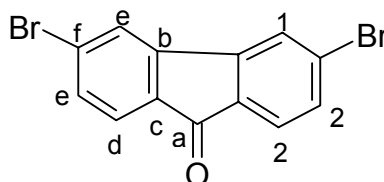
Synthesized by the following modified procedure:[341]

9.2 g (25.2 mmol) of 3,6-dibromophenanthrenequinone (**18**) and 300 mL of a saturated solution of KOH in H_2O at 85 °C were heated under reflux for 30 min. Within 2 h 21.0 g $KMnO_4$ were added and one more hour heated to reflux. After cooling to room temperarture carefully acidified with Conc. H_2SO_4 and the MnO_2 is reduced with sodium pyrosulfite. The mixture is sucked and the residue mixed three times with diluted KOH solution and again sucked. The pale yellow powder was washed with water, ethanol and afterwards, sublimed at 10 torr or recrystallized two times from dimethylformamide furnished 3,6-dibromo-9-fluorenone (**19**) as pale yellow needles. Yield: 6.62 g, 77 %. Mp: 320-321 °C, Lit.[341] Mp: 312 °C. ^{1}H-NMR (300 MHz, DMSO-d_6, 293K): δ = 8.08 (s, 2H, H-1); 7.56 (d, 4H, H-2). ^{13}C-NMR (62.5 MHz, DMSO-d_6, 293K): δ = 189.6 (C_a), 143.9 (C_b), 131.9 (C_c), 128.4 (C_d), 124.6 (C_e), 124.2 (C_f). FD$^+$- MS (m / z): 340.0 (molecular peak).

Elemental analysis:

$C_{13}H_6Br_2O$

(337.99)   Calculated: C, 46.20 %; H, 1.79 %; Br, 47.28 %

Found: C, 45.64 %; H, 1.72 %; Br, 46.82 %

5.6.3 Synthesis of 3,6-dianilino-9-fluorenone (20) as a model compound.
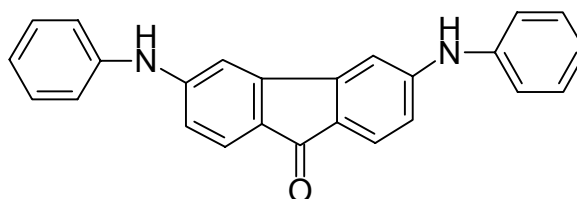
An oven-dried resealable Schlenk flask was evacuated and backfilled with argon. The flask was charged with Pd$_2$ (dba)$_3$ (18.3 mg, 0.02 mmol, 2.0 mol %), BINAP (37.4 mg, 0.06 mmol, 6.0 mol %), and NaOt-Bu (538.0 mg, 5.6 mmol). The flask was evacuated and backfilled with argon and then capped with a rubber septum. DMAc (5 mL), 3,6-dibromo-9-fluorenone (**19**) (675.99 mg, 2.0 mmol), aniline (373.0 mg, 4.0 mmol), and additional DMAc (2 mL) were added through the septum. The flask was fitted with a reflux condenser, and the mixture was heated to 100 °C with stirring for 20 h. The resulting solution was allowed to slowly cold to room temperature, filtered and subsequently poured into methanol, filtered and dried. The crude material was purified by recrystallization from chloroform/ methanol to afford (**20**) as red crystals. Yield: 602 mg, 83 %. Mp: > 400 °C. ^{1}H-NMR (300 MHz, DMSO-d_6, 293K): δ = 7.29 a broad peak represented the imino protons (NH) and all the aromatic protons (16H-Ar); FD$^+$- MS (m / z): 362.3 (molecular peak); FT-IR (KBr pellet): γNH at 3417 cm^{-1}; γC=O at 1708 cm^{-1}, γC-H aromatic at 3052 cm^{-1} and C-N at 1303 cm^{-1}; UV recorded in DMAc λ$_{max}$ at 450 and 604 nm; Anal. Calcd for $C_{25}H_{18}N_2O$ (362.44): C, 82.85; H, 5.01; N, 7.73. Found: C, 81.96; H, 4.84; N, 7.58.

5.6.4 Synthesis of PIFO polymers.
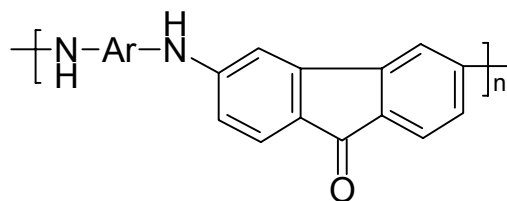
To a 50 mL an oven-dried resealable Schlenk flask equipped with magnetic stirrer, an argon outlet, inlet and water cooled condenser, 3,6-dibromo-9-fluorenone (**19**) (675.996 mg, 4.0 mmol), diamine (4.0 mmol), sodium *tert*-butoxide (1.076 g, 11.2 mmol), tris(dibenzylideneacetone)dipalladium(0) (36.6 mg, 0.04 mmol, BINAP (74.8 mg, 0.12 mmol), dimethylacetamide (3-5 mL) were added. The reaction mixture was evacuated and flushed with high purity argon. This procedure was repeated several times. The flask was immersed with contineous stirring in a 100 °C oil bath for 8 h, and in a 165 °C oil bath for 12 h. The resulting polymer solution was allowed to slowly cold to room temperature, filtered and precipitated by methanol, filtered, washed with water and methanol, then dried at 100 °C under vaccum.

PIFO-1:
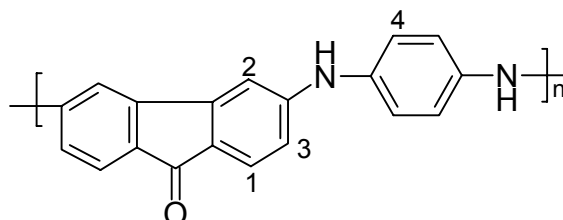
Yield: 530 mg, 93 %; FT-IR (KBr pellet): γNH at 3407 cm^{-1}; γC=O at 1702 cm^{-1}, and C-N at 1297 cm^{-1}; UV recorded in DMAc λ_{max} at 450 nm; ^{1}H-NMR (700 MHz, DMSO-d_6, 373K): δ = 7.59 (s, NH); 7.37 (s, H-1); 6.92 (s, H-2); 6.64 (s, H-3); 6.39 (s, H-4). The molecular weights of the polymer was calibrated by GPC: M_n = 4 500; M_w = 10 800; M_w / M_n = 2.4; DP = 15.

Elemental analysis:

$(C_{19}H_{12}N_2O)_n$ calculated: C, 80.27 %; H, 4.25 %; N, 9.85 %

$(284.32)_n$ found: C, 78.40 %; H, 4.34 %; N; 8.14 %

PIFO-2:
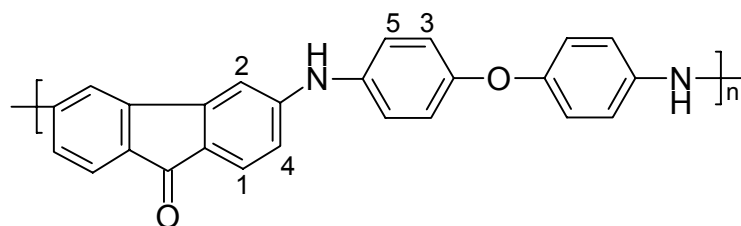
Yield: 678 mg, 90 %; FT-IR (KBr pellet): γNH at 3443 cm^{-1}; γC=O at 1708 cm^{-1}, γC-H aromatic at 3049 cm^{-1} and C-N at 1300 cm^{-1}; UV recorded in DMAc λ_{max} at 450 nm; ^{1}H-NMR (700 MHz, DMSO-d_6, 393K): δ = 7.35 (s, NH); 7.18 (s, H-1); 6.89 (s, H-2); 6.76 (s, H-3); 6.65 (s, H-4); 6.56 (s, H-5). The molecular weights of the polymer were calibrated by GPC: M_n = 6 400; M_w = 32 000; M_w / M_n = 5.0; DP = 17.

Elemental analysis:

$(C_{25}H_{16}N_2O_2)_n$ calculated: C, 79.77 %; H, 4.28 %; N, 7.44 %

(376.41)$_n$ found: C, 79.21 %; H, 4.40 %; N, 6.32 %

PIFO-3:
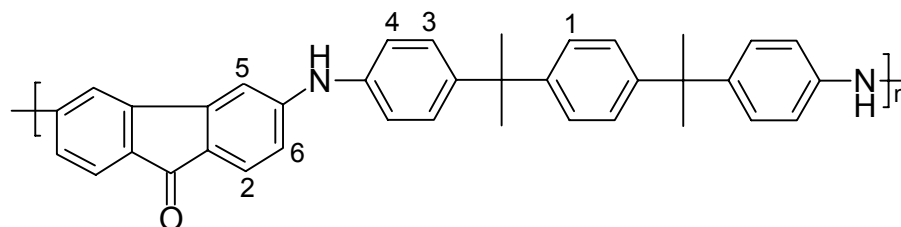
Yield: 896 mg, 86 %; FT-IR (KBr pellet): γNH at 3436 cm^{-1}; γC=O at 1709 cm^{-1}, γC-H aromatic at 3049 cm^{-1} and C-N at 1297 cm^{-1}; UV recorded in DMAc λ_{max} at 450 and 600 nm; ^{1}H-NMR (500 MHz, DMSO-d_6, 393K): δ = 7.09 (s, NH, H-1-H-4); 6.86 (s, H-5); 6.49 (s, H-6); 1.53 (s, CH$_3$). The molecular weights of the polymer was calibrated by GPC: M_n = 13 200; M_w = 83 800; M_w / M_n = 6.4; DP = 25.

Elemental analysis:

$(C_{37}H_{32}N_2O)_n$ calculated: C, 85.35 %; H, 6.19 %; N, 5.39 %

(520.67)$_n$ found: C, 83.19 %; H, 5.46 %; N, 4.31 %

PIFO-4:
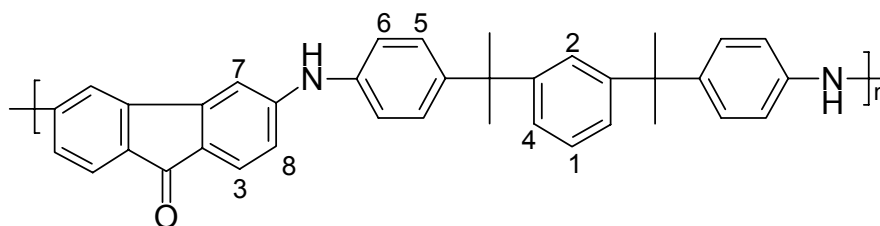
Yield: 947 mg, 91 %; FT-IR (KBr pellet): γNH at 3431 cm^{-1}; γC=O at 1710 cm^{-1}, γC-H aromatic at 3049 cm^{-1} and C-N at 1298 cm^{-1}; UV recorded in DMAc λ_{max} at 296.7 and 374.1 nm.; ^{1}H-NMR (500 MHz, DMSO-d_6, 373K): δ = 7.10 (broad s, NH, H-1-H-6); 6.86 (s, H-7); 6.49 (s, H-8); 1.54 (s, CH$_3$). The molecular weights of the polymer were calibrated by GPC: M$_n$ = 14 400; M$_w$ = 82 000; M$_w$ / M$_n$ = 5.7; DP = 27.

Elemental analysis:

(C$_{37}$H$_{32}$N$_2$O)$_n$	calculated:	C, 85.35 %; H, 6.19 %; N, 5.39 %
(520.67)$_n$	found:	C, 83.36 %; H, 5.25 %; N, 4.28 %

PIFO-5:
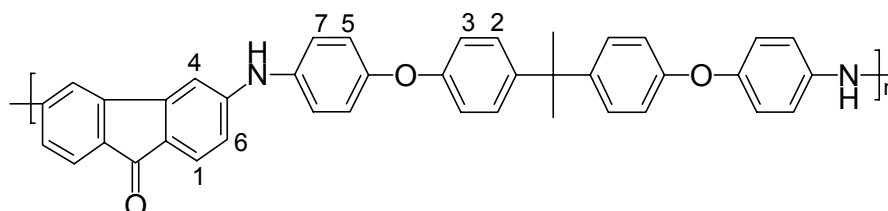
Yield: 986 g, 84 %; FT-IR (KBr pellet): γNH at 3430 cm^{-1}; γC=O at 1705 cm^{-1}, γC-H aromatic at 3049 cm^{-1} and C-N at 1301 cm^{-1}; UV recorded in DMAc λ_{max} at 450 and 600 nm; ^{1}H-NMR (700 MHz, DMSO-d_6, 413K): δ = 7.16 (s, NH, H-1,3); 6.92 (s, H-4); 6.82 (s, H-5); 6.73 (s, H-6); 6.62 (s, H-7); 1.66 (s, CH$_3$). The molecular weights of the polymer were calibrated by GPC: M$_n$ = 11 200; M$_w$ = 69 200; M$_w$ / M$_n$ = 6.2; DP = 19.

Elemental analysis:

(C$_{40}$H$_{30}$N$_2$O$_3$)$_n$	calculated:	C, 81.89 %; H, 5.15 %; N, 4.77 %
(586.69)$_n$	found:	C, 80.56 %; H, 6.21 %; N, 3.81 %

5.7 Synthesis of novel poly(imino carbazole)s (PICs)
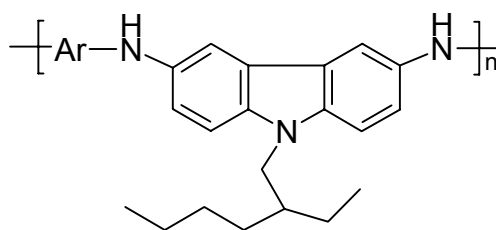
5.7.1 Method (a)

To a 50 mL an oven-dried resealable Schlenk flask equipped with magnetic stirrer, an argon outlet, inlet and water cooled condenser, dibromo compound (2.0 mmol), 3,6-diamino-9-(2-ethylhexyl)carbazole (618.92 mg, 2.0 mmol), sodium *tert*-butoxide (538.0 mg, 5.6 mmol), tris(dibenzylideneacetone)dipalladium(0) (18.3 mg, 0.02 mmol, 2.0 mol %), BINAP (37.4 mg, 0.06 mmol, 6.0 mol %), dimethylacetamide (3-5 mL) were added. The reaction mixture was evacuated and flushed with high purity argon. This procedure was repeated several times. The flask was immersed with contineous stirring in an 100 °C oil bath for 20 h. The resulting polymer solution was allowed to slowly cold to room temperature, filtered and precipitated by methanol, filtered, washed with water and methanol, then dried at 100 °C under vaccum.

PIC-1
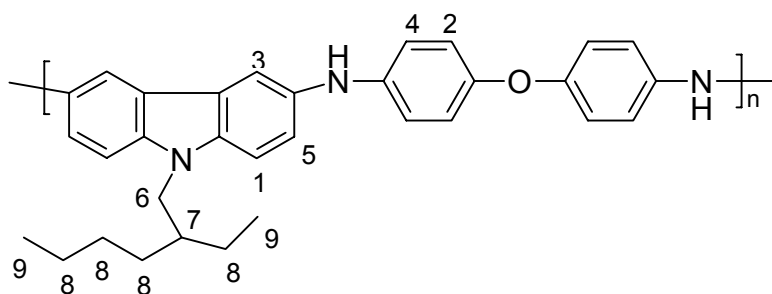
Yield: 830 mg, 87 %; FT-IR (KBr pellet): γNH at 3385 cm^{-1}; γC-H aromatic at 3029 cm^{-1} and C-N at 1305 cm^{-1}; UV recorded in DMAc λ_{max} at 280; 310 and 400 nm; ^{1}H-NMR (700 MHz, DMSO-d_6, 373K): δ = δ = 7.71 (s, NH); 7.37 (s, H-1); 7.20 (s, H-2); 6.91 (d, H-3,4,5); 4.14 (s, CH$_2$, H-6); 2.01 (s, CH, H-7); 1.25 (d, CH$_2$, H-8); 0.82 (d, CH$_3$; H-9). The molecular weights of the polymer was calibrated by GPC: M_n = 10 000; M_w =72 000; M_w / M_n = 7.2; DP = 21. Elemental analysis: (cf. Part 7, Table 3.7-3, P. 171).

(C$_{32}$H$_{33}$N$_3$O)$_n$ calculated: C, 80.81 %; H, 6.99 %; N, 8.83 %

(475.63)$_n$ found: C, 76.81 %; H, 6.46 %; N, 7.96 %

5.7.2 Method (b)

To a 50 mL an oven-dried resealable Schlenk flask equipped with magnetic stirrer, an argon outlet, inlet and water cooled condenser, dibromo compound (2.0 mmol), 3,6-diamino-9-(2-ethylhexyl)carbazole (618.92 mg, 2.0 mmol), sodium *tert*-butoxide (538.0 mg, 5.6 mmol), tris(dibenzylideneacetone)dipalladium(0) (18.3 mg, 0.02 mmol, 2.0 mol %), BINAP(37.4 mg, 0.06 mmol, 6.0 mol %), dimethylacetamide (3-5 mL) were added. The reaction mixture was evacuated and flushed with high purity argon. This procedure was repeated several times. The flask was immersed with contineous stirring in an 80 °C oil bath for 20 h. The resulting polymer solution was allowed to slowly cold to room temperature, filtered and precipitated by methanol, filtered, washed with water and methanol, then dried at 100 °C under vaccum.

PIC-7

Yield: 784 mg, 85 %; FT-IR (KBr pellet): γNH at 3389 cm^{-1}; γC-H aromatic at 3023 cm^{-1} and C-N at 1294 cm^{-1}; UV recorded in DMAc λ_{max} at 350 nm; ^{1}H-NMR (700 MHz, DMSO-d_6, 373K): δ = 7.79 (s, NH); 7.53 (s, H-1); 7.26 (s, H-3+4); 7.01 (s, H-5); 4.15 (s, CH$_2$, H-6); 2.02 (s, CH H-7); 1.26 (d, CH$_2$, H-8); 0.82 (d, CH$_3$; H-9). The molecular weights of the polymer were calibrated by GPC: M_n = 16 600; M_w = 135 000; M_w / M_n = 8.1; DP = 36.

Elemental analysis: (cf. Part 7, Table 3.7-3, P. 171).

    (C$_{32}$H$_{33}$N$_3$)$_n$ calculated: C, 83.62 %; H, 7.24 %; N, 9.14 %

     (459.63)$_n$ found: C, 81.22 %; H, 7.03 %; N, 8.55 %

5.7.3 Method (c)

To a 50 mL an oven-dried resealable Schlenk flask equipped with magnetic stirrer, an argon outlet, inlet and water cooled condenser, dibromo compound (2.0 mmol), 3,6-diamino-9-(2-ethylhexyl)carbazole (618.92 mg, 2.0 mmol), sodium *tert*-butoxide (538.0 mg, 5.6 mmol), tris(dibenzylideneacetone)dipalladium(0) (18.3 mg, 0.02 mmol, 2.0 mol %), BINAP (37.4

mg, 0.06 mmol, 6.0 mol %), lithium chloride (0.48-0.7 g), dimethylacetamide (3-5 mL) were added. The reaction mixture was evacuated and flushed with high purity argon. This procedure was repeated several times. The flask was immersed with contineous stirring in an 80 °C oil bath for 20 h. The resulting polymer solution was allowed to slowly cold to room temperature, filtered and precipitated by methanol, filtered, washed with water and methanol, then dried at 100 °C under vaccum.

PIC-5
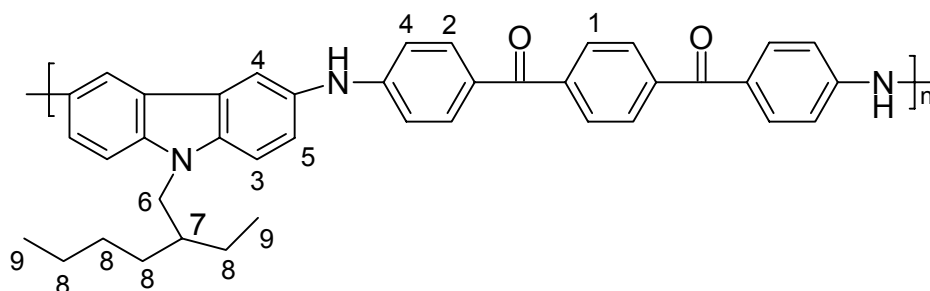
Yield: 1042 mg, 88 %; FT-IR (KBr pellet): γNH at 3415 cm^{-1}; γC=O at 1630 cm^{-1}, γC-H aromatic at 3049 cm^{-1} and C-N at 1310 cm^{-1}; UV recorded in DMAc λ_{max} at 380 nm.; ^{1}H-NMR (700 MHz, DMSO-d_6, 373K): δ = 7.94 (s, NH); 7.80 (s, H-1); 7.37 (s, H-2); 7.22 (s, H-3); 6.99 (s, H-4,5); 4.14 (s, CH$_2$, H-6); 1.94 (s, CH, H-7); 1.21 (d, CH$_2$, H-8); 0.77 (d, CH$_3$, H-9). The molecular weights of the polymer was calibrated by GPC: M_n = 9 800; M_w = 68 000; M_w / M_n = 6.9; DP = 16.

Elemental analysis: (cf. Part 7, Table 3.7-3, P. 171).

(C$_{40}$H$_{37}$N$_3$O$_2$)$_n$ calculated: C, 81.19 %; H, 6.30 %; N, 7.10 %

(591.75)$_n$ found: C, 76.14 %; H, 6.41 %; N, 7.19 %

PIC-8
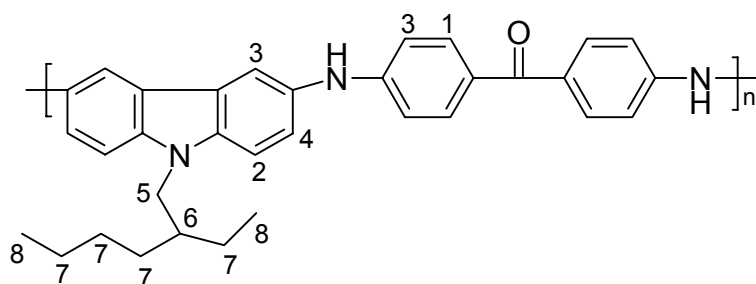
Yield: 878 mg, 90 %; FT-IR (KBr pellet): γNH at 3405 cm^{-1}; γC=O at 1630 cm^{-1}, γC-H aromatic at 3029 cm^{-1} and C-N at 1312 cm^{-1}; UV recorded in DMAc λ_{max} at 370 nm.; ^{1}H-NMR (500 MHz, DMSO-d_6, 373K): δ = 8.24 (s, NH); 7.93 (s, H-1); 7.59 (s, H-2); 7.32 (s, H-3); 6.96 (s, H-4); 4.19 (s, CH$_2$, H-5); 2.03 (s, CH, H-6); 1.23 (d, CH$_2$, H-7); 0.82 (d, CH$_3$, H-8). The molecular weights of the polymer was calibrated by GPC: M_n = 8 600; M_w = 23 000; M_w / M_n = 2.7; DP = 17.
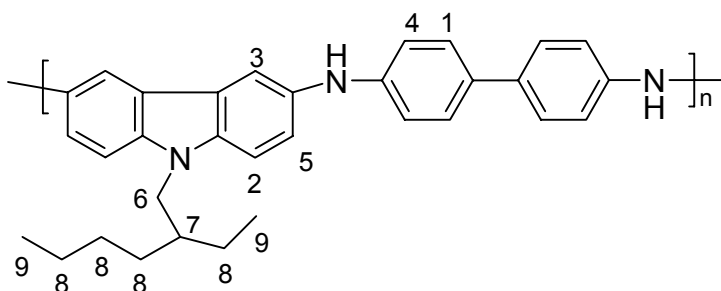
Elemental analysis: (cf. Part 7, Table 3.7-3, P. 171).

> (C$_{33}$H$_{33}$N$_3$O)$_n$ calculated: C, 81.28 %; H, 6.82 %; N, 8.62 %
> (487.64)$_n$ found: C, 77.84 %; H, 6.52 %; N, 8.45 %

[1] A. Le Guen, M. Klapper, K. Müllen, Macromolecules, 31, 6559 **(1998)**.

[2] A. Parthiban, A. Le Guen, Y. Yansheng, U. Hoffmann, M. Klapper, K. Müllen, Macromolecules, 30, 2238 **(1997)**.

[3] U. Hoffmann, F. Helmer-Metzmann, M. Klapper, K. Muellen, Macromolecules, 27, 3575 **(1994)**.

[4] R. J. Cotter, "Engineering Plastics" in: A Handbook of Polyarylethers, Gordon and Breach Publishers, Amsterdam, p. 132 **(1995).**

[5] A. Le Guen, M. Klapper, K. Müllen, Macromolecules, 31, 6559 **(1998)**.

[6] A. Parthiban, A. Le Guen, Y. Yansheng, U. Hoffmann, M. Klapper, K. Müllen, Macromolecules, 30, 2238 **(1997)**.

[7] U. Hoffmann, F. Helmer-Metzmann, M. Klapper, K. Müllen, Macromolecules, 27, 3575 **(1994)**.

[8] P. A. Staniland, In Comprehensive Polymer Science, Allen, G., Berington, J. C., Eds., Pergamon Press: New York, Vol. 5, p 483 **(1989)**.

[9] J. W. Labadie, J. L. Hedrick, M. Udea, In Step Growth Polymers for High-Performance Materials, New Synthetic Method, J. L. Hedrick, J. W. Labadie, Eds.; ACS Symposium Series 624; American Chemical Society: Washington, DC, p 210 **(1996)**.

[10] V. E. Radlmann, W. Schmits, G. E. Nischk, Makromol. Chem., 130, 45 **(1969)**.

[11] H. R. Kricheldorf, In Handbook of Polymer Synthesis; H. R. Kricheldorf, Eds., Marcel Dekker: New York, Part A, p. 586 **(1992)**.

[12] W. H. Bonner, U. S. Patent 3 442 857 **(1969)**.

[13] I. Goodman, J. E. McIntyre, W. Russell, British Patent 971 227 **(1964)**.

[14] B. M. Marks, U. S. Patent 3 442 857 **(1969)**.

[15] V. Jansons, K. Dahl, Makromol. Chem., Macromol. Symp., 51, 87 **(1991)**.

[16] R. J. Cotter, Engineering Plastics: A Handbook of Polyaryl ethers; Gordon and Breach Publishers: Amsterdam, p 20 **(1995)**.

[17] T. Takekoshi, J. G. Wirth, D. R. Heath, J. E. Kochanowski, J. S. Manello, M. J. Webber, J. Polym. Sci., Polym.Chem. Ed., 18, 3069 **(1980)**.

[18] V. E. Radlmann, W. Schmits, G. E. Nischk, Makromol. Chem., 130, 45 **(1969)**.

[19] H. R. Kricheldorf, In Handbook of Polymer Synthesis; Kricheldorf, H. R., Eds.; Marcel Dekker: New York, Part A, p 586 **(1992)**.

[20] J. W. Labadie, J. L. Hedrick, M. Udea, "Poly(aryl ether) synthesis" in: Step Growth Polymers for High Performance Materials, New Synthetic Method, J. L. Hedrick., J. W. Labadie, Eds., American Chemical Society, Washington, D. C., p. 210-221 **(1996)**.

[21] P. A. Staniland, "Poly(ether ketone)s" in: Comprehensive Polymer Science, G. Allen, J. C. Berington, Eds., PergamonPress, New York, p. V/484-497 **(1989)**; (b) T. Takekoshi, Polym. J., 19, 191 **(1989)**; (c) V. E. Radlmann, W. Schmits, G. E. Nischk, Makromol. Chem., 130, 45 **(1969)**; (d) H. R. Kricheldorf,"Aromatic Polyethers" in: Handbook of Polymer Synthesis, H. R. Kricheldorf, Ed., Marcel Dekker, Inc., New York, p. Part A/574-588 **(1992)**.

[22] (a) F. J. Williams, P. E. Donahue, J. Org. Chem., 42, 3414 **(1977)**.

 (b) R. L. Markezich, O. S. Zamek, J. Org. Chem., 42, 3431 **(1977)**.

(c) R. L. Markezich, O. S. Zamek, P. E. Donahue, F. J. Williams, J. Org. Chem., 42, 3435 **(1977)**.

(d) D. M. White, T. Takekoshi, F. J. Williams, H. M. Relles, P. E. Donahue, H. J. Klopfer, G. R. Loucks, J. S. Manello, R. O. Matthews, R. W. Schluenz, J. Polym. Sci., Polym.Chem. Ed., 19, 1635-1658 **(1981)**.

 (e) T. Takekoshi, Polym. J., 19, 191 **(1989)**.

[23] T. Takekoshi, J. G. Wirth, D. R. Heath, J. E. Kochanowski, J. S. Manello, M. J. Webber, J. Polym. Sci., Polym. Chem. Ed., 18, 3069 **(1980)**.

[24] S. K. Park, S. Y. Kim, Macromolecules, 31, 3385 **(1998)**.

[25] K. R. Carter, S. Y. Kim, J. L. Labadie, Polym. Prepr. (Am. Chem. Soc., Div. Polym. Chem.), 34, 415 **(1993)**.

[26] J. L. Hedrick, Macromolecules, 24, 812 **(1991)**.

[27] J. G. Hilborn, J. W. Labadie, J. L. Hedrick, Macromolecules, 23, 2854 **(1990)**.

[28] A. Pandya, J. Yang, H. W. Gibbson, Macromolecules, 27, 1367 **(1994)**.

[29] M. Lucas, P. Brock, J. L. Hedrick, J. Polym. Sci., Part A: Polym. Chem., 31, 2179 **(1993)**.

[30] S. K. Park, S. Y. Kim, Macromol. Chem. Phys., 199, 2717 **(1998)**.

[31] J. A. Miller Aromatic Nucleophilic Substitution; American Elsevier: New York, **(1968)**.

[32] J. March Advanced Organic Chemistry, Third ed.; John Wiley and Sons: New York, **(1985)**.

[33] R. Viswanathan, B. C. Johnson, J. E. McGrath, Polymer, 25, 1827 **(1984)**.

[34] J. Meisenheimer, Liebigs Ann. Chem., 323, 205 **(1902)**.

[35] C. A. Fyfe, A. Koll, S. W. H. Damji, C. D. Malkiewich, P. A. Forte, Can. J. Chem., 55, 1468 **(1977)**.

[36] G. G. Messmer, G. J. Palenik, Chem. Commun., 470 **(1969)**.

[37] N. Kornblum, L. Cheng, R. C. Kerber, M. M. Kestner, B. N. Newton, H. W. Pinnick, R. G. Smith, P. A. Wade, J. Org. Chem., 41, 1560 **(1976)**.

[38] J. F. Bunnett, R. E. Zahler, Chem. Rev., 49, 273 **(1951)**.

[39] F. A. Carey, R. J. Sundberg Advanced Organic Chemistry, Third ed., Plenum Press: New York, **(1990)**.

[40] R. Alexander, E. C. F. Ko, A. J. Parker, T. J. Broxton, J. Am. Chem. Soc., 90, 5049 **(1968)**.

[41] R. L. Fuchs, L. L. Cole, J. Am. Chem. Soc., 95, 3194 **(1973)**.

[42] T. F. Magnera, G. Caldwell, J. Sunner, S. Iduta, P. Kebarle, J. Am. Chem. Soc., 106, 6140 **(1984)**.

[43] A. G. MacDiarmid, J. C. Chiang, M. Halpern, W. S. Huang, S. L. Mu, N. L. Somasiri, W. Wu, S. I. Yaniger, Mol. Cryst. Liq. Cryst., 121, 173 **(1985)**.

[44] P. N. Adams, D. C. Apperley, A. P. Monkman, Polymer, 34, 328 **(1993)**.

[45] A. M. Kenwright, W. J. Feast, P. N. Adams, A. J. Milton, A. P. Monkman, B. J. Say, Polymer, 33, 4292 **(1992)**.

[46] (a) A. G. MacDiarmid, J. C. Chiang, A. F. Richter, N. L. D. Somasiri, A. J. Epstein, In Conducting Polymers; Alcacer, L., Ed.; Reifel: Dordrecht, The Netherlands, pp 105-120 **(1987)**; (b) N. Gospodinova, L. Terlemezyan, Prog. Polym. Sci., 23, 1443 **(1998)**; (c) J. C. Chiang, A. G. MacDiarmid, Synth. Met., 13, 193 **(1986)**.

[47] W. S. Huang, B. D. Humphrey, A. G. MacDiarmid, J. Chem. Soc., Faraday Trans., 82, 2385 **(1986)**.

[48] C. H. Ong, S. H. Goh, H. S. O. Chan, Polym. Bull., 39, 627 **(1997)**.

[49] P. N. Adams, P. J. Laughlin, A. P. Monkman, Synth. Met., 76, 157 **(1996)**.

[50] G. Boara, M. Sparpaglione, Synth. Met., 72, 135 **(1995)**.

[51] M. Vilčnik, M. Žigon, M. Zupan, A. Šebenik, Acta Chim. Slov., 45, 173 **(1998)**.

[52] A. G. MacDiarmid, Synth. Met., 125, p. 11 **(2002)**.

[53] A. G. MacDiarmid, A. J. Epstein, Faraday Discuss. Chem. Soc., 88, 317 **(1989)**.

[54] J. C. Chiang, A. G. MacDiarmid. Synth. Met., 13, 193 **(1986)**.

[55] A. G. MacDiarmid, J.-C. Chiang, A. F. Richter, A. J. Epstein. Synth. Met., 18, 285 **(1987)**.

[56] A. G. MacDiarmid, J. C. Chiang, A. F. Richter, N. L. D. Somasiri, A. J. Epstein, in: L. Alcacér (Ed.), Conducting Polymers, Reidel, Dordrecht, p. 105 **(1987)**.

[57] A. G. MacDiarmid, S. L. Mu, M. L. D. Somasiri, W. Wu, Mol. Cryst. Liq. Cryst., 121, 187 **(1985)**.

[58] A. Kitani, M. Kaya, K. Sasaki, J. Electrochem. Soc., 133,1069 **(1986)**.

[59] G. Gustafsson, Y. Cao, G. M. Treacy, F. Klavetter, N. Colaneri, A. Heeger, J. Nature, 357, 477 **(1992)**.

[60] Y. Yang, E. Westerweele, C. Zhang, P. Smith, A. J. Heeger, J. Appl. Phys., 77, 694 **(1995)**.

[61] M. Abe, A. Ohtani, Y. Umemoto, S. Akizuki, M. Ezoe, H. Higuchi, K. Nakamoto, A. Okuno, Y. Noda, J. Chem. Soc., Chem. Commun., 1736 **(1989)**.

[62] T. Mizoguchi, R. N. Adams, J. Am. Chem. Soc., 84, 2058 **(1962)**.

[63] D. M. Mohilner, R. N. Adams, W. J. Argersinger, J. Am. Chem. Soc., 84, 3618 **(1962)**.

[64] A. F. Diaz, J. A. Logan, J. Electroanal. Chem., 11, 111 **(1980)**.

[65] K. Yoshizawa, A. Ito, K. Tanaka, T. Yamabe, Synth. Met., 48, 271 **(1992)**.

[66] X.-L. Wei, Y. Z. Wang, S. M. Long, C. Bobeczko, A. J. Epstein, J. Am. Chem. Soc., 118, 2545 **(1996)**.

[67] L. H. C. Mattoso, R. M. Faria, L. O. S. Bulho˜es, A. G. MacDiarmid, J. Polym. Sci., Polym. Chem. Ed., 32, 2147 **(1994)**.

[68] Y. Wei, R. Hariharan, S. A. Patel, Macromolecules, 23, 758 **(1990)**.

[69] M. Leclerc, J. Guay, L. H. Dao, Macromolecules, 22, 649 **(1989)**.

[70] A. Ito, K. Ota, K. Tanaka, T. Yamabe, K. Yoshizawa, Macromolecules, 28, 5618 **(1995)**.

[71] K. Yoshizawa, A. Ito, K. Tanaka, T. Yamabe, Solid State Commun., 87, 935 **(1993)**.

[72] K. Yoshizawa, A. Takata, K. Tanaka, T. Yamabe, Polym. J., 24, 857 **(1992)**.

[73] K. Yoshizawa, K. Tanaka, T. Yamabe, Chem. Lett., 1311 **(1990)**.

[74] T. Ishida, H. Iwamura, Chem. Lett., 317**(1991)**.

[75] (a) J. P. Wolfe, S. Wagaw, J.-F. Marcoux, S. L. Buchwald, Acc. Chem. Res., 31, 805 **(1998)**; (b) Hartwig, J. F. Angew. Chem., Int. Ed. Engl., 37, 2046 **(1998)**; (c) B. Y. Yang, S. L. Buchwald, J. Organomet. Chem., 576, 125 **(1999)**.

[76] (a) E. A. Harwood, S. T. Sigurdsson, N. B. F. Edfeldt, B. R. Reid, P. B. Hopkins, J. Am. Chem. Soc., 121, 5081 **(1999)**; (b) L.-C. Liang, R. R. Schrock, W. M. Davis, D. H. McConville, J. Am. Chem. Soc., 121, 5797 **(1999)**; (c) S. Wagaw, B. H. Yang, S. L. Buchwald, J. Am. Chem. Soc., 121, 10251 **(1999)**.

[77] F. E. Goodson, S. I. Hauck, J. F. Hartwig, J. Am. Chem. Soc., 121, 7527 **(1999)**.

[78] X. X. Zhang, J. P. Sadighi, T. W. Mackewitz, S. L. Buchwald, J. Am. Chem. Soc., 122, 7606-7607 **(2000)**.

[79] H. S. Nalwa (Ed.), Handbook of Organic Conductive Materials and Polymers, Wiley, New York, **(1997)**.

[80] T. A. Skotheim, R. L. Elsenbaumer, J. F. Reynolds (Eds.), Handbook of Conducting Polymers, 2nd Ed., Marcel Dekker, New York, **(1998)**.

[81] A. G. MacDiarmid, A. J. Epstein, Faraday Discuss. Chem. Soc., 88, 317 **(1989)**.

[82] A. G. MacDiarmid, A. J. Heeger, Synth. Met., 1, 101 **(1979)**.

[83] T. A. Skotheim (Ed.), Handbook of Conducting Polymers, Vols. 1 and 2, Marcel Dekker, New York, **(1986)**.

[84] M. G. Kanatzidis, Chemical and Engineering News, Vol. 36, 3 December **(1990)**.

[85] C. K. Chiang, C. R. Fincher, Jr., Y. W. Park, A. J. Heeger, H. Shirakawa, E. J. Louis, A. G. MacDiarmid. Phys. Rev. Lett., 39, 1098 **(1977)**.

[86] C. K. Chiang, M. A. Druy, S. C. Gau, A. J. Heeger, E. J. Louis, A. G. MacDiarmid, J. Am. Chem. Soc., 100, 1013 **(1978)**.

[87] K. E. Ziemelis, A. T. Hussain, D. D. C. Bradley, R. H. Friend, J. Rilhe, G. Wegner, Phys. Rev. Lett., 66, 2231 **(1991)**.

[88] D. H. Reneker, I. Chun, Nanotechnology, 73, 216 **(1996)**.

[89] A. G. MacDiarmid Synthetic Metals, 125, 11 **(2001)**.

[90] J. Preston, "Aromatic Polyamides", in: Encyclopedia of Polymer Science and Engineering, Vol. 11, John Wiley & Sons, New York, p. 381 **(1988)**.

[91] J. Williams, Kunststoffe, 342 **(1994)**.

[92] H. J. Jeong, M. Kakimoto, Y. Imai, J. Polym. Sci., Part A: Polym.Chem., 29, 767 **(1991)**.

[93] [a] H. H. Yang, "Aromatic Polyamides", in: Aromatic High-Strength Fibers, John Wiley & Sons, New York **(1989)**; [b] P. E. Cassidy, "Thermally Stable Polymers", Dekker, New York **(1980)**.

[94] R. N. Johnson, A. G. Farnham, R. A. Clendinning, W. F. Hale, C. N. Merriman, J. Polym. Sci., Part A: Polym. Chem., 5, 2375 **(1967)**.

[95] P. W. Morgan, J. polym. Sci., Polym. Symp., 72, 27 **(1985)**.

[96] M. Schnell, Angew. Chem., 68, 633 **(1956)**.

[97] E. L. Witbecker, P. W. Morgan, J. polym. Sci., Part A: polym. Chem., 40, 289 **(1959)**.

[98] P. W. Morgan, Condensation Polymers by Interfacial and Solution Methods, Interscience, New York, **(1965)**.

[99] J. G. Delacampa, E. Guifarro, F. J. Serna, J. Deabojo, Eur. Polym. J., 21, 1013 **(1985)**.

[100] G. Cum, R. Gallo, F. Severini, A. Spadaro, Angew. Makromol. Chem., 138, 111 **(1986)**.

[101] H. W. Hill, S. L. Knowlek, P. W. Morgan, Fr. Pat., 1, 199, 460 **(1959)**.

[102] P. W. Morgan, S. L. Swalek, H. W. Hill, Synthesis of condensation polymers by interfacial polymerization in system with high phase miscibility, paper presented at National ACS meeting, Dallas, TX, April **(1973)**.

[103] D. Yajaprakash, M. Balasubramanian, M. J. Nanjan, J. polym. Sci., Part A: polym. Chem., 23, 2319 **(1985)**.

[104] Y. Kimura, H. Minamizawa, N. Yoshiyuki, Y. Nomura, K. Yoshida, T. Morinaga, Jpn: Kokai Tokkyo Koho, JP 4, 226, 532 **(1992)**.

[105] N. Yamazaki, M. Matsumoto, F. Higashi, J. polym. Sci., Part A: polym. Chem., 13, 1373 **(1975)**.

[106] J. Deabajo, J. p. Gabarda, J. Fontan, Angew. Makromol. Chem., 71, 143 **(1978)**.

[107] W. Wrasildo, J. M. Augl, J. polym. Sci., Part A: polym. Chem., 7, 321 **(1969)**.

[108] C. P. Yang, S. H. Hsiao, Makromol. Chem., 190, 2119 **(1989)**.

[109] S. H. Hsiao, C. P. Yang, J. polym. Sci., Part A: polym. Chem., 28, 1149 **(1990)**.

[110] S. H. Hsiao, C. P. Yang, Makromol. Chem., 191, 155 **(1990)**.

[111] S. H. Hsiao, C. P. Yang, J. polym. Sci., Part A: polym. Chem., 29, 447 **(1991)**.

[112] S. H. Hsiao, C. P. Yang, J. H. Lin, J. polym. Sci., Part A: polym. Chem., 29, 1175 **(1991)**.

[113] C. P. Yang, S. H. Hsiao, J. H. Lin, J. polym. Sci., Part A: polym. Chem., 30, 1865 **(1992)**.

[114] C. D. Diakoumakos, J. A. Mikroyannidis, Polymer, 35, 1986 **(1994)**.

[115] A. E. Lozano, J. G. de la Campa, J. de Abajo, J. Preston, Polymer, 35, 872 **(1994)**.

[116] A. E. Lozano, J. G. de la Campa, J. de Abajo, J. Preston, J. Polym Sci., Part A: Polym. Chem., 33, 1987 **(1995)**.

[117] D. J. Liaw, P. N. Hsu, J. J. Chen, B. Y. Liaw, C. Y. Hwang, J. Polym. Sci., Part A: Polym. Chem., 39, 1557 **(2001)**.

[118] J. A. Mikroyannidis, J. Polym. Sci., Part A: Polym. Chem., 30, 2371 **(1992)**.

[119] J. A. Mikroyannidis, Macromolecules, 28, 5177 **(1995)**.

[120] I. K. Spiliopoulos, J. A. Mikroyannidis, J. Polym. Sci., Part A: Polym. Chem., 34, 1685 **(1996)**.

[121] I. K. Spiliopoulos, J. A. Mikroyannidis, J. Polym. Sci., Part A: Polym. Chem., 34, 1703 **(1996)**.

[122] I. Sava, E. Hamciuc, C. Hamciuc, M. Bruma, FW. Mercer, VN. Reddy, Synthesis and properties of aromatic polyamides containing 5-(4-acetoxy-benzoylamino) side groups, High Perform. Polym., 11, 307 **(1999)**.

[123] I. Sava, M. Bruma, Synthesis of a new diacid chloride containing pendent benzamide group and study of aromatic polyamides based on it. Ann West Univ. Timisoara, Ser Chem., 10, 73 **(2001)**.

[124] I. Sava, M. Bruma, E. Hamciuc, C. Hamciuc, D. Timpu, FW. Mercer, J. Appl. Polym. Sci., 80, 650 **(2001)**.

[125] I. Sava, M.-D. Iosip, M. Bruma, C. Hamciuc, J. Robison, L. Okrasa, T. Pakula, Eur. Polym. J., 39, 725 **(2003)**.

[126] J. L. Hedrick, J. W. Labadie, "Step Growth Polymers for High-Performance Materials, New Synthetic Method", ACS Symposium Series, Vol. 624, American Chemical Society, Washington, DC, p. 210 **(1996)**.

[127] [a] F. J. Williams, P. E. Donahue, J. Org. Chem., 42, 3414; **(1977)** [b] R. L. Markezich, O. S. Zamek, J. Org. Chem., 42, 3431 **(1977)**; [c] D. M. White, T. Takekoshi, F. T. Willams, H. M. Relles, P. E. Donahue, H. J. Kloper, G. R. Loucks, J. S. Manello, R. O. Matthews, R. W. Schulenz, J. Polym. Sci., Polym. Chem. Ed., 19, 1635 **(1981)**; [d] T. Takekoshi, Polym. J., 19, 191 **(1987)**.

[128] [a] T. Takekoshi, J. G. Wirth, D. R. Heath, J. E. Kochanowski, J. S. Manello, M. J. Webber, J. Polym. Sci., Polym. Chem. Ed., 18, 3069 **(1980)**; [b] J. L. Hedrick, R. Twieg, Macromolecules, 25, 2021 **(1992)**; [c] S. K. Park, S. Y. Kim, Macromolecules, 31, 3385 **(1998)**; [d] S. K. Park, S. Y. Kim, Macromol. Chem. Phys., 199, 2717 **(1998)**; [e] I. S. Chung, S. Y. Kim, Macromolecules, 33, 9474 **(2000)**; [f] I. S. Chung, S. Y. Kim, J. Am. Chem. Soc., 123, 11071 **(2001)**.

[129] [a] J. L. Hedrick, Macromolecules, 24, 812 **(1991)**; [b] M. Lucas, J. L. Hedrick, Polym. Bull., 28, 129 **(1992)**.

[130] H. S. Lee, S. Y. Kim, Macromol. Rapid Commun., 23, 665 **(2002)**.

[131] K. R. Carter, S. Y. Kim, J. L. Labadie, Polym. Prepr. (Am. Chem. Soc., Div. Polym. Chem., 34, 415 **(1993)**.

[132] J. Buckingham. Dictionary of Natural Products (1 ed.), University Press, Cambridge, MA **(1994)**.

[133] R. O. Loutfy, C. K. Hsiao, P. M. Kazmaier, Photogr. Sci. Eng., 27, 5 **(1983)**.

[134] G. D'Aprano, M. Leclerc, G. Zotti, G. Schiavon, Chem. Mater., 7, 33 **(1995)**.

[135] J. March, Advanced Organic Chemistry, 4th ed., Wiley, New York, p. 641 **(1992)**.

[136] T. Hattori, J. Sakamoto, N. Hayashizaka, S. Miyano, Synthesis, 199 **(1994)**.

[137] W. Ten Hoeve, C. G. Kruse, J. M. Luteyn, J. R. G. Thiecke, H. Wynberg, J. Org. Chem., 58, 5101 **(1993)**.

[138] J. V. B. Kanth, M. Periasamy, J. Org. Chem., 58, 3156 **(1993)**.

[139] M. F. Semmelhack, H. Rhee.Tetrahedron Lett., 34, 1395 **(1993)**.

[140] A. S. Abd-El-Aziz, C. C. Lee, A. Piórko, R. G. Sutherland, J. Organomet. Chem., 348, 95 **(1988)**.

[141] A. Razzuk, E. R. Biehl, J. Org. Chem., 52, 2619 **(1987)**.

[142] H. Mitchell, Y. Leblanc, J. Org. Chem., 59, 682 **(1994)**.

[143] J. Lindley, Tetrahedron, 40, 1433 **(1984)**.

[144] A. J. Paine, J. Am. Chem. Soc., 109, 1496 **(1987)**.

[145] J. E. McMurry, S. Mohanraj, Tetrahedron Lett., 24, 2723 **(1983)**.

[146] A. Banfi, M. Bartoletti, E. Bellora, M. Bignotti, M. Turconi, Synthesis, 775 **(1994)**.

[147] D. H. R. Barton, J.-P Finet, J. Khamsi. Tetrahedron Lett., 27, 3615 **(1986)**.

[148] A. S. Guram, S. L. Buchwald. J. Am. Chem. Soc., 116, 7901 **(1994)**.

[149] A. S. Guram, R. A. Rennels, S. L. Buchwald. Angew. Chem. Int. Ed. Engl., 34, 1348 **(1995)**.

[150] A. J. Peat, S. L. Buchwald, J. Am. Chem. Soc., 118, 1028 **(1996)**.

[151] J. P. Wolfe, S. Wagaw, S. L. Buchwald, J. Am. Chem. Soc., 118, 7215 **(1996)**.

[152] J. P. Wolfe, S. L. Buchwald, J. Org. Chem., 61, 1133 **(1996)**.

[153] S. Wagaw, S. L. Buchwald, J. Org. Chem., 61, 7240 **(1996)**.

[154] J. P. Wolfe, R. A. Rennels, S. L. Buchwald, Tetrahedron, 21, 7525 **(1996)**.

[155] J. P. Wolfe, S. L. Buchwald, J. Am. Chem. Soc., 119, 6054 **(1997)**.

[156] S. Wagaw, R. A. Rennels, S. L. Buchwald, J. Am. Chem. Soc., 119, 8451 **(1997)**.

[157] J. P. Wolfe, S. L. Buchwald, J. Org. Chem., 62, 1264 **(1997)**.

[158] J. P. Wolfe, S. L. Buchwald, J. Org. Chem., 62, 6066 **(1997)**.

[159] J. P. Wolfe, S. L. Buchwald, Tetrahedron Lett., 38, 6359 **(1997)**.

[160] J. Åhman, S. L. Buchwald, Tetrahedron Lett., 38, 6363 **(1997)**.

[161] J. P. Wolfe, J. Åhman, J. P. Sadighi, R. A. Singer, S. L. Buchwald, Tetrahedron Lett., 38, p. 6367 **(1997)**.

[162] J.-F. Marcoux, S. Wagaw, S. L. Buchwald, J. Org. Chem., 62, 1568 **(1997)**.

[163] K. Aoki, A. J. Peat, S. L. Buchwald, J. Am. Chem. Soc., 120, 3068 **(1998)**.

[164] J. P. Sadighi, M. C. Harris, S. L. Buchwald, Tetrahedron Lett., 39, 5327 **(1998)**.

[165] F. Paul, J. Patt, J. F. Hartwig, J. Am. Chem. Soc., 116, 5969 **(1994)**.

[166] J. Louie, J. F. Hartwig, Tetrahedron Lett., 36, 3609 **(1995)**.

[167] M. S. Driver, J. F. Hartwig, J. Am. Chem. Soc., 118, 7217 **(1996)**.

[168] J. Louie, M. S. Driver, B. C. Hamann, J. F. Hartwig, J. Org. Chem., 62, 1268 **(1997)**.

[169] J. Louie, J. F. Hartwig, A. J. Fry, J. Am. Chem. Soc., 119, 11695 **(1997)**.

[170] F. E. Goodson, J. F. Hartwig, Macromolecules, 31, 1700 **(1998)**.

[171] G. Mann, J. F. Hartwig, M. S. Driver, C. Fernández-Rivas, J. Am. Chem. Soc., 120, 827 **(1998)**.

[172] J. P. Wolfe, S. Wagaw, J.-F. Marcoux, S. L. Buchwald, Acc. Chem. Res., 31, 805 **(1998)**.

[173] J. F. Hartwig, Synlett., 329 **(1997)**.

[174] M. Kosugi, M. Kameyama, T. Migita, Chem. Lett., 927 **(1983)**.

[175] K. Jones, M. F. Lappert, Organomet, Chem. Rev., 1, 67 **(1966)**.

[176] A. Miyashita, A. Yasuda, H. Takaya, K. Toriumi, T. Ito, T. Souchi, R. Noyori, J. Am. Chem. Soc., 102, 7932 **(1980)**.

[177] A. Miyashita, H. Takaya, T. Souchi, R. Noyori, Tetrahedron, 40, 1245 **(1984)**.

[178] T. Yamamoto, M. Nishiyama, Y. Koie. Tetrahedron Lett., 39, 2367 **(1998)**.

[179] N. P. Reddy, M. Tanaka, Tetrahedron Lett., 38, 4807 **(1997)**.

[180] J. F. Hartwig, S. Richards, D. Barañano, F. Paul, J. Am. Chem. Soc., 118, 3626 **(1996)**.

[181] M. Kranenburg, Y. E. M. van der Burgt, P. C. J. Kamer, P. W. N. M. van Leeuwan, K. Goubitz, J. Fraanje, Organometallics, 14, 3081 **(1995)**.

[182] V. Farina, in Comprehensive Organometallic Chemistry, 2nd Ed., Pergamon Press: Oxford, Vol. 12, pp 161-240 **(1995)**.

[183] (a) C. Amatore; G. Broeker, A. Jutand, F. Khalil, J. Am. Chem. Soc., 119, 5176 **(1997)**; (b) Amatore, C. Jutand, A. Coord. Chem. Rev., 178-180, 511 **(1998)**.

[184] Associative reactions of square-planar, d_8 transition metal complexes typically proceed *via* five-coordinate intermediates. See: J. P. Collman, L. S. Hegedus, J. R. Norton, R. G. Finke, Principles and Applications of Organotransition Metal Chemistry; University Science Books: Mill Valley, CA, **(1987)**; Chapter 5.

[185] G. Mann, J. F. Hartwig, J. Am. Chem. Soc., 118, 13109 **(1996)**.

[186] D. W. Old, J. P. Wolfe, S. L. Buchwald, J. Am. Chem. Soc., 120, 9722 **(1998)**.

[187] L. Wessjohann, G. McGaffin, A. deMeijere, Synthesis, 359 **(1989)**.

[188] M. J. O'Donnell, J. M. Boniece, S. E. Earp, Tetrahedron Lett., 2641 **(1978)**.

[189] D. L. Boger, J. S. Panek. Tetrahedron Lett., 25, 3175 **(1984)**.

[190] D. L. Boger, S. R. Duff, J. S. Panek, M. J. Yasuda. J. Org. Chem., 50, 5782 **(1985)**.

[191] D. L. Boger, S. R. Duff, J. S. Panek, M. J. Yasuda. J. Org. Chem., 50, 5790 **(1985)**.

[192] J. K. Stille. Angew. Chem. Int. Ed. Engl., 25, 508 **(1986)**.

[193] N. Miyaura, A. Suzuki. Chem. Rev., 95, 2457 **(1995)**.

[194] E.-I. Negishi. Acc. Chem. Res., 15, 340 **(1982)**.

[195] (a) T. Kanbara, A. Honma, K. Hasegawa, Chem. Lett., 1135 **(1996)**; (b) T. Kanbara, Y. Miyazaki, K. Hasegawa, T. Yamamoto, J. Polym. Sci., Polym. Chem. Ed., 38, 4194 **(2000)**; (c) T. Kanbara, Y. Nakadani, K. Hasegawa, Polym. J., 31, 206 **(1999)**.

[196] (a) J. F. Hartwig, Synlett., 329 **(1997)**; (b) J. F. Hartwig, Angew Chem Int Ed., 37, 2046 **(1998)**; (c) B. H.Yang, S. L. Buchwald, J. Organomet. Chem., 576, 125 **(1999)**; (d) M. C. Harris, O. Geis, S. L. Buchwald, J. Org. Chem., 64, 6019 **(1999)**; (e) J. P Wolfe, S. L. Buchwald, J. Org. Chem., 65, 1144 **(2000)**; (f) J. P. Wolfe, H. Tomori, J. P. Sadighi, J. Yin, S. L. Buchwald, J. Org. Chem., 65, 1158 **(2000)**; (g) B. C. Hamman, J. F. Hartwig, J. Am. Chem. Soc., 120, 7369 **(1998)**; (h) D. W. Old, J. P. Wolfe, S. L. Buchwald, J. Am. Chem. Soc., 120, 9722 **(1998)**; (i) T. Yamamoto, M. Nishiyama, Y. Koie, Tetrahedron Lett, 39, 2367 **(1998)**; (j) Y. Hong, C. H. Senanayake, T. Xiang, C. P. Vadenbossche, G. J. Tanoury, R. P. Bakale, S. A. Wald, Tetrahedron Lett., 39, 3121 **(1998)** (k) J. F. Hartwig, M. Kawatsura, S. I. Hauck, K. H. Shaughnessy, L. M. Alcazar-Roman, J. Org. Chem, 64, 5575 **(1999)**; (l) N. Prabhakar, M. Tanaka, Tetrahedron Lett., 38, 4807 **(1997)**; (m) X. Bei, A. S. Guram, H. W. Turner, W. H. Weinberg, Tetrahedron Lett., 40, 1237 **(1999)**; (n) J. Hang, G. Grasa, S. P. Nolan, Org. Lett., 1, 137 **(1999)**; (o) I. P. Beletskaya, A. G. BessmertnykhGuilard, R. Synlett., 1459 **(1999)**; and references therein.

[197] See for example: Y. F. Wang, K. P. Chan, A. S. Hay, React. Funct. Polym., 30, 205 **(1996)**. P. Hodge, H. M. Colquhoun, D. J. Williams, Chem. Ind. (London), 162 **(1998)**.

[198] H. Etori, T. Kanbara, T.Yamamoto, Chem. Lett., 461 **(1994)**.

[199] (a) Yamamoto, T.; Yamamoto, A. Chem. Lett., 353 **(1977)** (b) T. Yamamoto, Y. Hayashi, A.Yamamoto, Bull. Chem. SOC. Jpn., 51, 2091 **(1978)**, (c) T. Yamamoto, K. Sanechika, A. Yamamoto, J . Polym. Sci., Polym. Lett. Ed., 18, 9 **(1980)**.

[200] 6) Bao, Z.;Chan, W.; Yu, L. Chem. Mater., 5, 2 **(1993)**.

[201] P. M. Hergenrother, B. J. Jensen, S. J. Havens, Polymer, 29, 358 **(1988)**.

[202] H. Schnell, H. Krimm, Angew. Chem., 14, 662 **(1963)**.

[203] A. B. Galun, A. Kaluszyner, E. D. Bergmann, J. of Org. Chem., 27, 2373 **(1962)**.

[204] N. O. Calloway, Chem. Rev., 17, 327 **(1935)**.

[205] G. A. Olah, (Ed.) Friedel-Crafts and Related Reactions, Interscience, New York, Vol., 1,

P. 569 **(1963)**.

[206] G. A. Olah, (Ed.) Friedel-Crafts and Related Reactions, Interscience , New York, Vol., 3, P. 1003 **(1964)**.

[207] I. Cooke, B. P. Susz, Helv. Chim. Acta, 37, 1273 **(1954)**.

[208] L. K. Tan, S. J. Brownstein, J. Org. Chem., 47, 4737 **(1982)**.

[209] K. Zhu, L. Wang, X. Jing, F. Wang, J. Mater. Chem., 12, 181 **(2002)**.

[210] E. D. Bergmann, et al. Bull. Soc. Chim. Fr., 19, 703 **(1952)**.

[211] J. F. Hartwig, S. Richards, D. Barañano, F. Paul, J. Am. Chem. Soc., 118, 3626 (1996).

[212] "Textbook of Polymer Science" / Fred W. Billmeyer, Jr., 2nd Ed., Wiley-Interscience, New York, **(1971)**.

[213] Z. G. Qian, Z. Z. Pang, Z. X. Li, M. H. He, J. G. Liu, L. Fan, S. Y. Yang, J. Polym. Sci., Part A: Polym. Chem., 40, 3012 **(2002)**.

[214] P. Coppo, H. Adams, D. C. Cupertino, S. G. Yeates, M. L. Turner, Macromolecules, 36, 2705 **(2003)**.

[215] C. P. Yang, R. S. Chen, K. S. Hung, E. M. Woo, Polym. Int., 51, 406 **(2002)**.

[216] G. C. Pimentel, A. L. Mc.Clellan, the hydrogen bond, Freeman, San Francisco **(1960)**.

[217] F. Franks. Water, a comprehensive Treatise, Plenum, New York, Vols., 1-6 **(1972)**.

[218] M. D. Joesten, L. J. Schaad: Hydrogen Bonding, Marcel Dekker, New York, **(1979)**.

[219] R. M. Badger, S. H. Bauer, Spectroscopic studies of the hydrogen bond. II. The shifts of the OH vibrational Frequency in the formation of the hydrogen bond, J. Chem. Phys., 5, 839-851 **(1939)**.

[220] M. M. Coleman, J. F. Graf, P. C. Painter, In: Specific interactions and the miscibility of polymer blends, Technomic, Lancester, p. 159 **(1991)**.

[221] A. Bondi, J. Phys. Chem., 68, 441 **(1964)**.

[222] C. Aakeröy, T. A. Evans, K. R. Seddon, I. Pálinkó, New J. Chem., 145 **(1999)**.

[223] S. Jeon, J. Choo, D. Sohn, S. No Lee, Polymer, 42, 9915 **(2001)**.

[224] J. Coates, Encyclopedia of analytical chemistry, Copyright © John Wiley & Sons Ltd, Chichester, R. A. Meyers, Ed., PP. 10825 **(2000)**.

[225] J. C. Alvarez, J. G. de la Campa, A. E. Lozano, J. de Abajo, Macromol. Chem. Phys., 202, 3142 **(2001)**.

[226] D.-J. Liaw, B.-Y. Liaw, J. Polym. Sci., Part A Polym. Chem., 37, 2791 **(1999)**.

[227] P. Carty in Polymeric Materials Encyclopedia, J. C. Salamone, Ed. in chief, p 2422, CRC, New York, **(1996)**.

[228] I. K. Spiliopoulos, J. A. Mikroyannidis, J. Polym. Sci., Part A: Polym. Chem., 34, 1703 **(1996)**.

[229] V. Lakshmana Rao, J.M.S.Rev. Macromol. Chem. Phys., 35, 661 **(1995)**.

[230] A. E. Lozano, J. de Abajo, J. G. de la Campa, J. Preston, J. Polym. Sci., Part A: Polym. Chem., 33, 1987 **(1995)**.

[231] D. J. Dawson, W. W. Fleming, J. R. Lyerla, Economy, J. In ACS Symposium Series 282; F. W. Harris, H. J. Spinelli, Eds., American Chemical Society: Washington, DC, pp 63-79 **(1985)**.

[232] I. K. Spiliopoulos, J. A. Mikroyannidis, J. Polym. Sci., Part A: Polym. Chem., 34, 1703 **(1996)**.

[233] T. Pakula, F. Kremer, A. Schönhals, Eds. Springer **(2002)**, Chapter 16. DIELECTRIC AND MECHANICAL SPECTROSCOPY A COMPARISON, in "Broadband dielectric spectroscopy"

[234] T. Pakula, S. Geyler, T Edling, D. Boese, Rheologica Acta, 35, 631 **(1996)**.

[235] S. Mullins, T. Pakula, M. Klapper, K. Müllen, An elastic modulus of G'~1GPa is measured under simular conditions for a PEK obtained from bisphenol-A and difluorobenzophenone (M_n = 22000), to be published.

[236] J. C. Barbour, D. R. Denison, J. H. Burkhart, C. A. Apblett, Advanced Materials & Technology **(2001)** (http://www.sandia.gov).

[237] M. Bruma, In: O. Olabisi, Editor, Handbook of thermoplastics, Marcel Dekker, New York p. 771 **(1997)**.

[238] C. E. Sroog. Prog. Polym. Sci., 16, 561 **(1991)**.

[239] F. W. Harris in Polyimides, D. Wilson, H. D. Stenzenberger, P. M. Hergenrother, Eds., Blackie & Son Ltd., Glasgow and London, **(1990)**.

[240] A. K. St. Clair, T. L. St. Clair, W. P. Winfree, Polym. Matl. Sci. & Eng., 59, 28 **(1988)**.

[241] C. Feger, H. Franke, in Polyimides, Fundamentals and Applications, M. K. Ghosh, K. L. Mittal, eds, p. 343, Marcel Dekker, New York, **(1996)**.

[242] D. R. Day, in Polyimides: Materials, Chemistry and Characterization, C. Feger, M. M. Khojasteh, J. E. McGrath, Eds., p. 537, Elsevier, Amsterdam, **(1989)**.

[243] N. Yada, Polym. Adv. Technol., 8, 215 **(1996)**.

[244] ``X-Ray Diffraction Methods in Polymer Science`` L. E. Alexander, R. E. Krieger Publishing Company, New York, **(1979)**.

[245] Y. Lee, R. S. Porter, Macromolecules, 20, 1336 **(1987)**.

[246] N. T. Wakelyn, J. Polym. Sci., Polym. Lett. Ed., 25, 25 **(1987)**.

[247] J. N. Hay, D. J. Kemmish, J. I. A. I. M. LangfordRae, Polym. Commun., 25, 175 **(1984)**.

[248] S.-H. Hsiao, C.-P. Yang, K.-Y. Chu, Macromolecules, 30, 165 **(1997)**.

[249] I. Fischbach, T. Pakula, P. Minkin, A. Fechtenkotter, K. Mullen, HW. Spiess, Saalwachter K; J. Phys. Chem.; B 106 (25): 6408-6418 **(2002)**.

[250] O. Herrmann-Schönherr O. A. Schneller, A. M. Seifert, M. Soliman, J. H. Wendorff, Makromol. Chem. Phys., 193, 1955 **(1992)**.

[251] Houben-Weyl Methoden Org. Chem., E20/1, 626 **(1987)**.

[252] P. Rempp, P. Lutz, E. Franta, J. Macromol. Sci., Pure Appl. Chem., A31, 891 **(1994)**.

[253] J. R. Ceresa, Block and Graft Copolymers, Butterworths, London, 1962. Houben-Weyl Methoden Org. Chem., E20/1, 628-640 **(1987)**.

[254] A. Chapiro, High Polymers. Radiation Chemistry of Polymeric Systems, Interscience: New York, 1962, Chapter XV. Houben-Weyl Methoden Org. Chem., E20/1, 632 **(1987)**.

[255] P. Rempp, E. Franta, Pure Appl. Chem., 30, 229 **(1972)**.

[256] P. Rempp, E. Franta, J. E. Herz, Adv. Polym. Sci., 86, 145 **(1988)**.

[257] M. Klapper, T. Wehrmeister, K. Müllen Macromolecules, 29, 5805 **(1996)**.

[258] P. Rempp, P. Lutz, E. Franta, J. Macromol. Sci., Pure Appl. Chem., A31, 891 **(1994)**.

[259] S. Becker, A. Bohm, K. Mullen, Chem.-A Eur. J., 6, 3984 (**2000**).

[260] Ferry, J. D., Viscoelastic properties of polymers, John Wiley & Sons Inc. New York **(1980)**.

[261] Pakula, T.; Geyler, S.; Edling, T.; Boese, D.; Rheologica Acta 35,631 **(1996)**.

[262] (a) R. L. Willson, Free Radical Res. Commun., 8, 201 **(1990)**. (b) A. Skancke, P. N. Skancke, Chem. Quinoid Compd. 2, 1 **(1988)**; (c) D. H. Evans, In Encvclowedia of Electrochemistry of the Elements; Bard, A. J.: L&d, H.; Eds.; Marcel Dekker: New York, Vol. XI, p 1, **(1978)**; (d) A. O. Patil, Macromolecules, 28, **(1995)**; D. Y. Curtin, Paul, I. C. J . Am. Chem. SOC., 106, 348 and 4010 **(1984)**; (e) K. E. Shea, M. A. Fox, J. Am. Chem. SOC., 113, 611 **(1991)**.

[263] (a) T. A. Skotheim, Ed. Handbook of Conducting Polymers; Marcel Dekker: New York, Vols. I and 11 **(1986)**; (b) W. R. Salaneck, D. L. Clark, E. J. Samuelsen, E. Science and Applications of Conducting Polymers; Adam Hilger: New York, **(1990)**. (c) A. G. MacDiarmid, A. J. Heeger, NRL Memorandum Report, Proceedings of the Molecular Electron Devices Workshop, AD-A 05816, 208 **(1981)**.

[264] H. Etori, T. Kanbara, T.Yamamoto, Chem. Lett., 461 **(1994)**.

[265] (a) T. Yamamoto, A. Yamamoto, Chem. Lett., 353 **(1977)**, (b) T. Yamamoto, Y. Hayashi, A.Yamamoto, Bull. Chem. SOC. Jpn., 51, 2091 **(1978)**, (c) T. Yamamoto, K. Sanechika, A. Yamamoto, J . Polym. Sci., Polym. Lett. Ed., 18, 9 **(1980)**.

[266] Z. Bao, W. Chan, L. Yu, Chem. Mater., 5, 2 **(1993)**.

[267] J. Tang, X. Jing, B. Wang, F. Wang, Synth. Met., 24, 231 **(1988)**.

[268] W. R. Salaneck, B. Liedberg, O. Inganas, R. Erlandsson, I. Lundstrom, A. G. MacDiarmid, M. Halpern, N. L. D. Domsdiri, Mol. Cryst. Liq Cryst., 121, 191 **(1985)**.

[269] S. Baek, J. J. Ree, M. Ree. J. Polym. Sci., Part A: Polym. Chem., 40, 983 **(2002)**.

[270] A. J. Epstein, J. M. Ginder, F. Zuo, R. W. Bigelow, H.-S. Woo, D. B. Tanner, A. F. Richter, W.-S. Huang, A. G. MacDiarmid. Synth. Met., 303, 18 **(1987)**.

[271] A. T. Royappa, D. D. Steadman, T. L. Tran, P. T. Nguyen, C. S. Prayaga, B. Cage, N. Dalal, Synth. Met., 273, 123 **(2001)**.

[272] S. H. Kim, S. M. Lee, J. H. Park, J. H. Kim, K. N. Koh, S. W. Kang, Dyes and Pigments 51, 45 **(2000)**.

[273] D. H. Choi, S. Y. Ban, J. H. Kim, Bull. Korean Chem. Soc., 4 441, 24 **(2003)**.

[274] C. H. Choi, M. Kertesz, M.-I. Boyer, M. Cochet, S. Quillard, G. Louarn, S. Lefrant, Chem. Mater., 11, 855 **(1999)**.

[275] M. Sandberg, T. Hjertberg, Synth. Met., 29, 257 (**1989**).

[276] (a) A. G. MacDiarmid, 215th National Meeting American Chemical Society, TX, Dallas, **(1998)**; (b) A. G. MacDiarmid, W. J. Zhang, J. Feng, F. Huang, B. R. Hsieh, Polymer Prepr., 39, 80 **(1998)**.

[277] N. Keitaro, D. Jacques Chemistry of materials (Huaxue Cailiao), 9, 2682 **(1997)**.

[278] P. Barbara, P. Rentzepis, L. Brus, Journal of America Chemical Society (Meigu Huaxue Huizhi), 102, 2786 **(1980)**.

[279] I. Wilner, Acc. Chem. Res., 30, 347 **(1997)**.

[280] G. Berkovic, V. Krongauz, V. Weiss, Chem. Rev., 100, 1741 **(2000)**.

[281] S. Kawata, Y. Kawata, Chem. Rev., 100, 1777 **(2000)**.

[282] E. Fischer, Y. Hirshberg, J. Chem. Soc., 4522 **(1952)**.

[283] For details cf. Organikum, Berlin p. 415 **(1981)**.

[284] J. Guillet, Polymer Photophysics and Photochemistry, Cambridge University Press, New York, **(1985)**.

[285] R. D. Stramel, S. E. Webber, M. A. J. Rodgers, J. Phys.Chem., 93, 1928 **(1989)**. J.-S. Hsiao, S. E. Webber, J. Phys. Chem., 96, 2892 (**1992**); K. Shigehara, H. Sano, E. Tsuchida, Makromol. Chem., 179, 1531 **(1978)**.

[286] M. Suzuki, Y. Mori, N. Yokoyama, M. Kimura, K. Hanabusa, H. Shirai, Macromol. Chem. Phys., 198, 959 **(1997)**; M. Kaneko and A. Yamada, Inorg. Chim. Acta, 45, L73 **(1980)**; W. E. Jones, Jr., S. M. Baxter, G. F. Strouse, T. J. Meyer, J. Am. Chem. Soc., 115, 7363 **(1993)**; Z. Peng, A. R. Gharavi, L. Yu, J. Am. Chem. Soc., 119, 4622 **(1997)**.

[287] a) K. Kalyanasundaram, D. Dung, J. Phys. Chem., 84, 2402 **(1980)**; b) P. B. Sweeter, Anal. Chem., 39, 979 **(1967)**; c) M.-P. Pileni, M. Grätzel, J. Phys. Chem., 84, 2402 **(1980)**.

[288] a) H. Ushiki, M. Ozu, Eur. Polym. J., 22, 835 **(1986)**; b) H. M. Gajiwala, R. zand, Macromolecules, 28, 481 **(1995)**; c) S. Das, C. S. Rajesh, C. H. Suresh, K. G. Thomas, A. Ajayaghosh, C. Nasr, P. V. Kamat, M. V. George, Macromolecules, 28, 4249 **(1995)**.

[289] H. M. Gajiwala, R. Zand, Macromolecules, 28, 481 **(1995)**.

[290] H. M. Colquhoun, C. C. Dudman, M. Thomas, C. A. O'Mahoney, D. J. Williams, J. Chem. Soc., Chem. Commun., 336 **(1990)**.

[291] D. J. Brunelle, T. G. Shannon, Macromolecules, 24, 3035 **(1991)**.

[292] S. Ganguly, H. W. Gibson, Macromolecules, 26, 2408 **(1993)**.

[293] Y.-F. Wang, K. P. Chan, A. S. Hay, Macromolecules , 28, 6371 **(1995)**.

[294] H. Jiang, T. Chen, J. Xu, Macromolecules, 30, 2839 **(1997)**.

[295] A. Jonas, R. Legras, Macromolecules, 26, 2674 **(1993)**.

[296] P. Carty in Polymeric Materials Encyclopedia, J. C. Salamone, Ed. in chief, p. 2422, CRC, New York, **(1996)**.

[297] M.-P. Pileni, M. J . Gratzel, Phys. Chem., 84, 2402 **(1980)**.

[298] S. De Silvestri, P. Laporta, Chem. Phys. Lett.,103,275 **(1984)**.

[299] S. A. Jankes, S. I. Van Dijk, K. Goubitz, C. A. Reiss, W. Schuddeboom, J. W. Verboeven, Mol. Cryst. Liq. Cryst., pp. 273 **(1990)**.

[300] J. Tian, C. C. Wu, M. E. Thompson, J. C. Sturm, R. A. Register, Chem. Mater., 7, 2190 **(1995)**.

[301] Sharp, Sutherland and Wilson, J. Chem. Soc., 344 **(1943)**.

[302] Albert and Goldacre, ibid., 454 **(1943)**.

[303] Bradbury and Jordan, Biochern. J ., 36, 287 **(1942)**.

[304] (a) O. Nuyken, C. Scherer, A. Baindl, A. R. Brenner, U. Dahn, R. Gärtner, S. Kaiser-Röhrich, R. Kollefrath, P. Matusche, B. Voit, Prog. Polym. Sci., 22, 93 **(1997)**; (b) G. S.

Kumar, D. C. Neckers. Chem. Rev., 89, 1915 **(1989)**; (c) A. Altomare, F. Ciardelli, N. Tirelli, R. Solaro, Macromolecules, 30,1298 **(1997)**; (d) A. Altomare, F. Ciardelli, M. S. Ghiloni, R. Salaro, N. Tirelli, Macromol. Chem. Phys., 198, 1739 **(1997)**; (e) X. Meng, A. Natansohn, P. Rochon, Polymer, 38, 2677 **(1997)**; (f) D. Junge, D. V. McGrath, Chem. Commun., 857 **(1997)**; (g) J. P. Chen, J. P. Gao, Z. Y. Wang, J. Polym. Sci., Part A: Polym. Chem., 35, 9 **(1997)**; (h) G. Mao, J. Wang, R. Clingman, C. K. Ober, J. T. Chen, Thomas, E. L. Macromolecules, 30, 2556 **(1997)**; (i) Wu, Y. Demachi, Y. Tsutsumi, O. Kanazawa, A. Shiono, T. Ikeda, Macromolecules, 31, 349 **(1998)**; (j) O. Tsutsumi, T. Kitsunai, A. Kanazawa, T. Shiono, T. Ikeda, Macromolecules, 31, 355 **(1998)**; (k) Y. Imai, K. Naka, Y. Chujo, Macromolecules, 31, 532 **(1998)**; (l) S. Shinkai, T. Nakaji, Y. Nishida, T. Ogawa; O. Manabe, J. Am.Chem. Soc., 102, 5860 **(1980)**; (m) M. Irie, Y. Hirano, S. Hashimoto, K. Hayashi, Macromolecules, 14, 262 **(1981)**.

[305] (a) T. J. Yamamoto, Synth. Org. Chem. Jpn., 53, 999 **(1995)**; Prog. Polym. Sci., 17, 1153 **(1992)**; (b) A.-D. Schlüter, G. Wegner, Acta Polym., 44, 53 **(1993)**; (c) E. Drent; H. M. Budzelaar, Chem. Rev., 96, 663 **(1996)**; (d) M. Schuster, S. Blechert, Angew. Chem., Int. Ed. Engl., 36, 2036 **(1997)**.

[306] M. Yoneyama, M. Kakimoto, Y. Imai, Macromolecules, 21, 1908 **(1988)**, 22, 2593 **(1989)**; M.Yoneyama, M. Kakimoto, Y. Imai, J. Polym. Sci., Part A: Polym. Chem., 27, 1985 **(1989)**.

[307] (a) Y. D. Ward, V. Farina, Tetrahedron Lett., 39, 6993 **(1996)**; (b) C. A. Willoughby, K. T. Chapman, Tetrahedron Lett.,39, 7184 **(1996)**.

[308] P. Carty in Polymeric Materials Encyclopedia, J. C. Salamone, Ed. in chief, p 2422, CRC, New York, **(1996)**.

[309] E. Sawicki, J. Org. Chem., 22, 621 **(1957)**.

[310] T. Kanbara, M. Oshima, T. Imayasu, K. Hasegawa, Macromolecules, 31, 8725 (**1998**).

[311] B. Valeur, Eds.; WILEY-VCH (**2002**) Section 3.3.4, MOLECULAR FLUORESCENCE, "principles and applications" P. 54.

[312] B. Valeur, Eds.; WILEY-VCH (**2002**) Section 3.4.2, MOLECULAR FLUORESCENCE, "principles and applications" P. 56

[313] N. G. Pschirer, K. Byrd, U. H. F. Bunz, Macromolecules, 34, 8590 (**2001**).

[314] M. Irie, Adv. Polym. Sci., 94, 27 (**1990**).

[315] Applied photochromic polymer systems; Mc Ardle, C. B., Ed.; Chapman & Hall: New York, **(1992)**.

[316] Y. R. Shen, The principles of Nonlinear Optics; Wiley: New York, **(1985)**.

[317] G. Vanermen, C. Samyn, G. S'heeren, A. Persoons, Makromol. Chem., 193, 3057 **(1992)**.

[318] J. H. Burroughes, D. D. C. Bradley, A. R. Brown, R. N. Marks, K. Mackay, R. H. Friend, P. L. Burn, A. B. Holmes, Nature, 347, 539 **(1990)**.

[319] G. Grem, G. Leditzky, B. Ullrich, G. Leising, Adv. Mater., 4, 36 **(1992)**.

[320] M. Remmers, D. Neher, J. Grüner, R. H. Friend, G. H. Gelinck, J. M. Warman, C. Quattrocchi, D. A. dos Santos, J.-L. Brédas, Macromolecules, 29, 7432 **(1996)**.

[321] Y. Ohmori, M. Uchia, K. Muro, K. Yoshino, Jpn. J. Appl. Phys., 30, L 1941 **(1991)**.

[322] H. N. Cho, J. K. Kim, D. Y. Kim, C. Y. Kim, N. W. Song, D. Kim, Macromolecules, 32, 1476 **(1999)**.

[323] P. L. Burn, A. B. Holmes, A. J. Kraft, D. D. C. Bradley, R. H. Friend, A. R. Brown, J. Chem. Soc., Chem. Commun., 32 **(1992)**.

[324] D.-H. Hwang, H.-K. Shim, J.-I. Lee, K.-S. Lee, J. Chem. Soc., Chem. Commun., 2461 **(1994)**.

[325] R. M. Gurge, A. M. Sarker, P. M. Lahti, B. Hu, F. E. Karasz, Macromolecules, 30, 8286 **(1997)**.

[326] N. C. Greenham, S. C. Moratti, D. D. C. Bradley, R. H. Friend, A. B. Holmes, Nature, 365, 628 **(1993)**.

[327] R. E. Gill, G. G. Malliaras, J. Wildeman, G. Hadziioannou, Adv. Mater., 1994, 6, 132

[328] H. L. Wang, M. J. Marsella, D.-K. Fu, T. M. Swager, A. G. MacDiarmid, A. J. Epstein, Polym. Mater. Sci. Eng., 73, 473 **(1995)**.

[329] A. Kraft, A. C. Grimsdale, A. B. Holmes, Angew. Chem., Int. Ed., 37, 2 **(1998)**.

[330] M. Hamaguchi, H. Sawada, J. Kyokane, K. Yoshino, Chem. Lett., 525 **(1996)**.

[331] T. E. McCarthy, H. Witteler, T. Pakula, G. Wegner, Macromolecules, 28, 239 **(1995)**.

[332] R. H. Friend, R. W. Gymer, A. B. Holmes, J. H. Burroughes, R. N. Marks, C. Taliani, D. D. C. Bradley, D. A. Dos Santos, J. L. Brédas, M. Lögdlund, W. R. Salaneck, Nature, 397, 121 **(1999)**.

[333] A. W. Grice, D. D. C. Bradley, M. T. Bemius, M. Inbasekaran, W. W. Wu, E. P. Woo, Appl. Phys. Lett., 73, 629 **(1998)**.

[334] A. Kraft, A. C. Grimsdale, A. B. Holmes, Angew. Chem., Int. Ed. Engl., 110, 402 **(1998)**.

[335] R. H. Friend, N. C. Greenham, In Handbook of Conducting Polymers, 2nd Ed., T. A. Skotheim, R. L. Elsenbaumer, J. R. Reynolds, Eds., Marcel Dekker: New York, p 823 **(1997)**.

[336] J. I. Segura, Acta Polym., 49, 319 **(1998)**.

[337] J. Salbeck, Ber. Bunsen-Ges. Phys. Chem., 100, 1667 **(1996)**.

[338] U. Scherf, In Handbook of Conducting Polymers, 2nd Ed., T. A. Skotheim, R. L. Elsenbaumer, J. R. Reynolds, Eds., Marcel Dekker: New York, p 363 **(1997)**.

[339] F. Uckert, S. Setayesh, K. Müllen, Macromolecules, 32, 4519 **(1999)**.

[340] J. Schmidt, M. Eitel, J. Prakt. Chem., 134, 167 **(1932)**.

[341] J. Ipaktschi, R. Hosseinzadeh, P. Schlaf, E. Dreiseidler, R. Goddard, Helv. Chim. Acta, 81, 1821 **(1998)**.

[342] B. Valeur, Eds.; WILEY-VCH **(2002)** Section 3.4.4, MOLECULAR FLUORESCENCE, "principles and applications" P. 62.

[343] H. Zollinger, Weinheim; Color chemistry: syntheses, properties and applications of organic dyes and pigments, New York: VCH, p. 168 **(1987)**.

[344] J. F. Hartwig, S. Richards, D. Barañano, F. Paul, J. Am. Chem. Soc., 118, 3626, **(1996)**.

[345] Chem Draw Ultra, version 6.0.1, **(1985-2000)**, © Cambridgesoft.com.

[346] J. C. Alvarez, J. G. de la Campa, A. E. Lozano, J. de Abajo, Macromol. Chem. Phys., 202, 3142 **(2001)**.

[347] D.-J. Liaw, B.-Y. Liaw, J. Polym. Sci., Part A: Polym. Chem., 37, 2791 **(1999)**.

[348] A. Parthiban, A. Le Guen, Y. Yansheng, U. Hoffmann, M. Klapper, K. Müllen Macromolecules, Amino-Functionalized Poly(arylene ether ketone)s, 30, 2238 **(1997)**.

[349] D. J. Liaw, B.Y. Liaw, C. M. Yang. Macromolecules, 32, p. 7248 **(1999)**.

[350] E. D. Bergmann, et al. Bull. Soc. Chim. Fr., 19, 703 **(1952)**.

[351] M. Gaal, E. J. W. List, U. Scherf, Macromolecules, 36, 4236 (**2003**).

[352] N. G. Pschirer, K. Byrd, U. H. F. Bunz, Macromolecules, 34, 8590 (**2001**).

[353] A. S. Al-Hussaini, M. Klapper, T. Pakula, K. Müllen, Macromolecules, 37, 8269 (**2004**).

[354] D.-J. Liaw, B.-Y. Liaw, Polymer, 42, 839 **(2001)**.

[355] D. J. Liaw, B. Y. Liaw, C. M. Yang. Macromolecules, 32, 7248 **(1999)**.

[356] W. Wu, M. Bernius, M. Dibbs, M. Inbasekaran, E. Woo, L. Wujkowski, Polym. Prepr., 41, 821 **(2000)**.

[357] C. Wang, C. Yuan, H. Wu, Y. Wei, J. Appl. Lett., 78, 4264 **(1995)**.

[358] H. C. Kim, J.-S. Kim, K.- S. Kim, H. K. Park, S. Baek, M. Ree, J. Polym Sci Part A: Polym Chem, 42, 825 **(2004)**.

[359] G. S. Liou, S. H. Hsiao, Polym. J., 35, 402 **(2003)**.

[360] K.Takeda, CMC, Shibaura Institute of Technology 3-9-14 Shibaura, Minato-ku, Tokyo 108 ''Recycling Problems and Combustion of Flame-Retardant Organic Materials''.

[361] C. Xia, R. C. Advincula, Macromolecules, 34, 5854 **(2001)**.

[362] N. Nemoto, H. Kameshima, Y. Okano, T. Endo, J. of Polym. Sci.; Part A: Polym. Chem., 41, 1521 **(2003)**.

[363] W. Lifeng, P. Huagen, W. Xiaogong, L. Deshan, Z. Qixiang, TSINGHUA SCIENCE AND TECHNOLOGY, 6, 173 **(2001)**.

[364] M. Konas, T. M. Moy, M. E. Rogers, A. R. Shultz, T. C. Ward, J. E. McGrath, J. Polym. Sci., Polym. Phys., 33, 1429 **(1995)**.